

Multiproduct Terpene Synthases: Catalytic Promiscuity and Cyclization of Substrate Geometric Isomers

Dissertation

(kumulativ)

zur Erlangung des akademischen Grades doctor rerum
naturalium (Dr. rer. nat.)

vorgelegt dem Rat der Chemisch-Geowissenschaftlichen Fakultät
der Friedrich-Schiller-Universität Jena

von Master of Science
Abith Ramadevan Vattekkatte
geboren am 12 Juli 1982 in Trichur (Indien)

1. Gutachter Prof. Dr. Wilhelm Boland

2. Gutachter Prof. Dr. Rainer Beckert

3. Gutachter Prof. Dr. Wittko Francke

Tag der Verteidigung 25.11.2015

1 Table of Contents

1	Table of Contents	1
2	Statement of Authorship.....	5
3	Preface and Acknowledgement.....	17
4	Introduction	21
4.1	General Introduction.....	23
4.1.1	Discovery and Milestones	24
4.1.2	Commercial Applications of Terpenes	24
4.2	Terpene Diversity	26
4.2.1	Ecological Significance: Defense with Mixtures	26
4.2.2	Communication using Terpene Diversity.....	28
4.3	Terpenoid Biosynthesis: The Acyclic Substrates	28
4.3.1	The Initial C5 Precursors.....	28
4.3.2	Biosynthesis of Acyclic Precursors of The Terpene Family	30
4.4	Regulation of Terpene Biosynthesis	31
4.4.1	Subcellular Localization of Terpene Biosynthesis in Plants	31
4.4.2	Regulation of Terpene Biosynthesis in Plants.....	32
4.5	Terpene Synthases	33
4.5.1	Enzymology.....	33
4.5.2	Multiproduct Terpene Synthases.....	34
4.5.3	Reaction Mechanism of Multiproduct Synthases	35
4.6	Discovering Catalytic Promiscuity	37
4.6.1	Site Directed Mutagenesis Studies	38
4.6.2	Terpene Synthases Can Accept Multiple Substrates	38
5	Aim of the thesis	41
6	Manuscripts	47
6.1	Manuscript I: Isotope sensitive branching and kinetic isotope effects to analyse multiproduct terpenoid synthases from <i>Zea mays</i>	49
6.2	Manuscript II: Substrate geometry controls the cyclization cascade in multiproduct terpene synthases from <i>Zea mays</i>	55
6.3	Manuscript III: Inhibition of a multiproduct terpene synthase from <i>Medicago truncatula</i> by 3-bromoprenyl diphosphates	67
6.4	Manuscript IV: Novel biosynthetic products from multiproduct terpene synthase from <i>Medicago truncatula</i> using non-natural isomers of prenyl diphosphates.....	79
7	General Discussion.....	93
7.1	Multiproduct terpene synthases	95
7.1.1	Multiproduct Enzymes from <i>Zea mays</i>	96
7.1.2	Multiproduct Terpene Synthase from <i>Medicago truncatula</i>	98
7.2	Isotope Sensitive Branching in Multiproduct enzymes (Manuscript I)	100
7.2.1	Substrates for Isotope Sensitive Branching Experiments	102
7.2.2	Kinetic Isotope Effects in Multiproduct Terpene Synthases from <i>Zea mays</i>	103
7.3	Effects of Substrate Geometry on Terpene Synthases (Manuscript II)	104
7.3.1	Effects Of Geometry on Multiproduct Terpene Synthase from <i>Zea Mays</i>	105
7.3.2	Labelled Stereoisomers as Substrates.....	105
7.3.3	Product Distribution with Geometric Isomers.....	106
7.4	Development of Co-Crystallization Candidate (Manuscript III).....	107
7.5	Substrate Geometric Isomers as a Tool for Novel Biosynthetic Products (Manuscript IV).....	109
8	Summary	111
9	Future Perspectives	117
10	Zusammenfassung.....	121

11	Supporting Information.....	127
11.1	Manuscript I.....	129
11.2	Manuscript II.....	145
11.3	Manuscript III.....	167
11.4	Manuscript IV.....	177
12	Citations.....	199
13	Curriculum Vitae.....	209
14	List of Publications.....	211
15	Conference Presentations.....	213
15.1	Oral Presentations.....	213
15.2	Poster Presentations.....	214
16	Eigenständigkeitserklärung.....	215

2 Statement of Authorship

This section contains a list of the individual author contributions to the publications reprinted in this thesis.

Manuscript I:

Isotope sensitive branching and kinetic isotope effects to analyse multiproduct terpenoid synthases from *Zea mays*

Dr. Nathalie Gatto,¹ Abith Vattekkatte,² Dr. Tobias Köllner,³ Prof. Dr. Jörg Degenhardt,⁴ Prof. Dr. Jonathan Gershenzon⁵ and Prof. Dr. Wilhelm Boland⁶

Chemical Communications, 2015, 51, 3797-3800

Contribution	Authors					
	1	2	3	4	5	6
Conceptual development	X	X				X
Manuscript preparation	X	X				
Synthesis of substrates	X	X				
Enzymatic assays		X				
Biosynthesis elucidation		X	X			
Conceptual contribution					X	X
Manuscript correction			X	X	X	X
Supervision						X
	1.0	1.0				

Manuscript II:

Substrate geometry controls the cyclization cascade in multiproduct terpene synthases from *Zea mays*

Abith Vattekkatte,¹ Dr. Nathalie Gatto,² Dr. Tobias Köllner,³ Prof. Dr. Jörg Degenhardt,⁴
Prof. Dr. Jonathan Gershenzon⁵ and Prof. Dr. Wilhelm Boland⁶

Organic & Biomolecular Chemistry, 2015, 13, 6021-6030

Contribution	Authors					
	1	2	3	4	5	6
Conceptual development	X	X				X
Manuscript preparation	X					
Synthesis of substrates	X	X				
Enzymatic assays	X					
Biosynthesis elucidation	X		X			
Conceptual contribution					X	X
Manuscript correction		X	X	X	X	X
Supervision						X
	1.0					

Manuscript III:

Inhibition of a multiproduct terpene synthase from *Medicago truncatula* by 3-bromoprenyl diphosphates

Abith Vattekkatte,¹ Dr. Nathalie Gatto,² Eva Schulze,³ PD Dr. Wolfgang Brandt⁴ and
Prof. Dr. Wilhelm Boland⁵

Organic & Biomolecular Chemistry, 2015, 16, 4776-4784

Contribution	Authors				
	1	2	3	4	5
Conceptual development	X	X			X
Manuscript preparation	X				
Synthesis of substrates	X	X			
Enzymatic assays	X				
Modelling Studies			X	X	
Manuscript correction	X		X	X	X
Supervision					X
	1.0				

Manuscript IV:

Novel biosynthetic products from multiproduct terpene synthase from *Medicago truncatula* using non-natural isomers of prenyl diphosphates

Abith Vattekkatte,¹ Dr. Stefan Garms² and Prof. Dr. Wilhelm Boland³

(Under preparation)

Contribution	Authors		
	1	2	3
Conceptual development	X	X	X
Manuscript preparation	X		
Synthesis of substrates	X	X	
Enzymatic assays	X	X	
Biosynthesis elucidation	X	X	X
Manuscript correction	X		X
Supervision			X
	1.0		

Erklärung zu den Eigenanteilen des Promovenden/der Promovendin sowie der weiteren Doktoranden/Doktorandinnen als Koautoren an den Publikationen und Zweitpublikationsrechten bei einer kumulativen Dissertation

Für alle in dieser kumulativen Dissertation verwendeten Manuskripte liegen die notwendigen Genehmigungen der Verlage („Reprint permissions“) für die Zweitpublikation vor.

Die Co-Autoren der in dieser kumulativen Dissertation verwendeten Manuskripte sind sowohl über die Nutzung, als auch über die oben angegebenen Eigenanteile informiert und stimmen dem zu.

Die Anteile der Co-Autoren an den Publikationen sind in diesem Kapitel aufgeführt.

Ich bin mit der Abfassung der Dissertation als publikationsbasiert, d.h. kumulativ, einverstanden und bestätige die vorstehenden Angaben. Eine entsprechend begründete Befürwortung mit Angabe des wissenschaftlichen Anteils des Doktoranden/der Doktorandin an den verwendeten Publikationen werde ich parallel an den Rat der Fakultät der Chemisch-Geowissenschaftlichen Fakultät richten.

PROF. DR. WILHELM BOLAND

Name Erstbetreuer

20/07/15

Datum

JENA

Ort



Unterschrift

Prof. Dr. Rainer Becket

Name Erstbetreuer

21.07.15

Datum

JENA

Ort



Unterschrift

ABITH R. VATTEKKATTE


Name

21.07.15

Datum

JENA

Ort



Unterschrift

3 Preface and Acknowledgements

This is by far the most important part of my thesis. None of this work would have been possible without the support of many people I have been lucky to be associated with.

First and foremost I would like to express my gratitude to **Prof. Wilhelm Boland** for unflinching support and guidance all through my doctoral studies. You are a mentor par excellence, helping me as an organic chemist to develop insights into biological questions. I still remember our first meeting and the passion with which you introduced me to multiproduct terpene synthases. No wonder the enthusiasm rubbed off immediately and the pursuits to crystallize the enzyme started. Even though we are still awaiting the treasure, one important lesson I learnt from your motivation is that we are only one step away from success. You have been so generous, with your open door approach and resources that I cannot begin to say enough. You will be a person I look up to for guidance all throughout my career.

I am personally thankful to all the past and present members of Boland group for the wonderful work atmosphere and honestly cooperative attitude. I would especially like to thank **Grit Winnefeld** for going out of her way to make literally everything in Jena comfortable. Thank you, with your help with everything from house to travel, I would like to add nothing seems impossible in your efficient hands. Another person who deserves my special gratitude is **Stephan von Reuss**; my smooth ride over all the bumps not only scientific has been due to your eager attitude to help. Special thanks to you for all those midnight discussions and help with all things like talks, posters, insurance etc. and not to mention German contracts. The marathon run at completing this thesis would not have been possible without your supportive mailbox deliveries. I would also like to thank **Stefan Bartram** for all his help during my novice days and terpene synthase chemistry. I would like to thank **Prof. Rainer Beckert** for his valuable inputs during thesis committee meetings and prompt help with all regulations.

The research in this thesis could not have been performed without the help of the absolutely incredible scientists as my collaborators. Deserving special mention are **Tobias Köllner**, **Nathalie Gatto** and **Stefan Garms**. It was their initial hard work into this topic that allowed me to move ahead with this research. I would like especially acknowledge Stefan Garms for coming back to initiate my smooth transition into the world of enzymes. My first collaboration was with **Kornelius Zeth** and **Enea Sancho**, no effort was spared to cajole the enzyme to crystallize and have fun in Bilbao. Our biannual tradition of Naturstoffchemie workshop resulted in successful collaboration with **Eva Schulze** and **Wolfgang Brandt**, thank you for the quick modelling studies. I would like also to thank **Prof. Jonathan Gershenzon** and **Prof. Jörg Degenhardt** for their guidance and critical inputs for manuscripts.

A special advantage of working in Boland department is its true interdisciplinary nature, being a synthetic chemist it was a major advantage to be surrounded by experts in biochemistry, microbiology and evolutionary biology. I would like to thank **Peter Rahfeld** and **Rita Buchler** for endless help with protein purification and training in biochemistry techniques. Thanks to **Sindy Frick** for sharing PcIDS1 enzyme, **Susan Kugel** and **Tim Schöner** for the help with clones and standardization. I would like to additionally thank **Franziska Beran** for her patient help and **Maritta Kunert, Kerstin Ploss** with MS-instruments.

I am grateful to all the past and present members of the popular office in the department (also thanks to coffee machine). It was fun to be a member of this office with all the cheerful discussion, technical and personal help starting with settling into Jena, daily stuff and lovely postcards. A special note of thanks to **Nadja, Anne, Ilka, Daniela** and **Stephan**, I will cherish this friendship for a long time and fun continues with newer members too. Additionally, I would to thank **Anja David** and **Martin Niebergall** for all help and **Kost Group** for the lively lunch group and walks to Zeiss Mensa.

I have been always lucky to be surrounded with great friends all throughout my life. That's been the case over my doctoral studies too, I found some awesome like-minded friends, ready for the same crazy plans at the drop of a hat. Starting with South Africa, the thousands of kilometers of road trips all over Europe and game nights are stuff for life long memories. Thank you **Samay, Glen, Latha, Shraddha, Sailen, Eisha** and **Revathi** not only for the fun but being there with all the support. I would also like to acknowledge the **Jena Malayalees** for get-togethers. Apart from those in Jena, I would like to acknowledge all my Albany friends, among them especially **Siji** for the inspiration to apply here, **Lakshman, Sherin, Abhijit, Gayathri, The 253 Manning** and **Albany Boys** for being more than friends. Thank you **Sneha Kochak** for always being one phone call away and **KVA99** for everlasting friendship.

None of this work would have been possible without the strong foundation of my family. **Achan**, you have always encouraged and supported me to pursue my dreams. I owe it all to your inspiration; your confidence in my abilities gave me strength to make this thesis a reality. **Amma**, you are a reservoir of strength, your courage and prayers inspired me to keep the focus on the goal. I promise I'll be home soon.

Being far from home, I've been fortunate enough to have the company of my wife, **Thulasi**. Your honest and understanding demeanor have been the key drivers behind success of this thesis. Thanks for your encouragement and support. We are close to accomplishing our first goal and I look forward to our journey through life.

Finally, I would like to thank **Max Planck Society** for funding my doctoral studies and **Max Planck Institute for Chemical Ecology** for the amazing work place atmosphere.

4 Introduction

4.1 General Introduction

Terpenes are the most diverse class of natural products with some 55,000 known compounds, including monoterpenes (C_{10}), sesquiterpenes (C_{15}), and diterpenes (C_{20}) representing nearly 400 distinct structural families.¹⁻⁶ These ubiquitous natural products are present almost everywhere in nature and have been isolated from both terrestrial and marine plants, liverworts, and fungi.⁷⁻¹¹ Most of the terpenoids originate from plants, where these compounds are classified either as primary metabolites necessary for cellular function and development, or as secondary metabolites which are not involved in any growth or maintenance processes. For much of the last century terpenes were thought to be products of detoxification or overflow metabolism in plants.⁶ However, since the 1970s, many terpenes have been shown to have significant ecological roles in antagonistic or mutualistic interactions.¹² As primary metabolites they serve many biological functions such as hormones (steroids, gibberellins),¹³ structural components of membranes (phytosterols), as electron and proton scavenger in the respiratory chain (ubiquinones), as carotenoids in photosynthesis and as chromophores in the visual process (all-*trans* retinal) (Figure 1).¹²⁻¹⁷

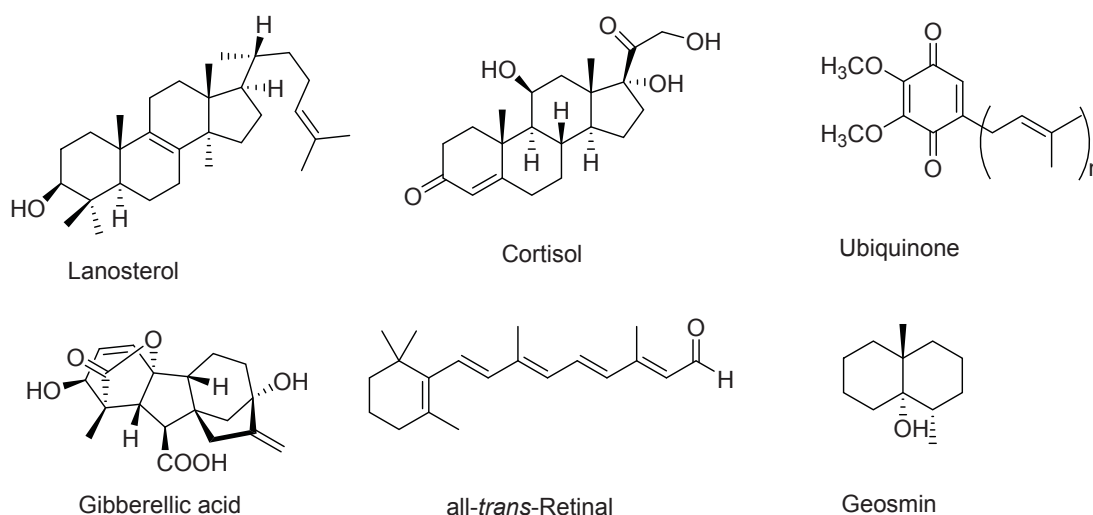


Figure 1: Examples of terpenes with established functions in nature. Very few terpenes have been investigated from a functional perspective; some of compounds with known biological relevance are shown above. Their functions range from hormones (steroids, gibberellins), structural components of membranes (phytosterols), as an electron and proton scavenger in the respiratory chain (ubiquinones) and as chromophores (all-*trans* retinal).

Majority of the terpenes are still considered to be secondary metabolites, which are used by plants in direct defense and protection mechanisms, such as high concentrations of terpenes in cotton leaves and in the xylem of conifers act as feeding deterrents, toxins or as a mechanical barrier.^{12,18,19} Apart from direct defense they are also involved in indirect defense against herbivores through recruitment of predators, for example emission of volatile organic compounds that may attract herbivore's enemies, such as predators or parasitoids.²⁰ Moreover, volatile terpenes serve as attractants for pollinators,¹⁴ feeding or oviposition deterrents to a large variety of insects¹⁵ as well as toxins¹². Furthermore, terpenes have always been

historically attractive for commercial purposes due to their applications in flavor, fragrance, agrochemical and pharmaceutical industry.^{21,22}

4.1.1 Discovery and Milestones

Historically terpenes have found various important applications in different cultures. Due to their ubiquitous presence in plant essential oils, their applications have been known since ancient Egyptian times. In Europe, camphor was introduced by the Arabs around the 11th century and the structure of camphor was established by Brecht in 1893.^{1,22} The structure of pinene was found by Wagner in 1894 and β -Carotene was isolated in 1837 by Wackenrodder from carrots, and its structure determined in 1907 by Willstätter.¹ In 1891 the characteristic odor of freshly plowed soil was first reported to be due to actinomycetes and identified by M.N. Gerber in 1965 as a degraded sesquiterpene alcohol, geosmin (meaning earth odor) (Figure 1).²³ Since 1945 there has been massive progress in terpene research due to the advent of chromatographic and spectrometric techniques. The discovery of the isoprene rule was initiated by Ruzicka.²⁴⁻²⁶ in 1953 and mevalonic acid as the biosynthetic precursor of cholesterol²⁷ in 1956 and later, its incorporation into a number of terpenoids were major milestones in scientific progress regarding terpenoids. More recently in 1996, Rohmer and coworkers showed that 1-deoxyxylulose-5-phosphate (DXP) as the first intermediate in DXP pathway.^{28,29} These ground breaking investigations have been awarded the Nobel Prize in physiology (Lynen and Bloch in 1964) and in chemistry (Cornforth in 1975). Thereafter, an increasing number of terpenoids have been shown to have important biological activities and associated applications.³⁰

4.1.2 Commercial Applications of Terpenes

Human societies have been quite adept at discovering applications of terpenes for commercial purposes.³¹ The diverse array of terpenoid structures and functions had provoked great interest in their commercial use since ancient times. Pharmaceutical and food industries have been the most effective in realizing the potential of terpenes as medicines and flavor enhancers (Figure 2). Perhaps the most widely known terpene is rubber (a polyterpene), which has been extensively used by humans.³² Other commercially important terpenes are limonene (cosmetics), carvone (aroma), hecogenin (detergent), and digitoxigenin (medicine). Agriculture has also shown increasing interest in terpenes with their antimicrobial activities, as a potential to replace antibiotics in livestock.¹⁶ They also act as natural insecticides and can be of use as protective substances in storing agriculture products.^{16,33}

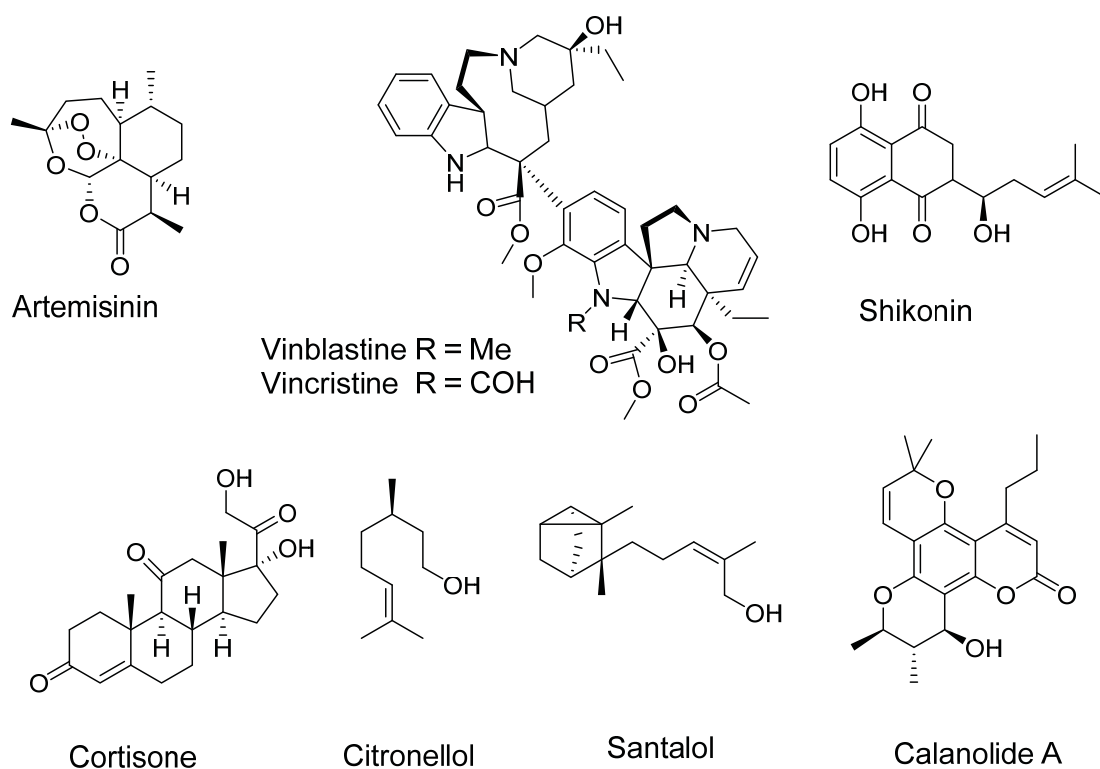


Figure 2: Representative examples of terpenoids of commercial significance. The diverse array of terpenoid structures and functions has found immense commercial applications. Terpenoids have been found to be useful in the prevention and therapy of several diseases (artemisinin against malaria, coumarins, including calanolide A from and shikonin against HIV and terpenoid indole alkaloids, vincristine and vinblastine from against cancer), and as flavor and fragrance ingredients (citronellol and santalol) and various agriculture applications.

Terpenes are precursors to many well-known essential compounds in the human body such as squalenes, coenzyme Q₁₀ and cholesterol. Polyisoprenoid alcohols called dolichols are necessary for the biosynthesis of biologically important glycoproteins. Sex hormones are one of the rapidly metabolized steroids in the human body all from a common precursor, cholesterol. The most notable ones are female sex hormones oestradiol and progesterone, whereas testosterone and androst-5-en-3 β -ol-17-one are male sex hormones. Synthetic oestrogens and progestins such as mestranol and norethindrone are the basis of the contraceptive pill; they act by disrupting the delicate balance of progesterone during the menstrual cycle. Cortisone (Figure 2) and 4-hydroxyandrostenedione are steroid hormones that have a broad spectrum of activity other than the sex hormones. Vitamin D leads the group of sterol compounds, necessary for the metabolism of calcium and phosphorus in humans.^{16,34,35}

Terpenoids have been found to be useful in the prevention and therapy of several diseases, including cancer, and also to have antimicrobial, antifungal, antiparasitic, antiviral, anti-allergenic, antispasmodic, anti-inflammatory, and immunomodulatory properties.^{33,36} A wide range of terpenoids (Figure 2) have demonstrated pharmaceutical activity against diseases, e.g. artemisinin from *Artemisia annua* against malaria, coumarins, including calanolide A from *Calophyllum lanigerum* and shikonin against HIV³⁷ and taxanes,

paclitaxel like compound from *Taxus* spp., and terpenoid indole alkaloids (TIAs), vincristine and vinblastine from *Catharanthus roseus* against cancer.³⁸⁻⁴⁰ The commercial importance of essential oils has been well established in flavor and fragrance industry. Today such oils and resins also form the basis of a wide range of taste and odor compounds such as menthol, oil of lavender (linalool), oil of lemongrass (citral), oil of sandalwood (santalols), oil of patchouli (patchouli alcohol), scent of roses (geraniol), and citronellol.^{32,41} In addition to their use in the fragrance and flavor industry, terpenes today are used for rubber production and as synthetic intermediates or as a solvent for paints and resins.^{8,42,43} There are diverse classes of terpenes waiting to be explored for potential commercial applications.

4.2 Terpene Diversity

The vast diversity of terpenoid structures is due to efficient mechanism of regioselective and stereospecific cyclization of the acyclic substrates like geranyl diphosphate (GDP, C₁₀), farnesyl diphosphate (FDP, C₁₅) and geranylgeranyl diphosphate (GGDP, C₂₀) catalyzed by enzymes known as terpene synthases.^{1,30,44,45} The resulting blends of terpenes have classically been identified as natural products and often referred to as secondary metabolites that do not seem to participate in essential cellular metabolism. Over the last century they were thought to be metabolic wastes, however this classification does not do justice to their ecological and natural significance. Recent advances in genetic and molecular studies have helped us decipher the natural and ecological roles of terpenes.^{46,47} This led to major advances in our knowledge about functions of these terpene mixtures within and among individual organisms.⁴

4.2.1 Ecological Significance: Defense with Mixtures

During the co-evolution of plants and insects, they have developed variety of biosynthetic mechanisms to deal with a wide range of enemies. One of the advantages of such diversity is that apart from concurrent defense against numerous predators, they also increase the probability of individuals in a population having unique compositions of terpenes for defense.⁶ Possession of such novel blends provides individuals better chance of survival in comparison with population⁴⁸ and other chemical mixtures have already been known to impede evolution of resistance in the adversary.⁴⁹

There is also significant advantage of terpene mixtures as defense tool as they can have more deterrence or toxicity value than similar amounts of a single component.^{45,50} Such synergistic capabilities are due to the ability of one component to increase defensive capabilities of others by inhibiting the detoxification in evolved adversaries.^{51,52} Alternatively, these mixtures with different physical properties also possess significant advantage of speed of movement over single compounds. This advantage may be in terms

of rapid movement to the site of attack or in terms of longer duration of persistence of defensive action by terpenes. One such example can be found in the defense of conifer resins against herbivory attack using both monoterpene olefins and diterpene acids (Figure 3). The more volatile monoterpenes act as a solvent enabling fast deployment of less volatile and feeding deterrent diterpenes from the resin ducts to the site of attack.⁵³ The evaporation of volatile monoterpenes is also reduced by the presence of less volatile diterpenes.⁵⁴

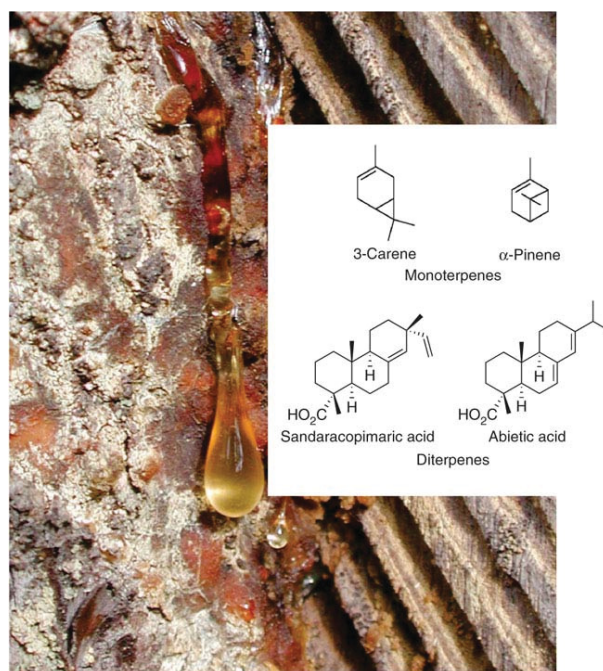


Figure 3: Plant Defense with Terpene Mixtures. The resin of conifers contains two classes of terpenes: monoterpene olefins and diterpene acids. On attack, the more volatile monoterpenes act as solvents enabling a rapid flow of the less volatile diterpene acids. The diterpene acids are toxins and feeding deterrents to herbivores, and they also polymerizing agents that seals the wound. Adapted with permission from Gershenzon *et al.*⁶

Apart from synergistic capabilities, there might also exist “contingency” effects of these complex blends. This term was originally coined for secondary metabolites from *Streptomyces* spp. that do not act synergistically but are produced independently by organisms to act on a single target in different ways. These contingency properties have also been shown for a group of sesquiterpenes from the plant *Landolphia dulcis* which have similar physical and chemical properties to breach the enemies’ biological barriers.⁵⁵

4.2.2 Communication using terpene diversity

For immobile organisms like plants, terpenes serve not only as important defense mechanism but also as signal for mutually beneficial interactions among species. Due to their low molecular weight and high vapor pressure, these blends of lipophilic monoterpenes and sesquiterpenes act as ideal long distance communication signal.⁶ The added advantage of chemodiversity is the communication with higher specificity and more information. It is a well-known fact that major components of herbivory-induced chemicals from foliage are terpenes.⁵⁶⁻⁵⁸ Interestingly, it is not only feeding but also much less invasive events such as egg-

laying that can induce emission of terpenoid mixtures that serve as signals for specific parasites. For example, in case of the pine sawfly (*Diprion pini*), when it lays its eggs on pine twigs, the terpene volatiles attract a wasp that parasitizes the sawfly eggs.¹⁵ Even though the major compound in the active mixture was found to be (*E*)- β -farnesene,⁵⁹ but devoid of other terpenoids in the blend the activity was absent.⁶⁰ Thus, terpene blends offer better cues that are more specific and informative in nature than single compounds.

Apart from beneficial interactions, sometimes these volatiles can also be picked up by insects or parasitic plants to locate their hosts. A blend of monoterpenes from nearby tomato plants are used by seedlings of the parasitic plant dodder (*Cuscuta pentagona*) as growth cues,⁶¹ whereas strigolactones are used by *Striga spp.* and *Orobancha spp.*, as germination stimulants for promoting mycorrhizal associations in the soil.⁶² A blend of volatiles rich in terpenes from lima bean leaves also serves to stimulate plant signaling and their release leads to indirect defense by attracting the enemy of herbivores.⁶³ There are also some examples of terpene blends acting as aerial cues by herbivore attacked neighbors to ramp up their own plant defense machinery in anticipation of attack.⁶⁴⁻⁶⁶ Overall, these examples demonstrate the importance of terpene blends in chemical communication between multitudes of ecological interactions.

4.3 Terpenoid Biosynthesis: the acyclic substrates

4.3.1 The initial C₅ precursors

The early interest in the biochemistry of terpene biosynthesis was largely driven by the desire to understand cholesterol formation. Terpene biosynthesis in nature can be divided into three phases. The vast diversity produced by isoprenoid biosynthetic pathways is essentially derived from two five carbon compounds, isopentenyl diphosphate (IDP) and its allylic isomer dimethylallyl diphosphate (DMADP). The formation of IDP and DMADP via the mevalonate (MVA) or methylerythritol (MEP) pathway marks the first stage.^{30,44}

For a long time, the classic mevalonate pathway (MVA pathway) was considered to be the sole source of all the C₅ precursors. Discovery of the MVA pathway was initiated in 1939 by Leopold Ruzicka who suggested isoprene unit as an universal building block for the biosynthesis of all terpenoids.²⁴ Later in 1950's the biosynthesis of IDP was elucidated mainly by Feodor Lynen, Konrad Bloch, John Cornforth and George Popjak.^{25,67-70} The MVA pathway (Figure 4) starts with two consecutive condensations of three acetyl-CoA molecules generates 3-hydroxy-3-methylglutaryl-CoA (HMG-CoA), which is further converted to mevalonic acid in a NADPH dependent process. Mevalonic acid is then further converted to 5-pyrophosphomevalonate

via consecutive ATP dependent phosphorylation. Then further fragmentation reaction leads to the formation of IDP and associated inorganic phosphate and CO_2 .⁷¹

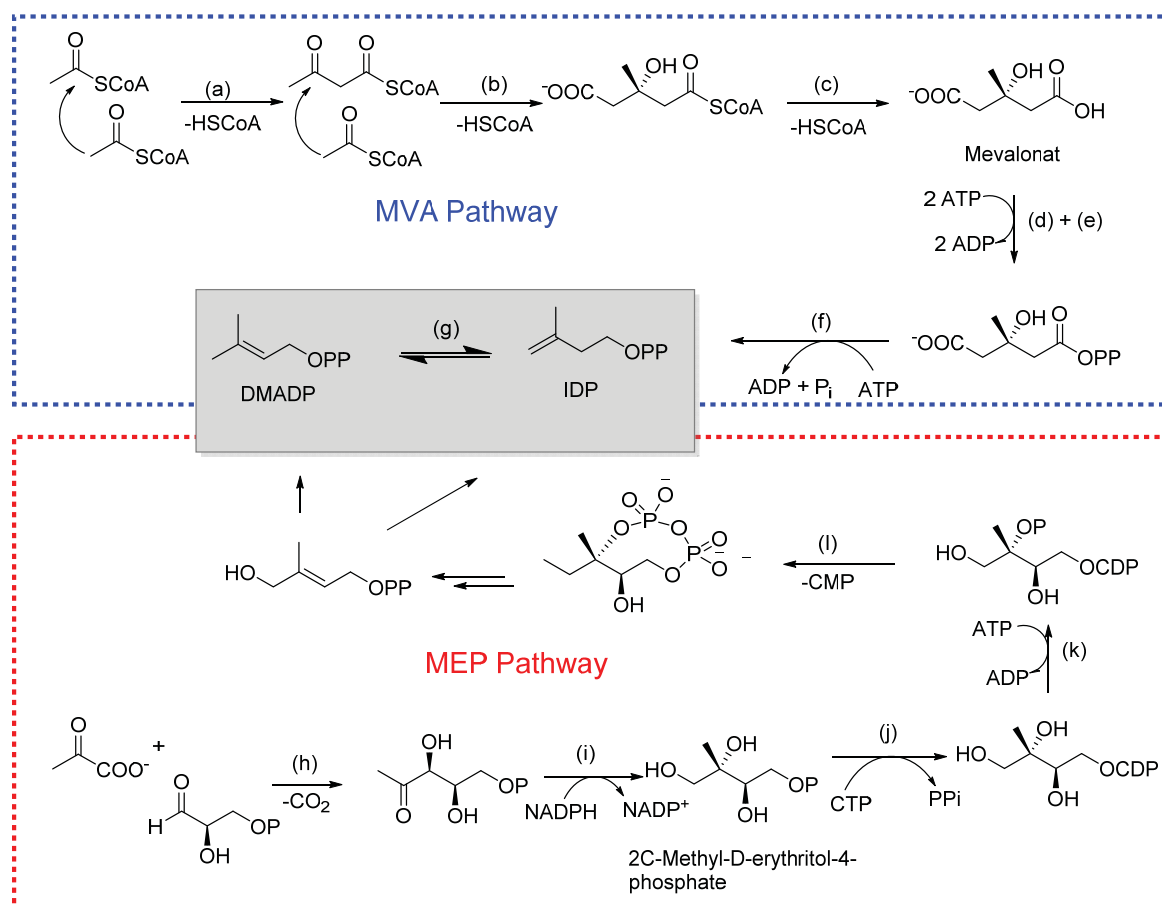


Figure 4: Biosynthesis of the active isoprene units IDP and DMADP via MVA (blue) and MEP pathway (red). Enzymes involved: a) acetoacetyl-CoA-thiolase (b) 3-hydroxy-3-methylglutaryl-CoA-synthase (c) HMG-CoA-reductase (d) mevalonate kinase (e) phosphomevalonate kinase (f) phosphomevalonate decarboxylase (g) isopentenylpyrophosphate-2,3-isomerase (h) 1-deoxy-D-xylulose-5-phosphate-synthase (i) 1-deoxy-D-xylulose-5-phosphate-reductoisomerase (j) diphosphocytidyl-2C-methyl-D-erythritol-synthase (k) diphosphocytidyl-2-Cmethyl-D-erythritol kinase (l) 2C-methyl-D-erythritol-2,4-cyclodiphosphate synthase (m) 1-hydroxy-2-methylbutenyl-4-diphosphate-reductase.

In 1996, some inexplicable results of feeding experiments and inhibitor studies led to the discovery of the alternative methylerythritol pathway (MEP pathway) by Rohmer and co-workers.²⁸ Interestingly, only the MVA pathway is present in animals, fungi, yeast and archaeobacteria as a source of C_5 precursors. However, various algae, plants and bacteria are known to utilize both biosynthetic pathways.^{72,73} In contrast to the mevalonate pathway, the MEP pathway produces both IDP and DMADP starting from glyceraldehyde-3-phosphate and pyruvate to form 1-deoxy-D-xylulose-5-phosphate (DXP). Formation of 2C-methyl-D-erythritol 4-phosphate (MEP) via a NADPH dependent reaction from DXP is followed by enzymatic conversion to a cyclic diphosphate. The cyclic diphosphate is then transformed into 1-hydroxy-2-methyl-2-buten-4-yl diphosphate (HDMADP). Unlike the MVA pathway which leads only to the formation of IDP, in case of MEP pathway, both IDP and DMADP are produced in the final step.⁸

4.3.2 Biosynthesis of acyclic precursors of the terpene family

In the second phase, the two isomeric C₅ diphosphates form longer substrates via head-to-tail linkages by prenyl transferases.^{74,75} In the first step, the cleavage of the diphosphate anions of DMADP takes place to afford an allyl cation (head), which undergoes electrophilic addition to the double bond (tail) of IDP (Figure 5). Further elimination of a proton yields (2*E*)-geranyl diphosphate (GDP), the direct precursor of the monoterpenes (C₁₀). Chain elongation by additional incorporation of IDP in an analogous reaction sequences provides (2*E*,6*E*)-farnesyl diphosphate (FDP), the precursor of the sesquiterpenes (C₁₅), and (2*E*,6*E*,10*E*) geranylgeranyl diphosphate (GGDP), the starting compound for the diterpenes (C₂₀). Attaching more IDP units leads to macromolecular polyisoprenes of different chain lengths (e.g. rubber).

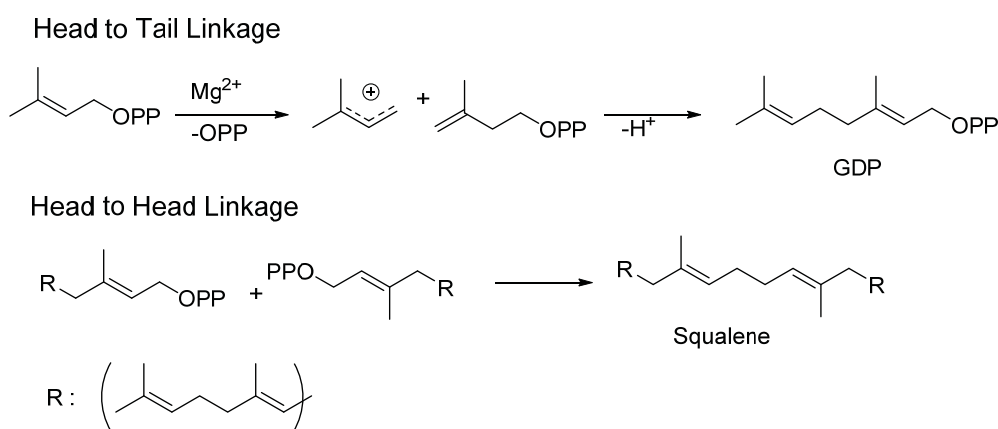


Figure 5: Biosynthesis of GDP (top) and squalene (below). The cleavage of the diphosphate anions of DMADP yields an allyl cation (head), which undergoes electrophilic linkage of IDP (tail) to generate geranyl diphosphate (GDP). This head to tail linkage is also the process behind chain elongation that leads to FDP, GGDP and other substrates. Another possibility is the head to head linkage which by dimerization of two units of FDP leads to triterpene squalene.

In an optional third phase, diversification proceeds by the polymerization of IPP units by prenyl transferases. Three acyclic precursors undergo various reactions like head-to-head dimerization of FDP or GGDP to yield triterpene squalene (C₃₀, Figure 6) and the tetraterpene phytoene (C₄₀) respectively. FDP or GGDP undergo additional polymerization reaction with additional isoprene units (C₅₀₊ for dolichols and rubber) or cyclization into complex structures. Prenyl side chains can additionally be linked by to proteins, quinones or other biomolecules by alkylation.⁷⁶ Furthermore GDP, FDP and GGDP act as substrates for reactions in the metal-mediated intramolecular cyclization that generates diversity of compounds with complex ring systems (Figure 6). In plants and microbes, these ring systems are often referred to as the terpene hydrocarbons and oxygenated terpenoids.

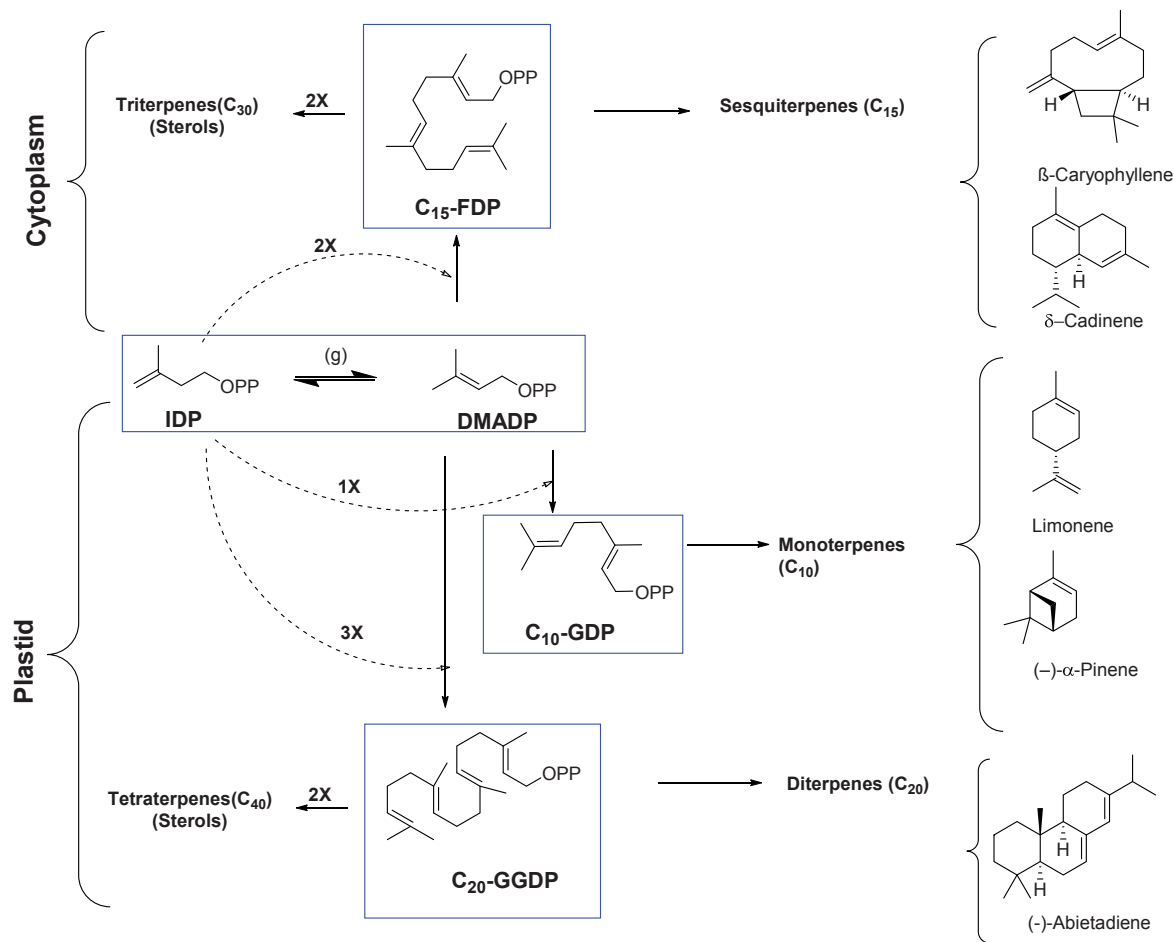


Figure 6: Biosynthetic pathway behind the terpenoid diversity. IDP and DMADP are the basic substrates behind all the terpenoid diversity. The chain elongation leads to geranyl diphosphate (GDP), the direct precursor of the monoterpenes (C₁₀). Further, chain elongation by incorporation of IDP provides farnesyl diphosphate (FDP), the precursor of the sesquiterpenes (C₁₅), and geranylgeranyl diphosphate (GGDP), the substrate for the diterpenes (C₂₀). Furthermore GDP, FDP and GGDP act as substrates for reactions in the metal-mediated intramolecular cyclization that generates diversity of compounds with complex ring systems.

4.4 Regulation of Terpene Biosynthesis

4.4.1 Subcellular localization of terpene biosynthesis in plants

The IDP and DMADP biosynthesis pathways are localized in different cellular compartments in plants.⁷⁷⁻⁷⁹ The MEP pathway is located in the plastids and it supplies the biosynthetic precursors for isoprene, the mono (C₁₀)- and diterpenes (C₂₀), carotenoids (C₄₀), chlorophyll (C₂₀) and tocopherols. The MVA pathway is the characteristic of cytosol, where it is involved in the formation of sesqui (C₁₅) - and triterpenes (C₃₀) and phytosterols (Figure. 7). Although the localization in different compartments allows the two pathways to act independent of each other, certain exchange of precursors (metabolic crosstalk) has been observed, mostly from plastids towards the cytosol.⁸⁰⁻⁸³ The scope and direction of the exchange depends on the species and plays an important role in the regulation of terpene metabolism.^{47,84} This localization of initial precursors and further prenyl diphosphates and leads to the partitioning of corresponding terpene families

between plastids (GDP and GGDP, mono- and diterpenes) and cytosol (FDP, sesquiterpenes) (Figure. 7). However, the separation of the GDP and FDP pool is not strictly observed in all plants.^{84,85}

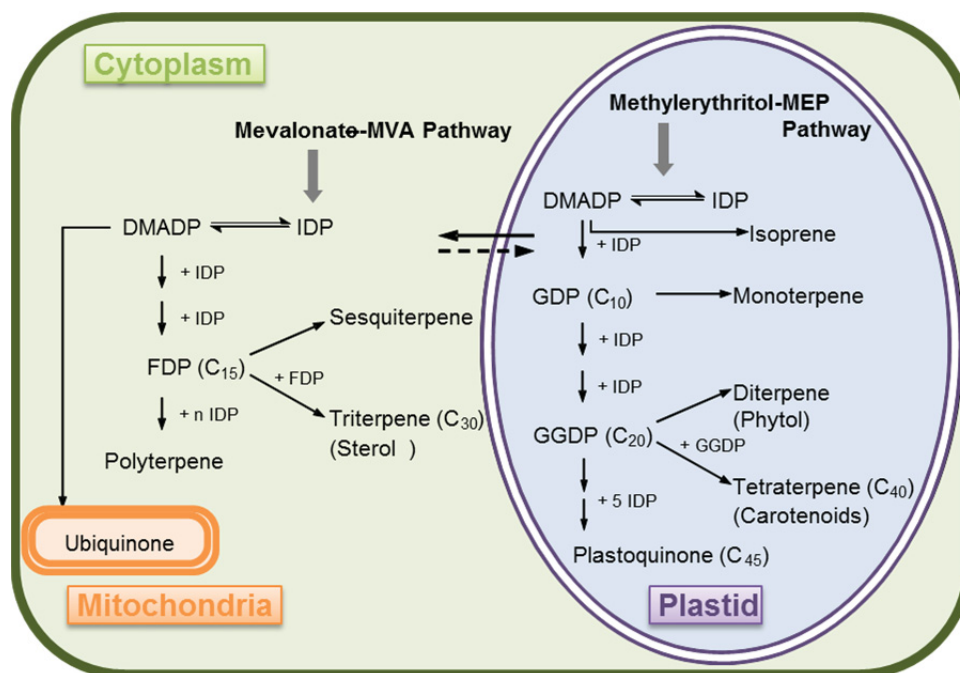


Figure 7: Compartmentalization of terpene biosynthesis. The two IDP and DMADP biosynthesis pathways are localized in different cellular compartments in plants. The MEP pathway is located in the plastids and it supplies the mono (C₁₀)- and diterpenes (C₂₀), carotenoids (C₄₀). The MVA pathway is located in cytosol, where it is involved in the formation of sesquiterpenes (C₁₅) and triterpenes (C₃₀) and phytosterols.

4.4.2 Regulation of terpene biosynthesis in Plants

Interestingly, terpenes are accumulated in plants in specific tissues or cell types, and moreover the biosynthesis of these compounds seems to be highly regulated. The accumulation of terpenes is tightly controlled by regulating the corresponding biosynthetic enzymes. The transcriptional control of corresponding genes has been shown to mediate the induction of sesquiterpenes biosynthesis in tobacco.^{86,87} The same acetyl-CoA units generated during the mevalonate pathway are utilized for both biosynthesis of sterols and primary isoprenoids as well as pathogen induced biosynthesis of antimicrobial sesquiterpenes.⁸⁸ Pathogen challenged cells suppress sterol biosynthesis and divert the carbon flow (~20%) into the new biosynthetic pathway of antimicrobial terpenes by upregulation of defense response induced branch pathways.⁸⁹ Otherwise, these compounds are produced and accumulated in specific cells and tissues, best examples being the pathogen-induced sesquiterpene accumulation in solanaceous plants (Figure 8).⁹⁰⁻⁹² The accumulation in specific compartments has been studied in case of insecticidal terpenes in glandular ducts of cotton,⁹³ resins^{94,95} and trichomes⁹⁶⁻⁹⁹. Thus it can be inferred that terpene biosynthesis in plants is both spatially and temporally regulated.

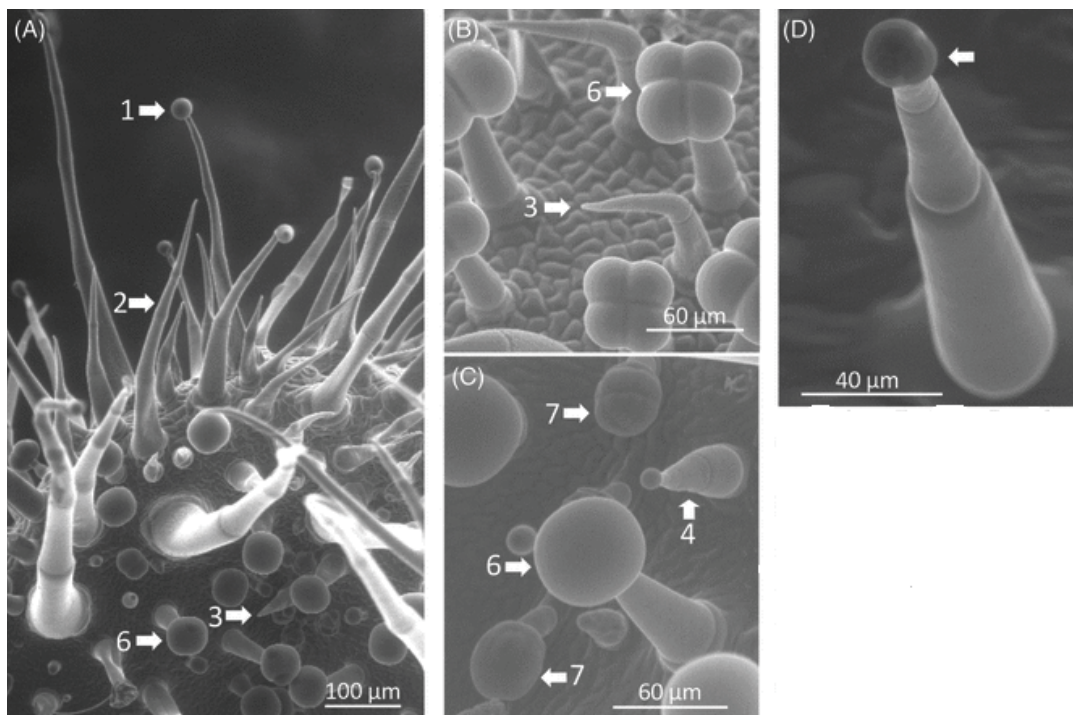


Figure 8: Sesquiterpene accumulation in solanaceous plants. (A) Scanning electron microscopy (SEM) image of a young wild tomato leaf (*Solanum habrochaites*). At least five trichome types can be observed: Type 1, tall glandular trichomes with a single secretory cell; Type 2, tall non-glandular trichomes; Type 3, short hooked non-glandular trichome; Type 6, glandular trichomes with four head cells; Type 7, short glandular trichomes. (B) Detail of a tomato leaf (*Solanum lycopersicum*) showing Type 6 and Type 3 trichomes. (C) Detail of a wild tomato leaf (*S. habrochaites*) showing Type 4, Type 6 and Type 7 trichomes. (D) Capitata trichome of *Nicotiana sylvestris*, similar to Type 4 trichomes of tomato. A droplet of diterpenoid-rich exudate can be seen on the side of the glandular head (white arrow). Adapted with permission from Tissier *et al.*⁹⁹

4.5 Terpene Synthases

4.5.1 Enzymology

The biosynthesis of vast diversity of terpenes with complex ring systems from the corresponding acyclic prenyl diphosphates is catalyzed by promiscuous enzymes known as terpene synthases. Sometimes, they are also called terpene cyclases when they catalyze primarily cyclization reaction.¹ Progress in understanding terpenoid diversity has predominantly been focused on the development of comprehensive enzymatic models for terpene synthase catalysis.¹⁰⁰⁻¹⁰⁵ Interestingly, all the terpene synthases that were cloned in the form of cDNA¹⁰⁶ or isolated directly from plants¹⁰⁷ were found to have similar biochemical properties. The encoding cDNAs for these enzymes exhibit chain length of 550 to 850 amino acids,¹⁰⁸ optimum pH in a range of 6.0 - 7.5,¹⁰⁹ and require divalent metal cations such as Mg^{2+} or Mn^{2+} ions as co-factors. However monoterpene synthases from gymnosperms are additionally dependent on a monovalent cation, usually K^+ and shows preference for Mn^{2+} and Fe^{2+} ions in contrast to Mg^{2+} ions.¹⁰⁸

Overall, the enzymes exhibit remarkable control of multiple stereochemical transformations along complicated reaction pathways. Cycloartenol synthase is a perfect example of the enzymatic control, it uses

the triterpenoid oxidosqualene as a substrate and forms the first multicyclic intermediate in the biosynthesis of plant sterols.¹¹⁰ In the cyclization process, eleven bonds are broken and the same number made with nine chiral centers. The control of the cyclase can be appreciated by the fact that it yields only 1 of approximately 500 possible stereoisomers (2^9).¹⁰⁰

The emphasis in terpenoid biochemistry has moved towards using molecular tools to decipher the structural characteristics of terpene synthases and correlating it with their corresponding reaction mechanism. Advances in cloning, expression and X-ray crystallography led to major advances towards connecting their primary amino acid sequence, resultant tertiary structure, and active site chemistry. This led to significant progress in understanding of monoterpene,¹⁰³ sesquiterpene¹⁰¹ and triterpene¹⁰⁰ synthase activity. Ten terpene synthases from plants, bacteria, and fungi have been successfully crystallized and their structures confirmed by X-ray crystallography.¹¹¹⁻¹²⁰ Terpene synthases can be classified into two major categories based on their functionality, Type I synthases are enzymes that initiate catalysis with the ionization of the allylic diphosphate substrate, whereas Type II enzymes starts by proton addition to the substrate. Another interesting fact is that Type I synthases consists of monoterpene, sesquiterpene and diterpene synthases, Type II synthases includes diterpene and triterpene synthases. Furthermore, interestingly terpene synthases share greater sequence similarity to those from the same species than to mechanistically related enzymes from other species.¹²¹ For example, monoterpene synthases from *Abies grandis* (Grand fir) exhibit a sequence similarity of 70-95% at the amino acid level but catalyze completely different reactions, while enzymes from other plant species like conifers, which have an amino acid similarity less than 30% may form the same products.¹²² For this reason, it is not possible to predict the catalytic function of a terpene cyclase based on their primary structure.

This thesis will focus on the enzymology of the Type I terpene synthases and mainly centered on the multiproduct terpene synthases TPS4 and TPS5 from *Zea mays* (maize) and MtTPS5 form *Medicago truncatula*. Both of them form multiple products by cyclization of FDP (C_{15}) and also accepts GDP (C_{10}) as substrate.

4.5.2 Multiproduct Terpene Synthases

Terpene synthases convert the acyclic prenyl diphosphates into a variety of cyclic and acyclic terpenoids. All sesquiterpenes known to date are derived from 300 basic hydrocarbon skeletons formed by sesquiterpene synthases from a single precursor FDP. The major factor behind terpene diversity is the large number of different terpene synthases and the fact that some of these enzymes produce multiple products.

This property was first noticed in terpene synthases of plants when it was realized that the production of multiple products in consistent proportions was retained even when the protein was expressed *in vitro*.¹⁰⁶ The variety of products that are generated by a single enzyme can also vary extremely. Apart from highly specific enzymes such as the aristolochene synthase from *Aspergillus terreus*, δ -selinene synthase and γ -humulene synthase from *Abies grandis* hold the current record producing 52 and 34 different sesquiterpenes, respectively.¹²²⁻¹²⁵ In addition to the main product, nearly half of all characterized monoterpene and sesquiterpene synthases form significant amounts of additional products (defined as at least 10% of the total) and are consequently classified as multiproduct synthases.^{106,126} It is believed that the ability to form a large number of products from one substrate is mainly due to the unusual electrophilic reaction mechanism of these enzymes.¹⁰⁶ At the same time, this reflects the tendency of nature, to form an evolving mechanism where a maximum number of products are formed by using least number of biosynthetic steps.^{2,111,127} But unfortunately, there is a lack of clear understanding about the structural characteristics leading to this flexibility, as so far none of the multiproduct synthases have been successfully crystallized.¹²⁸ The closest candidate to have confirmed crystal structure is the sesquiterpene cyclase *epi*-isozizaene synthase (EIZS) from *Streptomyces coelicolor*, but it is not a multiproduct synthase in its true sense as its product profile in addition to 79% *epi*-isozizaene has only five minor sesquiterpenes.¹²⁹⁻¹³¹

4.5.3 Reaction Mechanism of Multiproduct Synthases

4.5.3.1 Metal ion binding and diphosphate cleavage

The reaction cascade of a sesquiterpene synthases is initiated by the metal-mediated cleavage of the diphosphate of (2*E*,6*E*)-farnesyl diphosphate. All terpene synthases require a divalent cation for optimal activity *in vitro*. Insights into the mechanistic roles for the metal ions have been obtained from the crystallographic studies of 5-*epi*-aristolochene synthase (TEAS),¹¹² pentalenene synthase,¹¹¹ bornyl diphosphate synthase¹¹⁹ trichodiene synthase¹¹⁷ and more recently, sesquiterpene cyclase *epi*-isozizaene synthase (EIZS) from *Streptomyces coelicolor*. Sesquiterpene synthases have been reported to prefer Mg²⁺ *in vitro*, but they also accept Mn²⁺ at low concentrations.¹³²⁻¹³⁵ In general, monoterpene synthases seem to be less selective in their divalent cation requirements.¹⁰³ Interestingly, examination of the metal requirement of avian prenyltransferase,¹³⁶ supported the presence of two divalent metal ions in binding of the highly charged diphosphate group, leading to the formation of a substrate complex with the enzyme. At least a single DDxxD motif appears in nearly all Type I terpene synthases and these aspartates residues direct the substrate binding via the coordination of magnesium ions by forming salt bridges with the diphosphate group. This

binding mechanism has been confirmed by X-ray crystallography studies of trichodiene synthase,¹¹⁷ bornyl diphosphate synthase¹¹⁹ and farnesyl diphosphate synthase¹¹³. Additionally, based on various studies the metal cations have been suggested to neutralize the development of negative charge on the diphosphate, preventing the regeneration of the substrate.^{104,137-141} After initial substrate binding, the biosynthetic cascade is further divided into partial reactions and they follow logically into separate catalytic events.

4.5.3.2 Cationic reaction cascades in the active site

The cleavage of the diphosphate anion from the substrate leads to the formation of a highly reactive transoid farnesyl carbocation, after isomerization further down the cascade it undergoes various cyclizations and rearrangements, such as methyl or hydride shifts. Due to its constrained geometry, the electrophilic transoid farnesyl cation can only attack the distant C10-C11 double bond, whereby either the (2*E*,6*E*)-germacrene-11-yl cation or (2*E*,6*E*)-humul-10-yl cation are formed (Figure. 9).

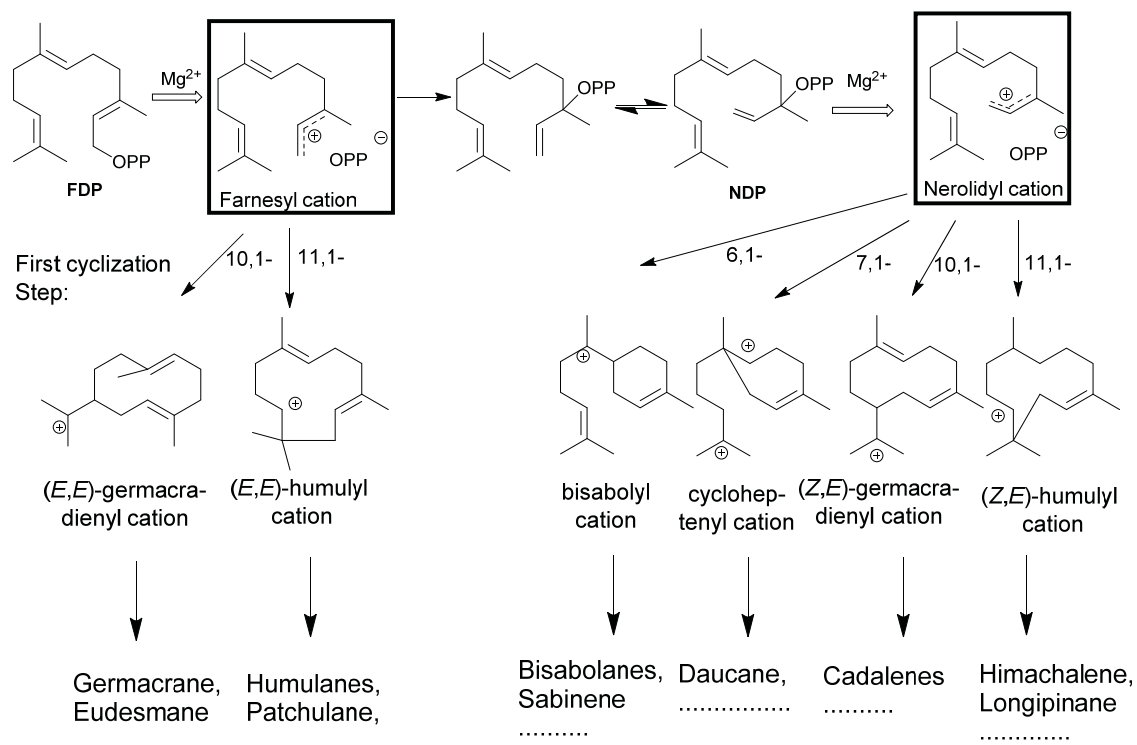


Figure 9: Possible cyclizations of (2*E*,6*E*)- or (2*Z*,6*E*)-farnesyl cations and some resulting carbon skeletons of sesquiterpenes. The loss of the diphosphate anion leads to the formation of a highly reactive transoid farnesyl cation, which after isomerization undergoes various cyclizations and rearrangements, such as methyl or hydride shifts. Due to its constrained geometry, the electrophilic transoid farnesyl cation can only attack on the distant C10-C11 double bond. However after rotation around C2-C3 double bond to (2*Z*,6*E*)-farnesyl cations, the geometrically suitable conformation leads to majority of cyclized products.

Some terpene synthases overcome this geometrical constraint by conversion to cisoid farnesyl cation and subdue the energy barrier of 12 kcalmol⁻¹^{103,142} by rotation around C2-C3 double bond and by the release and migration of diphosphate anion.^{103,105,143} The accepted mechanism leads to the generation of the tertiary allylic nerolidyl diphosphate intermediate by the recapture of diphosphate at the C3 position. A rotation

around the newly formed C2-C3 sigma bond and the subsequent dephosphorylation ultimately leads to the conformational desired (2Z,6E)-farnesyl cation (Figure. 9).¹⁴⁴ This mechanism is analogous to the upstream isomerization of (2E)-GDP to (2Z)-neryl cation via the intermediate linalyl diphosphate.¹⁰⁵ Majority of the cyclic monoterpenes are formed from the geometrically favorable cisoid cation, based on the electrophilic attack on distant bonds, which leads to the medium-sized C6-, C7-, C10- or C11 rings. In the case of sesquiterpenes, the bisabolyl cation, cycloheptenyl cation, (2Z,6E)-germacrene-11yl cation and (2Z, 6E)-10-humulyl cation lead to the corresponding bisabolane, daucane, cadalane and himachalane products.

In this thesis, the focus is on two sets of multiproduct synthases, TPS4 and TPS5 from *Zea mays*^{145,146} and MtTPS5 from *Medicago truncatula*.¹⁴⁷⁻¹⁴⁹ Garms. *et al.*,¹⁴⁹ had postulated the mechanistic pathway involved in the formation of 27 products from MtTPS5 using deuterium-labelled substrates. They were also able to determine the absolute configuration of individual products and further establish the initial conformation of the substrate and the stereochemical course of the reaction cascade.

The final hydrophilic products are released from the hydrophobic pocket either by elimination of a proton (sesquiterpene hydrocarbons) or by reaction with a water molecule (sesquiterpene alcohols). Pre-steady state kinetic studies of several sesquiterpene synthases has shown that slow release of the product is the rate limiting step after rapid accumulation of terpenoids in active site.^{150,151}

4.6 Discovering Catalytic Promiscuity

In many cases, enzymes can already catalyze more than one reaction. It is generally believed that enzymes with promiscuous functions evolved over time to acquire better specificity and activity. This is dependent on the plasticity of the protein to alter the product profile by minor amino acid mutations. The challenge is to use mechanistic reasoning to discover these new reactions. Thus enzyme promiscuity is considered an important tool towards understanding enzyme evolution and engineering them as better catalysts.^{152,153} Terpene synthases, especially sesquiterpene synthases are well known for their catalytic promiscuity. Multiproduct terpene synthases are ideal examples to study the promiscuity of these enzymes. The champion for this behavior is, δ -selinene synthase from *Abies grandis*, producing 52 different sesquiterpenes, from single substrate FDP. Yoshikuni *et al.*, were successfully able to control this reaction pathway of δ -selinene synthase, and by selective mutations of plasticity residues and were able to improve the product selectivity for these complex reaction cascade.¹⁵⁴

4.6.1 Site directed mutagenesis studies

The high fidelity of the multiproduct terpene synthases suggests that these enzymes must generate a specific sequence of reaction coordinates in the active site for the correct execution of the reaction cascade. In absence of crystal structure of multiproduct enzymes, inference can be drawn from aromatic residues lining the active site of 5-*epi*-aristolochene synthase from tobacco (TEAS) and pentalanene synthase. Chemical models based on these known structures suggest that the carbocation intermediates are directed through cation- π interactions^{155,156} involving phenylalanine, tryptophan and tyrosine residues. The crystal structure of the TEAS contains a catalytic triad of aspartate 444, tyrosine 520, and aspartate 525 which delivers a proton to the neutral intermediate germacrene A.^{112,157} A comparison of the sequence of MtTPS5 with TEAS and site-directed mutagenesis revealed the importance of tyrosine 526 in an equivalent position.¹⁴⁹ On exchange of Tyr520 with phenylalanine has dramatic effect on the product profile of TEAS, which changed to germacrene A as its sole product, and in case of MtTPS5, also generated almost exclusively germacrenes.^{149,157} In case of MtTPS5, this suggested an alternative route to the general accepted pathway to sesquiterpenes with a cadalane skeleton.¹⁴⁹ These studies showed the importance of proton transfer reactions in terpene biosynthesis and demonstrate how the alteration of only a single amino acid can have a dramatic effect on reshaping the active site. These highly versatile enzymes give the plants the opportunity to adapt very quickly to environmental stress and other changes. In a nutshell, deciphering the key amino acids that control the carbon flux in distinct cascades can be used to tailor enzymes for by simple mutations. The previous work on δ -selinene synthase and the work in our group on MtTPS5 demonstrate the feasibility of exploiting the underlying evolvability of active site, and provide useful approaches for novel enzyme design.

4.6.2 Terpene synthases can accept multiple substrates

Sesquiterpene synthase also display proclivity towards accepting different substrates, they not only accept FDP (C₁₅) but also shorter GDP (C₁₀) to generate a multiproduct profile. This promiscuity is an important cornerstone in rapid functional divergence of terpene synthases. Their broad substrate specificity gives them the liberty to utilize the available substrates in the system to generate different volatiles. Thus, substrate availability is an important factor that determines the type and quantity of terpenoids synthesized.

However, historically determining the correct substrate has been a major challenge for scientists working with terpene synthase enzymes.¹⁵⁸ This has evidently been shown in monoterpene synthases with the discovery by Schilmiller *et al.*, reporting the discovery of a new substrate for enzymes of plant monoterpene biosynthesis.¹⁵⁹ Monoterpene synthases have been found to be promiscuous *in vitro*,

employing geranyl diphosphate (GDP), as well as its (2*Z*)-isomer neryl diphosphate (NDP), and a tertiary isomer linalyl diphosphate as its substrate. From *in vitro* studies, early researchers had concluded that for monoterpene synthases that NDP was the general substrate instead of now recognized GDP.¹⁵⁸ This was also the predictable conclusion because with GDP, the enzyme would first have to isomerize the C2-C3 double bond before cyclization.^{160,161} In late 1970s, Rodney Croteau and his coworkers in their landmark work on monoterpene synthases demonstrated that for many plant monoterpene synthases, GDP was probably the native substrate. They were also able to show conclusively that these enzymes could carry out the double bond isomerization. Moreover, kinetic studies showed that GDP was much more efficient than its stereoisomer NDP.^{103,162} However recently, Schillmiller *et al.*, have shown convincing evidence that NDP is indeed the native substrate for NDP synthase from tomato (*Solanum lycopersicum*).¹⁵⁹ Similar promiscuous behavior was also suggested in case of sesquiterpene synthases, Cop4 and Cop6 from *Coprinus cinereus* that showed formation of different β -bisabolene carbocation depending on the substrate geometry.¹⁶³

In this thesis, mechanistic studies with purified multiproduct synthase MtTPS5 from *Medicago truncatula* and TPS4 and TPS5 from *Zea mays* were performed to investigate the different promiscuous behaviors of these three enzymes. In addition to using isotope labelled substrates to study and confirm the branching of sesquiterpene and monoterpene carbocationic intermediates. In addition, the effects of *cis-trans* isomers of FDP and GDP as a surrogate for secondary *cisoid* neryl cation intermediate generated by terpene synthases that can isomerize the π bond of all-*trans*-FDP have also been investigated. Moreover, in order to decipher the structural basis of the terpenoid chemodiversity in light of the lack of crystal structures of multiproduct synthases, the development of a structural mimic as inhibitor and possible co-crystallization candidate has also been reported.

5 Aim of the thesis

Terpene diversity can be explored further by using the catalytic promiscuity of multiproduct terpene synthases in combination with alternate substrates. A major goal of this thesis is to better define the multiproduct terpene synthase by using artificial substrates as metabolic molecular probes. The aim was to utilize the substrate promiscuity of the multiproduct terpene synthases MtTPS5 from *Medicago truncatula*¹⁴⁹ and TPS4 and TPS5 from *Zea Mays*¹⁴⁵ to study how alternate substrates might influence their catalytic activity. These labelled and (2Z)-configured substrates were used as metabolic probes to characterize the catalytic reaction cascade. This will also help evaluate the interaction with putative substrate recognition regions of the enzyme that contributes to the observed regio- and stereoselectivity.^{164,165} Another major intention was to find out whether the turnover with substrate stereoisomers¹⁶⁶ affects the catalytic turnover and the product profile. This will help dissect the mechanistic features of terpene synthases that catalyse the enigmatic isomerization reaction. Considering rapid advances in enzyme engineering over the last decade as a source of novel biosynthetic processes, the focus of this thesis was to explore the potential of using substrate analogs as biosynthetic tools. Ultimately, the objective was to further optimize and enhance existing catalytic capabilities or adding new catalytic functions to the existing enzymes.

Manuscript 1: Isotope sensitive branching and kinetic isotope effects to analyse multiproduct terpenoid synthases from *Zea mays*.

Isotope sensitive branching experiments constitute a valuable tool with respect to multiproduct enzymes, because they describe the effects of isotopic substitution in the substrate. The resulting kinetic isotope effect leads to rate enhancement in the formation of one product at the expense of a second product; this trade-off indicates that the two products arise from a common intermediate. Isotopically sensitive branching was investigated in case of the multiproduct terpene synthases TPS4-B73 and TPS5-Delprim from *Zea mays* that catalyze the formation of mono and sesquiterpene volatiles. This gives us the opportunity to examine the mechanistic details of multiproduct terpene synthases and to determine whether the final deprotonation of cationic intermediates en-route to mono- and sesquiterpenes is rate-limiting. Furthermore, deuterium kinetic isotope effects and product composition were also investigated for TPS4 and TPS5 enzymes.

Manuscript 2: Substrate geometry controls the cyclization cascade in multiproduct terpene synthases from *Zea mays*.

Two closely related multiproduct terpene synthase genes encoding enzymes, namely TPS4 and TPS5 accept GDP and FDP as substrates and convert them into two types of cyclic products with cyclohexenyl- or

bicyclo[3.1.0]hexyl moieties as common structural features. To reveal further details of the enzyme mechanism, we synthesized deuterium labelled substrate analogs for both geometric isomers of the critical C(2)–C(3) bond as the probe for isotope sensitive branching. These were used to evaluate the rate limiting effects of the initial isomerization step and to study whether the cyclization of (2Z)-GDP and (2Z,6E) FDP would proceed via the same cascade as observed with their corresponding natural substrates.

Manuscript 3: Inhibition of a multiproduct terpene synthase from *Medicago truncatula* by 3-bromoprenyl diphosphates.

The multiproduct sesquiterpene synthase MtTPS5 from *Medicago truncatula* catalyzes the conversion of farnesyl diphosphate (FDP) into a complex mixture of 27 sesquiterpenoids. There is a lack of definitive understanding about the structure of multiproduct terpene synthases due to the absence of any crystal structures. 3-Bromo substrate analogs of geranyl diphosphate and farnesyl diphosphate were synthesized because of their geometrical similarity and evaluated as substrates for MtTPS5. These substrates have additional advantage that the highly electronegative bromine atom can strongly influence the stability of the neighbouring carbocationic species but imposes no additional steric effect in comparison with the natural substrates. These analogs could either provide novel sesquiterpenes to investigate mechanistic aspects of the MtTPS5, or they could act as potent inhibitors of the enzyme. In case of inhibition it can be used to provide an active site resolved crystal structure and act as co-crystallization candidate like in the case of aristolochene synthase with farnesyl-thiolodiphosphate.¹⁶⁷

Manuscript 4: Novel biosynthetic products from multiproduct terpene synthase from *Medicago truncatula* using non-natural isomers of prenyl diphosphates

Terpene product diversity has been altered successfully in a few cases, but for the most part mutagenesis has resulted in either abbreviation or slight extension of a native reaction pathway.^{109,124,157,168-171} Redirection of enzymatic chemistry or the introduction of new catalytic activities has been elusive. Multiproduct terpene synthases with their remarkable flexibility provides an ideal active site scaffold to test the geometric isomers as substrates for new cyclization reactions. The multiproduct sesquiterpene synthase MtTPS5 from *Medicago truncatula* catalyzes the conversion of farnesyl diphosphate (FDP) into a complex mixture of 27 sesquiterpenoids. The aim was to test how the geometric conformation of the substrate determines the first cyclization event and also to characterize the resulting cyclization products of (2Z,6E)-FDP. This could either

lead to similar product profile as the natural substrate (*2E,6E*)-FDP or lead to novel products by alternate ring closure from a highly reactive nerolidyl carbocation.

This thesis is aimed towards gaining a better understanding of the highly promiscuous multiproduct terpene synthases which can act as a model system for designing better future catalysts. The alternate substrates would not only serve as metabolic probes for complex mechanistic pathways but also explore them as tools for new biosynthetic products. In order to understand the structural basis of these high fidelity enzymes, easy to synthesize inhibitors can be used as co-crystallization candidates, this could improve the chances of obtaining the crystals for X-ray studies.¹⁷² In conclusion, the scientific research described in this thesis is aimed at using artificial substrates towards characterizing the structural and mechanistic features that lead to catalytic promiscuity of multiproduct terpene synthases, and use them as a catalytic tool to achieve biosynthesis of desired terpenoid structures.

6 Manuscripts

6.1 Manuscript I: Isotope sensitive branching and kinetic isotope effects to analyse multiproduct terpenoid syntheses from *Zea mays*

Dr. Nathalie Gatto,¹ Abith Vattekkatte,² Dr. Tobias Köllner,³ Prof. Dr. Jörg Degenhardt,⁴

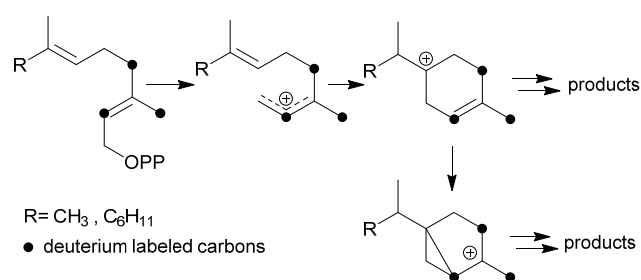
Prof. Dr. Jonathan Gershenzon⁵ and Prof. Dr. Wilhelm Boland⁶

Chem. Commun., 2015, 51, 3797-3800

DOI: 10.1039/C4CC10395E

Reproduced by permission of the Royal Society of Chemistry

Graphical Abstract



Summary

Multiproduct terpene synthases TPS4-*B73* and TPS5-*Delprim* from *Zea mays* exhibit isotopically sensitive branching in the formation of mono- and sesquiterpene volatiles. The impact of the kinetic isotope effects and the stabilization of the reactive intermediates by hyperconjugation along with the shift of products from alkenes to alcohols are discussed.



Cite this: *Chem. Commun.*, 2015, 51, 3797

Received 29th December 2014,
Accepted 30th January 2015

DOI: 10.1039/c4cc10395e

www.rsc.org/chemcomm

Isotope sensitive branching and kinetic isotope effects to analyse multiproduct terpenoid syntheses from *Zea mays*†

Nathalie Gatto,^a Abith Vattekkatte,^a Tobias Köllner,^a Jörg Degenhardt,^b Jonathan Gershenzon^a and Wilhelm Boland*^a

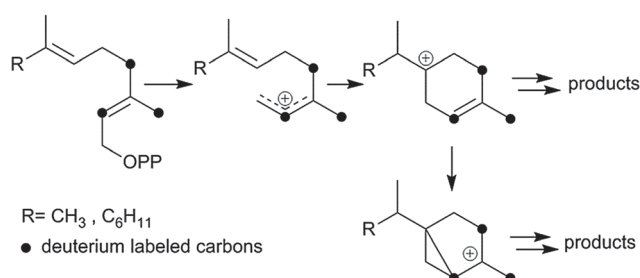
Multiproduct terpene synthases TPS4-B73 and TPS5-Delprim from *Zea mays* exhibit isotopically sensitive branching in the formation of mono- and sesquiterpene volatiles. The impact of the kinetic isotope effects and the stabilization of the reactive intermediates by hyperconjugation along with the shift of products from alkenes to alcohols are discussed.

Terpenes constitute the largest and most diverse class of plant natural products with more than 30 000 members.^{1,2} Volatile terpenes, which represent a major class among herbivore induced volatiles, are synthesized by specific terpene synthases. These enzymes have been extensively investigated in recent decades, and various cDNAs encoding plant terpene synthases involved in primary and secondary metabolism have been cloned and characterized.^{3,4} Terpene synthases are able to convert acyclic precursors such as geranyl diphosphate (GDP, C₁₀), farnesyl diphosphate (FDP, C₁₅) and geranylgeranyl diphosphates (GGDP, C₂₀) into cyclic monoterpenes (C₁₀), sesquiterpenes (C₁₅) and diterpenes (C₂₀), respectively.⁵ As the first reaction step, the unsaturated diphosphates dissociate into highly reactive carbocations and diphosphate anions. These cations interact with electron-rich double bonds in their vicinity resulting in intramolecular cyclizations. In addition, rearrangements, including hydride or methyl shifts, occur prior to stabilization by either deprotonation or reaction with a nucleophile.

In addition to terpene synthases, which generate a single product, there are multiproduct terpene synthases, which generate a bouquet of acyclic and cyclic products from a single precursor.³ These enzymes have the advantage that a single mutation may generate a bouquet of new compounds improving the plant's defense.⁶ The δ -selinene synthase and γ -humulene synthase from *Abies grandis* hold the current record, producing 52 and 34 different sesquiterpenes, respectively.³ To better understand the mechanistic details of multiproduct terpenoid syntheses and to determine

whether the final deprotonation of cationic intermediates *en route* to mono- and sesquiterpenes is rate-limiting, deuterium kinetic isotope effects and product composition were investigated for TPS4 and TPS5 enzymes from *B73* and *Delprim* maize varieties. The different terpene profiles were controlled by allelic variation of the closely related terpene synthase genes, TPS4 and TPS5.⁶ Although both enzymes showed the typical properties of sesquiterpene synthases, they not only accepted FDP (C₁₅) but also GDP (C₁₀) as a substrate. Both substrates were converted almost exclusively into two types of cyclic products, with cyclohexenyl- and bicyclo[3.1.0]hexyl moieties as structural elements (Scheme 1). To study the kinetics of the reaction cascade, we synthesized labeled substrates with deuterium atoms completely surrounding the cationic center at C(3) of the key intermediates (Scheme 1). Depending on their stability and ease with which deprotonation reactions, different reaction channels may be favoured.

[2-²H]- and [2,4,4,9,9,9-²H₆]-GDP as well as [2-²H]- and [2,4,4,13,13,13-²H₆]-FDP were prepared according to the protocol of Arigoni *et al.* (Scheme 2).⁷ For hexadeuterated analogues, [1,1,1,3,3-²H₅] ketones **1b** and **1d** were prepared by proton-deuterium exchange reaction in D₂O in presence of potassium carbonate. The subsequent Peterson olefination of the ketones **1a-d** with [2,2-²H₂]-trimethylsilylacetate **2** afforded the [2-²H]- or [2,4,4,9,9,9-²H₆]-carboxylic acids. The corresponding methyl esters were converted to the mono- and hexadeuterated alcohols **4a-d** using diisopropyl aluminum hydride. Labeled diphosphates were



Scheme 1 Isotope sensitive branching strategy.

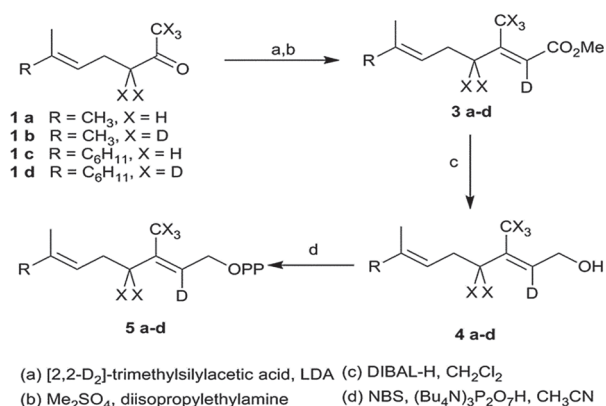
^a Max Planck Institute for Chemical Ecology, Hans-Knöll-Strasse 8, D-07745 Jena, Germany. E-mail: boland@ice.mpg.de

^b Institute for Pharmacy, University of Halle, Hoher Weg 8, D-06120 Halle, Germany

† Electronic supplementary information (ESI) available. See DOI: 10.1039/c4cc10395e



Communication



Scheme 2 Synthesis of deuterated GDP and FDP.

prepared according to Woodside *et al.*⁸ and yielded the corresponding trisammonium geranyl diphosphates **5a–b** and trisammonium farnesyl diphosphates **5c–d**.

The synthesized deuterium labelled GDP and FDP substrates were incubated with TPS4 and TPS5. The resulting terpenoid profiles were quantified by GC-FID and showed predominantly cyclic substances with a terpinan/sabinan (monoterpenes) and a bisabolane/sesquisabinane (sesquiterpenes) skeleton, respectively.⁹ Acyclic products were also present, including β -myrcene, and linalool from GDP and two sesquiterpenoids, (*E*)- β -farnesene and (3*R*)-(*E*)-nerolidol from FDP. The acyclic terpenes result from the deprotonation or water-capture of the first carbocation formed upon cleavage of the diphosphate. Comparing product ratios from labeled *versus* unlabeled precursors, we found that both cyclases exhibited a constant 1:2 ratio (acyclic/cyclic monoterpenes) for the GDP substrates as well as constant ratios of 1:5 for TPS4 and 1:10 for TPS5 for the FDP substrates. These results suggest that the labeling with stable isotopes did not influence the kinetics of the first ring closure, although the delocalized positive charge is partly surrounded by deuterium.

The relative overall rates of mono- and sesquiterpene formation from incubation of deuterated GDP and FDP with TPS4 and TPS5 and the apparent isotope effects k_H/k_D are given in Table 1. Incubation of monodeuterated [²H₁]-GDP **5a** and [²H₁]-FDP **5c** with both cyclases resulted in relative overall rates that were almost identical to those obtained with unlabeled substrates. The isotope effects for monodeuterated [²H₁]-GDP **5a** and [²H₁]-FDP **5c** are close to unity. However, the incubation of hexadeuterated substrates noticeably reduced the rate of product formation. The relative total rate was reduced by 15% (TPS4) or 25% (TPS5) upon incubation with [²H₆]-GDP **5b**. The rate of suppression corresponded to an apparent isotope effect k_H/k_D of 1.17 and 1.33, respectively. Similarly, enzymatic incubation with [²H₆]-FDP **5d** decreased the relative amount of sesquiterpenes (19% and 21% with TPS4 and TPS5, respectively) equivalent to k_H/k_D of 1.23 and 1.25, respectively. The observed overall rate reductions upon incubation with hexadeuterated GDP and FDP result from primary isotope effects (loss of ²H⁺). In contrast, the isotope labels in the monodeuterated substrates have no direct influence on the reaction mechanism, since the C(2)–D bond is not cleaved during the whole cyclization cascade. Moreover, the variations in the product profiles and the overall rates were a result of

Table 1 Effect of degree of labeling on total rate of monoterpene and sesquiterpene formation

Substrate	TPS4-B73		TPS5-Delprim	
	Relative rate ^a (%)	k_H/k_D	Relative rate ^a (%)	k_H/k_D
[² H ₁]-GDP 5a	101.09 ± 0.45	~1 ^b	99.98 ± 0.84	~1 ^b
[² H ₆]-GDP 5b	85.06 ± 0.84	1.17 ^b	75.02 ± 0.78	1.33 ^b
[² H ₁]-FDP 5c	106.21 ± 6.95	~1 ^b	101.30 ± 1.11	~1 ^b
[² H ₆]-FDP 5d	80.95 ± 7.55	1.23 ^b	79.65 ± 1.94	1.25 ^b

^a Relative overall rates compared to those of incubation with unlabeled GDP or FDP substrates (set at 100). Mean values from six replicates, ±1 SD. ^b Apparent total rate isotope effects compared to those of incubation with unlabeled GDP or FDP substrates. Note: oxygenated cyclic volatiles not considered.

apparent secondary isotope effects. The difference in the rate of volatile formation was even more pronounced in the case of sesquiterpenes. The production of all cyclic products requires an (*E/Z*)-isomerization step of the C(2)–C(3) double bond of the (*E*)-configured substrates, which is achieved through tertiary allylic phosphate intermediates, and linalyl- and nerolidyl diphosphate, respectively. This phenomenon has been reported for the product formation of maize sesquiterpene synthases TPS6, TPS10, TPS11,^{3,10} and other terpene synthases.¹¹

As mentioned above, the oxygenated cyclic volatiles were not considered in the present data. To estimate the weight of this approximation, quantitative kinetic measurements were carried out. For [²H₆]-FDP **5d** with TPS4 with $k_H/k_D = 1.15$, 13% fewer sesquiterpene formation (relative to FDP). Similar results were obtained when the oxygenated cyclic volatiles were not considered (a 19% decrease in the volatile production corresponded to a $k_H/k_D = 1.23$) and justify the approximation made above.

Both cyclases showed minor changes in the formation of limonene (4), α -terpinolene (6) and linalool (7) (Fig. 1). In contrast a significant decrease of α -thujene (1) and sabinene (2) along with a corresponding increase in sabinene hydrate (5) was observed when TPS4 and TPS5 were incubated with [²H₁]-GDP **5a** or [²H₆]-GDP **5b** when compared to incubation with GDP. The observed kinetic isotope effects (KIE)s, corresponding to a difference of 5 to 6 deuterium atoms between the substrates, are in the range of $k_H/k_D = 2.91$ –5.68. These values are in agreement with those observed for terminating deprotonation reactions of other monoterpene cyclases.^{12,13} In case of substrates differing by only one deuterium atom, the observed KIEs were much smaller (within a range of $k_H/k_D = 1.10$ –1.18).

The first set of sesquiterpenes, comprising (*S*)- β -bisabolene (11), (*E*)- γ -bisabolene (12) and zingiberene (9), (Fig. 2), were not affected by the isotopically sensitive branching experiments, and only minor changes in product composition were observed with hexadeuterated substrates (relative to unlabeled or monodeuterated analogues). A significant decrease in 7-*epi*-sesquithujene (1), sesquithujene (2), sesquisabinenes A (5) and B (6) and (*E*)- α -bergamotene isomers (3, 4) was observed after incubating [²H₆]-FDP **5d** with TPS4 (10–64%) and with TPS5 (26–61%), when compared to natural FDP (Fig. 2).

This rate suppression was coupled with a corresponding increase in the formation of γ - and β -curcumene isomers,



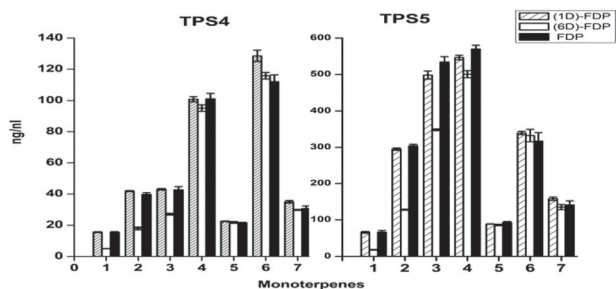


Fig. 1 Product distribution of main monoterpenes from incubations of deuterated GDP with TPS4 and TPS5. (1) α -Thujene, (2) sabinene, (3) β -myrcene, (4) limonene, (5) sabinene hydrate, (6) α -terpinolene, (7) linalool.

sesquithujene hydrate and 7-*epi*-sesquithujene hydrate by 175–400% for TPS4 and 193–255% for TPS5. Because the biosynthesis of sesquiterpene volatiles is mechanistically much more complex than that of monoterpenes volatiles, only the observed KIEs for the deprotonation reactions leading to 7-*epi*-sesquithujene and sesquithujene are presented. Thus, the observed KIEs were in the range of $k_{\text{H}}/k_{\text{D}} = 3.38\text{--}4.08$ for the terminating deprotonation reaction, leading to 7-*epi*-sesquithujene, and in the range of $k_{\text{H}}/k_{\text{D}} = 4.17\text{--}6.24$ for the terminating deprotonation reaction leading to sesquithujene. These values are in agreement with those obtained with the monoterpene series and with previous studies on other monoterpene cyclases.^{12,13} The corresponding KIEs were close to unity, demonstrating that the monodeuterated labelling at C(3) had almost no influence on the reaction cascade.

We previously proposed⁶ a reaction mechanism for the formation of mono- and sesquiterpene products by TPS4 and TPS5. The stabilization of the carbocationic intermediates is partly facilitated by interactions (*e.g.* π -cation interactions) with the hydrophobic, aromatic-rich environment and the DDxD motif of the active-site of the enzyme.⁹ Nevertheless, hyperconjugation is an important factor for the stability of carbocation intermediates. Hyperconjugation is considered to be the interaction of the vacant p-type orbital on the

cationic center with adjacent C–H or C–C σ -bonds. Because a C–D bond is stronger than a C–H bond, a C–H hyperconjugation stabilizes an adjacent positive charge more than a C–D hyperconjugation. Accordingly, reactions involving breaking C–D are slowed down. Such hyperconjugative weakening in reaction intermediates due to isotopes induces secondary KIEs. In the present study, all KIEs lead to the alteration of product distributions after isotopically sensitive branching. To illustrate the effects of hyperconjugation, the secondary KIEs of the cyclisation reactions of [²H₆]-FDP **5d** (Fig. 3) and [²H₆]-GDP **5b** (Fig. 4) are discussed.

From [²H₆]-FDP **5d**, after the initial ionization–isomerization–ionization sequence, the cyclization cascade is initiated by the formation of (*S*)- and (*R*)-bisaboyl cations (A and B). These first carbocations can be directly deprotonated to produce (*S*)- β -bisabolene without noticeable KIEs (the positive charge being located far from the deuterated center). Tertiary carbocations A₁ and B₁ are almost as stable as A and B because the positive charge is distant from the deuterium labeled carbon center and, hence, can be stabilized by C–H hyperconjugation. Secondary carbocations A₃ and B₃, which are energetically less favorable than tertiary ones (*e.g.* A₄ and B₄), are relatively stable due to surrounding hydrogen atoms. Carbocations A₄, A₅, B₄ and B₅ are the least stable ones, since the positive charge is fully surrounded by deuterium atoms and hence, cannot be delocalized and stabilized by C–D hyperconjugation. The stability of terminal carbocations results in the production of the corresponding cyclic terpene. Taken together, these observations are consistent with the product distribution obtained by isotopically sensitive branching experiments. Deuterium isotope effects are less pronounced in the monodeuterated analogues (Table 1). Nevertheless, strong KIEs for the formation of sesquithujene, 7-*epi*-sesquithujene or sesquisabinenes A and B were observed after incubation of both enzymes with hexadeuterated substrates (Fig. 4). In case of the bisaboyl carbocations A and B, (Fig. 3), minor KIEs were observed for β - or γ -bisabolene formation since the reactive carbocation intermediates are located in an exclusive [¹H]-environment. Similarly, only minor KIEs were observed for zingiberene isomers since the final deprotonation involves only the loss of a hydrogen atom (no primary KIE). Deuterium isotope effects on the monoterpene product distribution can also be rationalized in terms of hyperconjugation. As shown in Fig. 4, the first step of the cyclization cascade is the C(1)–C(6) ring closure of the linaloyl diphosphate, resulting in the formation of (*S*)- and (*R*)-terpinyl carbocations C₁ and C₂. As for bisaboyl intermediates A and B in the biosynthesis of sesquiterpenes, the positive charge is positioned far away from the influence of the deuterated carbons. Hence terminating steps *via* deprotonation or water capture leading to (*S*)-(*–*)-limonene and α -terpineol or α -terpinolene, can occur spontaneously and are not affected by kinetic isotope effects. As discussed below, minor variations in product distribution were observed when unlabeled or [²H₁]-GDP were used as substrates. These minor KIEs observed for limonene, α -terpinolene and α -terpineol reflect the absence of destabilizing effects in the two α -terpinyl carbocations. From C₁ and C₂, the cyclization cascade proceeded to carbocation D which was subsequently rearranged to the tertiary carbocations E₁ and E₂. Because the positive charge fully surrounded by deuterium atoms is less efficiently stabilized by

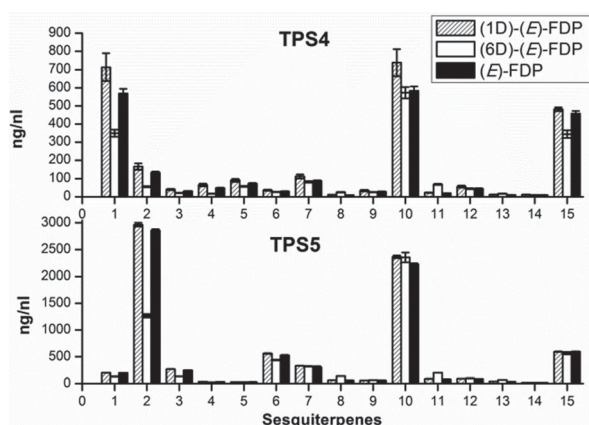


Fig. 2 Product distribution of main sesquiterpenes from incubations of deuterated FDP with TPS4 and TPS5. (1) 7-*epi*-Sesquithujene, (2) sesquithujene, (3) (*Z*)- α -bergamotene, (4) (*E*)- α -bergamotene, (5) sesquisabinene A, (6) sesquisabinene B, (7) (*E*)- β -farnesene, (8) γ -curcumene, (9) zingiberene, (10) (*S*)- β -bisabolene, (11) β -curcumene, (12) (*E*)- γ -bisabolene, (13) 7-*epi*-sesquithujene hydrate**, (14) sesquithujene hydrate**, (15) (*3R*)-(*E*)-nerolidol. ** Tentatively assigned structure.



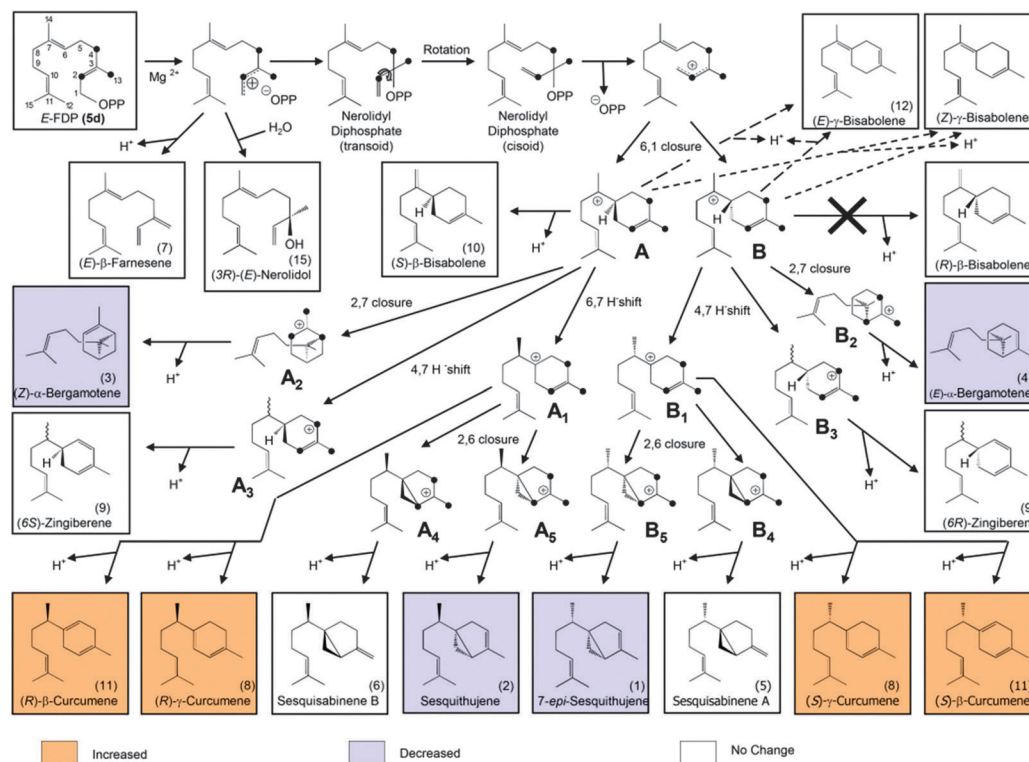


Fig. 3 Proposed mechanism for sesquiterpene formation from $[^2\text{H}_6]$ -FDP. The black dots represent deuterated carbons.⁶

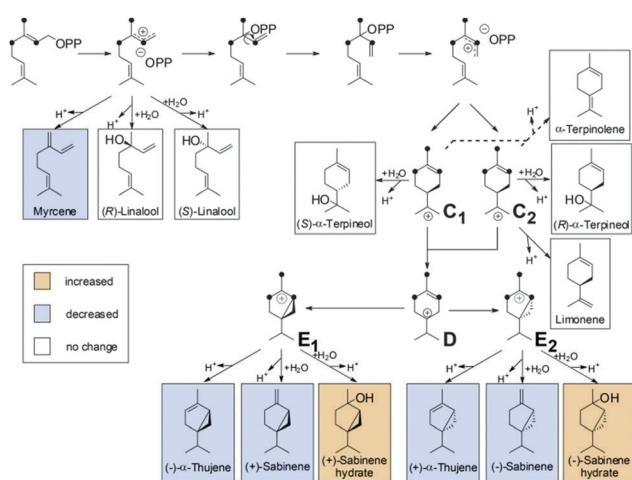


Fig. 4 Proposed reaction mechanism for the formation of monoterpenes by TPS4 and TPS5 from (E) - $[^2\text{H}_6]$ -GDP [7b].

C–H hyperconjugation, strong deuterium isotope effects on the formation of sabinene, sabinene hydrate and α -thujene were observed. Obviously, E_1 and E_2 preferentially stabilize by reacting with water as a nucleophile rather than losing a positively charged hydrogen isotope.

Multiproduct terpene synthases TPS4 and TPS5 from *Zea mays* show isotopically sensitive branching in the reaction cascade of prenyl diphosphates *en route* to mono- and sesquiterpene volatiles *via* a common carbocationic intermediate along a branched reaction sequence. The primary kinetic isotope

effects of deuterium atoms on terminating deprotonations and effects resulting from lower stabilization of the reactive intermediates by hyperconjugation direct the reaction to an enhanced formation of alcohols instead of olefinic products. Accordingly, the extensive deuterium labeling of intermediary cations is a valuable tool to identify branching points in complex cyclization sequences of multiproduct terpenoid synthases.

Notes and references

- J. D. Connolly and R. A. Hill, *Dictionary of Terpenoids*, Chapman & Hall, New York, 1992.
- J. C. Sacchetti and C. D. Poulter, *Science*, 1997, **277**, 1788–1789.
- J. Degenhardt, T. G. Köllner and J. Gershenzon, *Phytochemistry*, 2009, **70**, 1621–1637.
- D. J. Schenk, C. M. Starks, K. R. Manna, J. Chappell, J. P. Noel and R. M. Coates, *Arch. Biochem. Biophys.*, 2006, **448**, 31–44.
- E. M. Davis and R. Croteau, *Biosynthesis: Aromatic Polyketides, Isoprenoids, Alkaloids*, Springer-Verlag, Berlin, 2000, pp. 53–95.
- T. G. Köllner, C. Schnee, J. Gershenzon and J. Degenhardt, *Plant Cell*, 2004, **16**, 1115–1131.
- D. Arigoni, D. E. Cane, J. H. Shim, R. Croteau and K. A. Wagschal, *Phytochemistry*, 1993, **32**, 623–631.
- A. B. Woodside, Z. Huang and C. D. Poulter, *Org. Synth.*, 1993, **8**, 616–623.
- T. G. Köllner, P. E. O'Maille, N. Gatto, W. Boland, J. Gershenzon and J. Degenhardt, *Arch. Biochem. Biophys.*, 2006, **448**, 83–92.
- T. G. Köllner, C. Schnee, S. Li, A. Svatos, B. Schneider, J. Gershenzon and J. Degenhardt, *J. Biol. Chem.*, 2008, **283**, 20779–20788.
- D. E. Cane, H. T. Chiu, P. H. Liang and K. S. Anderson, *Biochemistry*, 1997, **36**, 8332–8339.
- H. J. Pyun, R. M. Coates, K. C. Wagschal, P. McGeary and R. B. Croteau, *J. Org. Chem.*, 1993, **58**, 3998–4009.
- K. C. Wagschal, H. J. Pyun, R. M. Coates and R. Croteau, *Arch. Biochem. Biophys.*, 1994, **308**, 477.



6.2 Manuscript II: Substrate geometry controls the cyclization cascade in multiproduct terpene synthases from *Zea mays*

Abith Vattekkatte,¹ Dr. Nathalie Gatto,² Dr. Tobias Köllner,³ Prof. Dr. Jörg Degenhardt,⁴

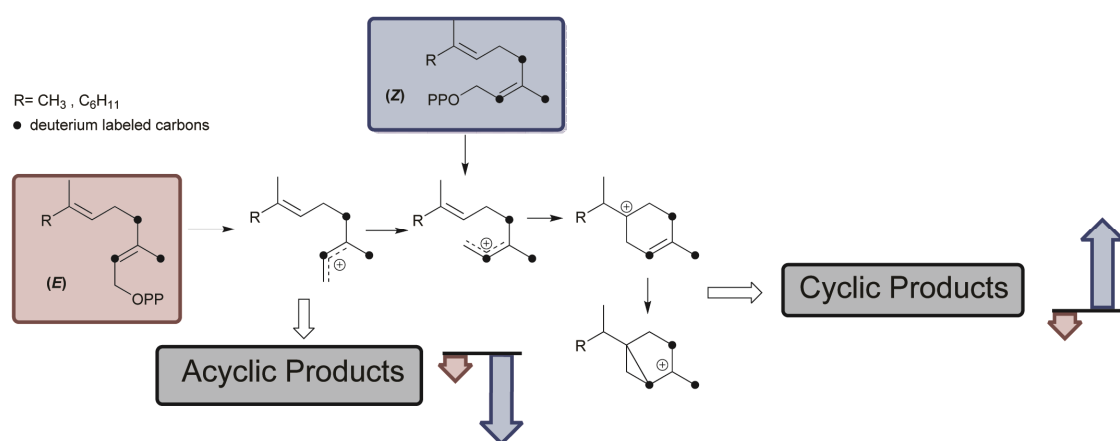
Prof. Dr. Jonathan Gershenzon⁵ and Prof. Dr. Wilhelm Boland⁶

Org. Biomol. Chem., 2015, 13, 6021-6030

DOI: 10.1039/C5OB00711A

Reproduced by permission of the Royal Society of Chemistry

Graphical Abstract



Summary

Multiproduct terpene synthases TPS4-*B73* and TPS5-*Delprim* from maize (*Zea mays*) catalyze the conversion of farnesyl diphosphate (FDP) and geranyl diphosphate (GDP) into a complex mixture of sesquiterpenes and monoterpenes, respectively. On incubation with labeled (2*Z*) substrates, TPS4 and TPS5 showed much lower kinetic isotope effects than the labeled (2*E*) substrates. The products arising from the deuterated (2*Z*)-precursors revealed a distinct preference for cyclic products and exhibited an enhanced turnover. This increase in the efficiency due to (2*Z*) configuration emphasizes the rate limiting effect of the initial (2*E*) → (2*Z*) isomerization step in the reaction cascade of the multiproduct terpene synthases.



Cite this: *Org. Biomol. Chem.*, 2015, **13**, 6021

Substrate geometry controls the cyclization cascade in multiproduct terpene synthases from *Zea mays*[†]

Abith Vattekkatte,^a Nathalie Gatto,^a Tobias G. Köllner,^b Jörg Degenhardt,^c Jonathan Gershenzon^b and Wilhelm Boland^{*a}

Multiproduct terpene synthases TPS4-*B73* and TPS5-*Delprim* from maize (*Zea mays*) catalyze the conversion of farnesyl diphosphate (FDP) and geranyl diphosphate (GDP) into a complex mixture of sesquiterpenes and monoterpenes, respectively. Various isotopic and geometric isomers of natural substrates like (2*Z*)-[2-²H]- and [2,4,4,9,9,9-²H₆]- (GDP) and (2*Z*,6*E*)-[2-²H]- and [2,4,4,13,13,13-²H₆]- (FDP) were synthesized analogous to presumptive reaction intermediates. On incubation with labeled (2*Z*) substrates, TPS4 and TPS5 showed much lower kinetic isotope effects than the labeled (2*E*) substrates. Interestingly, the products arising from the deuterated (2*Z*)-precursors revealed a distinct preference for cyclic products and exhibited an enhanced turnover on comparison with natural (2*E*)-substrates. This increase in the efficiency due to (2*Z*) configuration emphasizes the rate limiting effect of the initial (2*E*) → (2*Z*) isomerization step in the reaction cascade of the multiproduct terpene synthases. Apart from turnover advantages, these results suggest that substrate geometry can be used as a tool to optimize the biosynthetic reaction cascade towards valuable cyclic terpenoids.

Received 8th April 2015,
Accepted 28th April 2015

DOI: 10.1039/c5ob00711a

www.rsc.org/obc

Introduction

Plants produce a huge variety of secondary metabolites that continue to amaze both plant biologists and natural product chemists.¹ The largest group of plant secondary metabolites comprises the terpenes with more than 30 000 known compounds.² These molecules have applications ranging from flavor and fragrance to biological functions such as hormones, attractants for pollinators, or toxins.³ In addition, the terpenoid composition shows major qualitative and quantitative variation among species and also within single species.⁴ The structural diversity of terpenes is due to terpene synthases, enzymes that convert the prenyl diphosphate substrates like

geranyl diphosphate (GDP, C₁₀), farnesyl diphosphate (FDP, C₁₅) and geranylgeranyl diphosphate (GGDP, C₂₀) into monoterpenes (C₁₀), sesquiterpenes (C₁₅) and diterpenes (C₂₀), respectively.^{2b} Terpene synthases have been intensively investigated in recent decades and various cDNAs encoding plant terpene synthases responsible for the structural diversity have been characterized.⁵

Certain terpene synthases are known for their catalytic promiscuity. This catalytic promiscuity is due to a common electrophilic reaction mechanism which is important for deciphering evolution of enzymes and engineering future enzymatic catalysts.⁶ One of the unique features of terpene synthases is their ability to produce multiple products from a single prenyl diphosphate substrate.⁷ The δ-selinene synthase and the γ-humulene synthase from *Abies grandis* hold the present record by producing 52 and 34 different sesquiterpenes.⁸ Despite their overall sequence diversity, terpene synthases possess several highly conserved amino acid residues.⁹ An aspartate-rich DDxxD motif located at the entrance of the active site was shown to be involved in the binding of the metal ion-complexed diphosphate ester substrate.¹⁰ In the N-terminal part of monoterpene synthases, two arginine residues are present that are believed to influence the isomerization of the initial substrate.¹¹

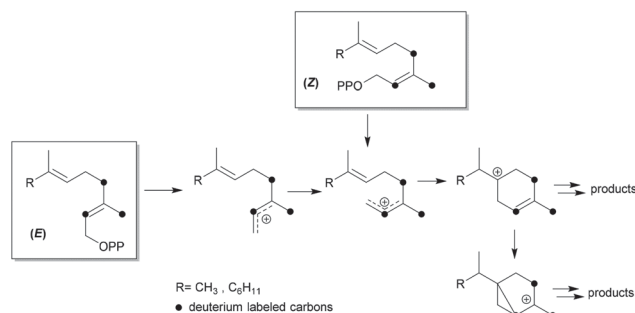
^aDepartment of Bioorganic Chemistry, Max Planck Institute for Chemical Ecology, Hans-Knöll-Strasse 8, D-07745 Jena, Germany. E-mail: boland@ice.mpg.de

^bDepartment of Biochemistry, Max Planck Institute for Chemical Ecology, Hans-Knöll-Strasse 8, D-07745 Jena, Germany

^cInstitute for Pharmacy, University of Halle, Hoher Weg 8, D-06120 Halle, Germany

[†]Electronic supplementary information (ESI) available: Product distributions of main monoterpenes and sesquiterpenes from incubations of deuterated GDP and FDP, respectively, with TPS4 and TPS5. Synthetic procedure and ¹H, ¹³C NMR spectra of compounds **3b**, **3d**, **4**, **5a-d**, **6a-d**, **7a-d**, **8a-d**, **1a-d** and **2a-d** and ³¹P NMR spectra of compounds **1a-d** and **2a-d**. IR spectra of compounds **3b**, **3d**, **4**, **5a-d**, **6a-d**, **1a-d** and **2a-d**. See DOI: 10.1039/c5ob00711a

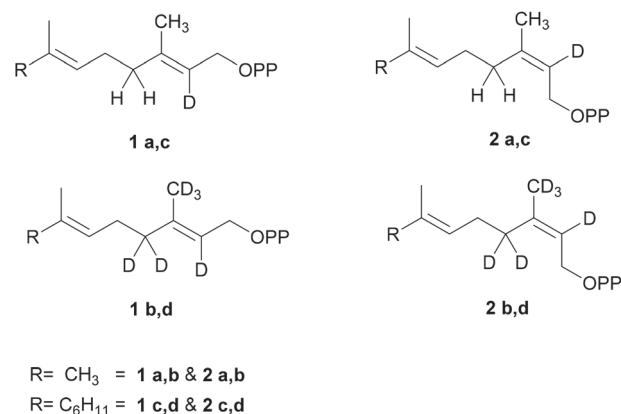




Scheme 1 Isotope sensitive branching strategy.

Two closely related terpene synthase genes encoding multi-product enzymes, namely TPS4 and TPS5, were recently cloned from *Zea mays*.¹² Both recombinant proteins accepted GDP and FDP as substrates and converted them into two types of cyclic products with cyclohexenyl- and bicyclo[3.1.0]hexyl moieties as common structural features (Scheme 1). Product formation is achieved by initial isomerization of the substrate (*E*)-GDP or (*E*)-FDP into the tertiary allylic diphosphates (Scheme 1). After dissociation, the rearranged linaloyl- or nerolidyl-cation cyclizes easily to a cyclohexenyl cation or by formation of a bicyclo[3.1.0]hexyl moiety stabilized in both cases by further deprotonation. Modeling of the TPS4 active site cavity and docking studies with cationic intermediates suggested that discrete steps of the reaction cascade are controlled by two different enzyme pockets.¹³ We have recently reported about the kinetic isotope effects and enhanced formation of alcohols over olefinic products by deuterated precursors of (*2E*)-GDP and (*2E,6E*)-FDP as compared to natural substrates.¹⁴

To reveal further details of the enzyme mechanism, we synthesized geranyl- and farnesyl diphosphates including both geometric isomers of the critical C(2)–C(3) bond (Scheme 1) using deuterium labels as a probe for isotope sensitive branching. We were interested in whether the cyclization of *cis*-isomers (*2Z*)-GDP (**2a–b**) and (*2Z,6E*) FDP (**2c–d**) would proceed *via* the same cascade as observed with their corresponding *trans*-substrates (**1a–d**) (Scheme 2). Most studies involving several sesquiterpene synthases using FDP isomers and analogues have been used to compare their kinetic properties and further determine the mechanism of carbocation quenching¹⁵ and the initial ionization-isomerization of all-*trans*-FDP for *cis*–*trans*-pathway-specific enzymes.^{13,16} Here, we describe the effects of substrate's conformation on the initial cyclization and the further course of individual protonation and deprotonation reactions by means of deuterium labeling. In contrast to our previous study,¹⁴ both TPS4 and TPS5 cyclize labeled (*2Z,6E*)-FDP (**2c–d**) and (*2Z*)-GDP (**2a–b**) showed quantitative difference in volatile composition as compared to natural substrates. Interestingly, they exhibited much higher turnover with (*2Z*) substrates (**2a–d**) than with their natural (*2E*) substrates (**1a–d**) and a reduced ratio of acyclic to cyclic products.



Scheme 2 Monodeuterated and hexadeuterated (*2E*)-GDP, FDP (**1a–d**) and (*2Z*)-GDP, FDP (**2a–d**).

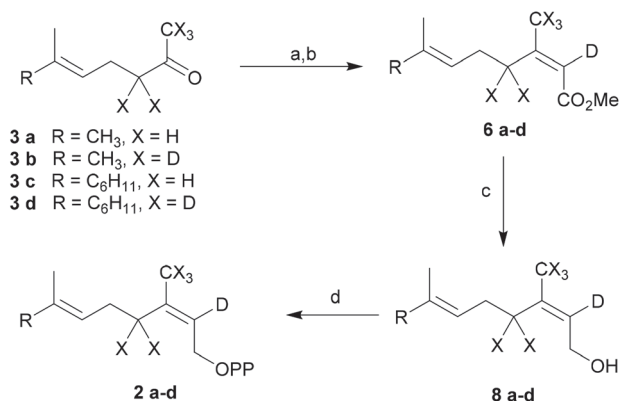
Results and discussion

To study the rate limiting effects of the initial isomerization step catalyzed by TPS4 and TPS5 and their consequences for the reaction cascade we synthesized labeled substrates (**2a–d**) with deuterium atoms completely surrounding the C(3) cationic center of the key intermediates (Scheme 1). The deuterium labels serve to investigate the alterations in product distribution that might occur as a consequence of changing the geometry of the C2–C3 double bond, which undergoes isomerization in the reaction sequence. These product alterations depend on the nature of the initial carbocationic intermediates formed whose stability and ease of deprotonation may favor different reaction channels.

Synthesis of substrates

[2-²H]- and [2,4,4,9,9,9-²H₆]-GDP (**2a–b**) and [2-²H]- and [2,4,4,13,13,13-²H₆]-FDP (**2c–d**) were prepared by modifying the protocol of Arigoni *et al.*¹⁷ (Scheme 3 and ESI[†]). For hexadeuterated analogues, [1,1,1,3,3-²H₅] ketones **3b** and **3d** were first prepared by proton-deuterium exchange reaction in MeOD in presence of DBN (1,5-diazabicyclo[4.3.0]non-5-ene).¹⁸ Subsequent Peterson olefination of the ketones (**3a–d**) with [2,2-²H₂]-trimethylsilylacetic acid **4** afforded a mixture of carboxylic acids, additionally labeled at C(2). After esterification, the isomers were easily separated by flash chromatography and provided the pure methyl esters (*2E*)-(**5a–d**) and (*2Z*)-(**6a–d**). Mono- and hexadeuterated alcohols (*2Z*)-(**8a–d**) were generated by reduction of the methyl esters with diisopropyl aluminium hydride. Labeled diphosphates were prepared according to Woodside *et al.*¹⁹ and yielded the corresponding trisammonium (*2Z*)-geranyl diphosphates (**2a–b**) and trisammonium (*2Z,6E*)-farnesyl diphosphates (**2c–d**). The corresponding (*2E*) substrates (**1a–d**) were synthesized from (*2E*)-(**5a–d**) and have already been described.¹⁴ This procedure provides an easy access to various labeled and unlabeled isomers of prenyl diphosphates.





Scheme 3 Synthesis of deuterated substrates. Reagents and conditions: (a) [2,2-²H₂]-trimethylsilylacetic acid, 2 eq. mol. LDA, THF, -78 °C to reflux; (b) Me₂SO₄, DIPEA; (c) DIBAL-H, CH₂Cl₂; (d) (i) NBS, Me₂S, CH₂Cl₂; (ii) (Bu₄N)₃P₂O₇H, CH₃CN; (iii) ion exchange; (iv) cellulose, CH₃CN/NH₄HCO₃.

Enzymatic transformations of labeled GDP and FDP by TPS4 and TPS5

Impact of the substrate geometry on the catalytic turnover.

Both maize terpene synthases, TPS4 from the variety *B73*, and TPS5 from *Delprim*, were incubated with both (*2E*)-series labeled GDP (**1a–b**) and FDP (**1c–d**) and (*2Z*)-series labeled GDP (**2a–b**) and FDP (**2c–d**). The terpenoid profiles resulting from the incubation experiments were analyzed by gas chromatography-flame ionization detection analysis (GC-FID) and compared with those resulting from unlabeled substrates. Fig. 1 compares the total rate of terpene formation resulting from incubations of these substrates with TPS4 and TPS5.

Both TPS4 and TPS5 exhibited much higher turnover when incubated with (*2Z*)-(2**a–d**) vs. (*2E*)-(1**a–d**) substrates (Fig. 1). In Fig. 1, horizontal line at 100 represents the relative rate obtained from unlabeled (*2E*)-GDP (A) and (*2E*)-FDP (B) respectively. All labeled (*2E*)-isomers of C₁₀ and C₁₅ substrates either show a decrease or values around the reference line for both monoterpenes and sesquiterpenes. Whereas in case of labeled (*2Z*)-isomers of C₁₀ and C₁₅ substrates there was a substantial increase in product formation on comparison with unlabeled reference substrates.

The rate of monoterpene production showed 30% increase after incubation with **2a** and 17% with **2b** in comparison to their corresponding unlabeled (*2E*)-analogues. The difference in the rate of volatile formation was even more pronounced in the case of sesquiterpenes (**2c–d**). When incubated with the monodeuterated **2c** the sesquiterpene production increased by ~200% and with the hexadeuterated **2d** the corresponding increase was ~150% when compared with unlabeled (*2E*)-FDP. The production of all C₁₀ and C₁₅ cyclic products requires an initial isomerization of the C(2)–C(3) double bond of the original substrate, achieved through the intermediate tertiary allylic phosphates linalyl- and nerolidyl diphosphate, respectively (Scheme 4). The substrates of the (*2Z*)-series (**2a–d**) already possess the double bond in the correct configuration

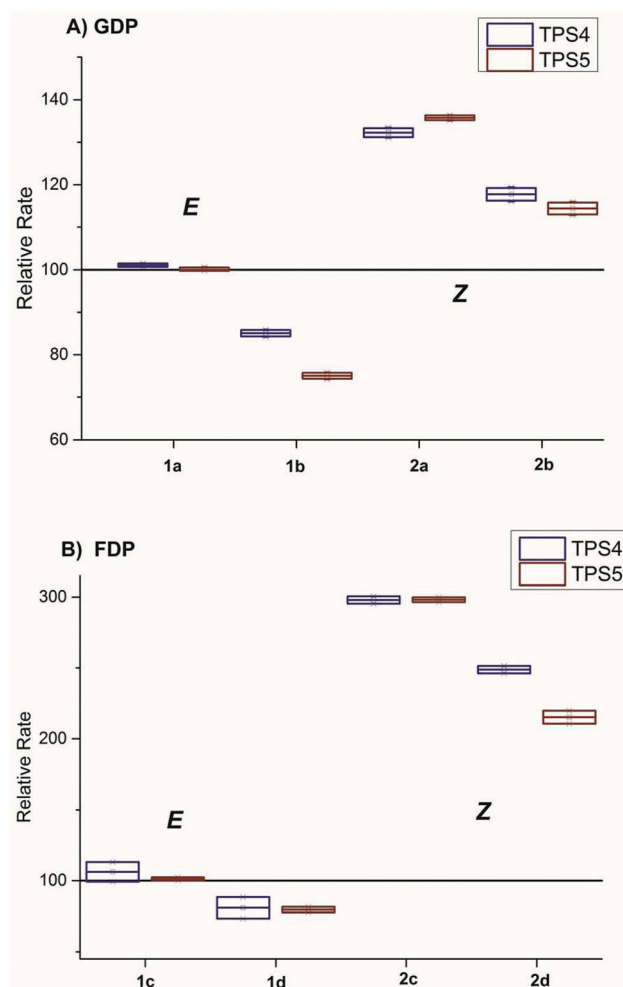
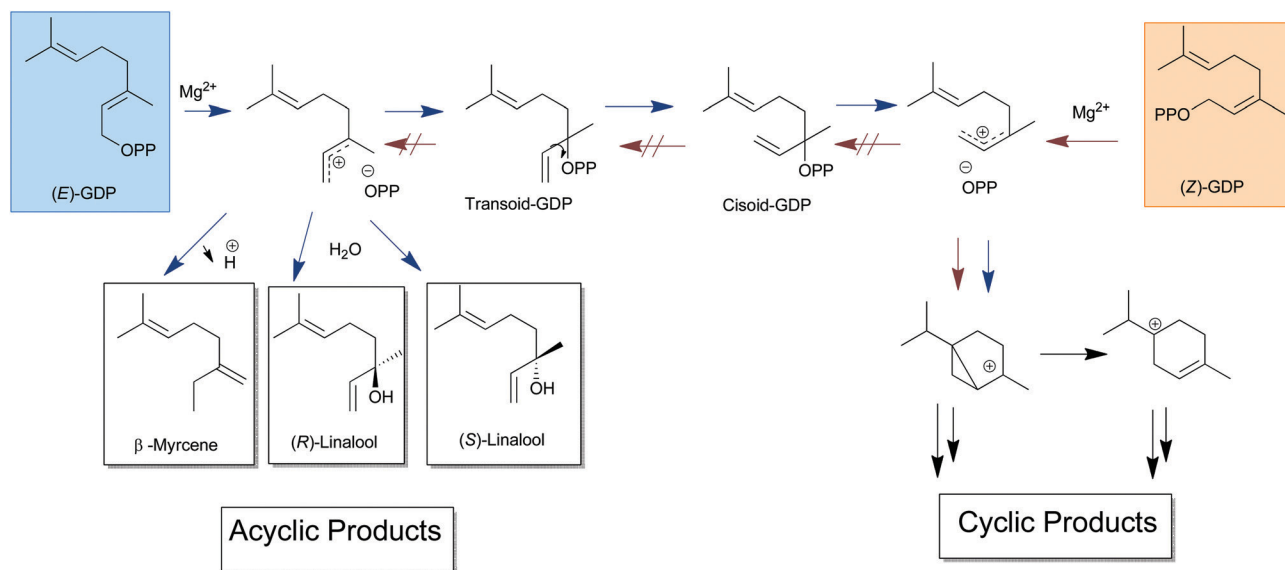


Fig. 1 Comparison of total rate of monoterpene (A) and sesquiterpene (B) formation with incubations of deuterated (*E*)/(*Z*)-GDP and FDP with TPS4-*B73* and TPS5-*Delprim*. Horizontal line at 100 represents the relative rate obtained from unlabeled (*2E*)-GDP (A) and (*2E*)-FDP (B) respectively. Boxplot: median (horizontal lines in boxes), interquartile range (boxes), 1.5x-interquartile range (whiskers).

allowing the direct cyclization of the emerging carbocationic intermediate after ionization. The increased turnover clearly indicates that the isomerization is the rate limiting step in the reaction cascade with natural substrates. Removal of this rate limiting factor leads to much higher efficiency in terpenoid cyclization by these enzymes.

The production of all C₁₀ and C₁₅ cyclic products requires an isomerization of the C(2)–C(3) double bond of the original substrate, achieved through the intermediate tertiary allylic phosphates linalyl- and nerolidyl diphosphate, respectively. The substrates of the (*2Z*)-series possess the double bond already in the correct configuration allowing the direct cyclization of the emerging carbocationic intermediate after diphosphate cleavage. This phenomenon has also been reported for the product formation of some other sesquiterpene synthases like trichodiene synthase from *Fusarium sporotrichioides*,²⁰ and two terpene synthases from *Coprinus cinereus* Cop4 and Cop6.^{16f,21}





Scheme 4 General mechanism for generation of acyclic compounds and cyclic compounds by TPS4 and TPS5.

Impact of the precursor diphosphate on the ratio of acyclic versus cyclic volatiles. The terpenoid profiles from $(2E)$ -GDP and $(2E,6E)$ -FDP substrates (**1a–d**) were dominated by cyclic substances with terpinane/sabinane (monoterpenes) and bisabolane/sesquisabinane (sesquiterpenes) skeletons, respectively. Incubation experiments with labeled $(2Z)$ -GDP and $(2Z,6E)$ -FDP (**2a–d**) resulted in qualitatively the same series of cyclic mono- and sesquiterpenes. This confirms that the formation of cyclic products leads down the same pathway as for the $(2E)$ -isomer despite the generation of $(2Z)$ instead of the $(2E)$ -carbocations *via* isomerization of the C(2)–C(3) double bond. A few recent examples also reported that the products from $(2Z)$ -FDP are comparable to those obtained from the *all-trans*-FDP.^{13,16f,21b} In contrast the different product profiles obtained from $(2E)$ - and $(2Z)$ -FDP by the *epi*-aristolochene synthase from tobacco and sesquiterpene synthase from *Coprinus cinereus* (Cop4) were attributed to different starting conformations of the isomeric substrates.^{21c,22}

Three acyclic monoterpene olefins, (E) - β -myrcene, (R) -linalool and (S) -linalool from $(2E)$ -GDP and two acyclic sesquiterpenes, (E) - β -farnesene and $(3R)$ - (E) -nerolidol from $(2E,6E)$ -FDP were also present in the product mixtures of these enzymes. These acyclic terpenes result from deprotonation or water-capture of the first cation formed after cleavage of the diphosphate group. However, a very strong depletion in the amount of acyclic monoterpenes, myrcene (98% reduction) and linalool (65% reduction) was observed after incubation with **2a** ($(2Z)$ -GDP (Fig. 2) in comparison to unlabeled $(2E)$ -GDP for both maize cyclases. The rate suppression was even more pronounced with TPS4 after incubation of **2a**, resulting in a complete absence of β -myrcene and an 88% reduction of linalool. The same effect was observed after incubation of hexadeuterated $(2Z)$ -GDP **2b** with both enzymes: β -myrcene (almost complete elimination) and linalool (48–80% reduction). Similarly,

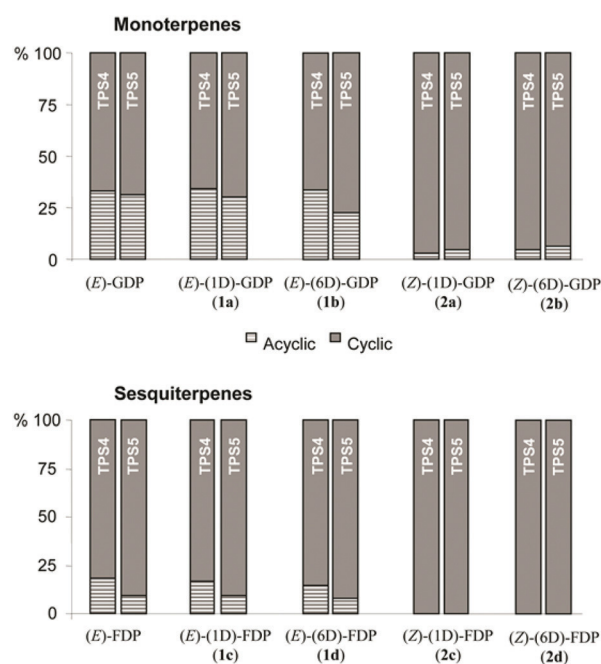


Fig. 2 Ratio acyclic/cyclic volatiles released after incubation of labeled substrates with TPS4-B73 and TPS5-Delprim.

strong decrease in the proportion of the acyclic sesquiterpenes were observed with deuterated $(2Z,6E)$ -FDP (**2c**, **2d**). Thus, incubation with hexadeuterated $(2Z,6E)$ -FDP **2d** led to a complete absence of (E) - β -farnesene and nerolidol production with both enzymes. Likewise, monodeuterated $(2Z,6E)$ -FDP **2c** lead to a decrease in (E) - β -farnesene formation (97% with TPS5 and complete elimination with TPS4) and nerolidol formation (complete elimination with both enzymes). Nevertheless, the pro-



duction of minute amounts of acyclic volatiles from (2*Z*)-substrates can be explained by direct deprotonation from the resulting carbocation or capture of a water molecule. These results strongly support a mechanism by which the substrates of the (2*Z*)-series (**2a–d**) are directly cyclized after ionization due to the C(2)–C(3) double bond already being in a suitable configuration for C(6)–C(1) ring closure (Scheme 4).

Interestingly, both TPS4 and TPS5 showed similar behavior when incubated with same set of isomers, (2*Z*)-series (**2a–d**) and (2*E*)-series (**1a–d**) (Fig. 2). They maintained a constant ratio between acyclic and cyclic products from the same geometric isomer. This ratio was 1:2 (acyclic/cyclic monoterpenes) for the (2*E*)-GDP substrates (unlabeled and **1a–b**) while an average ratio of 1:22 was observed for the corresponding (2*Z*)-GDP (**2a–b**). Similarly, for the unlabeled or deuterated (2*E,6E*)-FDP, this ratio was 1:5 (acyclic/cyclic sesquiterpenes) for TPS4 and 1:10 for TPS5. These results suggest that labeling with stable isotopes did not influence the kinetics of the first ring closure although the delocalized positive charge is partly surrounded by deuterium. Studies with monoterpene synthases have shown that only terpene synthases that can isomerize the C(2)–C(3) π bond of (2*E*)-GDP can make cyclic monoterpenes.²³ Likewise, only sesquiterpene synthases known to isomerize the C(2)–C(3) π bond of (2*E,6E*)-FDP have been reported to synthesize cyclic products from (2*E*)-GDP.²⁴ Thus, when incubated with (2*Z*)-series labeled GDP and FDP (**2a–d**) both enzymes showed strong preference for cyclic products with only a weak tendency for isomerization as evidenced by reduced formation of acyclic products (Scheme 4).

Kinetic isotope effects. In previous studies we observed changes in the product profiles of terpene synthases when incubated with natural (2*E*)-(**1a–d**) isomers when these had deuterium substitutions at sensitive branching positions leading to induced isotope effects.¹⁴ Now we examined the kinetic isotope effects associated with the (2*Z*)-(**2a–d**) substrates. The relative overall rates of mono- and sesquiterpenes with deuterated GDP and FDP (**1a–d**, **2a–d**) produced by TPS4 and TPS5 and the apparent total rate isotope effects k_H/k_D are given in Table 1. Because of the complex mono- and sesquiterpene biosynthetic pathways with multiple branching points (Fig. 5), oxygenated cyclic volatiles were not considered.

The relative overall rates of reaction with (2*Z*)-[²H]-GDP **2a** and (2*Z,6E*)-[²H]-FDP **2c** were used as reference for the determination of the apparent total rate isotope effects k_H/k_D for the hexadeuterated (2*Z*)-substrates (**2b**, **2d**). Thus the relative overall rate of monoterpene formation with (2*Z*)-[²H₆]-GDP **2b** decreased for TPS4 (11%) and TPS5 (16%). These rate suppressions correspond to an apparent total rate isotope effect k_H/k_D of 1.12 and 1.19, respectively. Furthermore TPS4 and TPS5 showed a depletion (17% and 28%, respectively) in the total rates of sesquiterpene volatiles after incubation with (2*Z,6E*)-[²H₆]-FDP **2d**, corresponding to an approximated apparent total rate isotope effect k_H/k_D of 1.20 and 1.38. The observed overall rate reductions after incubation with hexadeuterated GDP (**1b**, **2b**) and FDP (**1d**, **2d**) primarily result from induced primary isotope effects. In contrast the labeling pattern of the

Table 1 Effect of the degree of labeling (deuterium substitution) on the total rate of monoterpene and sesquiterpene formation resulting from incubations of deuterated GDP and FDP with TPS4-B73 and TPS5-Delprim from maize (*Zea mays*)

Substrate	TPS4-B73		TPS5-Delprim	
	Relative rate ^a (%)	k_H/k_D	Relative rate ^a (%)	k_H/k_D
(2 <i>E</i>)-[² H]-GDP 1a	101.09 ± 0.45	~1 ^b	99.98 ± 0.84	~1 ^b
(2 <i>E</i>)-[² H ₆]-GDP 1b	85.06 ± 0.84	1.17 ^b	75.02 ± 0.78	1.33 ^b
(2 <i>Z</i>)-[² H]-GDP 2a	132.25 ± 1.18	—	135.75 ± 0.63	—
(2 <i>Z</i>)-[² H ₆]-GDP 2b	117.72 ± 1.67	1.12 ^c	114.38 ± 1.55	1.19 ^c
(2 <i>E,6E</i>)-[² H]-FDP 1c	106.21 ± 6.95	~1 ^b	101.30 ± 1.11	~1 ^b
(2 <i>E,6E</i>)-[² H ₆]-FDP 2d	80.95 ± 7.55	1.23 ^b	79.65 ± 1.94	1.25 ^b
(2 <i>Z,6E</i>)-[² H]-FDP 2c	297.91 ± 2.59	—	298.14 ± 1.69	—
(2 <i>Z,6E</i>)-[² H ₆]-FDP 2d	248.75 ± 2.63	1.20 ^c	215.20 ± 4.58	1.38 ^c

^a Relative overall rates compared to those of incubation with unlabeled (E)-GDP or (E,E)-FDP substrates (set at 100). Each experiment was run by the mean of three to six independent replicates. ^b Apparent total rate isotope effects compared to those of incubation with unlabeled (E)-GDP or (E,E)-FDP substrates. ^c Apparent total rate isotope effects compared to those of incubation with (2*Z*)-[²H]-GDP or (2*Z,6E*)-[²H]-FDP substrates. Note: oxygenated cyclic volatiles not considered.

monodeuterated GDP (**1a**, **2c**) and FDP (**1a**, **2c**) had no direct influence on the reaction mechanism, since the C–D-bond is not cleaved during the entire cyclization cascade. Moreover, the variations in the product profiles and the overall rates were a result of apparent secondary isotope effects.

Isotope effects on product distributions. In order to investigate the impact of the isotope sensitive branching on product distributions, the olefinic products were quantified after incubation of TPS4 and TPS5 with (**2a–d**) (Fig. 3, 4 and ES†). The primary kinetic isotope effects were calculated using the shift in the product distribution after conversion of the unlabeled substrate (used as reference) or the mono- or hexadeuterated products according the following relationship:

$$\frac{k_H}{k_D} = \left[\frac{\% \text{ comp. X}}{\% \text{ comp. Y}} \right]_H \times \left[\frac{\% \text{ comp. X}}{\% \text{ comp. Y}} \right]_D \quad (1)$$

X and Y are pairs of cyclic products arising from a same branched point.

As mentioned above, the oxygenated cyclic volatiles were not considered in the present data.¹⁴ To estimate the weight of this approximation, quantitative kinetic measurements were carried out. Since TPS4-B73 and TPS5-Delprim exhibit similar basic features, only deuterium isotope effects on the catalytic activity of TPS4 were evaluated using the noncompetitive method. Both unlabeled (2*E,6E*)-FDP and (2*E,6E*)-[²H₆]-FDP **1d** substrates were used in two independent enzyme assays. Standard enzyme assays were performed in triplicate with aliquots of the same enzyme extracts under saturated substrate conditions. A decrease of 13% (relative to the reference substrate) of the maximal rate for sesquiterpene formation was observed when (2*E,6E*)-[²H₆]-FDP **1d** was incubated with TPS4, while similar K_m were obtained for both substrates. Since the kinetic experiments were performed using the same enzyme extract,



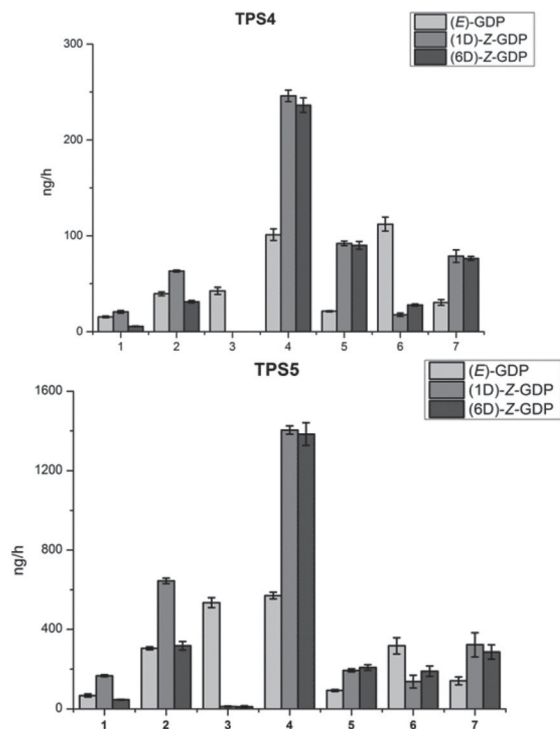


Fig. 3 Product distribution of main monoterpenes from incubations of deuterated GDP ($(2Z)$ - $[\text{H}]$ -GDP (**2a**) and $(2Z)$ - $[\text{H}_6]$ -GDP (**2b**) with TPS4-B73 and TPS5-*Delprim* from maize (*Zea mays*). (1) α -Thujene, (2) sabinene, (3) β -myrcene, (4) limonene, (5) α -terpinolene, (6) linalool, (7) α -terpineol.

the total enzyme concentration $[E_T]$ was identical for both assays. Therefore, the turnover number (k_{cat}) of the enzyme, usually defined as the ratio of $V_{\text{max}}/[E_T]$, can be approximated to V_{max} . The apparent total rate isotope effect $k_{\text{H}}/k_{\text{D}}$, determined from the maximal rates, equals 1.15. As discussed before, similar results were obtained when the oxygenated cyclic volatiles were not considered (19% decrease in the volatile production corresponding to a $k_{\text{H}}/k_{\text{D}} = 1.23$) and justify the approximation made above.

Monoterpene product distribution

Within a series ($2E$ (**1a-b**) or $2Z$ (**2a-b**)) both cyclases showed negligible changes in the formation of limonene, α -terpinolene and α -terpineol (Fig. 3) independent of the degree of labeling of the substrate used. Thus, minor kinetic isotope effects (KIE) were measured after incubation of $(2E)$ - $[\text{H}]$ -GDP **1a** or $(2E)$ - $[\text{H}_6]$ -GDP **1b** in comparison to the unlabeled $(2E)$ -GDP as well as after incubation of hexadeuterated $(2Z)$ - $[\text{H}_6]$ -GDP **2b** in comparison to the monodeuterated analog $(2Z)$ - $[\text{H}]$ -GDP **2a**. In contrast sabinene and α -thujene showed decreases associated with a corresponding increase in sabinene hydrate after incubation with TPS4 and TPS5. The observed KIEs for the sabinene and α -thujene deprotonation reactions were calculated from eqn (1). In case of substrates differing by only one deuterium atom, the observed KIEs ($k_{\text{H}}/k_{1\text{D}}$) $_E$ were much

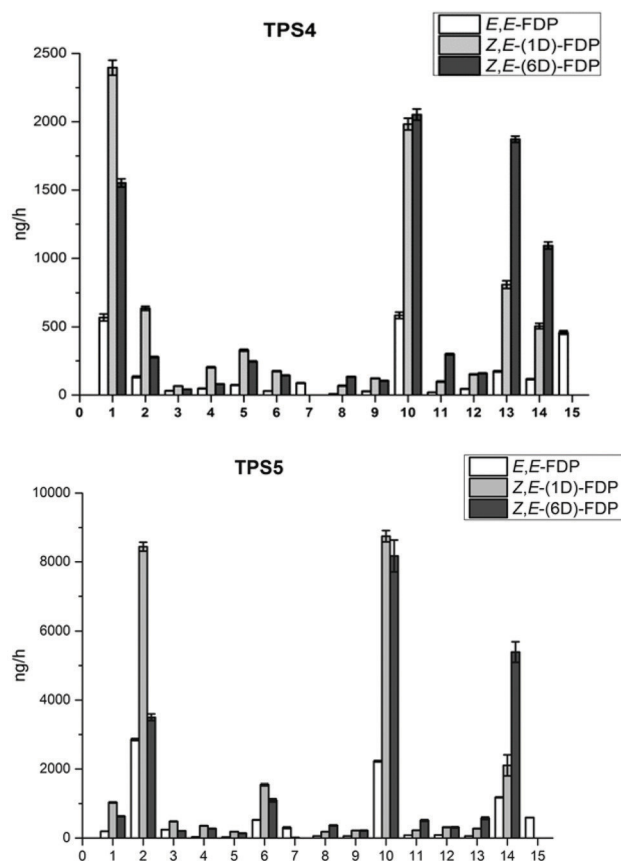


Fig. 4 Product distribution of main sesquiterpenes from incubations of deuterated FDP ($(2Z,6E)$ - $[\text{H}]$ -GDP (**2c**) and $(2Z,6E)$ - $[\text{H}_6]$ -GDP (**2d**) with TPS4-B73 and TPS5-*Delprim* from *Zea mays*. Major sesquiterpene products: (1) 7-*epi*-sesquithujene, (2) sesquithujene, (3) (Z) - α -bergamotene, (4) (E) - α -bergamotene, (5) sesquisabinene A, (6) sesquisabinene B, (7) (E) - β -farnesene, (8) γ -curcumene, (9) zingiberene, (10) (S) - β -bisabolene, (11) β -curcumene, (12) (E) - γ -bisabolene, (13) 7-*epi*-sesquithujene hydrate, (14) sesquithujene hydrate, (15) $(3R)$ - (E) -nerolidol.

weaker (a range of $k_{\text{H}}/k_{\text{D}} = 1.10$ – 1.18). However, the observed KIEs [$(k_{\text{H}}/k_{6\text{D}})_E$, $(k_{1\text{D}}/k_{6\text{D}})_E$ or $(k_{1\text{D}}/k_{6\text{D}})_Z$], corresponding to a difference of 5 to 6 deuterium atoms between the substrates, lie in the range of $k_{\text{H}}/k_{\text{D}} = 1.91$ – 5.68 . The interesting fact was that the $(2Z)$ -substrates ($k_{1\text{D}}/k_{6\text{D}})_Z$ showed the lowest KIEs and this effect was negligible when comparison is made with $(2E)$ -substrates.

Sesquiterpene product distribution

The same approach was used to evaluate the shift of products after incubation with different FDP substrates (E (**1c-d**) and Z (**2c-d**)) (Fig. 4). Despite the blend of volatiles being much more complex than in the case of monoterpenes, isotope effects on sesquiterpene volatiles can be observed after incubation with deuterated substrates. The first set of sesquiterpenes, comprising (S) - β -bisabolene, (E) - γ -bisabolene and zingiberene, were not affected by the isotope sensitive branching experiments and minor changes in product formation were observed after incubation with hexadeuterated substrates.



An important decrease in the formation of 7-*epi*-sesquithujene, sesquithujene, sesquisabinenes A and B and (*E*)- and (*Z*)- α -bergamotene isomers were observed from (2*E*,6*E*)- or (2*Z*,6*E*)-[²H₆]-FDP (**1d** or **2d**) (10–64% with TPS4 and 26–61% with TPS5, in comparison with unlabeled (2*E*,6*E*)-FDP or (2*Z*,6*E*)-[²H]-FDP **2c**, respectively). This rate suppression was coupled with a corresponding enhancement in the formation rate of β - and γ -curcumene isomers, sesquithujene hydrate and 7-*epi*-sesquithujene hydrate (175–400% for TPS4 and 193–255% for TPS5, in comparison with unlabeled (2*E*,6*E*)-FDP or (2*E*,6*Z*)-[²H]-FDP **2c**, respectively). Because of higher complexity involved in biosynthesis of sesquiterpene volatiles as compared to monoterpenes, only the observed KIEs for the deprotonation reactions leading to 7-*epi*-sesquithujene and sesquithujene were determined. The corresponding KIEs ($k_{\text{H}}/k_{\text{D}}$)_E were close to unity, demonstrating that the deuterium label at C(3) had almost no influence on the reaction cascade. The observed KIEs [($k_{\text{H}}/k_{\text{6D}}$)_E, ($k_{\text{1D}}/k_{\text{6D}}$)_E or ($k_{\text{1D}}/k_{\text{6D}}$)_Z] were in the range of $k_{\text{H}}/k_{\text{D}} = 1.38$ –4.08 for the terminating deprotonation reaction leading to 7-*epi*-sesquithujene and $k_{\text{H}}/k_{\text{D}} = 2.17$ –6.24 for the terminating deprotonation reaction leading to sesquithujene. Again as observed with monoterpenes the lowest KIEs (($k_{\text{1D}}/k_{\text{6D}}$)_Z) were calculated between (*ZZ*)-substrates and were much lower as compared with natural isomers. The huge turnover difference and lower KIEs suggest that enzyme is much more efficient when incubated with (*ZZ*)-substrates (**2a–d**) in spite of isotope effects.

β -Secondary KIEs and hyperconjugation

Terpene cyclization cascades catalyzed by cyclases involve the internal additions to remaining double bond, hydride shifts or rearrangements of highly reactive carbocations before their ultimate quenching by deprotonation or nucleophile capture. We had previously proposed¹² a reaction mechanism for the formation of mono- and sesquiterpene products by TPS4 and TPS5 consistent with the carbocationic mechanisms described for other sesquiterpene syntheses.²⁵ Stabilization of the carbocationic intermediates is partly ensured by interactions with the hydrophobic, aromatic-rich active-site of the enzyme (*e.g.* π -cation interactions with aromatic residues of the active site).²⁶ Nevertheless, hyperconjugative interactions within carbocations themselves also play an important role in their stability. In molecular orbital terms, hyperconjugation is described as the interaction of the vacant p-type orbital on the cationic center with adjacent C–H or C–C σ -bonds.²⁰ Magnitude of this hyperconjugative effect depends on the number of hydrogen atoms attached to the carbon atom immediately adjacent to the unsaturated system. Because the energy required for breaking a C–D bond is higher than that for a C–H bond, a C–D hyperconjugation stabilizes an adjacent positive charge less than a C–H hyperconjugation. Consequently, reactions in which C–D bonds are broken proceed more slowly than reactions in which C–H bonds are broken. Such hyperconjugative weakening in intermediates due to isotope substitution induces secondary kinetic isotope effects. In the present study, these secondary KIEs combine with the primary KIEs and alter

the product distributions after isotopically sensitive branching with both enzymes.

To illustrate the effects of hyperconjugation and the secondary KIEs, the case of (*ZZ*)-[²H₆]-GDP **2b** is depicted in Fig. 5 as a representative example. From (*ZZ*)-[²H₆]-GDP **2b** (Fig. 5), there is distinct lack of acyclic products due to the lack of an isomerization step. The cyclization cascade is initiated by the formation of the (*S*)- and (*R*)-terpinyl carbocations **A**₁ and **A**₂. Deuterium isotope effects on the monoterpene product distribution can be rationalized in terms of hyperconjugation. The positive charge is positioned far from the area of the deuterated carbons, hence deprotonation or water capture terminating steps leading to (*S*)-(-)-limonene and α -terpineol or α -terpinolene are not influenced by kinetic isotope effects. The minor KIEs observed for limonene, α -terpinolene and α -terpineol reflect the low destabilizing influence of the labeled carbon center in the two α -terpinyl carbocations. From **A**₁ and **A**₂ the cyclization cascade can proceed with the formation of carbocation **B** followed by subsequent rearrangement into the tertiary highly unstable carbocations **C**₁ and **C**₂. Here, the positive charge is fully surrounded by deuterium atoms and consequently less stabilized by C–H hyperconjugation than in the corresponding unlabeled compound. This leads to comparatively higher deuterium isotope effects on the formation of sabinene, sabinene hydrate and α -thujene. This leads to decreased deprotonation and higher formation of sabinene hydrate after capture by water molecule.

Similar considerations apply to the formation of sesquiterpenes by maize TPS4 and TPS5. From (2*Z*,6*E*)-[²H₆]-FDP **2d**, few acyclic products are formed and the cyclization cascade is initiated by the formation of (*S*)- and (*R*)-bisabolyl cations. These first carbocations can be directly deprotonated to produce (*S*)- β -bisabolene without noticeable KIEs. These observations are consistent with the product distribution obtained from isotopically sensitive branching experiments. Deuterium isotope effects are less pronounced in the case of the mono-deuterated analogue **2c** vs. hexadeuterated analogue **2d** since the positive charge can at most be surrounded by only one deuterium atom, with the other hydrogen atoms being able to undergo C–H hyperconjugative interactions. Higher KIEs were obtained for the formation of sesquithujene, 7-*epi*-sesquithujene or sesquisabinenes A and B after incubation with the hexadeuterated (*ZZ*)-substrate (**2d**) since these products are formed from carbocations that are fully surrounded by deuterium labeled carbons. This results in higher KIEs as the final product formation can only proceed *via* isotope labeled centers. In case of bisabolyl carbocations, minor KIEs were observed for β or γ -bisabolene formation because the positive charge is not disturbed by the deuterium labeled carbon center. Similarly, slight KIEs were observed for zingiberene isomers because carbocations were not highly destabilized by deuterium substitution. These experiments clearly show that isotope effects follow the same patterns within both the geometric isomers. Thus, (*ZZ*) substrate geometry provides an advantage in the early steps of reaction cascade that accounts for higher turnover and selection towards cyclic products.



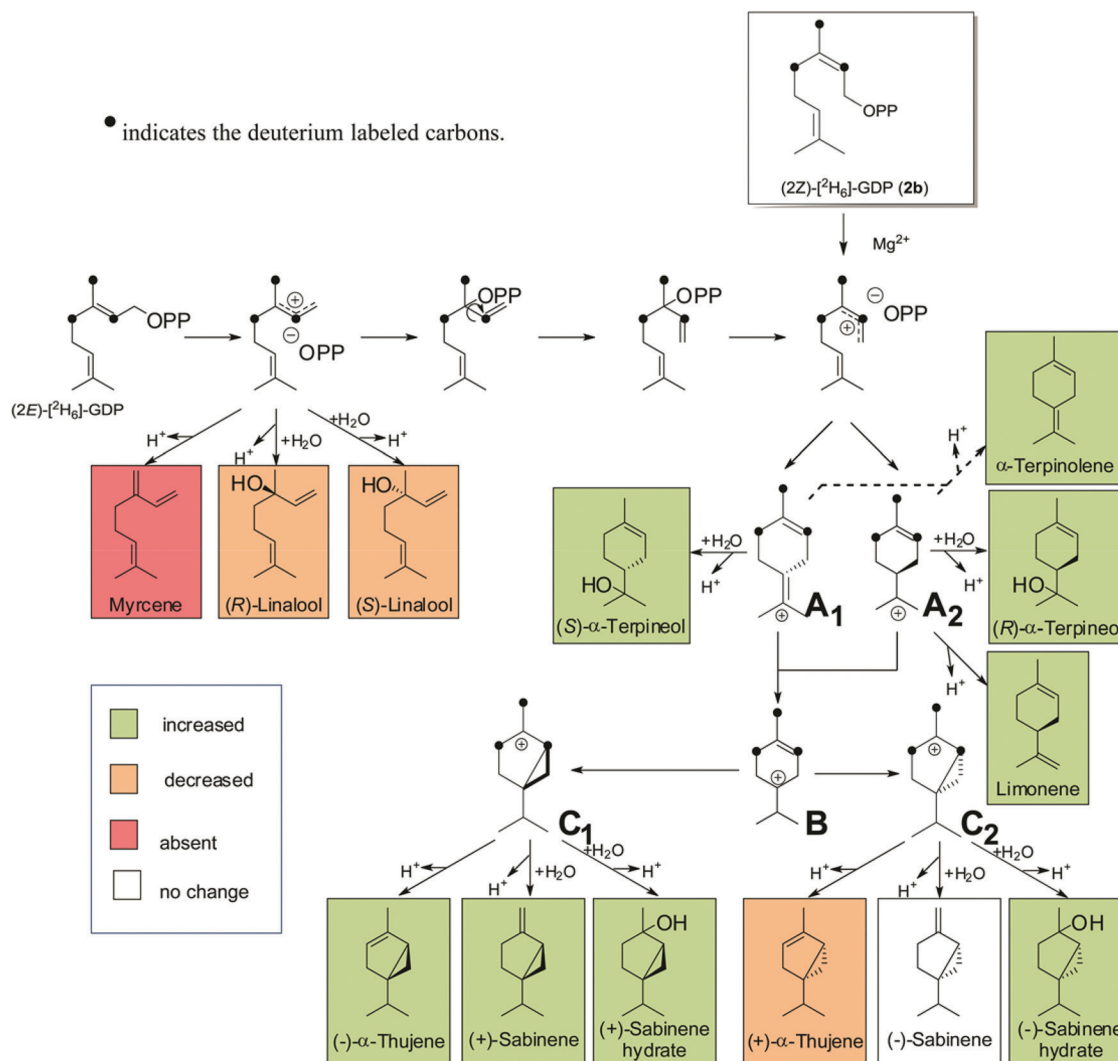


Fig. 5 Proposed reaction mechanism for the formation of monoterpenes by TPS4 and TPS5 from (2Z)-[²H₆]-GDP (2b) and (2E)-[²H₆]-GDP (1b).

A major determinant of product selectivity is the degree of conformational flexibility of the substrate in the active site of a terpene synthase. To explore the structural basis for the proposed reaction mechanism of maize TPS4, we had modeled the protein structure of this enzyme (TPS4) using the data available for 5-*epi*-aristolochene synthase (TEAS).¹³ The active site cavity of TPS4 is divided into two pockets by the G2 helix which reaches slightly into the cavity. Previously, four of the amino acids that make up the G2 helix were shown to have a major impact on the product specificity of TPS4.¹² Docking of the (*E,E*)-FDP substrate showed that the olefin moiety of the FDP substrate is located predominantly in one of the two pockets (pocket I). The early steps of the catalytic sequence including dephosphorylation, isomerization, and cyclization, up to the formation of the bisabolyl carbocation, all take place in pocket I. When the bisabolyl carbocation adopts an alternate conformation, it shifts to pocket II. Then, a variety of additional cyclizations, hydride shifts, and deprotonations occur in pocket II

leading to the formation of bicyclic products like 7-*epi*-sesquithujene. The energy requirement for the conformational change that drives pocket shifting is likely to be very small determined both by the chemical nature of the intermediate and the surrounding amino acids.¹³ This structural feature of having two pockets, is likely to be advantageous for initial interactions of enzyme with the deuterated (2Z)-GDP and (2Z,6E)-FDP tested in this study. Both of these have already undergone isomerization around the C(2)–C(3) bond, so the only activity left in pocket I is conversion to the corresponding carbocation. After these 2Z substrates cross the small energy barrier to pocket II, they are converted to a larger proportion of cyclic products than the (2E)-substrates. The enzyme likely has better efficiency with (2Z)-substrates because of lower energy requirements, as substrates are directly cyclized after ionization. This could explain not only the reduction in acyclic substrates and smaller kinetic isotope effects, but also the availability of more energy that can be utilized for processes in pocket II.



Recently, isotopically sensitive branching experiments have been used to identify the carbocation cascade reaction leading to the tricyclic sesquiterpene pentalene which was first predicted using quantum chemical calculations.²⁷ Deuterium isotope effects have also been used to study the reaction kinetics of initial dissociation of pyrophosphate moiety in sesquiterpene cyclization by tobacco *epi*-aristolochene synthase and monoterpene cyclization by pinene synthases from *Salvia officinalis*.^{15c,28} In this study we have utilized isotope sensitive branching experiments to study the effects of alternate substrate geometry around the C(2)–C(3) double bond on volatile production in multiproduct terpene synthase enzymes. The observation of increased turnover of cyclic products with (2*Z*)-substrate geometry may be useful in direction terpene synthase reaction cascades towards desired cyclic products.

Conclusion

In this work we investigate the effects of alternate substrate stereochemistry on the reaction mechanism of two maize multiproduct synthases that isomerize the C(2)–C(3) π bond of (2*E*,6*E*)-FDP via an NDP intermediate. We were interested in the impact of geometry as well as isotope effects on the product distribution of multiproduct enzymes. There was indeed major influence of the (2*Z*)-isomers on the enzymatic cascade as confirmed by deuterium labeling of products. The product distribution results showed a strong preference for cyclic products as a result of the alternate C(2)–C(3) geometry, indicating the rate limiting effects of the isomerization step in the natural biosynthesis of terpenes. There was also a major impact on efficiency with higher turnover and lower kinetic isotope effects observed with (2*Z*)-isomers as compared with natural (2*E*)-substrates. This can be rationalized in terms of availability of a preferable conformer and lower energy requirements which increases the efficiency of catalysis. This strong preference for cyclic products and huge turnover can be exploited to direct biosynthesis by certain terpene synthases already known for their catalytic promiscuity.

Acknowledgements

We thank Kerstin Ploss for the HRMS measurements, Stephan von Reuss and Stefan Garms for editorial assistance and Grit Winnefeld for administrative support. This work was supported by the Max Planck Society.

References

- M. Wink, *Phytochemistry*, 2003, **64**, 3.
- (a) J. S. Dickschat, *Nat. Prod. Rep.*, 2011, **28**, 1917; (b) J. D. Connolly and R. A. Hill, *Dictionary of Terpenoids*, Chapman & Hall, New York, 1992.
- (a) E. Nambara and A. Marion-Poll, *Annu. Rev. Plant Biol.*, 2005, **56**, 165; (b) E. Pichersky and J. Gershenzon, *Curr. Opin. Plant Biol.*, 2002, **5**, 237; (c) J. H. Langenheim, *J. Chem. Ecol.*, 1994, **20**, 1223.
- (a) T. G. Köllner, C. Schnee, J. Gershenzon and J. Degenhardt, *Plant Cell*, 2004, **16**, 1115; (b) J. Gershenzon and R. B. Croteau, *Lipid Metab. Plants*, 1993, 339.
- (a) J. Degenhardt, T. G. Köllner and J. Gershenzon, *Phytochemistry*, 2009, **70**, 1621; (b) D. J. Schenk, C. M. Starks, K. R. Manna, J. Chappell, J. P. Noel and R. M. Coates, *Arch. Biochem. Biophys.*, 2006, **448**, 31.
- (a) N. Tokuriki and D. S. Tawfik, *Science*, 2009, **324**, 203; (b) D. W. Christianson, *Curr. Opin. Chem. Biol.*, 2008, **12**, 141.
- E. M. Davis and R. Croteau, in *Biosynthesis: Aromatic Polyketides, Isoprenoids, Alkaloids*, Springer-Verlag, Berlin, 2000, pp. 53–95.
- D. B. Little and R. B. Croteau, *Arch. Biochem. Biophys.*, 2002, **402**, 1201.
- J. Bohlmann, G. Meyer-Gauen and R. Croteau, *Proc. Natl. Acad. Sci. U. S. A.*, 1998, **95**, 4126.
- C. M. Starks, K. W. Back, J. Chappell and J. P. Noel, *Science*, 1997, **277**, 1815.
- D. C. Williams, D. J. McGarvey, E. J. Katahira and R. Croteau, *Biochemistry*, 1998, **37**, 12213.
- T. G. Köllner, C. Schnee, J. Gershenzon and J. Degenhardt, *Plant Cell*, 2004, **16**, 1115.
- T. G. Köllner, P. E. O'Maille, N. Gatto, W. Boland, J. Gershenzon and J. Degenhardt, *Arch. Biochem. Biophys.*, 2006, **448**, 83.
- N. Gatto, A. Vattekkatte, T. Köllner, J. Degenhardt, J. Gershenzon and W. Boland, *Chem. Commun.*, 2015, **51**, 3797.
- (a) I. Alchanati, J. A. A. Patel, J. Liu, C. R. Benedict, R. D. Stipanovic, A. A. Bell, Y. Cui and C. W. Magill, *Phytochemistry*, 1998, **47**, 961; (b) S. Picaud, P. Mercke, X. F. He, O. Sterner, M. Brodelius, D. E. Cane and P. E. Brodelius, *Arch. Biochem. Biophys.*, 2006, **448**, 150; (c) D. J. Schenk, C. M. Starks, K. R. Manna, J. Chappell, J. P. Noel and R. M. Coates, *Arch. Biochem. Biophys.*, 2006, **448**, 31; (d) S.-H. Kim, K. Heo, Y.-J. Chang, S.-H. Park, S.-K. Rhee and S.-U. Kim, *J. Nat. Prod.*, 2006, **69**, 758.
- (a) C. R. Benedict, J. L. Lu, D. W. Pettigrew, J. G. Liu, R. D. Stipanovic and H. J. Williams, *Plant Physiol.*, 2001, **125**, 1754; (b) D. E. Cane, G. H. Yang, Q. Xue and J. H. Shim, *Biochemistry*, 1995, **34**, 2471; (c) L. S. Vedula, D. E. Cane and D. W. Christianson, *Biochemistry*, 2005, **44**, 12719; (d) L. S. Vedula, M. J. Rynkiewicz, H.-J. Pyun, R. M. Coates, D. E. Cane and D. W. Christianson, *Biochemistry*, 2005, **44**, 6153; (e) J. Degenhardt, T. G. Köllner and J. Gershenzon, *Phytochemistry*, 2009, **70**, 1621; (f) T. G. Köllner, C. Schnee, S. Li, A. Svatos, B. Schneider, J. Gershenzon and J. Degenhardt, *J. Biol. Chem.*, 2008, **283**, 20779.
- D. Arigoni, D. E. Cane, J. H. Shim, R. Croteau and K. a. Wagschal, *Phytochemistry*, 1993, **32**, 623.
- M. Kunert, P. Rahfeld, K. H. Shaker, B. Schneider, A. David, K. Dettner, J. M. Pasteels and W. Boland, *ChemBioChem*, 2013, **14**, 353.



- 19 A. B. Woodside, Z. Huang and C. D. Poulter, *Org. Synth.*, 1993, **8**, 616.
- 20 D. E. Cane, H. T. Chiu, P. H. Liang and K. S. Anderson, *Biochemistry*, 1997, **36**, 8332.
- 21 (a) P. E. O'Maille, J. Chappell and J. P. Noel, *Arch. Biochem. Biophys.*, 2006, **448**, 73; (b) T. G. Köllner, J. Gershenzon and J. Degenhardt, *Phytochemistry*, 2009, **70**, 1139; (c) F. Lopez-Gallego, S. A. Agger, D. Abate-Pella, M. D. Distefano and C. Schmidt-Dannert, *ChemBioChem*, 2010, **11**, 1093.
- 22 (a) J. A. Faraldos, P. E. O'Maille, N. Dellas, J. P. Noel and R. M. Coates, *J. Am. Chem. Soc.*, 2010, **132**, 4281; (b) J. P. Noel, N. Dellas, J. A. Faraldos, M. Zhao, B. A. Hess, L. Smentek, R. M. Coates and P. E. O'Maille, *ACS Chem. Biol.*, 2010, **5**, 377.
- 23 (a) R. Croteau and D. M. Satterwhite, *J. Biol. Chem.*, 1989, **264**, 15309; (b) W. Schwab, D. C. Williams, E. M. Davis and R. Croteau, *Arch. Biochem. Biophys.*, 2001, **392**, 123.
- 24 (a) C. L. Steele, J. Crock, J. Bohlmann and R. Croteau, *J. Biol. Chem.*, 1998, **273**, 2078; (b) S. Picaud, M. E. Olsson, M. Brodelius and P. E. Brodelius, *Arch. Biochem. Biophys.*, 2006, **452**, 17; (c) J. Bohlmann, J. Crock, R. Jetter and R. a. Croteau, *Proc. Natl. Acad. Sci. U. S. A.*, 1998, **95**, 6756; (d) S. M. Colby, J. E. Crock, P. G. Lemaux and R. B. Croteau, *Official Gazette of the United States Patent and Trademark Office Patents*, 1254, 2002.
- 25 D. E. Cane, *Compr. Nat. Prod. Chem.*, 1999, **2**, 155.
- 26 C. A. Lesburg, J. M. Caruthers, C. M. Paschall and D. W. Christianson, *Curr. Opin. Struct. Biol.*, 1998, **8**, 695.
- 27 L. Zu, M. Xu, M. W. Lodewyk, D. E. Cane, R. J. Peters and D. J. Tantillo, *J. Am. Chem. Soc.*, 2012, **134**, 11369.
- 28 (a) K. C. Wagschal, H. J. Pyun, R. M. Coates and R. Croteau, *Arch. Biochem. Biophys.*, 1994, **308**, 477; (b) J. R. Mathis, K. Back, C. Starks, J. Noel, C. D. Poulter and J. Chappell, *Biochemistry*, 1997, **36**, 8340.



6.3 Manuscript III: Inhibition of a multiproduct terpene synthase from *Medicago truncatula* by 3-bromoprenyl diphosphates

Abith Vattekkatte,¹ Dr. Nathalie Gatto,² Eva Schulze,³ PD Dr. Wolfgang Brandt⁴ and

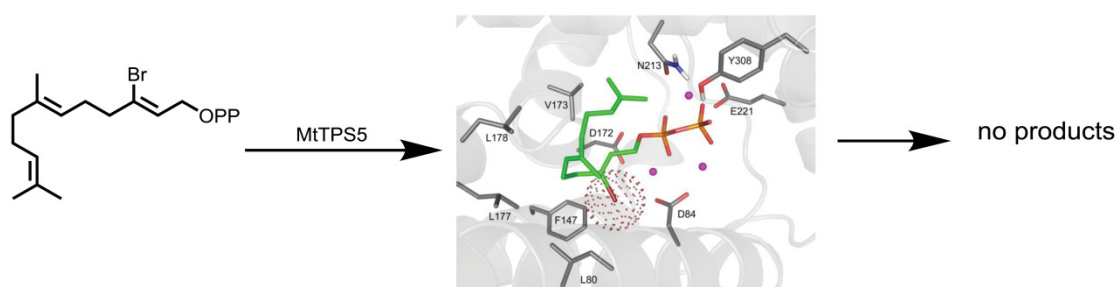
Prof. Dr. Wilhelm Boland⁵

Org. Biomol. Chem., 2015, 16, 4776-4784

DOI: 10.1039/C5OB00506J

Reproduced by permission of the Royal Society of Chemistry

Graphical Abstract



Summary

The multiproduct sesquiterpene synthase MtTSP5 from *Medicago truncatula* catalyzes the conversion of farnesyl diphosphate (FDP) into a complex mixture of 27 terpenoids. 3-Bromo substrate analogues of geranyl diphosphate (3-BrGDP) and farnesyl diphosphate (3-BrFDP) were evaluated as substrates of MTSP5 enzyme. Kinetic studies demonstrated that these compounds were highly potent competitive inhibitors of the MtTSP5 enzyme with fast binding and slow reversibility. These molecules might be ideal candidates for obtaining a co-crystal structure with multiproduct terpene synthases. Due to the structural and mechanistic similarity between various terpene synthases we expect these 3-bromo isoprenoids to be ideal probes for crystal structure studies.



Cite this: *Org. Biomol. Chem.*, 2015, **13**, 4776

Inhibition of a multiproduct terpene synthase from *Medicago truncatula* by 3-bromoprenyl diphosphates†

Abith Vattekkatte,^a Nathalie Gatto,^a Eva Schulze,^b Wolfgang Brandt^b and Wilhelm Boland*^a

The multiproduct sesquiterpene synthase MtTPS5 from *Medicago truncatula* catalyzes the conversion of farnesyl diphosphate (FDP) into a complex mixture of 27 terpenoids. 3-Bromo substrate analogues of geranyl diphosphate (3-BrGDP) and farnesyl diphosphate (3-BrFDP) were evaluated as substrates of MTPS5 enzyme. Kinetic studies demonstrated that these compounds were highly potent competitive inhibitors of the MtTPS5 enzyme with fast binding and slow reversibility. Since there is a lack of knowledge about the crystal structure of multiproduct terpene synthases, these molecules might be ideal candidates for obtaining a co-crystal structure with multiproduct terpene synthases. Due to the structural and mechanistic similarity between various terpene synthases we expect these 3-bromo isoprenoids to be ideal probes for crystal structure studies.

Received 13th March 2015,
Accepted 18th March 2015

DOI: 10.1039/c5ob00506j

www.rsc.org/obc

Terpenes constitute the largest and most diverse class of plant natural products with more than 55 000 members.¹ They serve many biological functions such as hormones, structural components of membranes, attractants for pollinators, toxins, feeding or as oviposition deterrents to insects.^{2–5} Despite their enormous structural variety, all terpenes are essentially derived from simple linear precursors such as geranyl diphosphate (GDP), farnesyl diphosphate (FDP), and geranylgeranyl diphosphate (GGDP). The cyclization of GDP to monoterpenes, FDP to sesquiterpenes and GGDP to diterpenes is accomplished by enzymes known as terpene synthases. Structurally, sesquiterpenes are one of the most diverse classes of terpenes isolated from plants, fungi, bacteria, and marine invertebrates.⁶ All sesquiterpenoids known to date are based on 300 basic hydrocarbon skeletons; these skeletons are generated by cyclization of FDP by sesquiterpene synthases.⁷

Sesquiterpene synthases are capable of catalyzing the formation of some of the most complex carbon–carbon bond forming reactions found in nature.⁸ Despite of their promiscuous nature, active site of these synthases strictly control the reaction pathway by directing the way isoprenoid chain folds, shielding the cation from early nucleophilic attack, and guiding carbocation cascade to its final products by quench-

ing. Even in sesquiterpene synthases, while some generate a single product, others produce complex bouquets of acyclic and cyclic products from a single precursor.⁹ The δ -selinene synthase and the γ -humulene synthase from *Abies grandis* hold the current record for producing 52 and 34 different sesquiterpenes, respectively.¹⁰ The lack of crystal structures of multiproduct terpene synthases, has led to great interest in the three-dimensional contour of the active site which retains such control over the reaction cascade. This knowledge is pivotal as it forms the mechanistic basis for the varying selectivity resulting in different conformations of the reactive cationic intermediates. Earlier we had reported that a multiproduct terpene synthase MtTPS5 (Fig. 1) from *Medicago truncatula* produces 27 products from FDP.^{11,12}

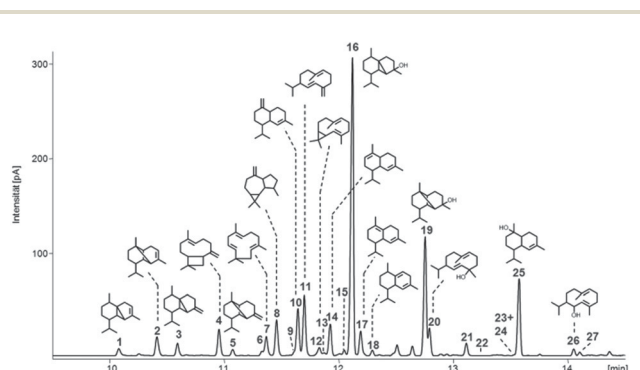


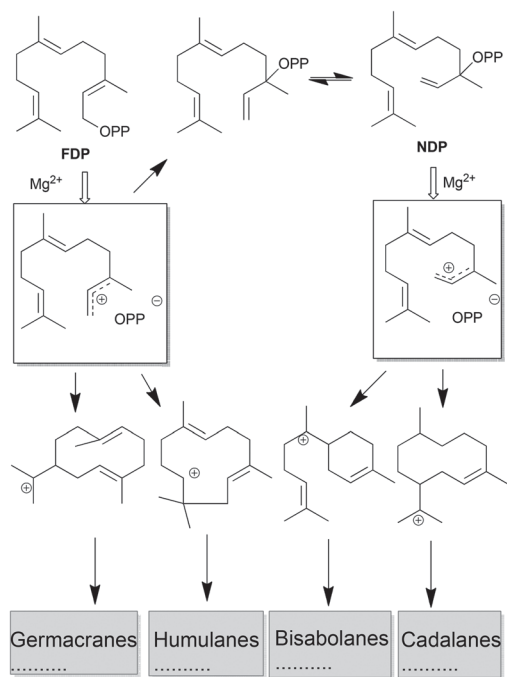
Fig. 1 GC chromatogram of sesquiterpenoids formed on incubation of FDP with MtTPS5 from *M. truncatula*.

^aDepartment of Bioorganic Chemistry, Max Planck Institute for Chemical Ecology, Hans-Knöll-Strasse 8, D-07745 Jena, Germany. E-mail: boland@ice.mpg.de

^bDepartment of Bioorganic Chemistry, Leibniz Institute of Plant Biochemistry, Weinberg 3, 06120 Halle (Saale), Germany

† Electronic supplementary information (ESI) available: Experimental procedure and spectra are included. See DOI: 10.1039/c5ob00506j





Scheme 1 Simplified cyclization pathways of FDP with MtTPS5.

We had also previously proposed the complex mechanistic pathway controlled by the MtTPS5 using a combination of techniques including labelling experiments.¹¹ In brief, the reaction cascade is initiated by the formation of a highly reactive farnesyl carbocation by the disassociation of diphosphate moiety. The C1 to C11 ring closure affords the humulyl cation, which generates terpenoids such as α-humulene and β-caryophyllene (Scheme 1). Most of the products require the initial C1 to C10 closure generating the germacren-11-yl cation which is further cyclized to products like germacrene D and germacrene based alcohols. The other key cationic intermediates are (2Z,6E)-germacren-1-yl cation and cadinan-7-yl cation, leading to about 80% of products. These intermediates are generated by isomerization of FDP to nerolidyl diphosphate (NDP). Even alteration of a single amino acid has a dramatic effect on the product profile; alteration of tyrosine to phenylalanine in MtTPS5 prevents the formation of a key intermediate *via* protonation of germacrene D. The tight control of the enzyme leads to optically pure products resulting from cyclization steps and hydride shifts. Hence, it is of vital importance to understand the electrostatic interactions within active site. One possibility is to link the structure with complex catalytic cascade by using alternate substrates.¹³

Substrate analogues have been used successfully to probe the specificity of the enzymes and obtain a substrate-bound crystal structure of enzymes.^{14–16} Natural biosynthesis allows these substrates to carry only methyl substituents, but synthetic approaches can provide various analogues of the natural substrates. Especially, substitution with sulphur has been used quite successfully for co-crystallization with different terpene synthases.^{17,18} In a recent example from Heaps *et al.*,¹⁴ chlori-

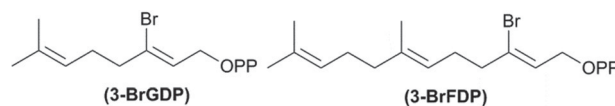


Fig. 2 GDP analogue (3-BrGDP) and FDP analogue (3-BrFDP).

nated substrates have been shown to be alternative co-substrates for farnesyl diphosphate synthase and also acting as inhibitors when both substrates were chlorinated. Fluorinated substrates have been successfully used to study the cyclization mechanism of several terpene synthases, in particular the aristolochene synthases.¹⁹ Thus, non-natural substrates have shown great potential as substrates or inhibitors to probe mechanisms and can be further utilized for the investigation of multiproduct terpene synthases.

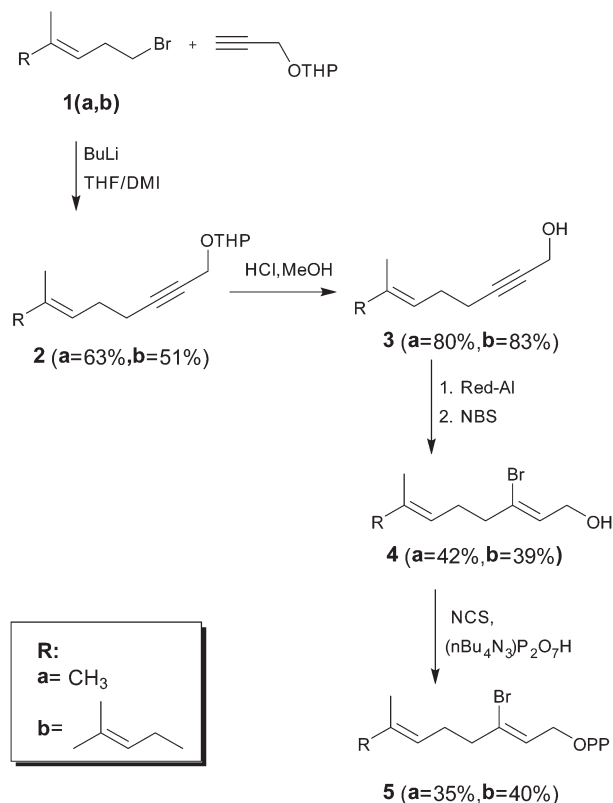
Based on the information obtained from mechanistic studies of MtTPS5,¹¹ we have designed a set of functional analogues of prenyl diphosphates for this enzyme that could destabilize the developing allylic carbocation. The GDP analogue (3-BrGDP) and FDP analogue (3-BrFDP) (Fig. 2) were considered because of their geometrical similarity and virtually identical van der Waals radius and volume (*ca.* 2.0 Å,²⁰ *cf.* also Fig. 6) with the methyl group at C3 position of natural substrates. The highly electronegative bromine atom can strongly influence the stability of the neighboring carbocationic species but imposes no additional steric effect in comparison with the corresponding natural substrates. These analogues could either provide novel sesquiterpenes that could be further utilized to investigate mechanistic aspects of the MtTPS5, or they could act as potent inhibitors of MtTPS5. In case of inhibition it can be used to provide an active site resolved crystal structure like in the case of aristolochene synthase with farnesyl-*S*-thiolodiphosphate.²¹ There is a lack of definitive understanding about the structure of multiproduct terpene synthases due to the absence of their crystal structures. These easy to synthesize inhibitors with identical sterical features could prove to be valuable tool for understanding the complex cyclization sequences in the active sites of these terpene cyclases.

Results and discussion

Synthesis

In order to investigate the potential of modified prenyl diphosphates, we have synthesized 3-bromo analogs of GDP (3-BrGDP) and FDP (3-BrFDP) as shown in Scheme 2. Alkylation of the THP ether of propargyl alcohol with 1-bromo-3-methylbut-2-ene (**1a**) and (*E*)-1-bromo-3,7-dimethylocta-2,6-diene (**1b**) provided the alkynes (**2a,b**) that were deprotected (MeOH, PPTS) to the propargyl alcohols (**3a**) and (**3b**). Reduction of the alcohols (**3a**) and (**3b**) with Red-Al, followed by reaction with *N*-bromosuccinimide gave the 3-bromo (*E*)-allylic alcohols (**4a**) and (**4b**). These alcohols were converted to 3-BrGDP (**5a**) and 3-BrFDP (**5b**) by sequential treatment with





Scheme 2 Synthesis of 3-BrGDP (5a) and 3-BrFDP (5b).

N-chlorosuccinimide and tris-(tetrabutyl-ammonium) hydrogen pyrophosphate in acetonitrile to yield the corresponding 3-bromoprenyl diphosphates.

Enzymatic characterizations of substrates

Inhibition studies. To test whether MtTPS5 would accommodate the replacement of a methyl group with a bromine atom, the terpene synthase from *Medicago truncatula* was incubated with the brominated analogues 3-BrGDP (5a) and 3-BrFDP (5b). Standard assays contained purified protein in assay buffer with substrate. The reaction mixture was covered with pentane containing dodecane as an internal standard to allow the quantification of reaction products. After being incubated for 90 min at 30 °C, the reaction was stopped and frozen in liquid nitrogen, and the pentane layer removed. The terpeneoid profiles resulting from the incubation experiments were analyzed by gas chromatography and compared to the profiles resulting from (2*E*)-GDP and (2*E*,6*E*)-FDP with the same enzyme. Results obtained by incubating both 3-BrGDP (5a) and 3-BrFDP (5b) with MtTPS5 showed no detectable formation of products. Longer incubation times (up to 24 hours) along with increased substrate and enzyme concentrations neither gave detectable amounts of brominated products or any other terpene-based derivatives. This indicated that enzyme is not able to initiate its catalytic cascade using 3-bromo substrates.

Both 3-BrGDP (5a) and 3-BrFDP (5b) were then assayed as inhibitors of the MtTPS5. With immediate mixing of enzyme, substrate, and inhibitor (no preincubation of enzyme and inhibitor), 3-BrGDP (5a) and 3-BrFDP (5b) were found to inhibit the MtTPS5 (Fig. 3). After preincubation for 1 h, standard assays containing protein in assay buffer with inhibitor and with natural substrate were performed (Fig. 3). The K_i , which was measured against MtTPS5 with 3-BrFDP (5b), was determined to be $1.54 \pm 0.21 \mu\text{M}$ and K_i with BrGDP (5a) was determined to be $1.25 \pm 0.23 \mu\text{M}$. Additional preincubations with the enzyme for 1, 2, 4 and 12 h prior to substrate addition at $t = 0$, showed no increase in potency of inhibition, demonstrating a fast onset of the inhibition of the enzyme.

Reversibility of inhibition. To determine whether the mechanism of inhibition of MtTPS5 by these compounds is rapidly reversible, slowly reversible, or irreversible, the activity was evaluated using a preincubation/dilution assay.²² To test the reversibility of the inhibition with 3-BrFDP (5b), MtTPS5 at

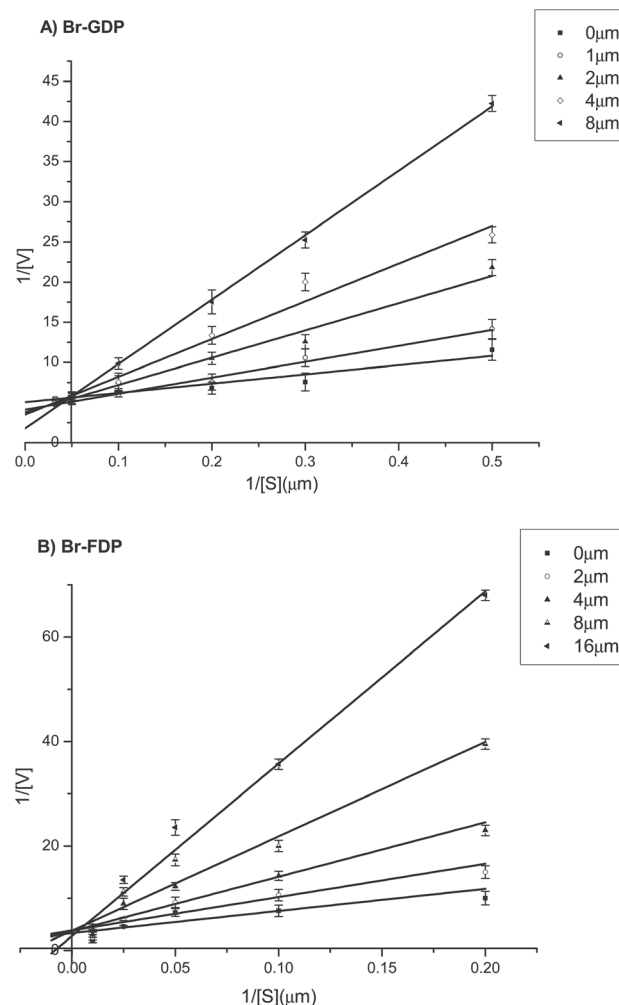


Fig. 3 Double reciprocal plots of initial rates versus the concentration of substrate for MtTPS5 catalyzed turnover of FDP in the presence of 3-BrGDP (5a) and 3-BrFDP (5b) are shown on panels A and B respectively.



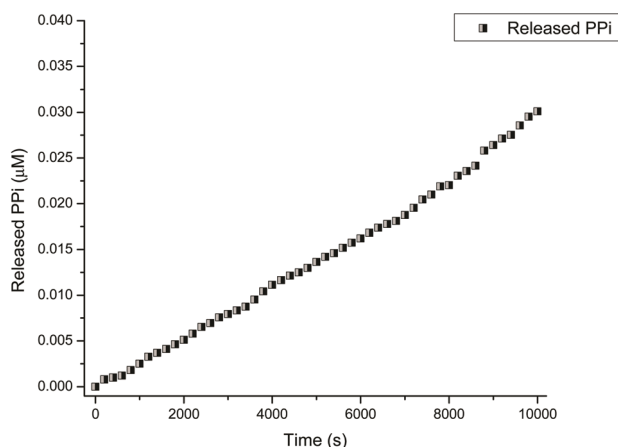


Fig. 4 Reversibility of Inhibition of MtTPS5 by 3-BrFDP (5b).

100-fold (its final assay concentration), and inhibitor at 10-fold its calculated IC_{50} , a condition is created where >90% of the enzyme should be in an enzyme-inhibitor complex. Upon 100-fold dilution of the enzyme pre-incubated mixture of enzyme-inhibitor complex and addition to assay buffer with substrate FDP, product formation was inhibited immediately after the addition of substrate because almost all the inhibitor 3-BrFDP (5b) was bound to the enzyme. Following the preincubated enzyme-inhibitor reaction condition for activity in separate assays, approximately 11% of the enzymatic activity in the inhibited reaction was returned after 50 minutes (Fig. 4). After 150 minutes, the rate of product formation for the pre-incubated reaction was about 5 times greater than the initial rate of product formation, showing that the inhibitor was being released from the enzyme-inhibitor complex and enzymatic activity was indeed recovering. Accordingly, 3-BrFDP (5b) acts as a very slow reversible inhibitor of the MtTPS5.

Ab initio calculations. This established that 3-BrGDP (5a) and 3-BrFDP (5b) inhibit the cyclization process of MtTPS5. It has already been shown that the allylic and vinyl fluoro substituents also have a retarding effect on the reactivity of various fluoro geranyl methanesulfonates.^{16,23} The bromo substituent at C3 has a large inductive electron withdrawing effect on the electron density of the adjoining double bond which evidently decreases its π basicity. This effect dramatically alters the stability of the allylic carbocations during the activation of the diphosphate substrate. Thus, for all enzymes proceeding through particular type of carbocationic intermediates as shown in Fig. 5, 3-bromo analogues would be poor substrates.

To investigate the influence of the 3-bromo substitution on the destabilization of the intermediate allyl cation, reaction energies calculations were carried out using TURBOMOLE²⁴ using DFT (B3-LYP^{25,26}) with the def-TZVPP basis set.²⁷ These calculations were performed for the corresponding cleavage of dimethylallyl diphosphate (DMAPP) and compared with 3-bromoallyl diphosphate (3-BrDMAPP) (Fig. 5). Whereas the cleavage of DMAPP requires only $31.9 \text{ kcal mol}^{-1}$, the corresponding 3-bromo analogue requires much more energy

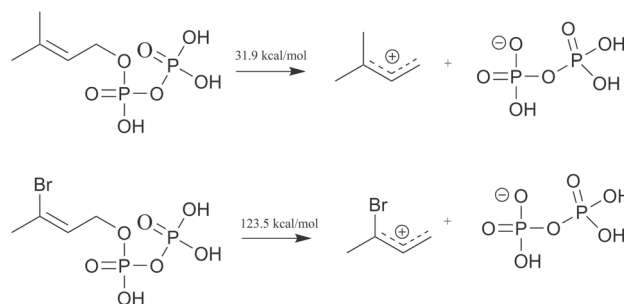


Fig. 5 *Ab initio* energy calculations for cleavage of DMAPP and 3-BrDMAPP.

($123.5 \text{ kcal mol}^{-1}$) and is clearly not energetically favorable. In the case of longer isoprenyl chains like GDP and FDP, the resulting carbocations are stabilized by specific cyclizations guided by the enzymatic active site. However, in case of 3-bromo analogues the huge endothermic energy required for the formation of the intermediate allyl cation prevents its formation, and hence, subsequent energy gain by cyclization is not possible. However, 3-Br GDP and 3-Br FDP are able to bind to the enzyme because there is no steric difference on comparison with the natural substrates. Since the dissociation of the diphosphate moiety is the first step, common to all prenyl diphosphate based terpenoid synthases and cyclases, we expect this simple analogues as a broadly applicable inhibitors. Preliminary experiments with a terpenoid synthase from insects isoprenyl diphosphate synthase 1 (PcIDS1)²⁸ from *Phaedon cochleariae* showed no catalytic formation of GDP with the incubation of substrates DMAPP and IDP.

Molecular mechanics simulations

In the case of the MtTPS5 enzyme, the three-dimensional contour of the active site forms the structural basis of varying selectivity that allows different conformations of the reactive cationic intermediates. Since the crystal structure for MtTPS5 is not yet known, we earlier compared the structure with the 5-*epi*-aristolochene synthase (TEAS) from *Nicotiana tabacum* that transforms FDP to 5-*epi*-aristolochene through the stable intermediate germacrene A which is also an intermediate of the MtTPS5 catalyzed reaction sequence.⁷ Starting from the TEAS crystal structure, Starks *et al.*²⁹ suspected that the hydroxyl group of tyrosine in the interaction with the two aspartate participates as a proton donor in the activation of germacrene A and forms a catalytic triad.²⁹ A comparison of the TEAS amino acid sequence shows that all three amino acids were conserved in MtTPS5 as well. This sequence similarity can be used to our advantage to model the active site interactions leading to products.

Recently, the co-crystal structure of aristolochene synthase (PDB code: 4KUX) from *Aspergillus terreus* with a bound FDP, a stable FDP analogue was reported. Despite differences in sequence alignment, the discussed triad the 84DDXXE motif essential for the diphosphate recognition corresponds with a



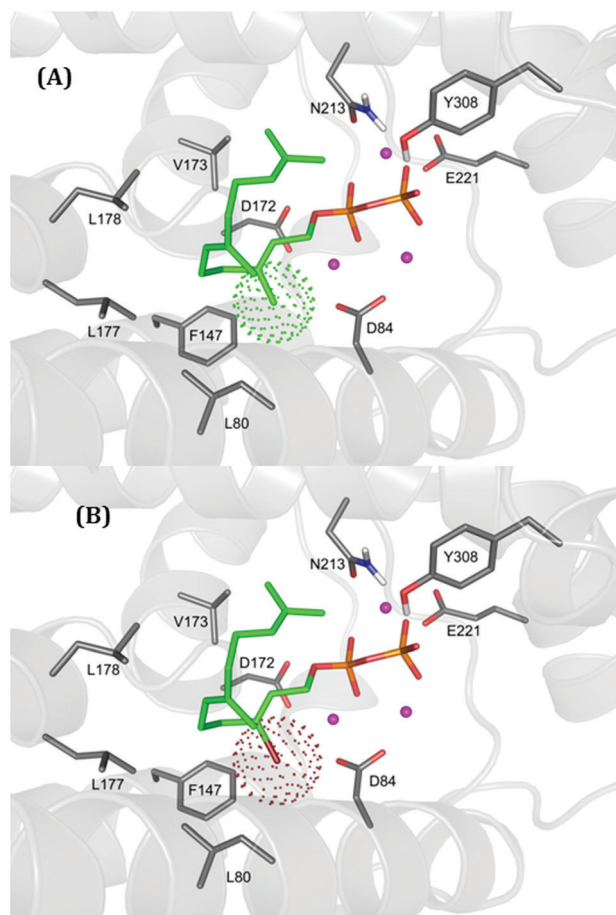


Fig. 6 Docking arrangement of FDP (A) and 3-BrFDP (5b) (B) in the active site of the X-ray structure of aristolochene synthase (4KUX). The van der Waals radii are shown by a cloud around CH₃ and Br groups.

similar motif 306DDXXD in MtTPS5. Thus, there is more likely to be comparable binding of the substrate or inhibitor is more likely. This is further supported when analyzing the active site (Fig. 6) of 4KUX with bound FSDP. The influence of the bromine substitution was analyzed first by replacement of the sulfur in FSDP with oxygen to form FDP and further modifying the ligand to 3-BrFDP (5b). The active site with ligands was energy minimized within an area of 7 Å around the ligand using the YASARA package.³⁰ There were no changes in key structural features in case of interaction between the catalytic triad and C3 methyl group placed in the hydrophobic area created by F147 and partly by L80 (Fig. 4). The sequence alignment with MtTPS5 shows that both F147 and L80 are superposed with F374 and L302, respectively, Thus, almost identical hydrophobic interactions especially of the 3-Me or 3-Br moiety in MtTPS5 can be expected. The folding pattern of both substrates in the active site might be identical and the dissociation of the diphosphate moiety should lead to initiation of formation of cyclic products. To check if the bromine is able to exhibit special stabilizing interactions, distances to spatially neighboring atoms were measured. Except of the mentioned interactions with the side chains of F147 and L80

there is only one carboxyl oxygen atoms of D84 in a distance of 3.9 Å which is, however, too large for significant stabilizing interactions. This distance is larger than 3.4 Å, the sums of the respective van der Waals radii, and also the C–Br–O angle (50°) is not appropriate to lead to an ideal scenario for the formation of an attractive Br–O halogen bond.³¹ Thus, we can conclude that natural FDP and 3-BrFDP (5b) bind to the active site in identical ways, and due to higher endothermic energy requirements the cleavage to a carbocation intermediate is not possible leading to absence of products.

Conclusion

The 3-bromo substituted GDP (3-BrGDP) and FDP (3-BrFDP) were evaluated as substrates or inhibitors for the MtTPS5 enzyme. The brominated analogues were not accepted as natural substrates for MtTPS5 and no product formation was observed. Our kinetic analyses demonstrated that these compounds were highly potent, acting as linear competitive inhibitors of the MtTPS5 enzyme, with fast binding and slow reversibility. Since there is a lack of knowledge about the crystal structure of multiproduct terpene synthases, these molecules would be ideal candidates for obtaining a co-crystal structure with *e.g.* the MtTPS5 from *M. truncatula*. They would not only support the co-crystallization process, but also give information on the conformation of the substrate bound in the crystal structure which is imperative in determining the precise nature of mechanism catalyzed by the enzyme. Due to the structural similarity between various terpene synthases, and similarity in behavior in active site, we expect these 3-bromo isoprenoids as ideal probes for crystal structure studies. The bromo substituent provides additional advantage to determine the absolute configuration based on the anomalous dispersion effect.^{32,33}

Experimental

General methods

Reactions were performed under Ar. Solvents were dried according to standard procedures. ¹H, ¹³C and ³¹P NMR were recorded at 400 MHz. Chemical shifts of ¹H, ¹³C and ³¹P NMR are given in ppm (δ) based on solvent peaks. CDCl₃: 7.27 (¹H NMR) and 77.4 ppm (¹³C NMR). D₂O/ND₄OD: 4.79 (¹H NMR); ¹³C NMR and ³¹P NMR were referenced to external standard 3-(trimethylsilyl)-propionic acid-d₄ sodium salt (TSP; 3% in D₂O) and phosphoric acid (H₃PO₄, 10% in D₂O), respectively. IR: Bruker Equinox 55 FTIR spectrophotometer.

Protein expression

Strains of *E. coli* (BL21-CodonPlus(DE3)) with recombinant vectors of MtTPS5¹² and N-terminal His₈-tag were grown to A₆₀₀ = 0.5 at 37 °C in LB-medium with kanamycin (50 µg ml⁻¹). After induction with isopropyl β-D-1-thiogalactopyranoside (IPTG), cultures were shaken overnight at 16 °C. Cells were



harvested by centrifugation and the pellet was resuspended in lysis buffer (50 mM NaH₂PO₄, 300 mM NaCl, 10 mM imidazole, pH 8.0) and incubated with lysozyme. After disruption of the cells by sonication, cell debris were removed by centrifugation. The supernatant was passed over a column of Ni²⁺-NTA-Agarose (QIAGEN, Germany), equilibrated with lysis buffer. After being washed twice with washing buffer (50 mM NaH₂PO₄, 300 mM NaCl, 20 mM imidazole), the protein was eluted with elution buffer (50 mM NaH₂PO₄, 300 mM NaCl, 250 mM imidazole). The purified protein was desalted into a TRIS-buffer (50 mM TRIS, pH 7.5, 10 mM NaCl, 10% glycerol) by passing through a NAP 25 column (Amersham Biosciences, Sweden), diluted to reach a concentration of 0.2 and 1 mg ml⁻¹ and stored at -20 °C.

Assay for terpene synthase activity

Standard assays contained 600 nM purified protein in assay buffer (25 mM HEPES, pH 7.5, 10% glycerol, 10 mM MgCl₂, 1 mM DTT) with 50 μM substrate in 1 mL final volume. The reaction mixture was covered with 100 μL of pentane (1 ng μL⁻¹ of dodecane as an internal standard) to trap the reaction products. After being incubated for 90 min at 30 °C, the reaction was stopped by vortexing for 20 s. The whole mixture was frozen in liquid nitrogen, and the pentane layer was removed after thawing and analyzed by GC-MS.

Gas chromatography

GC-MS analysis was performed on an instrument equipped with a ZB-5 capillary column (0.25 mm i.d. × 15 m with 0.25 μm film). One microliter of the sample was injected in splitless mode at injection port temperature of 220 °C. The oven temperature was kept at 50 °C for 2 min followed by a ramp of 10 °C min⁻¹ to 240 °C followed by an additional ramp of 30 °C min⁻¹ to 280 °C and finally kept for 2 min. Helium at a flow rate of 1.5 mL min⁻¹ served as carrier gas. Ionization potential was set to 70 eV, and scanning was performed from 40 to 250 amu. Compounds were identified by comparing their mass spectra and Kováts indices (retention indices) with published reference spectra (Garms *et al.*¹¹) For quantification of enzyme products, the compounds were first separated on a gas chromatograph (H₂ carrier gas 1.5 mL min⁻¹, injection volume 2 μL) under the conditions described above and subsequently analyzed on a flame ionization detector (FID) (250 °C). Correction of the different response factors of sesquiterpene hydrocarbons and alcohols was achieved using calibration curves obtained from samples with different concentrations of (*E*)-β-caryophyllene and torreyol. The average and standard deviations of relative ratios were determined by at least four independent samples setting the sum of identified compounds to 100%.

Kinetic characterization of 3-bromo analogues as inhibitors of MtTPS5

For kinetic studies, terpene synthase activity was determined by monitoring the decrease in absorbance at 340 nm as a consequence of the consumption of NADPH coupled to the

release of pyrophosphate. Pyrophosphate was detected using a coupled-enzyme system supplied as a pyrophosphate reagent by Sigma-Aldrich. This reagent was reconstituted in buffer (16.7 mg in 1 ml 10 mM Tris-HCl, 10 mM MgCl₂, 1 mM β-mercaptoethanol, pH 8). Assay reaction mixtures were prepared in 96-well microplates with 50 μl of pyrophosphate reagent, 90 μl of buffer (0–16 μM inhibitor, 25 mM HEPES, pH 7.5, 10% glycerol, 10 mM MgCl₂, 1 mM DTT) and 10 μl of various concentrations of FPP. Similarly, a blank reaction mixture without FPP (instead, 10 μl of buffer was used) was prepared, and both reaction mixtures were preheated at 30 °C for 5 min. Next, 5 μl of enzyme (0.2 mg ml⁻¹) was added to both mixtures to start the reactions. The activity was determined as the difference between the decrease in absorbance per minute of the sample and of the blank.

Apart from spectrophotometry based measurements, Assays (1 ml final volume) were initiated by addition of purified MTTPS5 solution (600 nM). Assays contained 0.1–5 μM farnesyl diphosphate, 0–3 μM inhibitor, 25 mM HEPES, pH 7.5, 10% glycerol, 10 mM MgCl₂, 1 mM DTT and were warmed to 30 °C prior to addition of enzyme solution. After incubation for 90 min. each assay was stopped by addition of 100 mM EDTA and 100 μL of pentane containing 1 ng μL⁻¹ of dodecane as an internal standard to trap the reaction products. After vortexing for 10 s, the pooled hexane extracts were vortexed with silica (50 mg) the sample was centrifuged at 13 000 rpm for 5 min and then the hexane was decanted into a vial and the activity quantified. K_M and $K_{M(app)}$ values were determined by a nonlinear fit of the data to the equation $V = V_{max}[S]/(K_M + [S])$ using Origin 8G. Mode of action of the inhibitors was determined by examination of double reciprocal plots of $1/v$ versus $1/[S]$. K_i values were determined using plots of $[I]$ versus $K_{M(app)}$ once each inhibitor was observed to be competitive.

Modelling studies

Ab initio calculations. To investigate the influence of the 3-Br methyl substitution on the (de)stabilization of the intermediately formed allyl cation energy optimizations were carried out with TURBOMOLE²⁴ using DFT (B3-LYP^{25,26}) with the def-TZVPP basis set²⁷ for the cleavage of dimethyl allyl diphosphate in comparison to 3-bromo methyl allyl diphosphate as model compounds.

Molecular mechanics simulations. The binding mode of FPP was further analyzed using an aristolochene synthase from *Aspergillus terreus*. A full crystal structure with bound FPP analogue is available of this enzyme (4UKX).²¹ Both enzymes, MtTPS5 and the aristolochene synthase, bind FPP and most likely also 3Br-FPP. The influence of the bromine substitution was analyzed by modifying the ligand and comparing the binding after energy minimization. Therefore, the crystal structure was used, hydrogens were added and the FPP analogue was changed to FPP (*i.e.* the sulfur atom at the diphosphate moiety was changed to oxygen) and the area of 7 Å around the ligand was minimized using the yasara 2 force field of the YASARA package.³⁰ The binding of the 3Br-FPP was similarly modelled. The methyl group at position 3 of the FPP was con-



verted into bromine and 7 Å around the ligand was minimized using the yasara 2 force field. The comparison of the two binding modes revealed FPP and 3Br-FPP could be bound similar by the enzyme.

Synthetic procedure

2-((7-Methyloct-6-en-2-yn-1-yl)oxy)tetrahydro-2H-pyran (2a).³⁴ The alkyne (2-(prop-2-yn-1-yloxy)tetrahydro-2H-pyran) (2.00 g, 14.3 mmol) was dissolved in dry DMI (20 ml). The solution was cooled to 0 °C, and *n*-butyllithium (1.39 M in hexanes, 10.3 ml, 14.3 mmol) was added by syringe over 15 min. Then stirred for 30 min, and further the 5-bromo-2-methylpent-2-ene **1a** (2.00 g, 9.52 mmol) in dry DMI (10 ml) was added. The reaction was warmed to room temperature and stirred for 5 h. Sat. aq. NaCl (50 ml) was added and the solution was extracted with petroleum ether (3 × 50 ml). The combined organic phase was dried (MgSO₄) and concentrated *in vacuo* to give yellow oil which was heated to 70 °C under vacuum to distill off most of the excess alkyne. The remaining oil was chromatographed on silica gel (9 : 1 hexanes–diethyl ether) to give 1.264 g of **2a** (63%) as a colorless oil data: (lit.³⁴) ¹H NMR (400 MHz, CDCl₃) δ: 5.12–5.14 (1H, m), 4.79 (1H, t, *J* = 3.3 Hz), 4.22 (2H, app q), 3.79–3.85 (1H, m), 3.49–3.53 (1H, m), 2.17–2.21 (4H, m), 1.68 (3H, s), 1.60 (3H, s), 1.50–1.91 (6H, m); ¹³C NMR (400 MHz, CDCl₃) δ: 132.9, 122.8, 96.5, 86.4, 75.7, 61.9, 54.5, 30.2, 27.3, 24.6, 25.3, 19.3, 19.1, 17.7. IR (neat) cm⁻¹: ν 2942, 2870, 1441, 1117, 1024.

(2E)-2-((7,11-Dimethyldodeca-6,10-dien-2-yn-1-yl)oxy)tetrahydro-2H-pyran (2b). First step in synthesis (2E)-2-((7,11-dimethyldodeca-6,10-dien-2-yn-1-yl)oxy)tetrahydro-2H-pyran (**2b**) was the conversion of homogeraniol to (2E)-9-bromo-2,6-dimethylnona-2,6-diene (**1b**) by following procedure of Oehlschlager *et al.*³⁵

(2E)-9-Bromo-2,6-dimethylnona-2,6-diene (1b).³⁵ To an ice-cooled solution of triphenylphosphine (1.5 g, 5.5 mmol) in 10 mL of CH₂Cl₂, bromine was added dropwise until a permanent yellow color appeared. A few milligrams of triphenylphosphine were added to consume excess Br₂ and then pyridine (0.8 mL, 10 mmol) was added and stirred for 10 min. Homogeraniol (0.85 g, 5 mmol) in 5 mL of CH₂Cl₂ was added dropwise and the reaction was stirred for further 90 min. The sample was concentrated and remainder precipitate was washed with pentane (4 × 50 mL), and the combined pentane extracts were washed with 1 N HCl (25 mL) and brine (2 × 30 mL), dried with MgSO₄, filtered and concentrated *in vacuo*. Distillation gave (2E)-2-((7,11-dimethyldodeca-6,10-dien-2-yn-1-yl)oxy)tetrahydro-2H-pyran (**2b**) (0.80 g, 71%): bp 90–92 °C ¹H NMR (400 MHz, CDCl₃) δ: 5.03–5.27 (m, 2H), 3.27–3.52 (t, 2H, C₁–CH₂, *J* = 6.66 Hz), 2.39–2.74 (q, 2H, C₂–CH₂, *J* = 6.67 Hz), 1.96–2.13 (m, 4H), 1.69 (s, 3H) 1.62 (s, 6H); MS, *m/z* (rel. intensity), 232 (10.5), 230 (11.7), 217 (5.8), 215 (8.2), 189 (28.2), 187 (30.5), 123 (18.8), 69 (100).

(2E)-2-((7,11-Dimethyldodeca-6,10-dien-2-yn-1-yl)oxy)tetrahydro-2H-pyran (2b). The alkyne (2-(prop-2-yn-1-yloxy)tetrahydro-2H-pyran) (2.00 g, 14.3 mmol) was dissolved in dry DMI (20 ml). The solution was cooled to 0 °C, and *n*-butyllithium (1.39 M in

hexanes, 10.3 ml, 14.3 mmol) was added slowly by syringe over 15 min. The reaction was stirred for 30 min, and then (2E)-9-bromo-2,6-dimethylnona-2,6-diene (**1b**) (2.76 g, 9.52 mmol) in dry DMI (10 ml) was added. The reaction was warmed to room temperature and stirred for 5 h. Sat. aq. NaCl (50 ml) was added and the solution was extracted with petroleum ether (3 × 50 ml). The combined organic phase was dried (MgSO₄) and concentrated *in vacuo* to give yellow oil which was heated to 70 °C under vacuum to distill off most of the excess alkyne. The remaining oil was chromatographed on silica gel (9 : 1 hexanes–diethyl ether) to give 1.051 g of **2a** (51%) as a colorless oil data: (lit.³⁶) ¹H NMR (400 MHz, CDCl₃) δ: 5.18 (s, 1H), 5.07 (s, 1H), 4.76 (s, 1H), 4.2 (t, *J* = 2 Hz, 2H), 3.6 (m, 2H), 2.9 (d, *J* = 7 Hz, 2H), 1.98 (m, 4H), 1.62 (m, 1H); ¹³C NMR (400 MHz, CDCl₃) δ: 135.9, 132.6, 122.8, 123.5, 100.2, 87.8, 75.7, 63.3, 54.5, 39.7, 30.2, 27.3, 25.9, 25.4, 24.6, 20.8, 19.3, 18.9, 17.3. IR (neat) cm⁻¹: ν 3060, 2960, 2240, 1140.

7-Methyloct-6-en-2-yn-1-ol (3a). The alkyne THP ether 2-((7-methyloct-6-en-2-yn-1-yl)oxy)tetrahydro-2H-pyran (**2a**) (1.667 g, 7.50 mmol) was dissolved in methanol (100 ml). Hydrochloric acid (concentrated, 5 drops, catalytic amount) was added. The reaction was stirred at room temperature for 1 h. The reaction was poured into a separatory funnel containing sat. aq. NaHCO₃ (15 ml) and extracted with dichloromethane (3 × 50 ml). The combined organic phase was dried (MgSO₄), concentrated *in vacuo*, and chromatographed on silica gel (1 : 1 hexanes–diethyl ether) to give 0.828 g of the alcohol **4a** (80%) as a colorless oil. (bp: 93–5 °C) as a colorless oil. *R*_f 0.43 (1 : 1 hexanes–ether); data: ¹H NMR (400 MHz, CDCl₃) δ: 5.18–5.13 (m, 1H), 4.25 (s, 2H), 2.26–2.17 (m, 4H), 1.70 (s, 3H), 1.62 (s, 3H), 1.52 (s, 1H); ¹³C NMR (400 MHz, CDCl₃) δ: 133.1, 122.6, 86.4, 78.3, 51.4, 27.3, 25.6, 19.2, 17.7; HRMS calcd for C₉H₁₄O 138.1045, found 138.1041. IR (neat) cm⁻¹: ν 3550–3160, 2970, 2920, 2860, 2280, 2220, 1470, 1370, 1130, 1100, 1010 cm⁻¹.

(2E)-7,11-Dimethyldodeca-6,10-dien-2-yn-1-ol (3b). The alkyne THP ether (2E)-2-((7,11-dimethyldodeca-6,10-dien-2-yn-1-yl)oxy)tetrahydro-2H-pyran (**2b**) (2.175 g, 7.50 mmol) was dissolved in methanol (100 ml). Hydrochloric acid (concentrated, 5 drops, catalytic amount) was added. The reaction was stirred at room temperature for 1 h. The reaction was poured into a separatory funnel containing sat. aq. NaHCO₃ (15 ml) and extracted with dichloromethane (3 × 50 ml). The combined organic phase was dried (MgSO₄), concentrated *in vacuo*, and chromatographed on silica gel (1 : 1 hexanes–diethyl ether) to give 1.282 g of the alcohol **4a** (83%) as a colorless oil. (bp 120–124 °C (0.5 mm)) as a colorless oil. *R*_f 0.40 (1 : 1 hexanes–ether); data: (lit.³⁷) ¹H NMR (400 MHz, CDCl₃) δ: 5.16 (m, 1H), 5.09 (m, 1H), 4.25 (d, 2H, *J* = 10.8), 2.22 (narrow m, 4H), 2.07 (m, 2H), 1.99 (m, 2H), 1.68 (s, 3H), 1.61 (s, 3H), 1.60 (s, 3H), 1.50 (t, 1H, *J* = 10.8), ¹³C NMR (400 MHz, CDCl₃) δ: 133.1, 122.6, 86.4, 78.3, 51.4, 27.3, 25.6, 19.2, 17.7; HRMS calcd for C₁₄H₂₂O: 206.1671, found 206.1667 IR (neat) cm⁻¹ 3334, 2287, 2224, 1670, 1020 cm⁻¹.

(2E)-3-Bromo-7-methylocta-2,6-dien-1-ol (4a). 7-Methyloct-6-en-2-yn-1-ol (**3a**) (0.317 g, 2.3 mmol) in 10 mL of dry THF was



added to a dry flask under N₂. Red-Al (1.17 mL, 3.9 mmol) was added dropwise *via* syringe and the reaction mixture was allowed to stir at rt for 36 h. The reaction mixture was cooled to -78 °C and *N*-bromosuccinimide (NBS) (0.783 g, 4.4 mmol) dissolved in THF was added dropwise and the reaction mixture was allowed to stir at -78 °C for an additional 1 h. The crude mixture was stirred at 0 °C for 2 h and was quenched by the addition of saturated sodium potassium tartrate (Rochelle's salt). The aqueous layer was extracted several times with ether. The organic layers were combined, washed with brine, dried over MgSO₄ and concentrated. This colorless oil consisted of desired (**4a**) as an isomeric mixture (GC). The residue was purified by chromatography on silica using 1 : 1 (v/v) hexane-ether to yield 200 mg (42%) of a colorless oil (GC: 96% pure). *R*_f = 0.43 (1 : 1 hexanes-ether); data: ¹H NMR (400 MHz, CDCl₃) δ: 5.93 (tt, 1H), 5.08 (t, 1H), 4.26 (d, 2H), 2.50 (t, 2H), 2.25 (dt, 2H), 1.78 (s, 1H), 1.70 (s, 3H), 1.64 (s, 3H); ¹³C NMR (400 MHz, CDCl₃): δ: 133.44, 130.2, 128.0, 122.5, 62.8, 42.0, 27.1, 26.0, 18.1. HRMS calcd for C₁₄H₂₂BrO (M - H₂O) 200.0195, found 200.0196. IR (neat) cm⁻¹: ν 3540–3100, 2970, 2930, 2850, 1705, 1635, 1445, 1375, 1080, 1020, 825.

(2E,6E)-3-Bromo-7,11-dimethyldodeca-2,6,10-trien-1-ol (4b). (*2E*)-7,11-Dimethyldodeca-6,10-dien-2-yn-1-ol (**3b**) (0.473 g, 2.3 mmol) in 10 mL of dry THF was added to a dry flask under N₂. Red-Al (1.17 mL, 3.9 mmol) was added dropwise *via* syringe and the reaction mixture was allowed to stir at rt for 48 h. The reaction mixture was cooled to -78 °C and *N*-bromosuccinimide (NBS) (0.783 g, 4.4 mmol) dissolved in THF was added dropwise and the reaction mixture was allowed to stir at -78 °C for an additional 1 h. The crude mixture was stirred at 0 °C for 2 h and was quenched by the addition of saturated sodium potassium tartrate (Rochelle's salt). The aqueous layer was extracted several times with ether. The organic layers were combined, washed with brine, dried over MgSO₄ and concentrated. This colorless oil consisted of desired (**4b**) as an isomeric mixture (GC). The residue was purified by chromatography on silica using 1 : 1 (v/v) hexane-ether to yield 257 mg (39%) of a colorless oil (GC: 96% pure). *R*_f = 0.40 (1 : 1 hexanes-ether); Data: ¹H NMR (400 MHz, CDCl₃) δ: 5.83 (t, *J* = 5.8 Hz, 1H) 5.08 (t, *J* = 5.7 Hz, 2H), 4.18 (d, *J* = 5.8 Hz, 2H), 2.52 (m, 2H), 2.21 (m, 2H), 2.06–1.95 (m, 4H), 1.73 (s, 1H), 1.68 (s, 3H), 1.62 (s, 3H), 1.59 (s, 3H) ¹³C NMR (400 MHz, CDCl₃) δ: 136.9, 133.8, 131.6, 124.4, 122.1, 110.3, 67.5, 45.6, 39.8, 28.1, 26.9, 25.9, 17.9, 16.4; HRMS calcd for C₁₄H₂₂BrO (M - H₂O) 268.0821, found 268.0820. IR (neat) cm⁻¹: ν 3540–3100, 2970, 2930, 2850, 1705, 1635, 1445, 1375, 1080, 1020, 825.

General procedure for the preparation of trisammonium diphosphates

Trisammonium diphosphates were prepared according to the modified method of Woodside *et al.*³⁸ To a solution of *N*-chlorosuccinimide (11.39 mmol) in CH₂Cl₂ (45 mL) at -30 °C under argon was added dropwise freshly distilled dimethyl sulfide (1.1 eq. mol). The mixture was warmed to 0 °C, stirred at this temperature for 10 min and cooled to -40 °C. A solution of

alcohol **4a** or **4b** (1 eq. mol) in CH₂Cl₂ (5 mL) was slowly added before the reaction mixture was warmed to 0 °C. Stirring was continued for 2 h at 0 °C and 15 min at rt. The clear solution was then washed with cold saturated NaCl (25 mL). The aqueous phase was extracted with pentane (2 × 20 mL). The combined organic layers were washed with cold saturated NaCl (20 mL), dried (MgSO₄), concentrated under reduced pressure (no water bath) and completely removed under high vacuum for 2 h. Corresponding alkyl chlorides were used without further purification. Freshly prepared tris(tetrabutylammonium) hydrogen pyrophosphate (1.2 eq. mol) was dissolved in ACN (5 mL) at rt under argon before dropwise addition of alkyl chloride in ACN (2 mL). Stirring was continued at rt overnight. The mixture was concentrated under reduced pressure. The residue was dissolved in (NH₄)₂CO₃ (3 mL) (0.25 mM, 2% isopropyl alcohol), loaded onto a 2 × 30 cm column of Dowex 50WX8-200 (NH₄⁺ form) before elution of two volumes column of (NH₄)₂CO₃ (0.25 mM, 2% isopropyl alcohol). The eluent was lyophilized and the resulting white powder was purified by chromatography on cellulose (1 : 9 (v/v) water in ACN). Fractions were monitored by TLC (silica gel, iPr-OH-water-AcOEt 6 : 3 : 1) and those containing trisammonium diphosphate were combined. Solvents were removed under reduced pressure and the resulting solution was lyophilized to afford **5a** or **5b**.

Trisammonium (2E)-1-(3-bromo-7-methylocta-2,6-dienyl)-diphosphate (5a). According to the general procedure, phosphorylation of **4a** (0.127 g) gave **5a** (0.153 g, 35% from **4a**) as a flocculent white solid. mp: 157–160 °C. Data: ¹H NMR (400 MHz, D₂O/ND₄OD) δ: 5.94 (t, 1H, *J* = 5.8 Hz), 5.07–5.07 (m, 1H), 4.39 (t, 2H, *J* = 6.4 Hz), 2.38–2.41 (m, 2H), 2.14–2.18 (m, 2H), 1.54 (s, 3H), 1.48 (s, 3H); ¹³C NMR (400 MHz, D₂O/ND₄OD) δ: 135.0, 130.6, 126.2, 122.8 (d, *J* = 7.3 Hz), 65.7 (d, *J* = 3.1 Hz), 41.4, 26.4, 25.2, 17.7; ³¹P NMR (400 MHz, D₂O/ND₄OD) δ: -5.81, -10.54; HRMS (ESIMS) calcd for C₉H₁₇BrO₇NaP₂ [M + Na]⁺ 400.9525, found 400.9525. IR (neat) cm⁻¹: ν 3150–2920 (br), 2320, 2197, 1649, 1447, 1207, 1092, 920.

Trisammonium ((2E,6E)-3-bromo-7,11-dimethyldodeca-2,6,10-trienyl)diphosphate (5b). According to the general procedure, phosphorylation of **4b** (0.141 g) gave **5b** (0.131 g, 40% from **4b**) as a flocculent white solid. mp: 155–160 °C. ¹H NMR (400 MHz, D₂O/ND₄OD) δ: 5.17–5.22 (m, 2H), 4.59 (t, 2H, *J* = 6.5 Hz), 2.40–2.44 (m, 2H), 2.27–2.31 (m, 2H), 2.09–2.14 (m, 2H), 2.02–2.04 (m, 2H), 1.69 (s, 3H), 1.63 (s, 3H), 1.62 (s, 3H); ¹³C NMR (400 MHz, D₂O/ND₄OD) δ: 138.3, 138.2, 134.2, 125.1, 123.5, 123.0 (d, *J* = 7.7 Hz), 63.4 (d, *J* = 4.5 Hz), 39.4, 39.3, 26.5, 26.0, 25.5, 16.0; ³¹P NMR (400 MHz, D₂O/ND₄OD) δ: -5.43, -10.51 HRMS (ESIMS) calcd for C₁₄H₂₅BrO₇P₂ [M + Na]⁺ 469.0151, found 469.0151. IR (neat) cm⁻¹: ν 3150–2920 (br), 2320, 2197, 1649, 1447, 1207, 1092, 920.

Trisammonium (E)-geranyl and (2E,6E)-farnesyl diphosphates. Unlabeled GDP and FDP were synthesized from commercial geranyl and farnesyl chloride (Aldrich) respectively, according to the phosphorylation procedure described above.



Acknowledgements

We would like to acknowledge Max Planck Society for funding. We would also like to acknowledge Stefan Garms and Stephan von Reuss for helpful discussions. We also like to thank Peter Rahfeld and Rita Buchler for their help with protein purification.

Notes and references

- H. V. Thulasiram, H. K. Erickson and C. D. Poulter, *Science*, 2007, **316**, 73–76.
- J. H. Langenheim, *J. Chem. Ecol.*, 1994, **20**, 1223–1280.
- E. Pichersky and J. Gershenzon, *Curr. Opin. Plant Biol.*, 2002, **5**, 237–243.
- E. Nambara and A. Marion-Poll, *Annu. Rev. Plant Biol.*, 2005, **56**, 165–185.
- M. Hilker, C. Kobs, M. Varama and K. Schrank, *J. Exp. Biol.*, 2002, **205**, 455–461.
- J. D. Connolly and R. A. Hill, *Dictionary of Terpenoids*, Chapman & Hall, New York, 1992.
- C. A. Lesburg, J. M. Caruthers, C. M. Paschall and D. W. Christianson, *Curr. Opin. Struct. Biol.*, 1998, **8**, 695.
- E. M. Davis and R. Croteau, in *Biosynthesis: Aromatic Polyketides, Isoprenoids, Alkaloids*, Springer-Verlag, Berlin, 2000, vol. 209, pp. 53–95.
- J. P. Jones, K. R. Korzekwa, A. E. Rettie and W. F. Trager, *J. Am. Chem. Soc.*, 1986, **108**, 7074.
- C. L. Steele, J. Crock, J. Bohlmann and R. Croteau, *J. Biol. Chem.*, 1998, **273**, 2078.
- S. Garms, T. G. Köllner and W. Boland, *J. Org. Chem.*, 2010, **75**, 5590–5600.
- G. I. Arimura, S. Garms, M. Maffei, S. Bossi, B. Schulze, M. Leitner, A. Mithöfer and W. Boland, *Planta*, 2008, **227**, 453–464.
- D. W. Christianson, *Chem. Rev.*, 2006, **106**, 3412–3442.
- N. A. Heaps and C. D. Poulter, *J. Org. Chem.*, 2011, **76**, 1838–1843.
- F. Y. David, J. Miller, D. W. Knight and R. K. Allemann, *Org. Biomol. Chem.*, 2009, **7**, 962–975.
- D. J. Hosfield, Y. Zhang, D. R. Dougan, A. Broun, L. W. Tari, R. V. Swanson and J. Finn, *J. Biol. Chem.*, 2004, **279**, 8526–8529.
- F.-Y. Lin, C.-I. Liu, Y.-L. Liu, Y. Zhang, K. Wang, W.-Y. Jeng, T.-P. Ko, R. Cao, A. H.-J. Wang and E. Oldfield, *Proc. Natl. Acad. Sci. U. S. A.*, 2010, **107**, 21337–21342.
- J. A. Faraldos and R. K. Allemann, *Org. Lett.*, 2011, **13**, 1202–1205.
- D. J. Miller, F. Yu, D. W. Knight and R. K. Allemann, *Org. Biomol. Chem.*, 2009, **7**, 962–975.
- A. Bondi, *J. Phys. Chem.*, 1964, **68**, 441–451.
- M. Chen, N. Al-lami, M. Janvier, E. L. D'Antonio, J. A. Faraldos, D. E. Cane, R. K. Allemann and D. W. Christianson, *Biochemistry*, 2013, **52**, 5441–5453.
- C. RA, *Evaluation of enzyme inhibitors in drug discovery: a guide for medicinal chemists and pharmacologists*, John Wiley & Sons, Hoboken, NJ, 2005.
- C. D. Poulter, J. C. Argyle and E. A. Mash, *J. Biol. Chem.*, 1978, **253**, 7227–7233.
- C. Steffen, K. Thomas, U. Huniar, A. Hellweg, O. Rubner and A. Schroer, *J. Comput. Chem.*, 2010, **31**, 2967–2970.
- K. Kim and K. D. Jordan, *J. Phys. Chem.*, 1994, **98**, 10089–10094.
- P. J. Stephens, F. J. Devlin, C. F. Chabalowski and M. J. Frisch, *J. Phys. Chem.*, 1994, **98**, 11623–11627.
- F. Weigend and R. Ahlrichs, *Phys. Chem. Chem. Phys.*, 2005, **7**, 3297–3305.
- S. Frick, R. Nagel, A. Schmidt, R. R. Bodemann, P. Rahfeld, G. Pauls, W. Brandt, J. Gershenzon, W. Boland and A. Burse, *Proc. Natl. Acad. Sci. U. S. A.*, 2013, **110**, 4194–4199.
- C. M. Starks, K. W. Back, J. Chappell and J. P. Noel, *Science*, 1997, **277**, 1815.
- E. Krieger, G. Koraimann and G. Vriend, *Proteins: Struct., Funct., Bioinf.*, 2002, **47**, 393–402.
- S. Sirimulla, J. B. Bailey, R. Vegesna and M. Narayan, *J. Chem. Inf. Model.*, 2013, **53**, 2781–2791.
- Z. Dauter, M. Dauter and K. R. Rajashankar, *Acta Crystallogr., Sect. D: Biol. Crystallogr.*, 2000, **56**, 232–237.
- J. M. Bijvoet, A. F. Peerdeman and A. J. van Bommel, *Nature*, 1951, **168**, 271–272.
- M. E. Jung and M. H. Parker, *J. Org. Chem.*, 1997, **62**, 7094–7095.
- A. C. Oehlschlager, S. M. Singh and S. Sharma, *J. Org. Chem.*, 1991, **56**, 3856–3861.
- S. Ghosal, M. Nirmal, J. C. Medina and K. S. Kyler, *Synth. Commun.*, 1987, **17**, 1683–1694.
- J. Hooz, J. Cabezas, S. Musmanni and J. Calzada, *Org. Synth.*, 1990, **69**, 120–128.
- A. B. Woodside, H. Zheng and C. D. Poulter, *Org. Synth.*, 1988, **66**, 211–219.

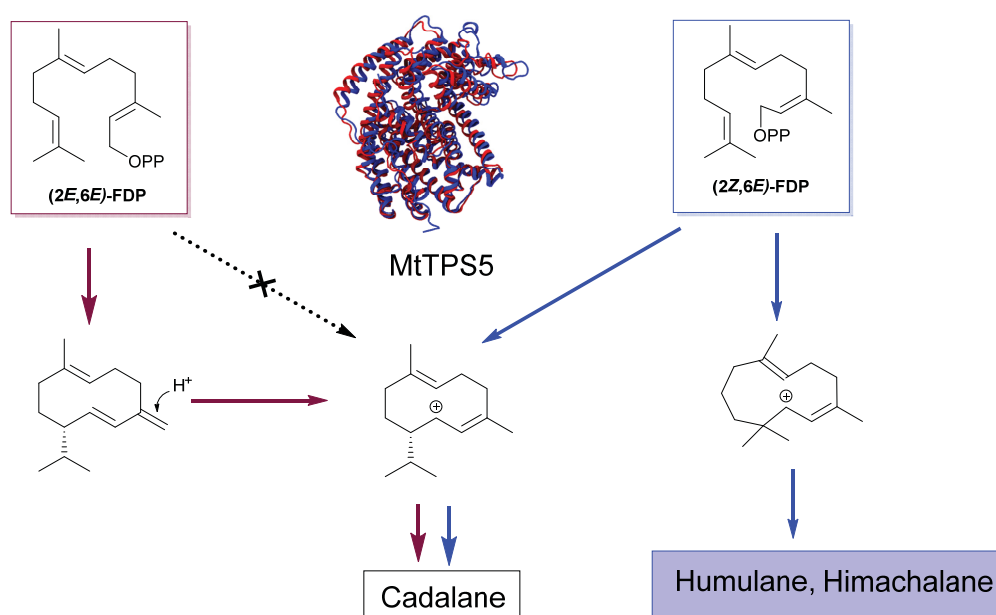


6.4 Manuscript IV: Novel biosynthetic products from multiproduct terpene synthase from *Medicago truncatula* using non-natural isomers of prenyl diphosphates

Abith Vattekkatte,¹ Dr. Stefan Garms² and Prof. Dr. Wilhelm Boland³

(Under preparation)

Graphical Abstract



Summary

The multiproduct sesquiterpene synthase MtTPS5 isolated from *Medicago truncatula* generates 27 products from (2E,6E)-farnesyl diphosphate (FDP). In this work, we report the reaction steps involved in the formation of novel products from (2Z,6E)-FDP. The absolute configuration of individual products was used to establish the stereochemical course of the reaction cascade after incubation with geometric isomers as substrates. Interestingly the unnatural precursor (2Z,6E)-FDP generated only one enantiomer of each product indicating the high stereospecificity of the reaction. These substrates showed a novel cyclization pathway leading to sesquiterpenes containing humulane, amorphene and himachalane skeletons, which were not observed with the (2E,6E)-(FDP).

Novel biosynthetic products from multiproduct
terpene synthase from *Medicago truncatula* using non-
natural isomers of prenyl diphosphates

Abith Vattekkatte, Stefan Garms and Wilhelm Boland

^aDepartment of Bioorganic Chemistry, Max Planck Institute for Chemical Ecology,
Beutenberg Campus, Hans-Knöll-Strasse 8, D-07745 Jena, Germany

boland@ice.mpg.de

*To whom correspondence should be addressed. Fax: +49(0) 3641 571 202

Abstract

Terpene synthases are highly promiscuous enzymes that responsible for a large diversity of terpenes found in nature. The multiproduct sesquiterpene synthase MtTPS5 isolated from *Medicago truncatula* generates 27 products from (2*E*,6*E*)-farnesyl diphosphate (FDP). In this paper, we report the reaction steps involved in the formation of the products from (2*Z*,6*E*)-FDP analogous to presumptive reaction intermediates. Using incubation experiments with geometric isomers as substrates; the absolute configuration of individual products was used to establish the stereochemical course of the reaction cascade. Interestingly the unnatural precursor (2*Z*,6*E*)-FDP generated only one enantiomer of each product indicating the stereospecificity of reaction. These substrates showed a novel cyclization pathway leading to sesquiterpenes containing humulane, amorphene and himachalane skeletons, which were not observed with the (2*E*)- isomer substrate. These geometric analogs can be used to generate novel cyclic products with highly promiscuous terpene synthases in combination with site directed mutagenesis of enzymes.

Introduction

Terpenes constitute the largest and most diverse class of plant natural products with more than 55,000 members found in almost all forms of life.¹ They serve many biological functions such as hormones (steroids, gibberellins, abscisic acid)², structural components of membranes (phytosterols), attractants for pollinators³, toxins⁴, feeding or oviposition deterrents to a large variety of insects.⁵ In addition to these direct defense strategies there are also indirect defenses which play a major role, for example emission of volatile organic compounds that may attract herbivore's enemies, such as predators or parasitoids.⁶ They are not only significant in chemical ecology but also are of high commercial significance as varied as medicines, materials, fuels, and chemicals especially as flavors and fragrance.⁶ Volatile terpenoids, which constitute a major class of induced volatiles, are synthesized by specific enzymes known as terpene synthases. These enzymes have been intensively investigated in the last decades and various cDNAs encoding plant terpenoid synthases involved in primary and secondary metabolisms have been cloned and characterized.⁷

Enzymes with promiscuous functions have long been believed to evolve and acquire higher specificity and activity and this plasticity has been achieved with a small number of amino acid substitutions.⁸ This promiscuity gives us the opportunity to study the enzyme evolution as well as design them as better future catalysts. Catalytic promiscuity has been for long known as one of the key features of terpene synthases, especially sesquiterpene synthases.^{6b, 6c} All sesquiterpenes known to date are derived from 300 basic hydrocarbon skeletons formed by sesquiterpene synthases from the universal precursor farnesyl

diphosphate (FDP).⁹ The structural diversity is created by generating an environment that binds the flexible isoprenoid substrate in a proper orientation and conformation to enforce specific trajectories for C-C bond formation. Besides terpene synthases generating single product, multiproduct terpene synthases are also known for producing a collection of acyclic and cyclic products from a single precursor.^{7a} The δ -selinene synthase and the γ -humulene synthase from *Abies grandis* hold the present record by producing 52 and 34 different sesquiterpenes.¹⁰ The biosynthetic promiscuity is assumed to result from an active site allowing alternative conformations of the substrate and later intermediates.

During terpenoid biosynthesis the unsaturated diphosphates (FDP etc.) are dissociated into highly reactive cations and phosphate anions. These electrophilic cations interact with electron-rich double bonds in the vicinity, followed by intramolecular cyclizations, rearrangements, including hydride or methyl shifts prior to stabilization by either deprotonation or a reaction with a nucleophile.¹¹ Due to the (*E*)-configuration of substrate, this intramolecular cyclization proceeds through the remote double bonds, for example in FDP medium-sized ring systems such as caryophyllene and humulene are generated. In contrast, the direct intramolecular cyclization of (*2E,6E*)-FDP with the neighbouring C(5)-C(6) double bond to cyclohexenyl cations is not possible and requires a preceding isomerization. This is achieved by a suprafacial migration of the diphosphate moiety of the substrate that leads to an enzyme-bound tertiary allylic intermediate.¹² In our previous work, we have shown that this rotation around the newly formed C(2)-C(3) bond and ionization of the corresponding *cisoid* conformer affords the neryl cation and the *trans*-farnesyl cation, having the right geometry for C(6)-C(1)-closure but also has rate limiting effects on whole cascade.¹³

In order to understand the catalytic promiscuity of multiproduct terpene synthases, we have performed mechanistic studies on multiproduct sesquiterpene synthase *MtTPS5* from *Medicago truncatula*.¹⁴ The promiscuous behavior of this enzyme was investigated by using (*2Z,6E*)-FDP as a mimic for the secondary *cisoid* neryl cation intermediate generated during biosynthesis from (*2E,6E*)-FDP in which the C2=C3 π bond is already in the *cis* configuration. This geometrical isomer has been used to study the kinetics of various terpene synthases, but very few studies have compared the cyclization properties of these highly promiscuous enzymes with geometric isomers.¹⁵ We were interested whether the cyclization cascade with (*2Z,6E*)-FDP would yield the same product profiles with *MtTPS5* as observed with their normal substrate (*2E,6E*)-FDP. This would be similar to what we observed with maize sesquiterpene synthases *TPS4* and *TPS5*, which resulted in the same volatile profile but with higher turnover.¹³ In a similar work with *Cop4* and *Cop6* from *Coprinus cinereus*, different products resulting from the opposite enantiomer (6*S*)- β -bisabolene as opposed to (6*R*)- β -bisabolene and (*2E,6E*)-germacradienyl carbocation respectively from (*2E,6E*)-FDP were

observed.¹⁶ Interestingly, in case of MtTPS5, the product formation saw a completely different product profile, with novel cyclic products not seen with (2*E*,6*E*)-FDP.

Results and discussion

To evaluate the impact of the stereochemistry of C(2)-C(3) double bond of the FDP-precursors, the (2*Z*)-isomers were synthesized. The highly efficient synthesis of (2*Z*,6*E*)-farnesyl diphosphate as its triammonium salt from (2*Z*,6*E*)-farnesol has been previously described.¹⁷ Recombinant MtTPS5 from *Medicago truncatula* was expressed and purified as described.¹⁴

Enzymatic characterization of substrates

We had also previously proposed the complex mechanistic pathway controlled by the MtTPS5 using a combination of techniques including labelling experiments.^{14b} In brief, the reaction cascade is initiated by the formation of a highly reactive farnesyl carbocation by the disassociation of diphosphate moiety. The C1 to C11 ring closure affords the humulyl cation, which generates terpenoids such as α -humulene and β -caryophyllene. Most of the products require the initial C1 to C10 closure generating the germacren-11-yl cation which is further cyclized to products like germacrene D and germacrenyl based alcohols. The other key cationic intermediates are (2*Z*,6*E*)-germacren-1-yl cation and cadinan-7-yl cation, leading to about 80% of products. These intermediates are generated by isomerization of FDP to nerolidyl diphosphate (NDP). Even alteration of a single amino acid has a dramatic effect on the product profile; alteration of tyrosine to phenylalanine in MtTPS5 prevents the formation of a key intermediate via protonation of germacrene D as a neutral intermediate. The tight control of the enzyme leads to 27 optically pure products resulting from cyclization steps and hydride shifts. Hence, it was of great interest to observe the response of the enzyme on incubation with (2*Z*,6*E*)-FDP, to study the rate limiting effects of the initial isomerization step and their consequences for the reaction cascade. These product alterations depend on the nature of the initial carbocationic intermediates formed whose stability and ease of deprotonation may favor different reaction channels.

Incubation with (2*Z*,6*E*)-FDP

Unlike the maize sesquiterpene synthases, the incubation of (2*Z*,6*E*)-FDP gave a completely different product profile as compared to (2*E*,6*E*)-FDP. They were different in both qualitative as well as quantitative terms. The GC-FID chromatogram product profile of MtTPS5, when incubated with (2*Z*,6*E*)-FDP showed the

presence of 23 different sesquiterpenes (Figure 1). Out of these 23 compounds, 14 sesquiterpenes were identified based on their retention indices and mass spectra in comparison with authentic references (Figure 2).

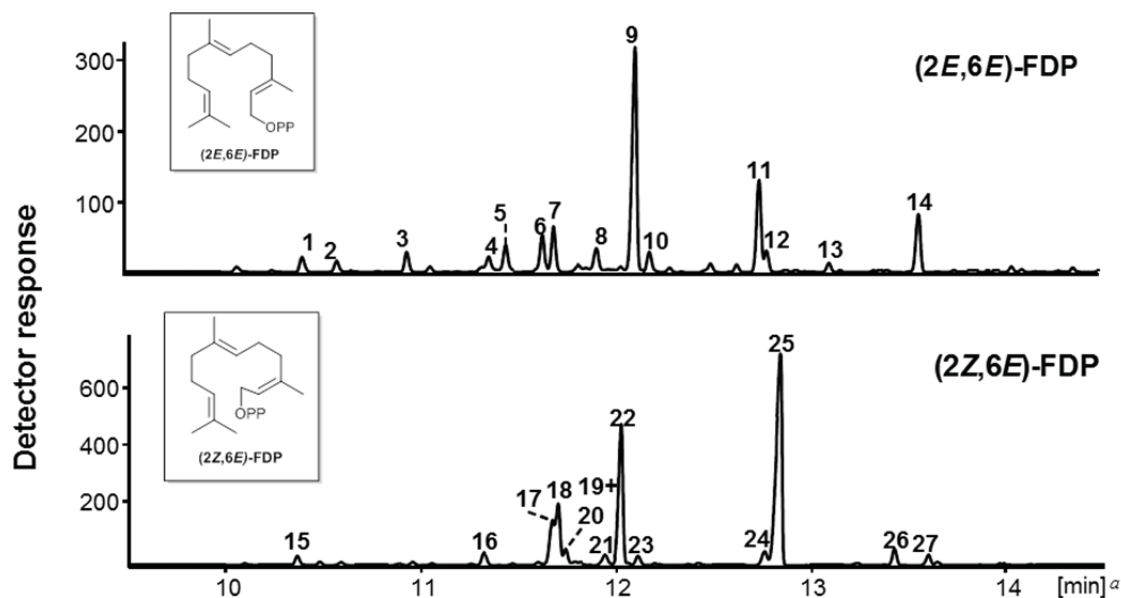


Figure 1: GC-FID Chromatogram of major sesquiterpenes on incubation of recombinant MtTPS5 with (2E,6E)-FDP and (2Z,6E)-FDP. The compounds were identified by their Kovats indices and mass spectra as compared to authentic references. Only major sesquiterpenes are labelled. (2E,6E)-FDP: 1 α -Copaen, 2 β -Cubebene, 3 (*E*)- β -Caryophyllene, 4 Cadina-3,5-diene, 5 *allo*-Aromadendrene, 6 γ -Muurolene, 7 Germacrene D, 8 α -Muurolene, 9 Cubebol, 10 δ -Cadinene, 11 Copan-3-ol, 12 4 α -Hydroxygermacra-1(10),5-diene, 13 Copaborneol, 14 Torreyol. (2Z,6E)-FDP: 15 α -Ylangen, 16 α -Himachalene, 17 Isobicyclo-germacrene, 18 α -Amorphene, 19 γ -Humulene, 20 γ -Himachalene, 21 β -Himachalene, 22 δ -Amorphene 25 Humulan-4,9-dien-8-ol and 27 2-Himachalen-7-ol. Sesquiterpene alcohols 23, 24 and 26 ($C_{15}H_{26}O$ II-IV) could not identified.

The most interesting aspect of these results with (2Z,6E)-FDP was that the dominant terpenoid skeletons were completely absent in case of (2E,6E)-FDP. The product profile of (2Z,6E)-FDP consisted predominantly of mono- and bicyclic sesquiterpenes containing humulane, amorphene and himachalane skeletons, which were not observed on the reaction with the (2E)- isomer substrate. This suggested that product formation with (2Z,6E)-FDP by MtTPS5 followed a completely novel pathway as compared with natural substrate.

Stereochemical analysis of products

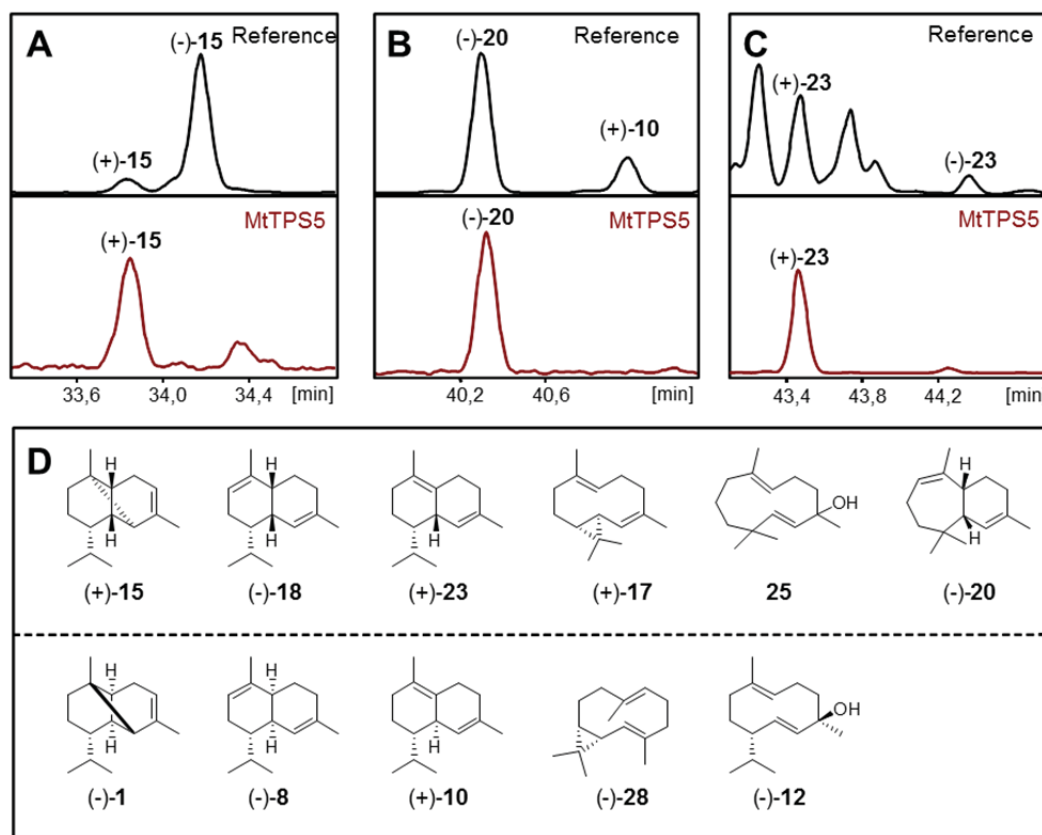


Figure 2: Determination of the absolute configurations of some products obtained after incubation of MtTPS5 with (2Z, 6E) -FDP. The separation of the enantiomers was carried out by GC-MS on a chiral phase (shown for 15 (A), 20 (B) and 23 (C)). D. Juxtaposition of isomeric compounds starting from (2Z,6E)-FDP (top row) and (2E,6E)-FDP (bottom row). Bicyclogermacrene (28).

The absolute configuration of α - and δ -Amorphene, α - and γ -himachalene, as well as of α -Ylangen was determined by GC-MS on a chiral phase column (Fig. 2, supporting information). The stereochemical analysis of the enzyme products reveals the conservation of configurations among compounds with the same hydrocarbon skeleton as well as between related structures with (2Z,6E)-FDP. One common factor observed with both geometric isomers is that the enantiomeric composition of all substances was high degree optical purity. The absolute configuration and identity of individual compounds was confirmed by comparing it with authentic standards obtained from various sources (supporting information). Accordingly, it can be inferred that MtTPS5 exerts a stronger control on the initial conformation of the farnesyl cation allowing only the formation of the one enantiomer of the products. In contrast, the multiproduct terpene synthase TPS4 from *Zea mays* and the trichodiene synthase from *Fusarium sporotrichioides* generate a mixture of racemic and diastereomeric products.¹⁸ For α -Amorphene (18) the determination of the enantiomeric excess was not possible because the (+)-enantiomer co-eluted with that of (+)- α -Amorphene (+)-23 (Supporting information). All compounds generated from MtTPS5 with (2E,6E)-FDP as substrate shared (S)-configured

stereochemistry at C10. In contrast, the bridgehead hydrogen atoms (C1-H, C6-H) of α -Ylangen, as well as α - und δ -Amorphene of (2Z,6E)-FDP had an opposite orientation to those from (2E,6E)-FDP generated volatiles (1, 8 and 10) (Fig. 2).

Structure elucidation of Major product Humulan 6,9-dien-3-ol

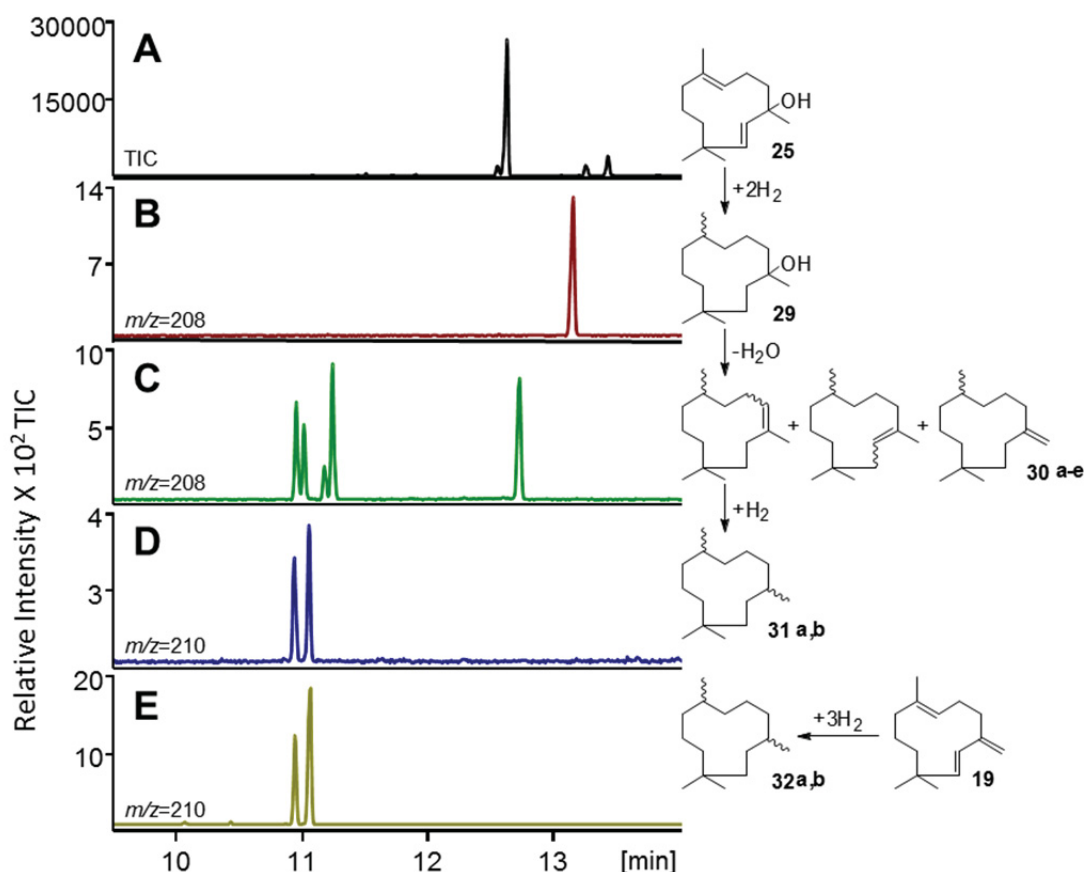


Figure 3: Structure elucidation of Humulan 6,9-dien-3-ol (25). GC-MS chromatograms which were obtained by reactions of a column chromatography on silica gel purified fraction of 25 and its secondary products. (A): an 25-enriched fraction, (B) products by catalytic hydrogenation of 25, (C) products after acid catalyzed dehydration of 29, (D) products by catalytic hydrogenation of 30a-e, (E) reference, obtained from 19 by hydrogenation 32a, b.

The available mass spectra libraries and Kovats indices were unsuccessful to match up 25 as their main product. The structure was thus elucidated by classical step by step derivatization (Fig. 3). The mass spectrum of 25 a weak molecular peak at $m/z=222$ and fragment ions at $m/z=207$ $[M-Me]^+$ and $m/z=204$ $([M-H_2O]^+)$, indicating the structure of a sesquiterpene. Catalytic hydrogenation of a highly enriched fraction 25 yielded a product (29) with a the increased mass of 4 amu of the fragment ion $[M-H_2O]^+$ $m/z = 208$. It could be deduced from this reaction that 25 is a monocyclic system in which two double bonds were reduced. After acid-catalyzed dehydration of 29 with trifluoroacetic anhydride five compounds (102a -e) were on separation by gas chromatography, which had the expected molecular peak at $m/z = 208$. This helped us further

conclude that the hydroxy group could be located only on a tertiary carbon atom, because the detection of five stereoisomeric products, as a secondary alcohol would have provided only four products. Further proof of the fact that 25 is a 11-membered ring system, was observed when by hydrogenation of the mixture of substances (30 a- e) yielded the same diastereomeric Humulane (32 a,b) on the hydrogenation of γ -humulene (19). On connecting all observed results, the product can be confirmed as Humula-4,9-dien-8-ol (25), which was isolated by Pentegova et al., from the resin of silver fir (*Abies alba*).¹⁹

Proposed mechanism of MtTPS5-catalyzed cyclizations of (2Z,6E)-FDP

Previous labelling and mechanistic studies of MtTPS5 with (2E,6E)-FDP showed that the enzyme is capable of generating cadalane sesquiterpenes via two different pathways. It was also observed that the reaction channel by which the isomerization of the initially formed (2E,6E)-farnesyl cations is converted to (2Z,6E)-farnesyl cation is comparatively suppressed.^{14b} Interestingly, when (2Z,6E)-FDP substrate analogue was used, a completely new range of products was obtained. A large proportion of the released compounds (~ 33%) had a cadalane backbone, which in contrast to the (2E,6E)-FDP products possessed opposite absolute configuration (1S, 6R) of the bridgehead carbon atoms. Due to the determination of the absolute configurations of some of the products, the stereochemical course of the reaction cascade and the starting conformation of the (2Z)-isomeric substrate could be reconstructed (Fig. 4). The highly reactive (2Z,6E)-farnesyl cation, which is formed after cleavage of the diphosphate group of (2Z,6E)-FDP is predominantly undergoes (~ 57%) by a C1-C11 ring closure to generate (2Z,6E)-Humul-10-yl cation. The transfer of positive charge from C10 to C1 is only possible by a direct hydride 1,3-shift. Due to the presence of a quaternary carbon atom between these two positions, the possibility of two consecutive 1,2-hydride shifts is eliminated. Deprotonation of the (2Z,6E)-Humul-1-yl cation (36) generates γ -humulene (19), this on further reaction with water, results in the main product Humulan-6,9-dien-3-ol (25). Furthermore, the Himachalanes 16, 21, 20 and 27 are released from 36 through an electrophilic attack on the *si* face of the C6-C7 double bond, followed by elimination of a proton or by reaction with a water molecule.

Another reaction channel, which starts from (2Z,6E)-farnesyl cation passes through the ten-membered macrocyclic (2Z,6E)-germacrene-11-yl cation (33) after initial C1-C10 cyclization. In this step, initially the (*R*) configuration at C10 is established, which is conserved in all the Cadalane sesquiterpenes. Analogous to the proposed reaction mechanism with (2E,6E)-FDP, a 1,3-deprotonation of C1-H_{RE} leading to bicyclogermacrene, a similar mechanism is observed with (2Z,6E)-FDP, wherein the isomer Isobicyclogermacrene (17) is formed. In addition, the absolute configuration at C1 of Isobicyclogermacrene

(17) suggests that the (2*Z*,6*E*)-germacrene-11-yl cation (33) is generated by a shift of 1- H_{Re} from C1 to C11. This assumption must be confirmed by incubation experiments with chirally deuterated substrates ((1*S*)- as well as (1*R*)-[1- 2H]-FDP). In the further course of the reaction C1-C6 ring-closure yields 35, and further to cadinane-7-yl cation (37c), this passes through loss of a proton in the two double-bond generating Amorphenes 23 and 18. The tricyclic rings are formed after an additional cyclization of 37c between C2 and C7 followed by deprotonation to (-)- α -Ylangen (15).

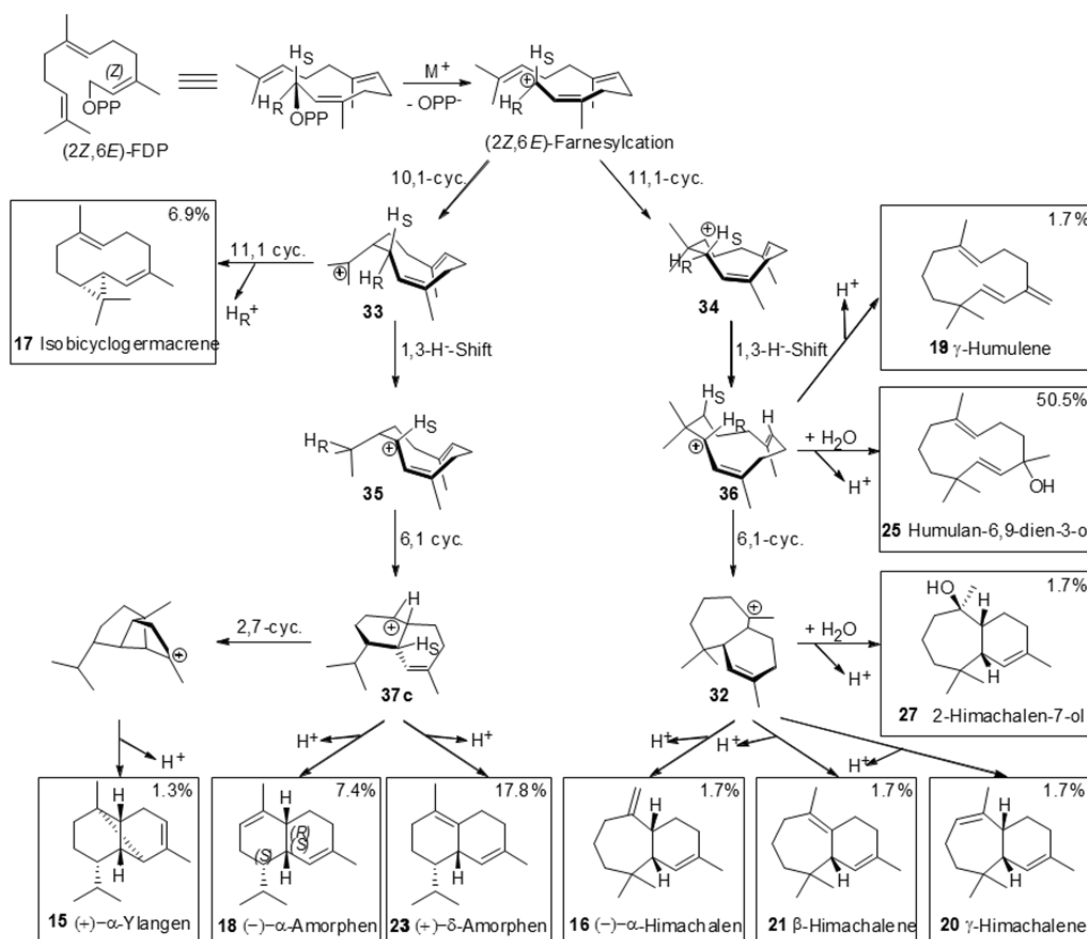


Figure 4: Proposed mechanism of formation of the products after incubation of (2*Z*, 6*E*)-FDP with M ϵ TPS5

A close correlation exists between the two reaction cascades that leads to terpenoid formation, starting from both (2*E*,6*E*)- and (2*Z*,6*E*)-FDP (Fig. 4). The essential elements such as 1,3-hydride shift, initial 1,10- or 1,11- cyclization and the formation of bicyclic compounds by a second ring closure are found in both reaction mechanisms. The huge structural difference in the products mainly due to the different starting conformation of the two substrates, as the reactive moieties each occupies a different spatial arrangement, which needs further examination with help of docking studies. The large influence of the initial folding of farnesyl cation in the active site depending on the configuration of the C2-C3 double bond has already shown in case of 5-

epi- aristolochene synthase (TEAS) of tobacco.²⁰ This was possible due to availability of crystal structures of enzyme-substrate complexes of TEAS with fluorine analogs of (2*E*,6*E*)- and (2*Z*,6*E*)-FDP. The different stereo- and regiochemical course of the reaction cascade two starting conformation is similar to MtTPS5 cannot confirmed due to lack of crystal structure of multiproduct terpene synthases.²⁰⁻²¹ Work is in progress to co-crystallize the 3-bromo substrate to decipher the structural basis of this diversity as well as catalytic promiscuity.²² The isolation of a (2*Z*,6*E*)-FDP synthase from *Mycobacterium tuberculosis*, which is involved in the bacterial cell wall biosynthesis, indicates the relevance of (2*Z*,6*E*)-FDP in other biological systems.²³ This also indicates the possibility of a "sleeping" cyclization pathway starting from (2*Z*,6*E*)-FDP but none has been found so far.

Conclusions

In this work we probe the reaction mechanism of multiproduct terpene synthase from *Medicago truncatula* that can isomerize the C2=C3 π bond of (2*E*,6*E*)-FDP via an NDP intermediate. This step precedes the catalysis of subsequent cyclization reactions generating 27 sesquiterpenoids. We were able to show that MtTPS5 is very promiscuous, generating multiple cyclization products from (2*Z*,6*E*)-FDP. The product profile of (2*Z*,6*E*)-FDP consisted predominantly of mono- and bicyclic sesquiterpenes containing humulane, amorphene and himachalane skeletons, which were not observed on the reaction with the (2*E*)- isomer substrate. The determination of absolute configuration of final products and the presence of only one enantiomer shows the exceptional stereochemical control of MtTPS5 over the reaction cascade. These alternative geometric analogs can be used to generate novel cyclic products with highly promiscuous terpene synthases with help of site directed mutagenesis.

Acknowledgements:

We thank Kerstin Ploss for the HRMS measurements. We would also like to thank Stephan von Reuss and Tobias G. Köllner for support with references. This work was supported by Max Planck Society.

Supporting Information

General analytical procedures, absolute configuration retention indices and mass spectra of terpenoids from MtTPS5 and their comparison with references are available

References

- 1(a) J. D. Connolly and R. A. Hill, Chapman & Hall, New York, 1992; (b) D. T. Major and M. Weitman, *Journal of the American Chemical Society*, 2012, **134**, 19454; (c) N. Dudareva, A. Klempien, J. K. Muhlemann and I. Kaplan, *New Phytol.*, 2013, **198**, 16.
- 2 E. Nambara and A. Marion-Poll, *Annual Review of Plant Biology*, 2005, **56**, 165.
- 3 E. Pichersky and J. Gershenzon, *Current Opinion in Plant Biology*, 2002, **5**, 237.
- 4 J. H. Langenheim, *Journal of Chemical Ecology*, 1994, **20**, 1223.
- 5 M. Hilker, C. Kobs, M. Varama and K. Schrank, *Journal of Experimental Biology*, 2002, **205**, 455.
- 6(a) P. M. Dewick, *Natural Product Reports*, 2002, **19**, 181; (b) B. M. Fraga, *Natural Product Reports*, 2011, **28**, 1580; (c) D. W. Christianson, *Current Opinion in Chemical Biology*, 2008, **12**, 141.
- 7(a) J. Degenhardt, T. G. Köllner and J. Gershenzon, *Phytochemistry*, 2009, **70**, 1621; (b) D. J. Schenk, C. M. Starks, K. R. Manna, J. Chappell, J. P. Noel and R. M. Coates, *Archives of Biochemistry and Biophysics*, 2006, **448**, 31.
- 8 Y. Yoshikuni, T. E. Ferrin and J. D. Keasling, *Nature*, 2006, **440**, 1078.
- 9 D. J. Miller and R. K. Allemann, *Natural Product Reports*, 2012, **29**, 60.
- 10 C. L. Steele, J. Crock, J. Bohlmann and R. Croteau, *Journal of Biological Chemistry*, 1998, **273**, 2078.
- 11 N. Gatto, A. Vattekkatte, T. Kollner, J. Degenhardt, J. Gershenzon and W. Boland, *Chem Commun (Camb)*, 2015, **51**, 3797.
- 12(a) D. E. a. Cane, *Chemical Reviews*, 1990, **90**, 1089; (b) D. M. Satterwhite, C. J. Wheeler and R. Croteau, *Journal of Biological Chemistry*, 1985, **260**, 3901.
- 13 A. Vattekkatte, N. Gatto, T. G. Kollner, J. Degenhardt, J. Gershenzon and W. Boland, *Organic & Biomolecular Chemistry*, 2015.
- 14(a) G. I. Arimura, S. Garms, M. Maffei, S. Bossi, B. Schulze, M. Leitner, A. Mithöfer and W. Boland, *Planta*, 2008, **227**, 453; (b) S. Garms, T. G. Köllner and W. Boland, *The Journal of Organic Chemistry*, 2010, **75**, 5590.
- 15(a) D. E. Cane, G. H. Yang, Q. Xue and J. H. Shim, *Biochemistry*, 1995, **34**, 2471; (b) K. Nabeta, M. Fujita, K. Komuro, K. Katayama and T. Takasawa, *J. Chem. Soc.-Perkin Trans. 1*, 1997, 2065; (c) T. G. Köllner, P. E. O'Maille, N. Gatto, W. Boland, J. Gershenzon and J. Degenhardt, *Archives of Biochemistry and Biophysics*, 2006, **448**, 83; (d) T. G. Köllner, C. Schnee, S. Li, A. Svatos, B. Schneider, J. Gershenzon and J. Degenhardt, *Journal of Biological Chemistry*, 2008, **283**, 20779.
- 16 F. Lopez-Gallego, S. A. Agger, D. Abate-Pella, M. D. Distefano and C. Schmidt-Dannert, *ChemBioChem*, 2010, **11**, 1093.
- 17 Y. Shao, J. T. Eumner and R. A. Gibbs, *Organic Letters*, 1999, **1**, 627.
- 18(a) T. G. Köllner, P. E. O'Maille, N. Gatto, W. Boland, J. Gershenzon and J. Degenhardt, *Archives of Biochemistry and Biophysics*, 2006, **448**, 83; (b) L. S. Vedula, J. Jiang, T. Zakharian, D. E. Cane and D. W. Christianson, *Archives of Biochemistry and Biophysics*, 2008, **469**, 184.
- 19 V. A. Khan, A. V. Tkachev and V. A. Pentegova, *Chem Nat Compd*, 1988, **24**, 606.
- 20 J. P. Noel, N. Dellas, J. A. Faraldos, M. Zhao, B. A. Hess, L. Smentek, R. M. Coates and P. E. O'Maille, *ACS Chemical Biology*, 2010, **5**, 377.
- 21 J. A. Faraldos, P. E. O'Maille, N. Dellas, J. P. Noel and R. M. Coates, *Journal of the American Chemical Society*, 2010, **132**, 4281.
- 22 A. Vattekkatte, N. Gatto, E. Schulze, W. Brandt and W. Boland, *Organic & Biomolecular Chemistry*, 2015, **13**, 4776.
- 23(a) M. C. Schulbach, S. Mahapatra, M. Macchia, S. Barontini, C. Papi, F. Minutolo, S. Bertini, P. J. Brennan and D. C. Crick, *Journal of Biological Chemistry*, 2001, **276**, 11624; (b) M. C. Schulbach, P. J. Brennan and D. C. Crick, *Journal of Biological Chemistry*, 2000, **275**, 22876.

7 General Discussion

7.1 Multiproduct terpene synthases

One of the unique traits associated with terpene synthases is their ability to convert an acyclic prenyl diphosphate into multiple products which ultimately leads to the huge diversity of known terpene compounds.^{1,106} Despite their ability to expand the abundance and diversity of terpenes as secondary metabolites, there are still large gaps in our knowledge about the structure of multiproduct terpene synthase and the mechanism that results in the formation of multiple products. The property of multiple product formation is found in nearly half of all characterized mono and sesquiterpene synthases but no common feature has been identified in known sequences that is linked to this capability.¹⁰⁶ Since this ability is so abundant it can be safely inferred that the carbocationic intermediates can be stabilized in multiple ways by the enzyme, but that is usually directed towards a single product.

In terms of structural features some knowledge has been gained despite the lack of crystal structure by characterizing the individual terpene synthases for generating multiple products. In case of the record holder δ -selinene synthase from *Abies grandis*, the formation of 52 different sesquiterpenes has been postulated to be due to presence of two DDxxD motifs located on opposite sides of active site cleft.^{94,168} This facilitates the possibility of substrate binding in two pockets in different conformations which leads to this massive product diversity by a single enzyme.⁹⁴ There is also the possibility that multiproduct formation by these enzymes is due to a NSE/DTE motif that is located at the same position as the second DDxxD motif in some terpene synthases.^{168,173} But a clear answer to this trait remains elusive due to the absence of clearly defined crystal structures of a multiproduct enzyme.¹²⁸

The conformational flexibility in the active site is supposed to be a major factor that allows formation of more reaction intermediates that subsequently result in more products. Nevertheless, based on various kinetic studies,^{151,174} we already know that the cationic cyclization cascades proceed rapidly; this limits the time scale for possible larger conformational changes in intermediates.^{175,176} Moreover, structural complexes of trichodiene synthase with substrate analogs demonstrated that the intermediates were bound in thermodynamically preferred conformations rather than ones expected as part of the mechanistic cascade.^{177,178} These results coupled with other studies point towards the fact that kinetic factors take precedence over thermodynamic process during product formation in terpene synthases.¹⁷⁵ This perspective led to the inference that multiproduct formation is dependent on the early stage of substrate conformational changes. Hence, it would be very interesting to study the multiproduct behaviour of these enzymes by using substrates as metabolic probes with incorporated conformational changes.

The best way to incorporate these conformational changes is by using the geometric double bond isomers of prenyl diphosphates as substrates for the multiproduct enzymes; which should provide new insights on multiple product formation. In fact till 2009, the (2*E*)-double bond isomer was universally accepted as the natural substrate for terpene synthases for both geranyl diphosphate (C₁₀) and farnesyl diphosphate (C₁₅). However in 2009, the work of Schillmiller *et al.*, described the discovery of a monoterpene synthase in tomato glandular trichomes that accepted nerolidyl diphosphate (NDP) the (2*Z*)-isomer of GDP as its natural substrate.¹⁵⁹ In case of sesquiterpene synthases, similar results were reported in case of wild tomato *Solanum habrochaites* where (2*Z*,6*Z*)-FDP was accepted as a precursor instead of traditionally accepted (2*E*,6*E*)-FDP.¹⁷⁹ These alternative substrates proved to be an invaluable tool to study the biosynthesis of monoterpenes and sesquiterpenes in tomato plants.¹⁰⁶

The major aim of this thesis was to employ alternative substrates to probe the characteristics of catalytic pathway in multiproduct terpene synthases. Different strategies of labelling and conformational changes were employed by using the stereoisomers of natural substrates (Manuscript I, II).^{180,181} Moreover the interest in elucidating the structural characteristics that leads to this diversity prompted the development of an easy to synthesize substrate mimic that binds in an identical manner to natural one (Manuscript III).¹⁸² Two sets of multiproduct terpene synthases were used for this purpose, one set comprising of two terpene synthase genes encoding stereoselective multiproduct enzymes TPS4 and TPS5 from *B73* and *Delprim* maize varieties respectively.¹⁴⁵ In the second set, MtTPS5 enzyme from model plant *Medicago truncatula* was used that produces 27 different sesquiterpene products from (2*E*,6*E*)-FDP.^{148,183,184}

7.1.1 Multiproduct enzymes from *Zea mays*

The TPS4-*B73* and TPS5-*Delprim* of *Zea mays* catalyze the formation of the same complex blend of terpene volatiles consisting predominantly of bisabolane-, sesquithujane-, and bergamotane-type sesquiterpenes albeit in distinctly different proportions.^{145,185-187} The terpenoid profiles from (2*E*)-GDP and (2*E*,6*E*)-FDP substrates were dominated by cyclic compounds with a terpinan/sabinan (monoterpenes) and bisabolane/sesquisabinane (sesquiterpenes) skeleton, respectively. Acyclic terpenoids were also present in the product mixture including the three acyclic monoterpenes, β -myrcene, (*R*)-linalool and (*S*)-linalool produced from (2*E*)-GDP and the two acyclic sesquiterpenes, (*E*)- β -farnesene and (3*R*)-(E)-nerolidol produced from (2*E*,6*E*)-FDP. These acyclic terpenes result from deprotonation or water-capture of the first cation formed after cleavage of the diphosphate group.

From the amino acid sequences, the difference between TPS4 and TPS5 was found to be four amino acids of which the replacement of Gly residue at position 409 with an Ala affected the catalytic site. As a result it was found that different terpene profiles were controlled by allelic variation of the closely related terpene synthase genes TPS4 and TPS5.¹⁴⁵ Although both enzymes showed the typical properties of sesquiterpene synthases (molecular mass, subunit architecture and the need for a divalent metal co-factor) they not only accepted FDP (C₁₅) but also the C₁₀ analog GDP as a substrate. Both substrates were almost exclusively converted into two types of cyclic products with cyclohexenyl- and bicyclo[3.1.0]hexyl moieties as common structural features (Figure 10). Interestingly, for the diastereoisomeric pairs of 7-*epi*-sesquithujene and sesquithujene, sesquisabinene A and sesquisabinene B, (*E*)- α -bergamotene and (*Z*)- α -bergamotene, and enantiomeric (*S*)- and (*R*)- β -curcumene, and (*S*)- and (*R*)- γ -curcumene, respectively the first compound is abundant in the product profile of TPS4 and the latter in case of TPS5.^{145,188}

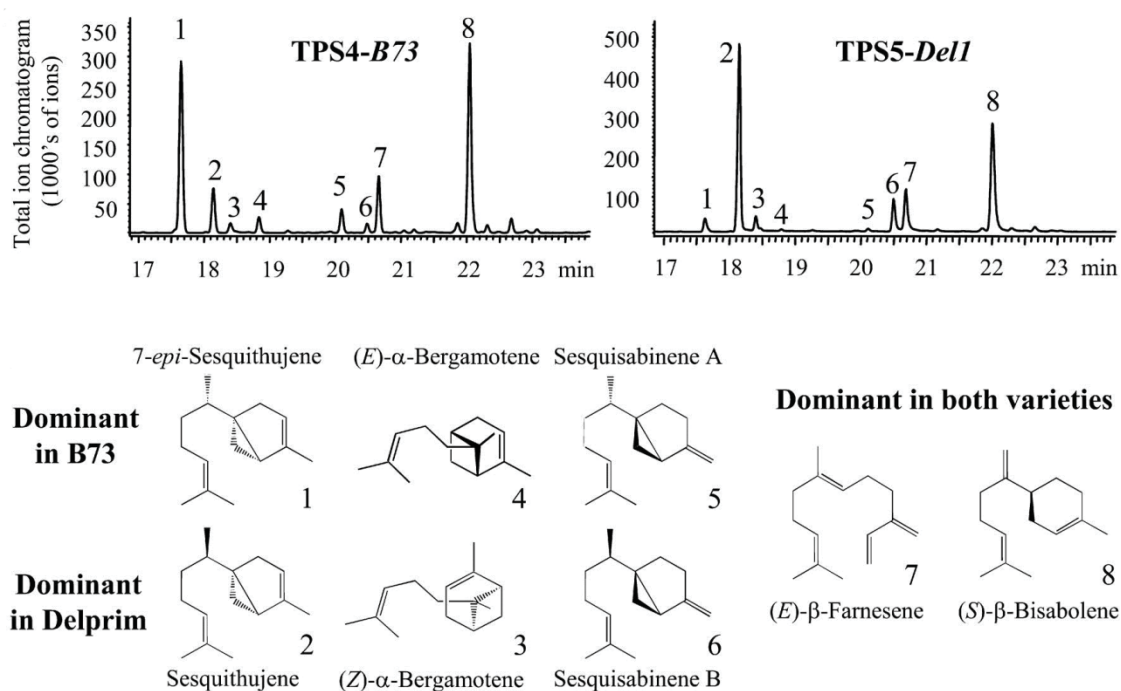


Figure 10: Volatile sesquiterpene products of two maize varieties and the corresponding terpene Synthase Enzymes (B) Comparison of products of terpene synthases TPS4 and TPS5 expressed in *E. coli* and incubated with FDP. A portion of the gas chromatography–mass spectrometry analysis of each sample is shown.(C) Structures of major sesquiterpene products. 1, 7-*epi*-sesquithujene; 2, sesquithujene; 3, (*Z*)- α -bergamotene; 4, (*E*)- α -bergamotene; 5, sesquisabinene B; 6, sesquisabinene A; 7, (*E*)- β -farnesene; 8, (*S*)- β -bisabolene. Adapted with permission Köllner, *et al.*¹⁴⁵

Interestingly, there is an extraordinary symmetry in the mechanistic cascade of both the enzymes starting with branching from the neryl cation. Both (*R*)- and (*S*)-bisabolyl cations further branch into an analogous mixture of products following parallel pathways, only exception being the (*6S*)-enantiomer of β -bisabolene. In terms of reaction rates, nearly 95% of the bisabolyl cation-derived products that originate from the (*S*)- configured bisabolyl cation in TPS5. While in case of TPS4, the split in the ratio of bisabolyl-derived products is almost equal between (*R*)- and (*S*)-bisabolyl cation, with a majority of the (*S*)-form represented by

(*S*)- β -bisabolene (Figure 11).¹⁴⁵ Catalysis with GDP showed the same principal pattern as FDP but at a lower velocity, with identical 13 monoterpenes being formed as products in both cases.

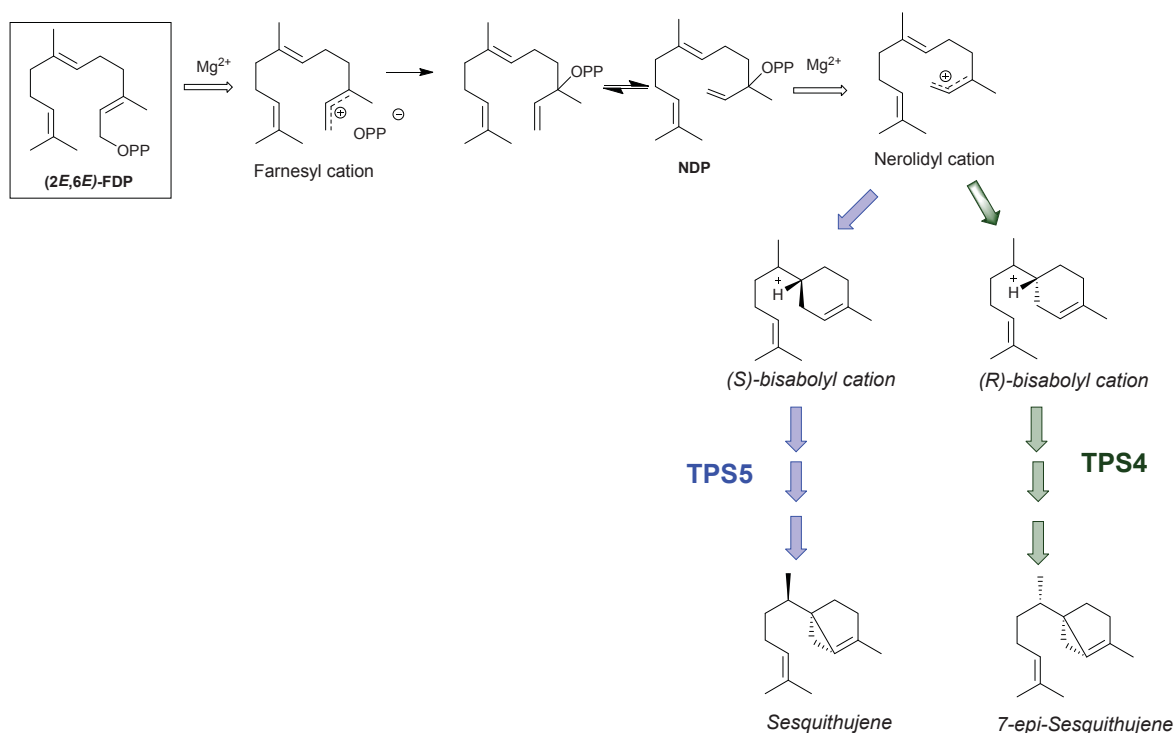


Figure 11: Abbreviated TPS4 (green) and TPS5 (blue) reaction cascade showing product specificity of each enzyme from (2*E*,6*E*)-FDP. Maize TPS4 and TPS5 catalyze the formation of the same complement of sesquiterpene products, albeit in distinctly different proportions. Abbreviated mechanisms depict the generation of 24% 7-*epi*-sesquithujene, and 6% sesquithujene for TPS4; and 2% 7-*epi*-sesquithujene, and 28% sesquithujene for TPS5. Blue and green arrows depict TPS5- and TPS4-preferred pathways, respectively.

The relationship between active site scaffolds and the diversity in product formation was studied with the terpene synthase TPS4. The results of active site modelling and docking simulations suggested that discrete steps of the reaction cascade take place in two different active site pockets, with a shift from one pocket to the other being caused by conformational changes in the bisabolyl cation intermediate. With the help of mutagenesis studies, it was inferred that early steps of the catalytic process up to the formation of the monocyclic bisabolyl cation are localized in pocket I and the secondary cyclization takes place primarily in the pocket II region.¹⁸⁸

7.1.2 Multiproduct terpene synthase from *Medicago truncatula*

To explore the regulatory mechanisms for herbivore-induced terpenoid emissions, three TPS cDNAs were cloned from *M. truncatula*.^{148,189} MtTPS5 is a multiproduct sesquiterpene synthase and incubation with FDP provides 18 sesquiterpene hydrocarbons and 10 sesquiterpene alcohols, with very different carbon skeletons comprising the germacrane, cubebane and *allo*-aromadendrene skeletons and other structures (Figure 12).^{149,190} Analysis of enantiomeric composition of the products revealed that all compounds were highly optically pure like optically pure (–)- β -cubebene and (–)-germacrene D.¹⁴⁹

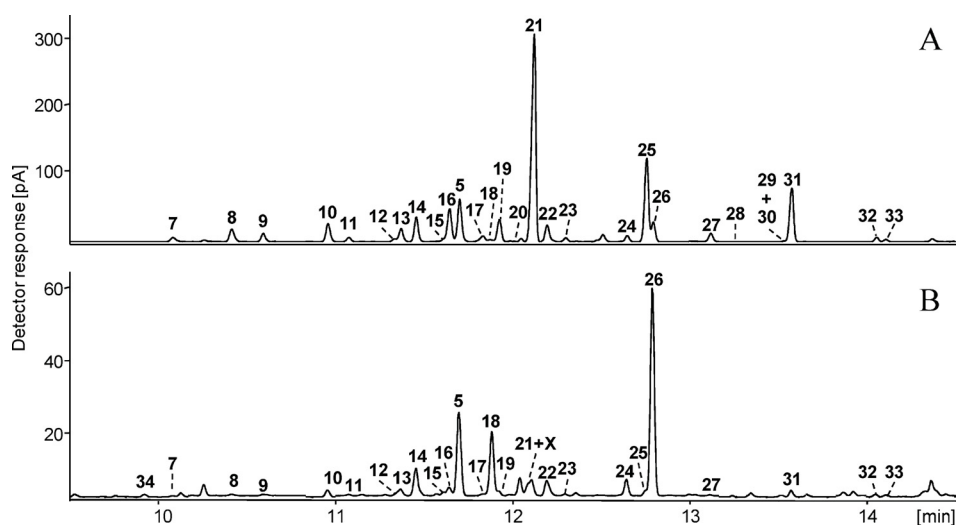


Figure 12: GC-FID chromatograms of enzymatic products of recombinant MtTPS5 wild type (A) and Y526F mutant (B) from incubation with (2E,6E)-FDP. The products were identified by Kováts indices and mass spectra in comparison to authentic samples: 7, α -cubebene; 8, α -copaene; 9, β -cubebene; 10, (*E*)- β -caryophyllene; 11, β -copaene; 12, cadina-3,5-diene; 13, α -humulene; 14, *allo*-aromadendrene; 15, *trans*-cadina-1(6),4-diene; 16, γ -muurolene; 5, germacrene D; 17, bicyclosquiphellandrene; 18, bicyclogermacrene; 19, α -muurolene; 20, δ -amorphene; 21, cubebol; 22, δ -cadinene; 23, cadina-1,4-diene; 24, nerolidol; 25, copan-3-ol; 26, 4 α -hydroxygermacra-1(10),5-diene; 27, copaborneol; 28, 1-*epi*-cubanol; 29, T-cadinol; 30, cubanol; 31, torreyol; 32, kunzeaol; 34, bicycloelemene. Adapted with permission from Garms *et al.*¹⁴⁹

The high enantiomeric excess of the products generated by MtTPS5 is remarkable; it indicated that the whole reaction cascade starting with the initial ionization of FDP, the isomerization of the farnesyl carbocation and subsequent cyclization to the final products is under tight control of the active site. The cyclization cascade was reconstructed (Figure 13) by following the products derived from a common carbocationic intermediate as they share the same configuration at all stereocenters. The farnesyl cation leads to the class of products linked to the bicyclogermacrane skeleton, humulene and caryophyllene,^{121,127,191} while the isomerization of the farnesyl to the nerolidyl cation results in the cubebenes and cadinenes.¹⁹²⁻¹⁹⁴ Based on a mechanism originally proposed by Arigoni in 1975, it was concluded that the series of cadalanes is generated by protonation of a neutral germacrene D intermediate, shown by labelling experiments in D₂O.¹⁶⁶ Tyrosine at position 526 is known to provide a proton to germacrene A *en route* to 5-*epi*-aristolochene in TEAS.¹⁵⁷ Exchange of this Tyr by a Phe in MtTPS5 (Y526F mutant) suppressed this reaction pathway confirming an analogous mechanism in the *Medicago truncatula* MtTPS5 enzyme. Interestingly, the Y526F mutant formed small amounts of the cadinene and cubebene family via the nerolidyl cation.¹⁴⁹

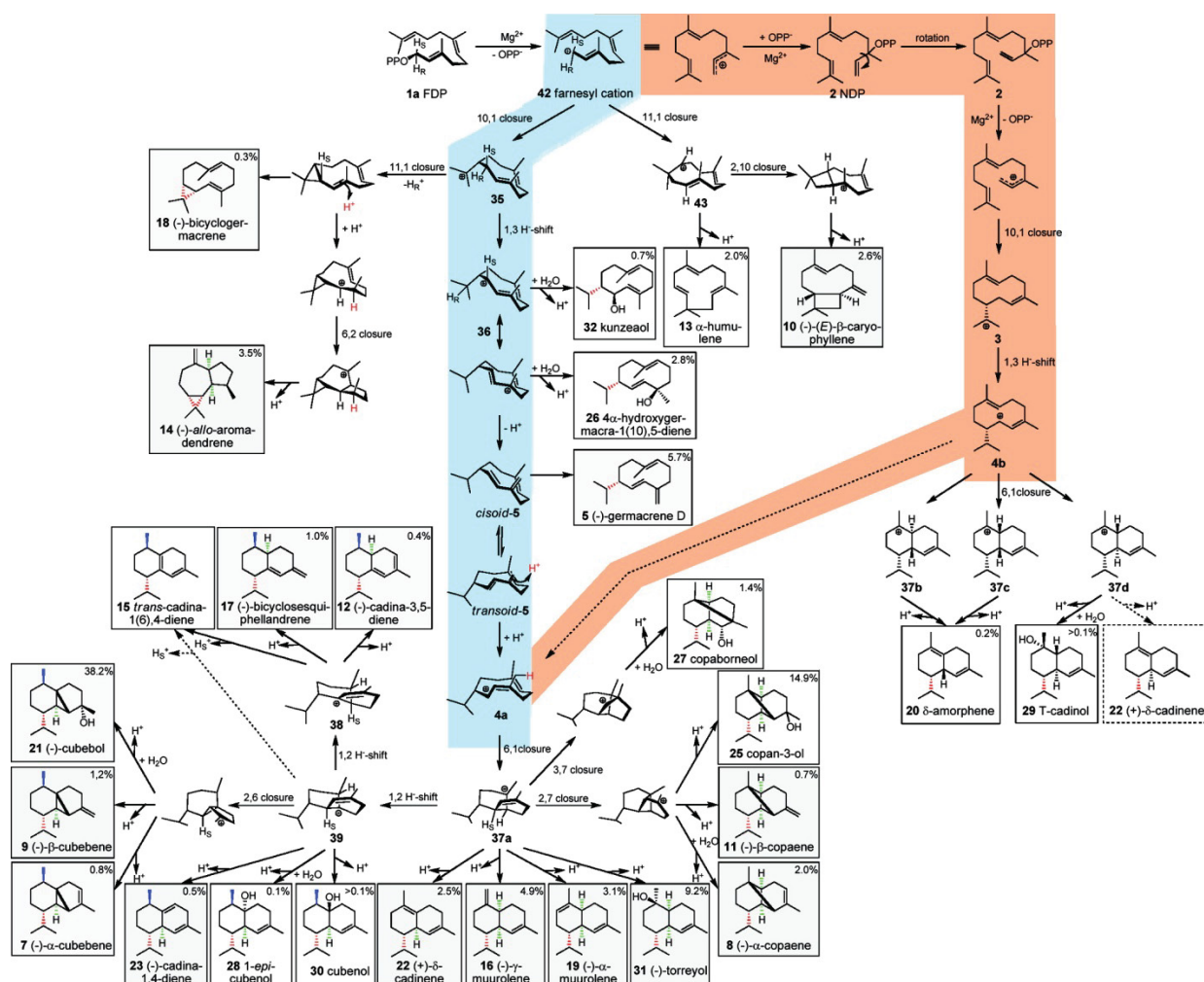


Figure 13: Proposed reaction mechanism for the formation of sesquiterpene products by MtTPS5 with (2*E*,6*E*)-farnesyl diphosphate. Stereocenters with the same absolute configuration are marked in green, red, and blue. Reaction channels leading to 4a,b by protonation of germacrene D (light blue) or by the intermediacy of NDP (2) (orange) are highlighted. Adapted with permission from Garms *et al.*¹⁴⁹

7.2 Isotope Sensitive Branching in Multiproduct enzymes (Manuscript I)

The reactions catalyzed by a typical terpene cyclase involve a complex series of isomerizations and intramolecular electrophilic reactions, frequently accompanied by molecular rearrangements and hydride shifts. They are usually terminated either by loss of a proton or by capture of an external nucleophile such as water or the pyrophosphate anion. All the carbocationic intermediates between the acyclic prenyl diphosphate and the final cyclization product are tightly sequestered by the cyclase in hydrophobic active site. Hence, unfortunately these complicated yet seamless transformations cannot be directly visualized.

Multiproduct terpene synthases provides an attractive opportunity to decipher the normally vague chain of events leading to the generation of individual terpenes. Since all of the terpenoid products are derived either from geranyl diphosphate (GDP) or farnesyl diphosphate (FDP). It can be safely assumed that all of the products represent the quenching of individual intermediates at various stages of the multistep isomerization-cyclization-rearrangement process. Hence, this logic can be used by means of labelled

substrates to clarify the sequence of biosynthetic reactions and to analyze the factors influencing the partitioning of the various carbocationic intermediates. The induced kinetic isotope effects are observed changes in product ratios in multiproduct enzymes resulting from an isotopically labeled substrate. In complicated enzymatic reaction cascades, this technique which uses intramolecular isotope effects has been used to examine the mechanistic hypotheses¹⁹⁵⁻¹⁹⁹. In such an experiment, the substrate is a molecule that is exactly equivalent except for isotopic substitution. Thus the observed isotope effects then reflect the intramolecular competition between the two otherwise equivalent sites.²⁰⁰ Harada *et al.*,²⁰¹ have shown that within a branched reaction sequence, the “metabolic switching” or isotopically sensitive branching can affect the magnitude of the isotope effect.¹⁹⁶

Isotopically sensitive branching in a multiproduct enzyme describes the rate enhancement in the formation of one product at the expense of a second product due to isotopic substitution.²⁰² Such an observation indicates that the two products arise from a common intermediate formed by the same enzyme. For the terpene cyclase reaction, a simplified kinetic model (Figure 14) is described as below:

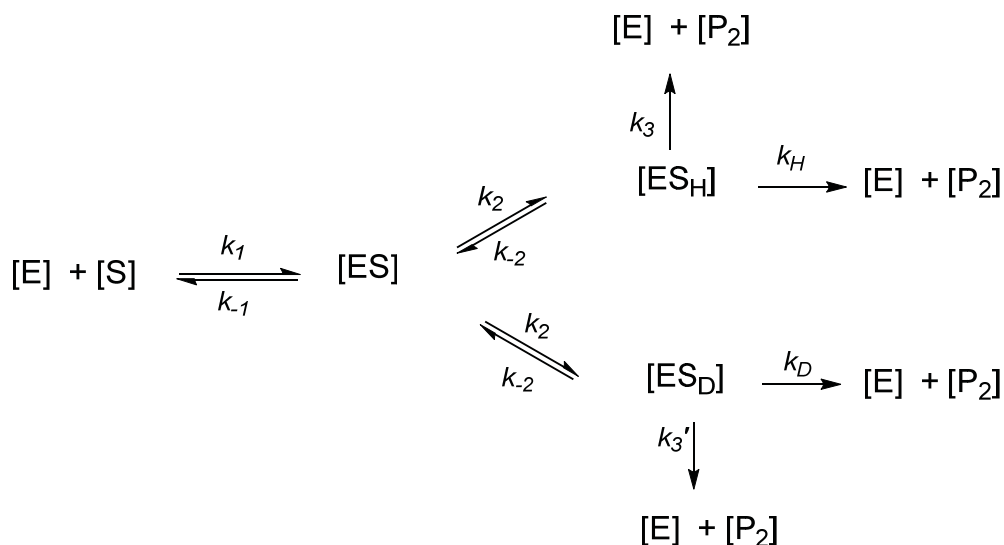


Figure 14: Kinetic model for isotopically sensitive branched reaction pathways. The model assumes that there is no isotope effect associated with binding (i.e., a single rate constant k_2 describes the fractionation of [ES] to [ESH] and [ES_D] and a single rate constant k_{-2} describes the formation of [ES] from [ESH] and [ES_D]) and that product formation is irreversible.²⁰⁰

Stabilization of the carbocationic intermediates is partly ensured by interactions with the hydrophobic, aromatic-rich active-site of the enzyme (e.g. π -cation interactions with aromatic residues of the active site).²⁰³ Nevertheless, hyperconjugative interactions within carbocations themselves also play an important role in their stability. In molecular orbital terms, hyperconjugation is described as the interaction of the vacant p -type orbital on the cationic center with adjacent C-H or C-C σ -bonds.²⁰ The magnitude of this hyperconjugative effect depends on the number of hydrogen atoms attached to the carbon atom immediately

adjacent to the unsaturated system. Because the energy required for breaking a C-D bond is higher than that for a C-H bond (i.e. a C-D bond is stronger than a C-H bond), a C-D hyperconjugation stabilizes an adjacent positive charge less than a C-H hyperconjugation. Consequently, reactions in which C-D bonds are broken proceed more slowly than reactions in which C-H bonds are broken. Such hyperconjugative weakening in reaction intermediates due to isotope (deuterium) substitution induces secondary kinetic isotope effects.

Isotope sensitive branching experiments have been successfully used to confirm the complex reaction cascades of various monoterpene synthases like pinene synthases from Sage,²⁰⁴ pinene cyclase from *Abies grandis*,²⁰⁵ phellandrene cyclase from lodgepole pine (*Pinus contorta*)²⁰⁵ and other monoterpene cyclases.^{204,206,207} This technique has also been successfully used to probe mechanism of sesquiterpene synthases, tobacco *epi*-aristolochene synthase and hyoscyamus premnaspirodiene synthases.¹⁰⁷ More recently, effects of isotopically sensitive branching on product distribution have been reported for pentalenene synthase and used to predict a new branching pathway.^{208,209}

7.2.1 Substrates for Isotope Sensitive Branching Experiments

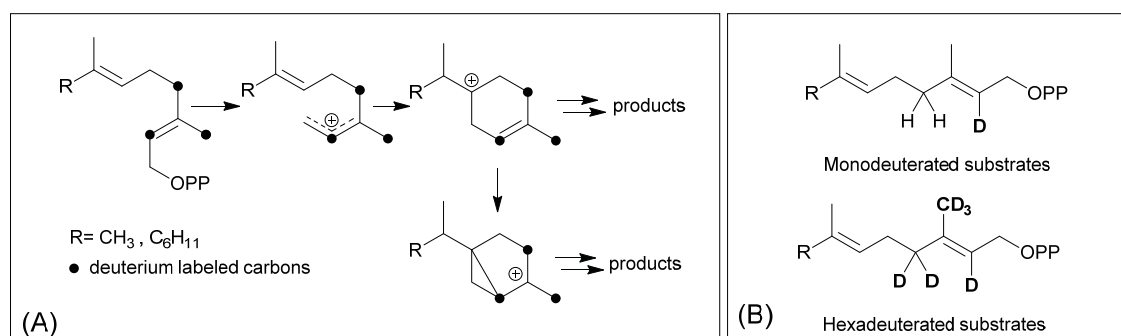


Figure 15: (A) Isotope sensitive branching strategy (B) monodeuterated and hexadeuterated of GDP and FDP. In case of hexadeuterated substrates, isotope labeled with deuterium atoms completely surrounding the C(3) carbon of the substrate and of the key intermediates were synthesized.

To gain insight into terpenoid biosynthesis in maize and determine whether the final deprotonation of cationic intermediates *en route* to mono- and sesquiterpenes is rate limiting, deuterium kinetic isotope effects were investigated for TPS4 and TPS5 enzymes from *B73* and *Delprim* maize varieties. The encoded terpene synthases were heterologously expressed in *E. coli*, purified and fully characterized. To study the kinetics of the reaction cascade and to understand the rate limiting role of the final deprotonations, stable isotope labeled substrates were synthesized with deuterium atoms completely surrounding the C(3) carbon of the substrate and of the key intermediates (Figure 15). Some of these cationic intermediates are flanked by protons; others are completely surrounded by deuterium atoms. Depending on their stability and ease of deprotonation reactions, different reaction channels may be favored. In order to study the impact of the

degree of isotope labelling both monodeuterated and hexadeuterated analogs of GDP (C_{10}) and FDP (C_{15}) were evaluated as substrates.¹⁸⁰

7.2.2 Kinetic isotope effects in multiproduct terpene synthases from *Zea mays*

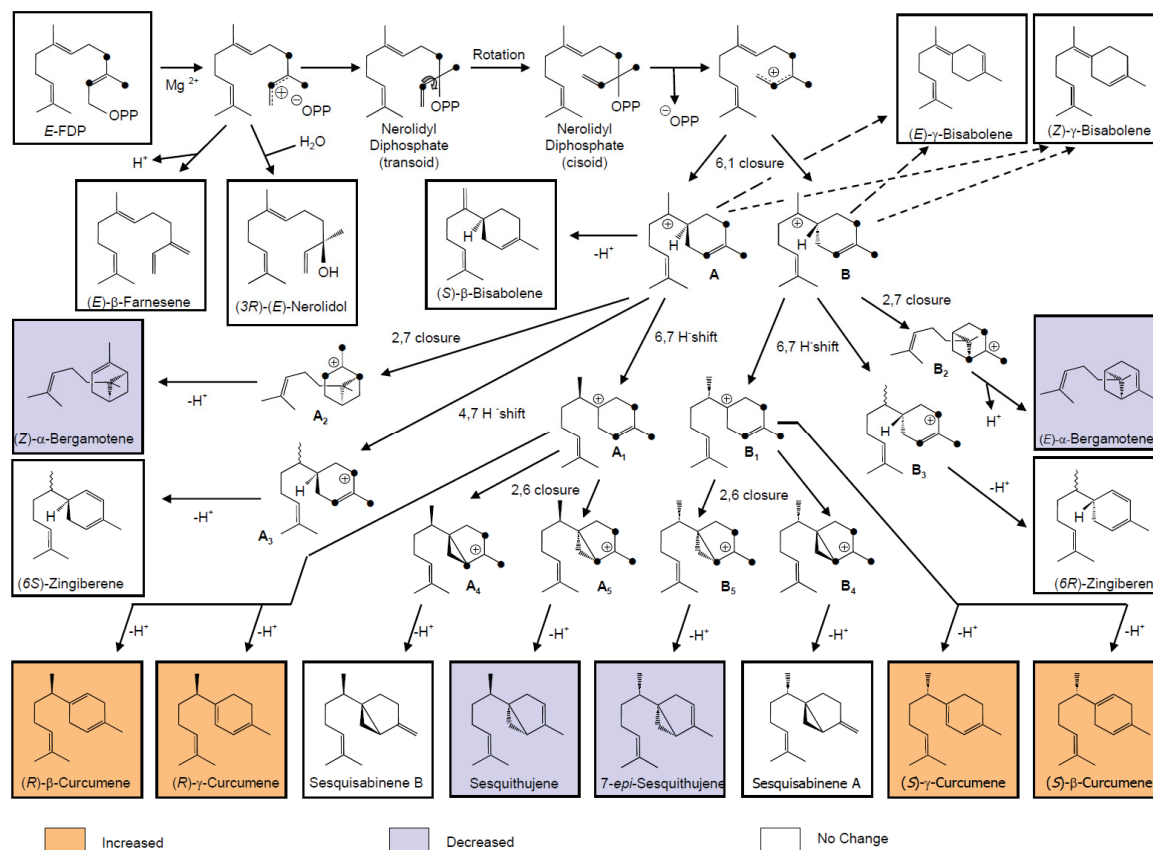


Figure 16: Proposed pathway for sesquiterpene formation from TPS4 and TPS5 using [2,4,4,13,13,13-²H₆]-FDP. The black dots represent deuterated carbons. Some of these cationic intermediates are flanked by protons; others are completely surrounded by deuterium atoms. Depending on their stability and ease of deprotonation reactions, different reaction channels are favored. (Orange depicts an increase, blue decrease and no color represents no change as compared to unlabeled substrate).

In the present study, the kinetic isotope effects (KIE) combine with the primary KIEs confirm the alteration of product distributions after isotopically sensitive branching. To illustrate the effects of hyperconjugation and the resulting secondary KIEs, the case of (2*E*,6*E*)-[2,4,4,13,13,13-²H₆]-FDP and (2*E*)-[2,4,4,9,9,9-²H₆]-GDP were considered and product formation from FDP are depicted in Figure 16. Deuterium isotope effects are less pronounced in the case of the monodeuterated analogues since the positive charge is surrounded by only one deuterium atom, the other hydrogen atoms being able to undergo C-H hyperconjugative interactions.

From (2*E*,6*E*)-[2,4,4,13,13,13-²H₆]-FDP, the cyclization cascade is initiated by the formation of (*S*)- and (*R*)-bisaboyl cations (A and B, respectively) (Figure 16). These first carbocations can be directly deprotonated to produce (*S*)-β-bisabolene without noticeable KIEs (the positive charge being located far from

the deuterated center). Carbocations **A**₄, **A**₅, **B**₄ and **B**₅ are the less stable ones since the positive charge fully surrounded by deuterium atoms cannot be delocalized and stabilized by C-D hyperconjugation. The stability of the terminal carbocation results in the corresponding cyclic terpene being produced. Nevertheless, strong KIEs for the formation of sesquithujene, 7-*epi*-sesquithujene or sesquisabinenes A and B were obtained. Similarly, slight KIEs were observed for zingiberene isomers because carbocations **A**₃ and **B**₃ were not highly destabilized after deuterium substitution. The rate suppression was coupled with a corresponding enhancement in the rate of formation of β - and γ -curcumene isomers, sesquithujene hydrate and 7-*epi*-sesquithujene hydrate, leading to enhanced formation of alcohols. This pattern of isotope sensitive branching was also observed in case of monoterpene formation.

Interestingly, the products arising from the deuterated precursors revealed an enhanced formation of alcohols instead of olefinic products in comparison with those from unlabeled (*2E*)-GDP and (*2E,6E*)-FDP. This observation of isotopically sensitive branching of product formation in maize supports the enzymatic biosynthesis of mono- and sesquiterpene volatiles from a common carbocationic intermediate along a branched reaction sequence.

7.3 Effects of Substrate Geometry on Terpene Synthases (Manuscript II)

The multiproduct formation in terpene synthases is dependent on the early stage substrate conformation changes.¹⁷⁵ Novel insight into the multiproduct behaviour of these enzymes can be gained by using isotope-labelled geometric stereoisomers as metabolic probes.²¹ Enzymes that catalyze the *trans*-pathway of catalysis rearrange and quench this initial transoid cation. Other enzymes that catalyze the *cis*-*trans* pathway of catalysis recapture the diphosphate leaving group at carbon C3, thereby allowing rotation around the generated C2-C3 bond to yield the nerolidyl diphosphate (NDP) intermediate. Even in nature we know that with the discovery of tomato monoterpene synthase that accepted NDP instead of (*E*)-GDP as its natural substrate.¹⁵⁹ Sesquiterpene synthases are known as very specific for either one or the other pathways, and yet there are examples of enzymes that use both pathways.²¹⁰

The advantage with using geometrical isomers of natural substrates like (*2Z,6E*)-FDP is that no isomerization step precedes the subsequent carbocation cyclization reactions as the desired cisoid farnesyl cation becomes readily available after cleavage of the diphosphate moiety. Various sesquiterpene synthases have been characterized using FDP isomers and analogues to determine the mechanism of carbocation quenching^{107,194,211,212} and also the initial ionization and isomerization of *all-trans*-FDP for *cis-trans*-pathway-specific enzymes.^{175,176,193,213} However, the focus of most research has been directed towards

determining the kinetic properties of different FDP isomers. Only recently has the investigative focus shifted towards using (2*Z*,6*E*)-FDP as a substrate for sesquiterpene cyclases, especially notable is the work on sesquiterpene synthases Cop4 and Cop6 from *Coprinus cinereus*.¹⁶³

7.3.1 Effects of geometry on multiproduct terpene synthase from *Zea Mays*

To reveal further details of the TPS4 and TPS5 enzymatic mechanism, various isotopic analogs of geranyl- and farnesyl diphosphates were synthesized. These included geometric isomers of the critical C(2)-C(3) bond) like [2-²H]- (2*Z*)- and [2,4,4,9,9,9-²H₆]- (GDP) and [2-²H]- (2*Z*,6*E*)- and [2,4,4,13,13,13-²H₆]-FDP using deuterium labels as metabolic probes for isotope sensitive branching. The interest was in whether the cyclization of (2*Z*)-isomers such as (2*Z*)-GDP and (2*Z*,6*E*) FDP would proceed via the same cascade as observed with their corresponding (*E*)-substrates. Here, the interest was to analyze by means of deuterium labeling how the substrate's conformation affects the initial cyclization as well as the course and site of the individual protonation and deprotonation steps. The idea was to combine the knowledge gained from previous isotope sensitive branching studies to decipher the effects of substrate geometry on the reaction cascade.¹⁸¹

7.3.2 Labelled stereoisomers as substrates

[2-²H]- and [2,4,4,9,9,9-²H₆]-GDP and [2-²H]- and [2,4,4,13,13,13-²H₆]-FDP were prepared by modifying the protocol of Arigoni *et al.*²¹⁴ Substrates were similar to the ones used in the previous study with deuterium atoms completely surrounding the C(3) cationic center of the key intermediates (Figure 17). The deuterium labels serve to investigate the alterations in product distribution that might occur as a consequence of changing the geometry of the C2-C3 double bond, which undergoes isomerization in the reaction sequence.

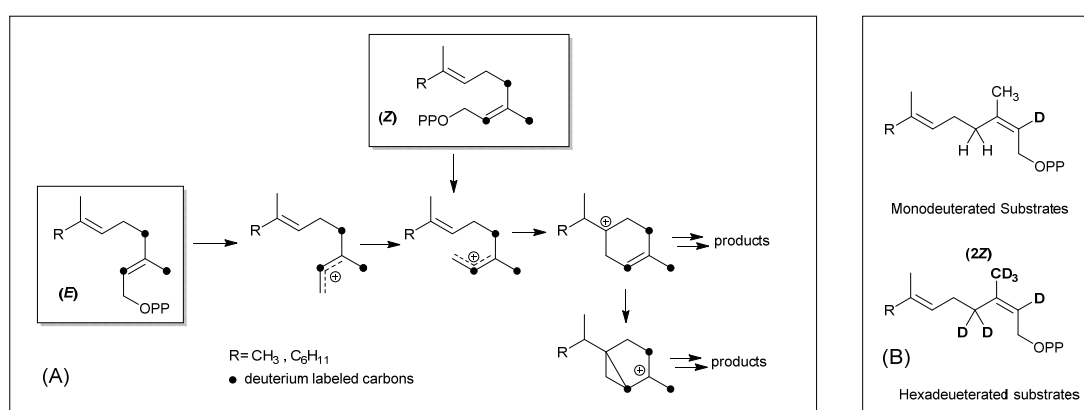


Figure 17: (A) Isotope sensitive branching strategy with stereoisomers (B) of monodeuterated and hexadeuterated of (2*Z*)-GDP and (2*Z*, 6*E*) FDP. Isotope labeled with deuterium atoms completely surrounding the C(3) carbon of the substrate and of the key intermediates with isomerization of the C(2)-C(3) double bond were synthesized.

7.3.3 Product distribution with geometric isomers

When compared with our previous results,¹⁸⁰ both TPS4 and TPS5 catalyze the cyclization of labeled (*2Z,6E*)-FDP and (*2Z*)-GDP showed only quantitative difference in volatile composition when compared to natural substrates. Interestingly, these enzymes exhibited much higher turnover with (*2Z*) substrates than with their natural (*2E*)-substrates and a reduced ratio of acyclic to cyclic products. The production of all C₁₀ and C₁₅ cyclic products requires an initial isomerization of the C(2)-C(3) double bond of the original substrate. The substrates of the (*2Z*)-series already possess the double bond in the correct configuration allowing the direct cyclization of the emerging carbocationic intermediate after ionization. The terpenoid profiles from (*2E*)-GDP and (*2E,6E*)-FDP substrates (Figure 18) were dominated by cyclic compounds with terpinane/sabinane and bisabolane/sesquisabinane skeletons. This confirms that the formation of cyclic products follows the same pathway as the (*2E*)-isomer. A few recent examples also report (*2Z,6E*)-FDP results comparable to those obtained from the FDP.^{146,188,215}

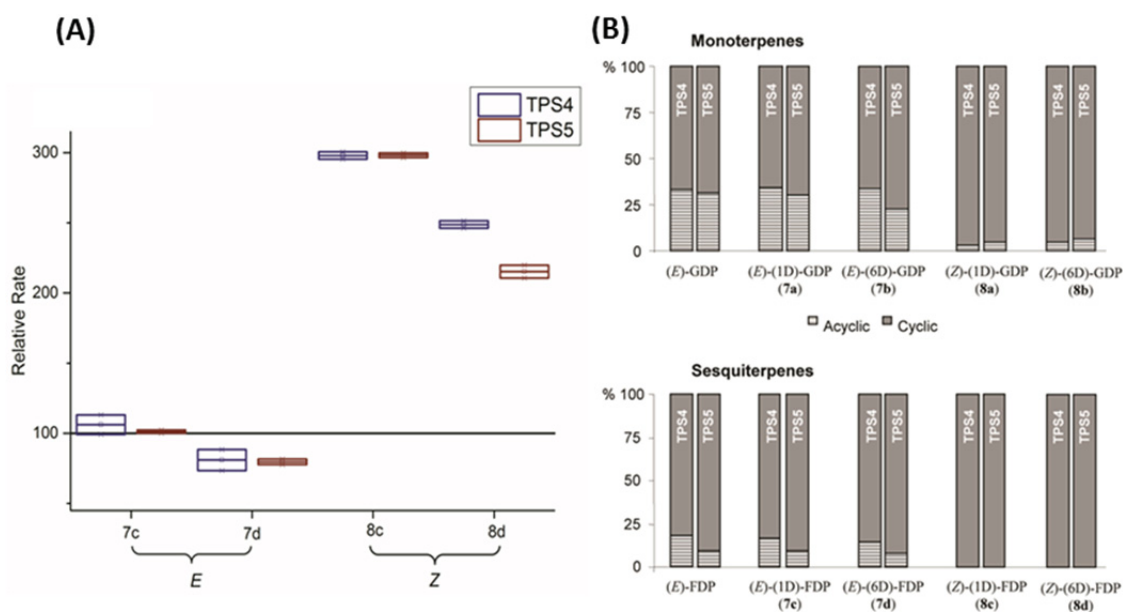


Figure 18: (A) Comparison of total rate of sesquiterpene and (B) Ratio acyclic/cyclic volatiles formation with incubations of deuterated (*E*)/(*Z*)-GDP and FDP with TPS4-B73 and TPS5-Delprim. (A) Comparison of relative rates of sesquiterpene volatile formation from Monodeuterated substrates (7c, 8c) and hexadeuterated substrates. Compounds 7 and 8 represent (*E*) and (*Z*)-FDP respectively. Sesquiterpene production increased by ~200% and the corresponding increase was ~150% with the hexadeuterated substrate when compared with unlabeled (*2E,6E*)-FDP. (B) There was a distinct absence of acyclic products in case substrate with (*2Z*)-substrates was seen in both monoterpenes and sesquiterpenes.

The rate of monoterpene production showed a 30% increase upon incubation with (*2Z*)-GDP and 17% with hexadeuterated substrates in comparison to their corresponding unlabeled (*2E*)-analogues. The difference in the rates of volatile formation was even more pronounced in the case of sesquiterpene. Sesquiterpene production increased by ~200% and the corresponding increase was ~150% with the (*2Z,6E*)-hexadeuterated substrate when compared with unlabeled (*2E,6E*)-FDP (Figure 18A). The increased turnover

clearly indicates that the isomerization is the rate limiting step in the reaction cascade with natural substrates. Docking studies had postulated the presence of two pockets, where the early steps of the catalytic sequence including dephosphorylation, isomerization, and cyclization, up to the formation of the bisabolyll carbocation, all take place in pocket-I of the enzyme.¹⁸⁸ Then on possibly crossing a low energy barrier to pocket II, they are converted to a larger proportion of cyclic products than the (*2E*)-substrates. This could explain not only the reduction in acyclic substrates and smaller kinetic isotope effects, but also the availability of more energy that can be utilized for processes in pocket II. This strong preference for cyclic products and huge turnover can be exploited to direct biosynthesis for other terpene synthases already known for their catalytic promiscuity.¹⁰⁶

7.4 Development of co-crystallization candidate (Manuscript III)

There is a lack of clear understanding about the structural characteristics that lead to catalytic promiscuity in multiproduct terpenoid synthases, as so far none of them has been successfully crystallized.¹²⁸ Examples of *trans*-pathway-specific enzymes with solved crystal structures include pentalenene-synthase from *Streptomyces* UC5319,²¹⁶ 5-*epi*-aristolochene-synthase from *Nicotiana-tobaccum*,^{112,217} and aristolochene-synthase from *Aspergillus terreus* and *Penicillium roqueforti*.^{116,218,219} Trichodiene-synthase from *F. sporotrichoides*,^{220,221} and very recently, δ -cadinene-synthase from *Gossypium arboreum*²²² are the only *cis-trans*-pathway-specific sesquiterpene synthases with solved crystal structures. The closest candidate to a multiproduct terpene synthase with a confirmed crystal structure is sesquiterpene cyclase *epi*-isozizaene synthase (EIZS) from *Streptomyces coelicolor*. However, it is not multiproduct synthase in true sense as its product profile has about 79% *epi*-isozizaene from the substrate FDP.¹²⁹⁻¹³¹

Substrate analogues have been successfully utilized to probe the specificity of the enzymes and to obtain a substrate-bound crystal structure of enzymes. Especially, sulphur substitution has been used quite successfully for co-crystallization with different terpene synthases.^{223,224} Fluorinated substrates have been successfully used to study the cyclization mechanism of several terpene synthases, in particular the aristolochene synthases.^{225,226} Thus, non-natural substrates have shown great potential as substrates or inhibitors to probe mechanisms and can be further utilized for multiproduct terpene synthases.

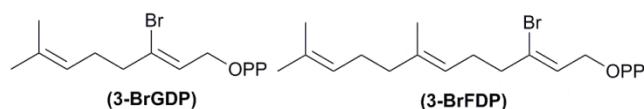


Figure 19: GDP analogues containing bromo substitution (3-BrGDP) and FDP analogue (3-BrFDP). Bromo substitution was chosen because of the geometrical similarity with the methyl group at C3 position.

Based on the information obtained from mechanistic studies of MtTPS5,¹⁴⁹ a set of easy to synthesize functional analogues of prenyl diphosphates was designed for this enzyme that could destabilize the intermediate allylic carbocation. The brominated GDP analogue (3-BrGDP) and FDP analogue (3-BrFDP) (Figure 19) were chosen because of their geometrical similarity and virtually identical van der Waals radius (ca. 2.0 Å,²²⁷ Figure 20) with the methyl group at C3 position. The highly electronegative bromine atoms can strongly influence the stability of neighboring carbocationic species but pose no additional steric differences in comparison with corresponding natural substrates. These analogues could either provide novel sesquiterpenes, or they could act as potent inhibitors of MtTPS5. In case of inhibition it can be used to provide an active site resolved crystal structure.¹⁶⁷ Kinetic studies demonstrated that these compounds constitute potent competitive inhibitors of the MtTPS5 enzyme with fast binding and slow reversibility.

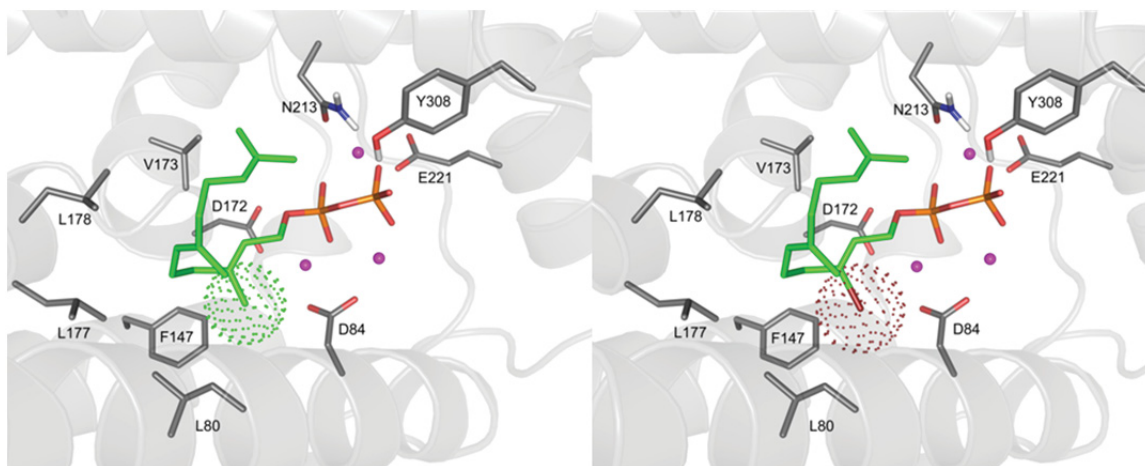


Figure 20: Docking arrangement of FDP (left) and 3-BrFDP (5b) (right) in the active site of the X-ray structure of aristolochene synthase (4KUX). The van der Waals radii are shown by a cloud around CH₃ and Br groups.

However, in case of 3-bromo analogues the huge endothermic energy required for the formation of the intermediate allyl cation prevents its formation, and hence, subsequent energy gain by cyclization is not possible. However, 3-Br GDP and 3-Br FDP are able to bind to the active site of enzyme because there is no steric difference in comparison with the natural substrates. Since the dissociation of the diphosphate moiety is the first step, common to all prenyl diphosphate based terpenoid synthases and cyclases; we expect these simple analogues broadly applicable inhibitors. Preliminary experiments with isoprenyl diphosphate synthase 1 (PcIDS1)²²⁸ from leaf beetle *Phaedon cochleariae* showed no catalytic formation of FDP upon incubation with the substrates GDP and IDP. Initial results indicate a possible co-crystallization of this enzyme with 3-Br-GDP, but this can only be confirmed after solving the crystal structure. Due to the structural similarity between various terpene synthases and the similarity in behavior of the active site, we expect these 3-bromo isoprenoids to constitute ideal probes for crystal structure studies. The 3-bromo substituent provides

additional advantage of determining the absolute configuration based on the anomalous dispersion effect.^{229,230}

7.5 Substrate geometric isomers as a tool for novel biosynthetic products (Manuscript IV)

Mechanistic studies of the catalytic cascade of MtTPS5 with (2*E*,6*E*)-FDP showed that the enzyme is capable of synthesizing cadalane sesquiterpenes in two different ways.¹⁴⁹ Here, the isomerization of the initially formed (2*E*,6*E*)-farnesyl cations to nerolidyl diphosphate (NDP) and further to (2*Z*,6*E*)-farnesyl (Figure 4, orange) is not preferred. Interestingly, (2*Z*,6*E*)-FDP on incubation with MtTPS5 provides a completely new array of products. A large proportion of the released compounds (~ 33%) have a cadalane skeleton, which is in contrast to the (2*E*,6*E*)-FDP products which exhibit the opposite absolute configuration at the bridgehead carbon atoms. This trend is unlike multiproduct terpene synthase TPS4 and TPS5 from *Zea mays* which generate the same product profile with both substrates but with quantitative differences. The determination of the absolute configurations of some products helped with reconstruction of the stereochemical course of the reaction cascade from the starting conformation of the (*Z*)-isomeric substrate. The highly reactive (2*Z*,6*E*)-farnesyl cation, which is formed upon cleavage of the diphosphate group predominantly undergoes a C1-C11 ring closure to the (2*Z*,6*E*)-humul-10-yl cation (~57%). This (2*Z*,6*E*)-Humul-1-yl cation undergoes deprotonation to form γ -humulene, and on further reaction with water, the main product humulan-6,9-dien-3-ol is formed. This product is not observed at all in case of the incubation of (2*E*,6*E*)-farnesyl diphosphate with MtTPS5.

The mechanistic considerations of product formation, starting from (2*E*,6*E*)- and (2*Z*,6*E*)-FDP clearly show a close correlation between the two reaction cascades. The essential elements such as 1,3-hydride shift, initial 1,10- or 1,11- cyclization and the construction of bicyclic compounds by a second ring closure are found in both reaction mechanisms. The synthase bypasses the geometric restriction which prevents the direct formation of cadalanes from the (2*E*)-isomer substrate to a lesser extent over an alternative path (Figure 21). The isomerization of (2*E*,6*E*)- to (2*Z*,6*E*)-farnesyl cation is realized via the rotation of the C2-C3 single bond of the tertiary allylic intermediate. This leads to the formation of major products with humulane and himachalane skeletons for (2*Z*,6*E*)-FDP which are not favored in case of using (2*E*,6*E*)-FDP as a substrate.

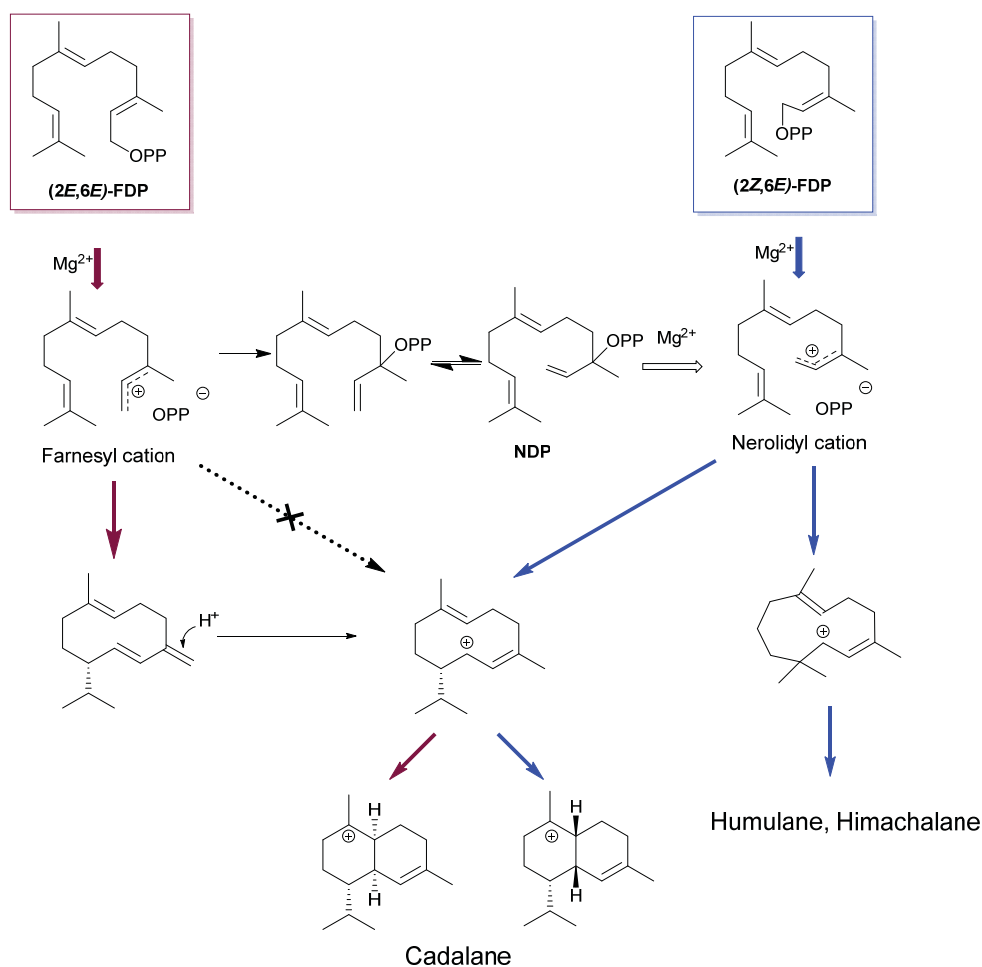
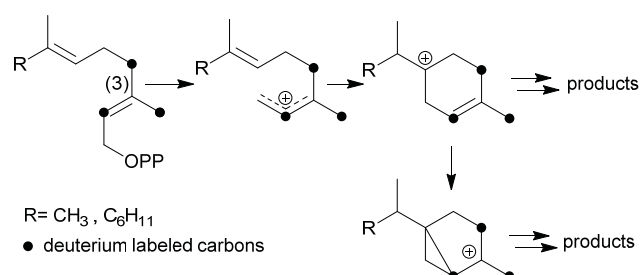


Figure 21: Possible cyclization pathway for MtTPS5 with (2Z,6E)-FDP and natural (2E,6E)-FDP. Use (2Z,6E)-FDP as substrate lead to an alternate cyclization to majority humulane and himachalane products. This was in contrast to cadalenes skeleton as major products as seen with natural stereoisomers (2E,6E)-FDP.

When using (2Z,6E)-farnesyl diphosphate as a substrate not only were the majority of the products novel when compared to (2E,6E)-FDP, but some peaks in the product profile could not be matched to any of the known compounds in the database. This was interesting as three peaks depicting sesquiterpenes could lead us to totally new compounds as all our efforts to match the mass data with known Kovats indices were futile. This interesting prospect forms the basis for efforts to isolate the compounds associated with these three unknown peaks using preparative gas chromatograph and further elucidating the structures by NMR. The most interesting aspect of these results is the fact that we can easily alter the product profile of a multiproduct enzyme by making changes in the double bond geometry of substrates. In fact, as observed in this case with MtTPS5, products with novel skeletons can be obtained from these substrates. Hence, in the quest for novel molecules we should definitely put a major focus on the substrate and altering its features apart from the focus on genetic mutation in the enzyme. The knowledge about multiproduct terpene synthases gained from this thesis can be utilized to engineer enzymes for future.

8 Summary

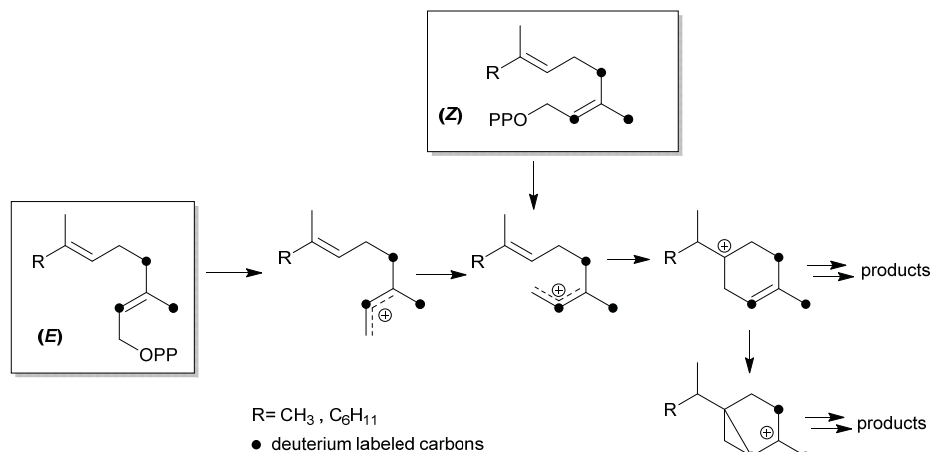
Terpenes constitute the largest and most diverse class of natural products, with about 55,000 compounds characterized throughout all forms of life serving diverse roles in primary as well as secondary metabolism.^{1,128,231} The wealth of terpene carbon skeletons can be attributed at least in part to a highly promiscuous class of enzymes known as the terpene synthases.⁴⁴ In addition to the high fidelity enzymes that produce only a single product, there are multiproduct terpene synthases, which generate a bouquet of acyclic and cyclic products from an acyclic precursor.¹⁰⁶ In order to study the catalytic promiscuity and the mechanistic cascade of the reaction pathways, three multiproduct sesquiterpene synthases were heterologously expressed and purified.^{145,183} Both TPS4 and TPS5 from *Zea mays* and MtTPS5 from *Medicago truncatula* generate a complex mixture of more than 20 sesquiterpenes and 10 monoterpenes.^{149,188} Research over the last decade has been focused towards using site-directed mutagenesis to decipher the complex catalytic capabilities of multiproduct terpene synthases.^{232,233} However, the minor differences in amino acid sequences that exist between terpene synthases are insufficient to explain their multiproduct nature.^{76,128} Furthermore, the lack of a defined crystal structure hinders their structural understanding. Research in this thesis was aimed at employing substrate analogs to evaluate the catalytic promiscuity of the multiproduct terpene synthases.



Scheme 1: Isotope sensitive branching strategy for multiproduct terpene synthases

This research utilized isotopically sensitive branching, defined as the change in the relative ratios of products from the same intermediates due to isotopic substitution in multiproduct enzymes.²³⁴ This has been especially effective in the investigation of the multiproduct reaction cascade of terpene synthases TPS4-B73 and TPS5-Delprim from *Zea mays*.¹⁸⁰ Labeled substrates with deuterium atoms completely surrounding the cationic center at C(3) of the key intermediates were used as metabolic probes (Scheme 1). This study not only confirmed the mechanistic details of the reaction cascade of multiproduct terpenoid synthases but also the rate-limiting effects of the final deprotonation steps en route to mono- and sesquiterpenes. The primary kinetic isotope effects on terminating deprotonations and lower stabilization of the reactive intermediates by hyperconjugation led to an enhanced formation of alcohols instead of olefinic products.

In addition, deuterium labeled substrates were used to investigate the alterations in product distribution and rate limiting effects that occur as a consequence of changing the geometry with (2*Z*,6*E*)-FDP (Scheme 2) resembling the nerolidyl diphosphate (NDP) intermediate generated during the catalytic cascade.¹⁸¹ In this work, the effects of alternate substrate stereochemistry as well as isotope effects on the product distribution on multiproduct terpene cyclase were investigated.



Scheme 2: Isotope sensitive branching strategy to study the effects of substrate geometry

There was indeed a major influence of the (2*Z*)-isomers on the enzymatic cascade of terpene synthases TPS4-*B73* and TPS5-*Delprim* from *Zea mays* as confirmed by deuterium labeling of products. Interestingly, the multiproduct terpene synthase TPS4 and TPS5 generate the same product profile but with increased preference for cyclic products.¹⁸¹ Major increase in enzymatic turnover that was observed with (2*Z*)-substrates emphasizes the rate limiting effect of the initial isomerization step in the reaction cascade. These results suggest that substrate geometry can be used as a tool to optimize the biosynthetic reaction cascade towards valuable cyclic terpenoids.

In contrast, use (2*Z*,6*E*)-FDP as a substrate with MtTPS5 from *Medicago truncatula* showed a completely different product profile. In fact majority of products are not observed with incubation of (2*E*,6*E*)-FDP with MtTPS5. The highly reactive (2*Z*,6*E*)-farnesyl cation predominantly undergoes (~57%) a C1-C11 ring closure to the (2*Z*,6*E*)-humul-10-yl cation. This cation undergoes deprotonation to form γ -humulene, and on further reaction with water, leads to the main product humula-6,9-dien-3-ol. The rest of products shared the cadalane backbone as with (2*E*,6*E*)-FDP but with the opposite absolute configuration of the bridgehead carbon atoms. This demonstrates the possibility of using substrate geometry as tool to generate novel products with multiproduct terpene synthases.

There exists a clear lack of understanding about the structural characteristics of multiproduct terpene synthases due to absence of defined crystal structures. In order to obtain an active site resolved structure, 3-

bromo analogs of geranyl diphosphate and farnesyl diphosphate were evaluated as substrates.¹⁸² They were found to be highly potent competitive inhibitors of the MtTPS5 enzyme with fast binding and slow reversibility. These molecules might considerably enhance the chances for obtaining a co-crystal structure with multiproduct terpene synthases and other terpene synthases.

With this work, substrate analogs as metabolic probes were successfully used to confirm the highly complex reaction cascade of multiproduct terpene synthases down to the last deprotonation step. Especially interesting was the finding that substrate geometry can be used to enhance the enzymatic turnover and divert the reaction cascade towards cyclic products. Moreover, in case of MtTPS5 these substrates generated completely novel cyclic products as compared to natural substrates. In order to decipher the structural features that define the structural diversity a co-crystallization candidate has also been developed. Consequently, the catalytic promiscuity of multiproduct terpene synthases can be employed to design better biocatalysts with improved turnover that also offer the possibility to generate novel cyclic products.

9 Future Perspectives

Multiproduct terpene synthases are highly promiscuous enzymes with catalytic capabilities to convert acyclic prenyl diphosphates into a complex bouquet of cyclic and acyclic products. In this thesis, alternative substrates were used as a tool to evaluate the details of complex reaction cascade and also to fine-tune the biosynthetic cascade in favor of certain class of products. Whereas, some alternate stereoisomers demonstrate the possibility of improved enzymatic turnover, others served as precursors to completely new array of products not seen with natural substrates. The knowledge gained from this research can be further expanded to better understand multiproduct terpene synthases and mould them into highly efficient catalysts for future applications.

Isotope sensitive branching

Isotope sensitive branching is a powerful tool for studying the minute mechanistic details of complex biosynthetic cascade and carbocationic intermediates through which the final products are formed. In the current work, the focus was on the effect of isotopic substitution on initial steps by surrounding the C3 carbon atom and confirms the biosynthetic cascade of TPS4 and TPS5 of *Zea mays*. The fluctuations in product composition and isotope labels on final products confirm the reaction scheme. In order to understand the theoretical basis of enhanced formation of alcohols and kinetic isotope effects, a collaborative work has been initiated with group of Dr. Lubomír Rulišek, Institute of Organic Chemistry and Biochemistry, Prague. This work can be expanded to other multiproduct terpene synthases with multiple reaction cascades like MtTPS5 from *Medicago truncatula*. In order to decipher individual steps in such biosynthetic cascades, the deuterium labels can be shifted to surround carbon atoms at different positions. These metabolic probes can be used to confirm the complicated cyclization pathways of individual products of other multiproduct terpene synthases.

Substrate geometry as a biosynthetic tool

The multiproduct terpene synthases from *Zea mays* and *Medicago truncatula* both accept unnatural precursors with differing double bond geometry as substrates. In case of multiproduct terpene synthases from *Zea mays*, the product composition changes only in quantitative terms, whereas in the case of *Medicago truncatula* these substrates lead to novel products, some of them possibly unknown. In both cases, the substrate used was (2*Z*,6*E*) FDP which underwent enhanced enzymatic turnover. In order to further probe the catalytic promiscuity of multiproduct terpene synthases, they were incubated with another geometric isomer (2*E*,6*Z*) FDP. Interestingly, with MtTPS5 this substrate also led to multiproduct blend of terpenoids, preliminary GC-MS analysis did not result in their identification with Kovats indices, suggesting new sesquiterpene products. This clearly demonstrates the flexibility of multiproduct synthase to accept unnatural

stereoisomers as substrates. The isolation of these unknown compounds by preparative GC and elucidation their structures is planned for future. The scope of this research will be further expanded by testing the catalytic promiscuity of other multiproduct terpene synthases as well as library of other terpene synthases using these artificial substrates.

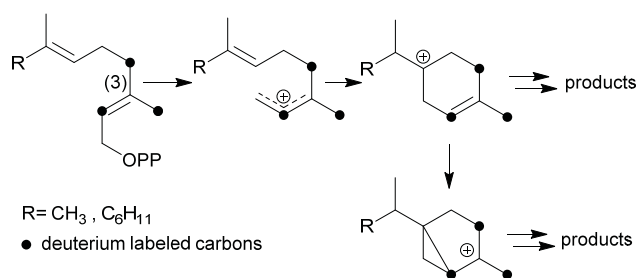
Co-crystallization candidate

The 3-bromo substrate analogs showed strong competitive inhibition of the MtTPS5 enzyme which makes them ideal tools for co-crystallization and structural analyses. In an ongoing collaboration with crystallography group of Prof. Dr. Michael Groll at Technische Universität München, there are preliminary results indicating the usefulness of 3-bromo substrates as co-crystallization candidate with FDP-synthase PcIDS1 enzyme from *Phaedon cochleariae*. This success indicates possibility of 3-bromo substrates as a co-crystallization candidate for multiproduct terpene synthases. This could provide the structural basis of their multiproduct nature in spite of their high sequence similarity with single product enzymes. This knowledge is critical for attempts to engineer highly promiscuous multiproduct enzymes towards producing desired products.

The focus of future research with multiproduct terpene synthases should be directed towards gaining more knowledge about the structural basis of this chemical diversity. This is possible by obtaining the crystal structure of multiproduct terpene synthases and further connecting it with current knowledge about their catalytic promiscuity by using these alternate substrates. More structural knowledge about active site flexibility that results in alternative conformations of the prenyl diphosphate substrate and later reaction intermediates is critical. This grasp of active site-alternate substrate interactions would form the basis of designing terpene synthases as future catalysts for synthesizing complicated cyclic terpenoids on demand.

10 Zusammenfassung

Mit ungefähr 55.000 Verbindungen bilden die Terpene die größte und vielfältigste Klasse der Naturstoffe welche in unterschiedlichsten Funktionen innerhalb des Primär- oder Sekundärmetabolismus in allen Lebensformen verbreitet sind.^{1,128,231} Die Vielfalt der terpenoiden Kohlenstoffgrundgerüste ergibt sich zumindest teilweise aus der Promiskuität einer als Terpensynthasen bekannten Klasse an Enzyme.⁴⁴ Neben hochgradig spezifischen Enzymen welche ausgehend von acylischen Vorstufen ausschließlich ein einziges Produkt liefern existieren auch Multiprodukt Terpensynthasen welche ein Gemisch acyclischer und cyclischer Produkte erzeugen.¹⁰⁶ Um die katalytische Promiskuität und die zugrundeliegende mechanistische Reaktionskaskade zu untersuchen wurden drei Multiprodukt Sesquiterpensynthasen heterolog exprimiert und aufgereinigt.^{145,183} TPS4 und TPS4 aus *Zea mays* und MtTPS5 aus *Medicago truncatula* produzieren eine komplexe Mischung aus mehr als 20 Sesquiterpenen oder 10 Monoterpenen.^{149,188} Untersuchungen innerhalb des letzten Jahrzehnts haben sich insbesondere darauf konzentriert die komplexen katalytischen Eigenschaften der Multiprodukt Terpensynthasen mittels gezielter Mutagenese zu entziffern.^{232,233} Die geringen Unterschiede in Aminosäuresequenzen zwischen Terpensynthasen können ihren Multiprodukt Charakter allerdings nicht erklären.^{76,128} Darüber hinaus wird unser Verständnis durch den Mangel an definierten Kristallstrukturen stark eingeschränkt. Die Forschungsarbeit dieser Dissertation zielte daher darauf ab die katalytische Promiskuität der Multiprodukt Terpensynthasen mittels Substratanaloga zu untersuchen.

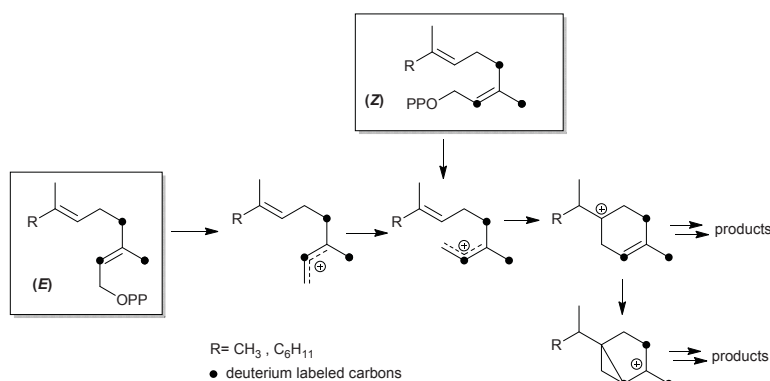


Schema 1: Isotopensensitive Verzweigungs Strategie für Multiprodukt Terpensynthasen.

In dieser Arbeit wurde die isotopensensitive Aufspaltung in Multiprodukt Enzymen untersucht, welche als die auf eine Isotopensubstitution basierende Änderung der relativen Verhältnisse zwischen zwei aus der gleichen Vorstufe hervorgehenden Produkte definiert ist.²³⁴ Dieser Ansatz hat sich insbesondere für die Untersuchung der Multiprodukt Reaktionskaskade der Terpensynthasen TPS4-B73 und TPS5-Delprim aus *Zea mays* als besonders effektiv erwiesen.¹⁸⁰ Markierte Substrate in denen das kationische Zentrum an C(3) in den Schlüsselintermediaten komplett mit Deuterium Atomen umgeben ist wurden als metabolische Sonden eingesetzt (Schema 1). Diese Untersuchungen bestätigten nicht nur mechanistische Details der Reaktionskaskade in Multiprodukt Terpensynthasen sondern auch die finale Deprotonierung als den

geschwindigkeitsbestimmenden Schritt bei der Bildung von Mono- und Sesquiterpenen. Die primären kinetischen Isotopeneffekte der terminierenden Deprotonierungen und die geringere Stabilisierung der reaktiven Intermediate mittels Hyperkonjugation führten zu einer gesteigerten Bildung von Alkoholen auf Kosten von olefinischen Produkten.

Darüber hinaus wurden Deuterium-markierte Substrate benutzt um Veränderungen in der Produktverteilung und die geschwindigkeitsbestimmenden Effekte zu bestimmen welche als Konsequenz einer geänderten Geometrie in (2Z,6E)-FDP (Schema 2) beobachtet werden, wobei dieses ein Substrat darstellt welches dem innerhalb der Reaktionskaskade generierten Nerolidyldiphosphat (NDP) ähnelt.¹⁸¹ In dieser Arbeit wurden die Effekte der alternativen Substratgeometrie sowie die Isotopen Effekte auf die Produkt Verteilung in Multiprodukt Terpencyclasen untersucht.



Schema 2: Isotopen sensitive Verzweigung Strategie zur Untersuchung der Auswirkung geänderter Substrat Geometrien.

Es gab in der Tat einen großen Einfluss der (2Z)-isomere auf die enzymatische Reaktionskaskade der Terpensynthasen TPS4-B73 und TPS5-Delprim aus *Zea mays* was durch Deuterium-Markierung der Produkte gezeigt wurde. Interessanterweise ergeben die Multiprodukt Terpensynthasen TPS4 und TPS5 dasselbe Produktprofil jedoch mit einer gesteigerten Präferenz für cyclische Produkte.¹⁸¹ Die große Zunahme der enzymatischen Umsetzung welche mit (Z)-Substraten beobachtet wurde belegt die Bedeutung der anfänglichen Isomerisierung als geschwindigkeitsbestimmenden Schritt für die gesamte Reaktionskaskade. Diese Ergebnisse weisen darauf hin, dass die Substratgeometrie als Werkzeug verwendet werden kann um biosynthetische Reaktionskaskaden für die Darstellung wertvoller cyclischer Terpene zu optimieren.

Im Gegensatz hierzu ergibt das (2Z,6E)-FDP als Substrat für MtTPS5 aus *Medicago truncatula* ein komplett verändertes Produktprofil. Tatsächlich werden die Mehrheit der Produkte nicht beobachtet wenn stattdessen (2E,6E)-FDP mit MtTPS5 inkubiert wird. Das hochreaktive (2Z,6E)-Farnesyl Kation unterläuft hauptsächlich einen C1-C11 Ringschluss zu dem (2Z,6E)-Humul-10-yl Kation (~57%). Dieses Kation erleidet dann eine Deprotonierung unter Bildung des γ -Humulens, und eine weitere Reaktion mit Wasser

führt zum Humula-6,9-dien-3-ol als Hauptprodukt. Die weiteren Produkte besitzen wie die mit (2*E*,6*E*)-FDP gebildeten ein Cadalan-Grundgerüst, weisen aber eine unterschiedliche relative Konfiguration auf. Dies zeigt die Möglichkeit die Substratgeometrie als ein Mittel zu verwenden um mit Hilfe von Multiprodukt Terpensynthesen neue Produkte herzustellen.

Unser Verständnis für die strukturellen Charakteristika von Multiprodukt Terpensynthesen ist stark begrenzt durch das Fehlen an definierten Kristallstrukturen. Um die Struktur des aktiven Zentrums aufzulösen wurden die 3-Brom Analoga des Geranyldiphosphat und des Farnesyldiphosphat als Substrate untersucht.¹⁸² Dabei wurde entdeckt dass diese sehr potente kompetitive Inhibitoren des MtTPS5 Enzymes mit schneller Bindung und langsamer Reversibilität darstellen. Diese Moleküle könnten unsere Chancen Co-Kristalle mit Multiprodukt Terpensynthesen Innerhalb dieser Arbeit wurden Substrat Analoga erfolgreich als metabolische Sonden verwendet um die hochkomplexe Reaktionskaskade der Multiprodukt Terpensynthesen bis zum abschließenden Deprotonierungs-Schritt hin zu untersuchen. Besonders interessant war die Entdeckung, dass die Substratgeometrie verwendet werden kann um die enzymatische Umsatzrate zu erhöhen und die Reaktionskaskade zu cyclischen Produkten hin umzuleiten.

Darüber hinaus konnte gezeigt werden, dass diese Substrate im Gegensatz zu den natürlichen Substraten mit MtTPS5 vollständig neue cyclische Produkte ergeben. Um die strukturellen Eigenschaften welche die strukturelle Diversität definieren zu entziffern wurde auch ein Kandidat für eine Co-Kristallisation entwickelt. Dementsprechend kann die Promiskuität der Multiprodukt Terpensynthesen verwendet werden um bessere Biokatalysatoren mit verbesserten Umsatzraten zu entwickeln, welche darüber hinaus auch die Möglichkeit anbieten neue cyclische Produkte zu generieren.

11 Supporting Information

11.1 Manuscript I

(**Note:** ^1H , ^{13}C and ^{31}P NMR and IR spectra of the synthetic compounds are attached in CD at the end this thesis)

Supporting Information

Isotope sensitive branching and kinetic isotope effects to analyze multiproduct terpenoid synthases from *Zea mays*

Nathalie Gatto,^a Abith Vattekkatte,^a Tobias Köllner,^b Jörg Degenhardt,^c Jonathan Gershenzon,^b and Wilhelm Boland^{a*}

^aDepartment of Bioorganic Chemistry, Max Planck Institute for Chemical Ecology, Beutenberg Campus, Hans-Knöll-Strasse 8, D-07745 Jena, Germany

^bDepartment of Biochemistry, Max Planck Institute for Chemical Ecology, Beutenberg Campus, Hans-Knöll-Strasse 8, D-07745 Jena, Germany

^c Institute for Pharmacy, University of Halle, Hoher Weg 8, D-06120 Halle, Germany
boland@ice.mpg.de

Table of contents

Product distribution of main monoterpenes from incubations of deuterated GDP with TPS4-B73 and TPS5- <i>Delprim</i> from maize (<i>Zea mays</i>)	S7
Product distribution of main sesquiterpenes from incubations of deuterated FDP with TPS4-B73 from maize (<i>Zea mays</i>)	S8
Product distribution of main sesquiterpenes from incubations of deuterated FDP with TPS5- <i>Delprim</i> from maize (<i>Zea mays</i>)	S9
<u>Synthetic Procedure:</u>	
[2,2- ² H ₂]-Trimethylsilylacetic acid (2)	S10
[1,1,1,3,3- ² H ₅]-6-Methyl-hept-5-en-2-one (1b)	S10
[1,1,1,3,3- ² H ₅]-6,10-Dimethyl-undeca-5,9-dien-2-one (1d)	S10
Methyl (2 <i>E</i>)-[2- ² H]-3,7-Dimethylocta-2,6-dienoate (3a)	S11
Methyl (2 <i>Z</i>)-[2- ² H]-3,7-Dimethylocta-2,6-dienoate (4a)	S11
Methyl (2 <i>E</i>)-[2,4,4,9,9,9- ² H ₆]-3,7-Dimethylocta-2,6-dienoate (3b)	S12
Methyl (2 <i>Z</i>)-[2,4,4,9,9,9- ² H ₆]-3,7-Dimethylocta-2,6-dienoate (4b)	S12
Methyl (2 <i>E</i> ,6 <i>E</i>)-[2- ² H]-3,7,11-Trimethyldodeca-2,6,10-trienoate (3c)	S12
Methyl (2 <i>Z</i> ,6 <i>E</i>)-[2- ² H]-3,7,11-Trimethyldodeca-2,6,10-trienoate (4c)	S12
Methyl (2 <i>E</i> ,6 <i>E</i>)-[2,4,4,13,13,13- ² H ₆]-3,7,11-Trimethyldodeca-2,6,10-trienoate (3d)	S13
Methyl (2 <i>Z</i> ,6 <i>E</i>)-[2,4,4,13,13,13- ² H ₆]-3,7,11-Trimethyldodeca-2,6,10-trienoate (4d)	S13
(2 <i>E</i>)-[2- ² H]-3,7-Dimethylocta-2,6-dien-1-ol (5a)	S13
(2 <i>E</i>)-[2,4,4,9,9,9- ² H ₆]-3,7-Dimethylocta-2,6-dien-1-ol (5b)	S13
(2 <i>E</i> ,6 <i>E</i>)-[2- ² H]-3,7,11-Trimethyldodeca-2,6,10-trien-1-ol (5c)	S14
(2 <i>E</i> ,6 <i>E</i>)-[2,4,4,13,13,13- ² H ₆]-3,7,11-Trimethyldodeca-2,6,10-trien-1-ol (5d)	S14
Trisammonium (2 <i>E</i>)-[2- ² H]-3,7-Dimethylocta-2,6-dienyl Diphosphate (7a)	S14

Trisammonium (2E)-[2,4,4,9,9,9- ² H ₆]-3,7-Dimethylocta-2,6-dienyl Diphosphate (7b)	S15
Trisammonium (2E,6E)-[2- ² H]-3,7,11-Trimethyldodeca-2,6,10-trienyl Diphosphate (7c)	S15
Trisammonium (2E,6E)-[2,4,4,13,13,13- ² H ₆]-3,7,11-Trimethyldodeca-2,6,10-trienyl Diphosphate (7d)	S15

(In the attached CD)

¹H, ¹³C spectra of the synthetic compounds

[2,2- ² H ₂]-Trimethylsilylacetic acid (2)	
[1,1,1,3,3- ² H ₅]-6-Methyl-hept-5-en-2-one (1b)	
[1,1,1,3,3- ² H ₅]-6,10-Dimethyl-undeca-5,9-dien-2-one (1d)	
Methyl (2E)-[2- ² H]-3,7-Dimethylocta-2,6-dienoate (3a)	
Methyl (2Z)-[2- ² H]-3,7-Dimethylocta-2,6-dienoate (4a)	
Methyl (2E)-[2,4,4,9,9,9- ² H ₆]-3,7-Dimethylocta-2,6-dienoate (3b)	
Methyl (2Z)-[2,4,4,9,9,9- ² H ₆]-3,7-Dimethylocta-2,6-dienoate (4b)	
Methyl (2E,6E)-[2- ² H]-3,7,11-Trimethyldodeca-2,6,10-trienoate (3c)	
Methyl (2Z,6E)-[2- ² H]-3,7,11-Trimethyldodeca-2,6,10-trienoate (4c)	
Methyl (2E,6E)-[2,4,4,13,13,13- ² H ₆]-3,7,11-Trimethyldodeca-2,6,10-trienoate (3d)	
Methyl (2Z,6E)-[2,4,4,13,13,13- ² H ₆]-3,7,11-Trimethyldodeca-2,6,10-trienoate (4d)	
(2E)-[2- ² H]-3,7-Dimethylocta-2,6-dien-1-ol (5a)	
(2E)-[2,4,4,9,9,9- ² H ₆]-3,7-Dimethylocta-2,6-dien-1-ol (5b)	
(2E,6E)-[2- ² H]-3,7,11-Trimethyldodeca-2,6,10-trien-1-ol (5c)	
(2E,6E)-[2,4,4,13,13,13- ² H ₆]-3,7,11-Trimethyldodeca-2,6,10-trien-1-ol (5d)	
Trisammonium (2E)-[2- ² H]-3,7-Dimethylocta-2,6-dienyl Diphosphate (7a)	
Trisammonium (2E)-[2,4,4,9,9,9- ² H ₆]-3,7-Dimethylocta-2,6-dienyl Diphosphate (7b)	
Trisammonium (2E,6E)-[2- ² H]-3,7,11-Trimethyldodeca-2,6,10-trienyl Diphosphate (7c)	

Trisammonium (2*E*,6*E*)-[2,4,4,13,13,13-²H₆]-3,7,11-Trimethyldodeca-2,6,10-trienyl
Diphosphate (**7d**)

³¹P NMR spectra of the synthetic compounds

Trisammonium (2*E*)-[2-²H]-3,7-Dimethylocta-2,6-dienyl Diphosphate (**7a**)

Trisammonium (2*E*)-[2,4,4,9,9,9-²H₆]-3,7-Dimethylocta-2,6-dienyl Diphosphate (**7b**)

Trisammonium (2*E*,6*E*)-[2-²H]-3,7,11-Trimethyldodeca-2,6,10-trienyl Diphosphate (**7c**)

Trisammonium (2*E*,6*E*)-[2,4,4,13,13,13-²H₆]-3,7,11-Trimethyldodeca-2,6,10-trienyl
Diphosphate (**7d**)

IR spectra of the synthetic compounds

[2,2-²H₂]-Trimethylsilylacetic acid (**2**)

[1,1,1,3,3-²H₅]-6-Methyl-hept-5-en-2-one (**1b**)

[1,1,1,3,3-²H₅]-6,10-Dimethyl-undeca-5,9-dien-2-one (**1d**)

Methyl (2*E*)-[2-²H]-3,7-Dimethylocta-2,6-dienoate (**3a**) and

Methyl (2*Z*)-[2-²H]-3,7-Dimethylocta-2,6-dienoate (**4a**)

Methyl (2*E*)-[2,4,4,9,9,9-²H₆]-3,7-Dimethylocta-2,6-dienoate (**3b**) and

Methyl (2*Z*)-[2,4,4,9,9,9-²H₆]-3,7-Dimethylocta-2,6-dienoate (**4b**)

Methyl (2*E*,6*E*)-[2-²H]-3,7,11-Trimethyldodeca-2,6,10-trienoate (**3c**) and

Methyl (2*Z*,6*E*)-[2-²H]-3,7,11-Trimethyldodeca-2,6,10-trienoate (**4c**)

Methyl (2*E*,6*E*)-[2,4,4,13,13,13-²H₆]-3,7,11-Trimethyldodeca-2,6,10-trienoate (**3d**) and

Methyl (2*Z*,6*E*)-[2,4,4,13,13,13-²H₆]-3,7,11-Trimethyldodeca-2,6,10-trienoate (**4d**)

Trisammonium (2*E*)-[2-²H]-3,7-Dimethylocta-2,6-dienyl Diphosphate (**7a**)

Trisammonium (2*E*)-[2,4,4,9,9,9-²H₆]-3,7-Dimethylocta-2,6-dienyl Diphosphate (**7b**)

Trisammonium (2*E*,6*E*)-[2-²H]-3,7,11-Trimethyldodeca-2,6,10-trienyl Diphosphate (**7c**)

Trisammonium (2*E*,6*E*)-[2,4,4,13,13,13-²H₆]-3,7,11-Trimethyldodeca-2,6,10-trienyl
Diphosphate (**7d**)

General Methods. Reactions were performed under Ar. Solvents were dried according to standard procedures. ^1H , ^{13}C and ^{31}P NMR were recorded at 400 MHz. Chemical shifts of ^1H , ^{13}C and ^{31}P NMR are given in ppm (δ) based on solvent picks. CDCl_3 : 7.27 (^1H NMR) and 77.4 ppm (^{13}C NMR). $\text{D}_2\text{O}/\text{ND}_4\text{OD}$: 4.79 (^1H NMR); ^{13}C NMR and ^{31}P NMR were referenced to external standard 3-(trimethylsilyl)-propionic acid- d_4 sodium salt (TSP; 3 % in D_2O) and phosphoric acid (H_3PO_4 , 10 % in D_2O), respectively. IR: Bruker Equinox 55 FTIR spectrophotometer.

Assay for terpene synthase activity. Each 200 μL assay contained 50 μL of the bacterial extract in assay buffer (10 mM 3-(*N*)-2-hydroxypropane sulfonic acid (Mopso), pH 7.0, 1 mM DTT, and 10 % (v/v) glycerol) with 350 μM substrate, 7.5 mM MgCl_2 , 1.5 mM NaWO_4 , and 0.75 mM NaF in a 2 ml screw-capped glass vial. The assay was overlaid with 100 μL pentane containing 2.5 μM (*E*)- β -caryophyllene (Aldrich, 98 % pure) as an internal standard and incubated for 20 min at 30 $^\circ\text{C}$. The reaction was stopped by mixing for 1 min, and an aliquot of the pentane layer was analyzed by GC-FID.

Gas chromatography. A Hewlett-Packard model 6890 gas chromatograph was employed with the carrier gas He at 1 ml min^{-1} , splitless injection (injector temperature: 220 $^\circ\text{C}$, injection volume: 2 μL), a DB-WAX column (polyethylene glycol, 30 m \times 0.25 mm ID \times 0.25 μm film thickness, J&W Scientific, Folsom, CA, USA) for sesquiterpenes and a DB5-MS column (30 m \times 0.25 mm ID \times 0.25 μm film thickness, J & W Scientific) for monoterpenes, respectively. Temperature was programmed from 50 $^\circ\text{C}$ (3 min hold) at 7 $^\circ\text{C}$ min^{-1} to 240 $^\circ\text{C}$ (2 min hold). Quantification was performed with the trace of a flame ionization detector (FID) operated at 250 $^\circ\text{C}$.

Trisammonium (*E*)-Geranyl and (2*E*,6*E*)-Farnesyl Diphosphates. Unlabeled GDP and FDP were synthesized from commercial geranyl and farnesyl chloride (Aldrich) respectively, according to the phosphorylation procedure described above.

Heterologous expression of terpene synthases. The open reading frames of *tps4-B73* and *tps5-Dell* were cloned as *EcoRI-NotI* fragments and inserted into the bacterial expression vector pHis8-3 which provided the expressed proteins with a His-tag at the *N*-terminal [23]. The constructs were transformed into the *Escherichia coli* strain BL21 (DE3) and fully sequenced to avoid errors introduced by DNA amplification. The recombinant proteins TPS4 and TPS5 were purified from *E. coli* as previously described [9].

Product distribution of main monoterpenes from incubations of deuterated GDP with TPS4-B73 and TPS5-Delprim from maize (*Zea mays*)

enzyme	product distribution ^{a, b} ng/h (% composition)	substrate				
		<i>E</i> -GDP ^c	<i>E</i> -(1D)-GDP 7a	<i>Z</i> -(1D)-GDP 8a	<i>E</i> -(6D)-GDP 7b	<i>Z</i> -(6D)-GDP 8b
TPS4	α -Thujene (M ₁)*	15.4 ± 0.5 (3.3)	15.6 ± 0.2 (3.1)	20.8 ± 0.8 (3.3)	5.0 ± 0.0 (1.2)	5.7 ± 0.1 (1.0)
	Sabinene (M ₂)*	39.7 ± 1.2 (8.4)	41.8 ± 0.3 (8.4)	63.1 ± 0.6 (9.9)	18.0 ± 0.9 (4.2)	31.4 ± 0.8 (5.3)
	β -Myrcene (M ₃)	42.6 ± 2.0 (9.1)	42.9 ± 0.5 (8.6)	-	26.9 ± 0.6 (6.4)	-
	(S)-(-)-Limonene (M ₄)	101.1 ± 3.5 (21.5)	100.9 ± 1.6 (20.3)	245.9 ± 3.4 (38.6)	95.2 ± 2.1 (22.5)	236.3 ± 4.3 (39.6)
	Sabinene hydrate (M ₅)**	26.7 ± 1.2 (5.7)	31.2 ± 1.0 (6.3)	38.8 ± 1.3 (6.1)	39.6 ± 0.7 (9.3)	62.6 ± 1.2 (10.5)
	α -Terpinolene (M ₆)	21.4 ± 0.4 (4.5)	22.4 ± 0.2 (4.5)	91.9 ± 1.4 (14.4)	21.7 ± 0.5 (5.1)	89.9 ± 2.3 (15.1)
	Linalool (M ₇)*	112.1 ± 4.2 (23.9)	128.5 ± 3.6 (25.9)	17.8 ± 1.0 (2.8)	115.8 ± 2.1 (27.3)	27.9 ± 0.6 (4.7)
	α -Terpineol (M ₈)*	30.6 ± 1.7 (6.5)	34.9 ± 0.8 (7.0)	78.6 ± 3.8 (12.3)	29.7 ± 0.3 (7.0)	76.2 ± 1.2 (12.8)
	Geraniol (M ₉)	79.7 ± 3.3 (17.0)	78.7 ± 2.7 (15.8)	80.7 ± 3.0 (12.6)	71.3 ± 1.8 (16.8)	66.0 ± 0.9 (11.1)

^a Product distribution was determined by GC-FID analysis. ^b Average of three independent replicates. ^c GDP denotes the geranyl diphosphate. * Stereoisomeric pairs chromatographically not resolved. ** Compound identified by mass spectra alone.

Enzyme	product distribution ^{a, b} ng/h (% composition)	substrate				
		<i>E</i> -GDP ^c	<i>E</i> -(1D)-GDP 7a	<i>Z</i> -(1D)-GDP 8a	<i>E</i> -(6D)-GDP 7b	<i>Z</i> -(6D)-GDP 8b
TPS5	α -Thujene (M ₁)*	67.0 ± 4.5 (2.5)	66.3 ± 2.4 (2.4)	166.9 ± 3.1 (5.0)	18.4 ± 1.1 (0.8)	46.4 ± 1.1 (1.5)
	Sabinene (M ₂)*	303.9 ± 4.4 (11.2)	294.8 ± 3.5 (10.7)	644.1 ± 8.3 (19.2)	127.9 ± 1.5 (5.4)	316.7 ± 12.4 (10.2)
	β -Myrcene (M ₃)	534.1 ± 14.6 (19.6)	498.0 ± 11.1 (18.0)	11.9 ± 1.6 (0.3)	348.1 ± 2.6 (14.8)	10.2 ± 2.9 (0.3)
	(S)-(-)-Limonene (M ₄)	570.0 ± 10.2 (20.9)	546.5 ± 6.3 (19.8)	1404.0 ± 12.1 (42.0)	500.4 ± 9.9 (21.3)	1383.4 ± 33.2 (44.6)
	Sabinene hydrate (M ₅)**	198.3 ± 13.2 (7.3)	212.6 ± 2.3 (7.7)	452.0 ± 4.7 (13.5)	304.0 ± 10.2 (12.9)	648.9 ± 48.0 (20.9)
	α -Terpinolene (M ₆)	92.6 ± 2.8 (3.4)	89.0 ± 0.2 (3.2)	194.0 ± 4.7 (5.8)	86.7 ± 2.0 (3.7)	208.8 ± 8.0 (6.7)
	Linalool (M ₇)*	317.0 ± 23.2 (11.6)	339.4 ± 4.7 (12.3)	137.6 ± 18.5 (4.1)	332.2 ± 17.3 (14.1)	189.9 ± 15.4 (6.1)
	α -Terpineol (M ₈)*	140.8 ± 11.5 (5.2)	157.9 ± 4.6 (5.7)	322.1 ± 34.73 (9.6)	135.3 ± 7.0 (5.8)	286.1 ± 20.2 (9.2)
	Geraniol (M ₉)	500.0 ± 47.3 (18.4)	559.2 ± 3.5 (20.2)	12.9 ± 4.1 (0.4)	495.8 ± 34.8 (21.1)	11.2 ± 0.4 (0.3)

^a Product distribution was determined by GC-FID analysis. ^b Average of three independent replicates. ^c GDP denotes the geranyl diphosphate. * Stereoisomeric pairs chromatographically not resolved. ** Compound identified by mass spectra alone.

Product distribution of main sesquiterpenes from incubations of deuterated FDP with TPS4-B73 from maize (*Zea mays*)

enzyme	product distribution ^{a, b} ng/h (% composition)	substrate				
		<i>E</i> -FDP ^c	<i>E,E</i> -(1D)-FDP 7c	<i>Z,E</i> -(1D)-FDP 8c	<i>E,E</i> -(6D)-FDP 7d	<i>Z,E</i> -(6D)-FDP 8d
TPS4	7- <i>epi</i> -Sesquithujene (S ₁)	568.8 ± 25.4 (18.5)	713.2 ± 75.9 (20.0)	2395.1 ± 55.3 (29.3)	349.4 ± 19.4 (12.1)	1552.2 ± 30.6 (16.8)
	Sesquithujene (S ₂)	133.3 ± 6.0 (4.3)	165.4 ± 17.3 (4.6)	635.7 ± 14.5 (7.8)	55.9 ± 3.0 (1.9)	278.4 ± 5.0 (3.0)
	(<i>Z</i>)- α -Bergamotene (S ₃)	30.5 ± 1.5 (1.0)	40.2 ± 4.0 (1.1)	66.3 ± 1.4 (0.8)	21.3 ± 1.1 (0.7)	42.2 ± 0.7 (0.4)
	(<i>E</i>)- α -Bergamotene (S ₄)	47.8 ± 2.0 (1.5)	65.4 ± 7.1 (1.8)	203.8 ± 4.7 (2.5)	16.7 ± 0.8 (0.6)	80.8 ± 1.6 (0.9)
	Sesquisabinene A (S ₅)	72.9 ± 2.9 (2.4)	91.0 ± 8.0 (2.5)	328.3 ± 6.9 (4.0)	57.5 ± 3.0 (2.0)	246.7 ± 4.0 (2.7)
	Sesquisabinene B (S ₆)	29.9 ± 1.2 (1.0)	36.5 ± 2.9 (1.0)	175.7 ± 3.7 (2.1)	26.3 ± 1.3 (0.9)	144.2 ± 2.3 (1.6)
	(<i>E</i>)- β -Farnesene (S ₇)	88.2 ± 3.4 (2.9)	112.5 ± 11.2 (3.1)	-	82.8 ± 4.2 (2.9)	-
	γ -Curcumene (S ₈)*	9.4 ± 0.3 (0.3)	11.0 ± 1.0 (0.3)	68.3 ± 3.4 (0.8)	25.2 ± 1.5 (0.9)	134.6 ± 2.0 (1.4)
	Zingiberene (S ₉)*	27.6 ± 2.0 (0.9)	34.3 ± 4.5 (1.0)	122.6 ± 2.7 (1.5)	25.4 ± 1.3 (0.9)	105.3 ± 2.3 (1.1)
	(<i>S</i>)- β -Bisabolene (S ₁₀)	584.4 ± 23.0 (19.1)	737.3 ± 74.2 (20.7)	1983.6 ± 42.8 (24.3)	573.1 ± 31.2 (19.9)	2053.2 ± 41.1 (22.2)
	β -Curcumene (S ₁₁)*	19.7 ± 0.6 (0.6)	23.0 ± 1.9 (0.6)	98.5 ± 5.0 (1.2)	68.5 ± 3.6 (2.4)	299.9 ± 4.9 (3.2)
	(<i>E</i>)- γ -Bisabolene (S ₁₂)	45.0 ± 1.6 (1.5)	56.1 ± 5.5 (1.6)	152.1 ± 3.3 (1.9)	44.2 ± 2.4 (1.5)	159.9 ± 3.1 (1.7)
	7- <i>epi</i> -Sesquithujene hydrate (S ₁₃)**	174.0 ± 4.8 (5.7)	182.3 ± 0.9 (5.1)	809.6 ± 28.3 (9.9)	363.5 ± 20.9 (12.6)	1873.0 ± 22.9 (20.3)
	Sesquithujene hydrate (S ₁₄)**	116.7 ± 3.6 (3.8)	116.1 ± 0.7 (3.2)	505.9 ± 19.1 (6.2)	200.8 ± 11.8 (7.0)	1093.8 ± 25.3 (11.8)
	(3 <i>R</i>)-(E)-Nerolidol (S ₁₅)	458.3 ± 13.8 (14.9)	481.4 ± 10.6 (13.5)	-	344.1 ± 21.1 (11.9)	-
	Unknown (A)***	525.6 ± 14.7 (17.1)	550.2 ± 2.8 (15.4)	7.1 ± 1.4 (0.1)	411.3 ± 23.6 (14.3)	8.12 ± 0.7 (0.1)
	Unknown (B)***	29.8 ± 0.9 (1.0)	30.9 ± 0.1 (0.9)	148.9 ± 6.7 (1.8)	69.8 ± 4.1 (2.4)	393.3 ± 6.9 (4.2)
	Unknown (C)***	51.7 ± 2.4 (1.7)	51.6 ± 0.7 (1.4)	229.2 ± 10.2 (2.8)	80.8 ± 4.7 (2.0)	487.4 ± 8.5 (5.3)

^a Product distribution was determined by GC-FID analysis. ^b Average of three independent replicates. ^c GDP denotes the geranyl diphosphate. * Absolute configuration of the stereoisomeric pairs uncertain. ** Hypothetic structure. Compounds identified by mass spectra alone. *** Unknown oxygenated cyclic sesquiterpenes.

**Product distribution of main sesquiterpenes from incubations of deuterated FDP with
TPS5-Delprim from maize (*Zea mays*)**

enzyme	product distribution ^{a, b} ng/h (% composition)	substrate				
		<i>E</i> -FDP ^c	<i>E,E</i> -(1D)-FDP 7c	<i>Z,E</i> -(1D)-FDP 8c	<i>E,E</i> -(6D)-FDP 7d	<i>Z,E</i> -(6D)-FDP 8d
TPS5	7- <i>epi</i> -Sesquithujene (S ₁)	196.6 ± 2.0 (2.0)	200.4 ± 2.1 (2.0)	1035.7 ± 14.6 (3.9)	132.0 ± 5.1 (1.2)	633.0 ± 13.7 (2.4)
	Sesquithujene (S ₂)	2854.3 ± 28.8 (29.3)	2967.0 ± 35.2 (29.2)	8442 ± 129.9 (32.3)	1265.8 ± 32.8 (11.6)	3497.7 ± 95.7 (13.2)
	(<i>Z</i>)- α -Bergamotene (S ₃)	245.4 ± 2.4 (2.5)	268.4 ± 2.7 (2.6)	484.0 ± 7.1 (1.8)	134.8 ± 2.8 (1.2)	209.8 ± 5.2 (0.8)
	(<i>E</i>)- α -Bergamotene (S ₄)	33.5 ± 0.4 (0.3)	36.1 ± 0.5 (0.3)	360.7 ± 5.9 (1.4)	23.6 ± 2.0 (0.2)	274.4 ± 9.0 (1.0)
	Sesquisabinene A (S ₅)	31.8 ± 0.4 (0.3)	30.5 ± 0.4 (0.3)	187.1 ± 2.8 (0.7)	28.1 ± 1.5 (0.2)	141.8 ± 5.4 (0.5)
	Sesquisabinene B (S ₆)	526.9 ± 5.1 (5.4)	557.5 ± 7.0 (5.5)	1545.5 ± 27.0 (5.9)	438.0 ± 8.1 (4.0)	1096.1 ± 46.9 (4.1)
	(<i>E</i>)- β -Farnesene (S ₇)	299.7 ± 22.1 (3.1)	330.5 ± 3.2 (3.2)	18.4 ± 1.8 (0.1)	321.1 ± 5.3 (2.9)	-
	γ -Curcumene (S ₈)*	60.3 ± 1.0 (0.6)	63.44 ± 1.5 (0.6)	184.2 ± 2.7 (0.7)	139.0 ± 0.2 (1.3)	367.6 ± 16.5 (1.4)
	Zingiberene (S ₉)*	60.5 ± 0.7 (0.6)	60.4 ± 0.6 (0.6)	219.5 ± 4.1 (0.8)	66.3 ± 1.7 (0.6)	219.9 ± 10.8 (0.8)
	(<i>S</i>)- β -Bisabolene (S ₁₀)	2223.7 ± 19.8 (22.8)	2363.6 ± 25.8 (23.3)	8746.3 ± 165 (33.4)	2352.5 ± 91.4 (21.6)	8172.4 ± 463 (30.9)
	β -Curcumene (S ₁₁)*	82.6 ± 1.5 (0.8)	90.0 ± 2.0 (0.9)	224.9 ± 2.8 (0.8)	201.9 ± 0.6 (1.8)	510.1 ± 25.2 (1.9)
	(<i>E</i>)- γ -Bisabolene (S ₁₂)	87.4 ± 0.9 (0.9)	91.8 ± 0.9 (0.9)	314.8 ± 6.1 (1.2)	98.4 ± 3.3 (0.9)	312.5 ± 18.9 (1.2)
	7- <i>epi</i> -Sesquithujene hydrate (S ₁₃)**	58.8 ± 0.8 (0.6)	60.4 ± 1.4 (0.6)	276.3 ± 5.1 (1.0)	138.1 ± 2.6 (1.3)	575.3 ± 32.8 (2.2)
	Sesquithujene hydrate (S ₁₄)**	1185.0 ± 13.0 (12.2)	1218.1 ± 15.9 (12.0)	2104.2 ± 304 (8.0)	2578.4 ± 45.3 (23.6)	5394.2 ± 299 (20.4)
	(3 <i>R</i>)-(E)-Nerolidol (S ₁₅)	596.8 ± 3.9 (6.1)	592.0 ± 5.1 (5.8)	-	566.5 ± 22.1 (5.2)	-
	Unknown (A)***	230.9 ± 2.4 (2.4)	221.0 ± 2.6 (2.2)	-	206.1 ± 6.0 (0.2)	3.0 ± 3.0 (0)
Unknown (B)***	12.5 ± 0.2 (0.1)	10.8 ± 0.9 (0.1)	69.3 ± 1.0 (0.3)	26.4 ± 0.7 (0.2)	154.0 ± 7.9 (0.6)	
Unknown (C)***	896.8 ± 9.2 (9.2)	918.6 ± 9.4 (9.0)	1792.2 ± 31.1 (6.8)	2104.1 ± 41.2 (19.3)	4449.7 ± 225 (16.8)	

^a Product distribution was determined by GC-FID analysis. ^b Average of three independent replicates. ^c GDP denotes the geranyl diphosphate. * Absolute configuration of the stereoisomeric pairs uncertain. ** Hypothetic structure. Compounds identified by mass spectra alone. *** Unknown oxygenated cyclic sesquiterpenes.

Experimental Section

[2,2-²H]-Trimethylsilylacetic acid [2]. A mixture of sodium acetate-*d*₃ (1.76 g, 20.7 mmol, Aldrich), 18-crown-6 ether (2g, 7.6 mmol) in dry ether (100 mL) was refluxed 2h under argon. Trimethylsilyl chloride (2.61 mL, 20.7 mmol) was added dropwise and the mixture was refluxed for 24h under argon. After cooling, the mixture was filtrated under argon. The resulting clear solution was added dropwise to a solution of lithium diisopropylamine at -78°C [prepared by reaction of *n*-butyl lithium 1.6 M in hexane (12.94 mL, 20.7 mmol) and diisopropylamine (2.90 mL, 20.7 mmol) in ether (40 mL)]. The mixture was stirred for 30 min at -78°C, warmed to rt and stirring was continued for additional 30 min. The yellow solution was then refluxed for 2h. The reaction was quenched by addition of saturated NH₄Cl at 0°C. The aqueous phase was acidified to pH = 3 with HCl (0.5 M) and the solution was extracted with ether (3 × 50 mL). The combined organic layers were dried (MgSO₄) and concentrated. Purification by flash chromatography (1:4 (v/v) ether in petroleum ether) gave **2** (1.16 g, 42 %) as a colorless oil which solidifies at low temperature. ¹H NMR (400 MHz, CDCl₃) δ 0.17 (s, 9H); ¹³C NMR (400 MHz, CDCl₃) δ (CO₂H not observed), -1.13; IR (neat) cm⁻¹: ν 2925, 2855, 1733, 1461, 1261, 799; ESI-HRMS calcd. for C₄H₇D₂O₂Si [M-CH₃]⁺ 119.0497, found 119.0501.

General Procedure for the Preparation of Pentadeuterated Ketones. A mixture of **1a,c** (39.6 mmol) and K₂CO₃ (0.25 g, previously dried at 80°C for 24h) in D₂O (8 mL) was vigorously stirred overnight at 70°C under argon. After cooling to rt, the mixture was extracted with dry CH₂Cl₂ (3 × 10 mL). The combined organic layers were dried (MgSO₄) and concentrated. The procedure was repeated 3-5 times with fresh D₂O and K₂CO₃. The degree of labeling was monitored by GC-MS (>96 atom % ²H). The pentadeuterated ketone was purified by flash chromatography (1:9 (v/v) ether in petroleum ether).

[1,1,1,3,3-²H₅]-6-Methyl-hept-5-en-2-one [1b]. According the general procedure, deuteration of 6-methyl-hept-5-en-2-one **1a** (5g) gave **1b** (4.21 g, 81 %) as a yellow pale oil. ¹H NMR (400 MHz, CDCl₃) δ 5.0-5.04 (m, 1H), 2.20 (d, *J* = 7.09 Hz, 2H), 1.63 (s, 3H), 1.57 (s, 3H); ¹³C NMR (400 MHz, CDCl₃) δ 209.4, 133.0, 122.9, 25.9, 22.7, 17.9; IR (neat) cm⁻¹: ν 2977, 2937, 2554, 1711, 1449, 1380, 1252, 1171, 1042; EI-MS [M⁺] 131 (4), 113 (85), 95 (65), 69 (60), 46 (100); ESI-HRMS calcd. for C₈H₉D₅O [M]⁺ 131.1358 found 131.1360 [21].

(5E)-[1,1,1,3,3-²H₅]-6,10-Dimethyl-undeca-5,9-dien-2-one [1d]. According the general procedure, deuteration of (5E)-6,10-dimethylundeca-5,9-dien-2-one **1c** (5g) gave **1d** (4.41 g, 86 %) as a yellow pale oil. ¹H NMR (400 MHz, CDCl₃) δ 5.07 (t, *J* = 7.8 Hz, 2H), 2.25 (d, *J* = 6.8 Hz, 2H), 1.95-2.08 (m, 4H), 1.68 (s, 3H), 1.61 (s, 3H), 1.60 (s, 3H); IR (neat) cm⁻¹: ν 2969, 2920, 2857, 1712, 1449, 1378, 1252, 1175, 1061; EI-MS [M⁺] 199 (3), 181 (4), 156

(28), 136 (39), 121 (15), 93 (21), 82 (9), 69 (78), 53 (17), 46 (100); ESI-HRMS calcd. for $C_8H_9D_5O$ $[M]^+$ 199.1984, found 199.1985 [22].

General Procedure for the Preparation of Methyl Esters. Methyl esters were prepared according to the modified method of Arigoni et al. [14]. To a solution of lithium diisopropylamine (2.2 eq. mol) in THF (15 mL) at -78°C was added dropwise a solution of **2** (1.16 g, 8.64 mmol) in THF (15 mL). The mixture was stirred for 30 min at -78°C , 30 min at 0°C and then cooled to -78°C before dropwise addition of the corresponding ketones **1a-d** (1.1 eq. mol) in THF (15 mL). The reaction mixture was then stirred 1h at -78°C , 1h at -10°C and 1h at rt. The reaction mixture was quenched by dropwise addition of HCl (0.1 N) at 0°C . THF was removed under reduced pressure and the residue was dissolved in hexane (30 mL). The solution was poured into 100 mL of an hexane:HCl (0.5 N) (3:1) mixture and the aqueous phase was extracted with hexane (3×40 mL). The combined organic layers were washed with brine, dried ($MgSO_4$) and concentrated. Purification by flash chromatography (1:4 (v/v) ether in petroleum ether) gave an isomeric mixture of corresponding carboxylic acids. The mixture of *E/Z* carboxylic acids was dissolved in ACN (20 mL) at 0°C and freshly distilled diisopropylamine (1.1 eq. mol) was added dropwise. The mixture was stirred 10 min at 0°C , 20 min at rt and then cooled to 0°C before dropwise addition of freshly distilled dimethyl sulfate (2 eq. mol). The reaction mixture was stirred for 3h at rt. The mixture was quenched by dropwise addition of NH_4OH (0.1N) and the solvent was removed under reduced pressure. The residue was taken up in Et_2O (10 mL), poured into an ether:water (3:1) mixture (80 mL) and the aqueous phase was extracted with ether (3×30 mL). The combined organic layers were washed with brine, dried ($MgSO_4$) and concentrated. Silica gel column chromatography (1:9 (v/v) ether in petroleum ether) gave isomerically pure methyl esters.

Methyl (2E)-[2- 2H_1]-3,7-Dimethylocta-2,6-dienoate [3a] and Methyl (2Z)-[2- 2H_1]-3,7-Dimethylocta-2,6-dienoate [4a]. According the general procedure, condensation of **1a** (1.14 g) and **2** (1.10 g), esterification of the mixture of *E/Z* carboxylic acids and subsequent purification by flash chromatography gave **4a** (0.20 g) as a colorless oil followed by **3a** (0.31 g) as a colorless oil (total yield 35 % from **2**, *Z/E* 4:6). IR (neat, mixture of *E*- and *Z*-isomers) cm^{-1} : ν 2962, 1261, 1094, 1021, 866, 800.

Data for **4a**: 1H NMR (400 MHz, $CDCl_3$) δ 5.14-5.18 (m, 1H), 3.68 (s, 3H), 2.64 (t, $J = 8.25$ Hz, 2H), 1.69 (q, $J = 7.52$ Hz, 2H), 1.90 (s, 3H); 1.69 (s br, 3H), 1.63 (s br, 3H); ^{13}C NMR (400 MHz, $CDCl_3$) δ 167.1, 160.8, 132.6, 124.5, 51.1, 33.8, 27.2, 26.0, 25.6, 18.0; EI-MS $[M]^+$ 183 (6), 152 (16), 124 (35), 115 (55), 84 (36), 69 (100), 41 (37); ESI-HRMS calcd. for $C_{11}H_{17}DO_2$ $[M]^+$ 183.1369, found 183.1360.

Data for **3a**: 1H NMR (400 MHz, $CDCl_3$) δ 5.07-5.10 (m, 1H), 3.69 (s, 3H), 2.17 (s, 7H), 1.69 (s, 3H), 1.61 (s, 3H); ^{13}C NMR (400 MHz, $CDCl_3$) δ 167.6, 160.4, 132.9, 123.4, 51.1, 41.2, 26.4, 26.0, 19.2, 18.1; EI-MS $[M]^+$ 183

(15), 152 (19), 124 (47), 115 (87), 84 (59), 69 (100), 41 (57); ESI-HRMS calcd. for $C_{11}H_{17}DO_2$ $[M]^+$ 183.1369, found 183.1362.

Methyl (2E)-[2,4,4,9,9,9- 2H_6]-3,7-Dimethylocta-2,6-dienoate [3b] and Methyl (2Z)-[2,4,4,9,9,9- 2H_6]-3,7-Dimethylocta-2,6-dienoate [4b]. According the general procedure, condensation of **1b** (1.25 g) and **2** (1.16 g), esterification of the mixture of *E/Z* carboxylic acids and subsequent purification by flash chromatography gave **4b** (0.24 g) as a colorless oil followed by **3b** (0.37 g) as a colorless oil (total yield 38 % from **2**, *Z/E* 4:6). IR (neat, mixture of *E*- and *Z*- isomers) cm^{-1} : ν 2964, 2918, 1719, 1629, 1435, 1230, 1102, 1041, 792.

Data for **4b**: 1H NMR (400 MHz, $CDCl_3$) δ 5.14-5.18 (m, 1H), 3.68 (s, 3H), 2.15 (d, $J = 7.30$ Hz, 2H), 1.69 (s, 3H), 1.63 (s, 3H); ^{13}C NMR (400 MHz, $CDCl_3$) δ 167.1, 160.5, 132.5, 124.1, 51.1, 27.0, 26.0, 18.0; EI-MS $[M]^+$ 188 (10), 156 (16), 128 (38), 119 (41), 88 (36), 69 (100), 41 (47); ESI-HRMS calcd. for $C_{11}H_{12}D_6O_2$ $[M]^+$ 188.1683, found 188.1691.

Data for **3b**: 1H NMR (400 MHz, $CDCl_3$) δ 5.07-5.10 (m, 1H), 3.69 (s, 3H), 2.15 (d, $J = 6.83$ Hz, 2H), 1.69 (s, 3H), 1.61 (s, 3H); ^{13}C NMR (400 MHz, $CDCl_3$) δ 167.6, 160.2, 132.9, 123.4, 51.1, 26.3, 26.0, 18.0; EI-MS $[M]^+$ 188 (7), 156 (13), 128 (27), 119 (50), 88 (26), 69 (100), 41 (38); ESI-HRMS calcd. for $C_{11}H_{12}D_6O_2$ $[M]^+$ 183.1683, found 188.1692.

Methyl (2E,6E)-[2- 2H_1]-3,7,11-Trimethyldodeca-2,6,10-trienoate [3c] and Methyl (2Z,6E)-[2- 2H_1]-3,7,11-Trimethyldodeca-2,6,10-trienoate [4c]. According the general procedure, condensation of **1c** (1.62 g) and **2** (1.02 g), esterification of the mixture of *E/Z* carboxylic acids and subsequent purification by flash chromatography gave **4c** (0.25 g) as a colorless oil followed by **3c** (0.41 g) as a colorless oil (total yield 35 % from **2**, *Z/E* 4:6). IR (neat, mixture of *E*- and *Z*- isomers) cm^{-1} : ν 2968, 2917, 1719, 1638, 1438, 1378, 1241, 1148, 1069, 928, 792.

Data for **4c**: 1H NMR (400 MHz, $CDCl_3$) δ 5.14-5.18 (m, 1H), 5.06-5.10 (m, 1H), 3.66 (s, 3H), 2.65 (t, $J = 7.79$ Hz, 2H), 2.17 (q, $J = 7.64$ Hz, 2H), 2.03-2.08 (m, 2H), 1.95-1.99 (m, 2H), 1.88 (s, 3H), 1.67 (s, 3H), 1.61 (s, 3H), 1.59 (s, 3H); ^{13}C NMR (400 MHz, $CDCl_3$) δ 167.0, 160.6, 136.1, 131.5, 124.7, 123.9, 50.9, 40.0, 33.7, 27.1, 27.0, 26.0, 25.5, 17.9, 16.2; EI-MS $[M]^+$ 251 (8), 208 (21), 136 (32), 115 (55), 81 (51), 69 (100), 41 (52); ESI-HRMS calcd. for $C_{16}H_{25}DO_2$ $[M]^+$ 251.1995, found 251.1999.

Data for **3c**: 1H NMR (400 MHz, $CDCl_3$) δ 5.07-5.10 (m, 2H), 3.69 (s, 3H), 2.17 (s br, 7H), 1.97-2.10 (m, 4H), 1.69 (s, 3H), 1.61 (s br, 6H); ^{13}C NMR (400 MHz, $CDCl_3$) δ 167.6, 160.3, 136.6, 131.7, 124.6, 123.3, 51.0, 41.3, 40.0, 27.1, 26.4, 26.0, 19.2, 18.0, 16.3; EI-MS $[M]^+$ 251 (25), 208 (56), 150 (57), 115 (60), 81 (57), 69 (100), 41 (67); ESI-HRMS calcd. for $C_{16}H_{25}DO_2$ $[M]^+$ 251.1995, found 251.2000.

Methyl (2E,6E)-[2,4,4,13,13,13-²H₆]-3,7,11-Trimethyldodeca-2,6,10-trienoate [3d] and Methyl (2Z,6E)-[2,4,4,13,13,13-²H₆]-3,7,11-Trimethyldodeca-2,6,10-trienoate [4d]. According the general procedure, condensation of **1d** (1.78 g) and **2** (1.09 g), esterification of the mixture of *E/Z* carboxylic acids and subsequent purification by flash chromatography gave **4d** (0.24 g) as a colorless oil followed by **3d** (0.41 g) as a colorless oil (total yield 31 % from **2**, *Z/E* 4:6). IR (neat, mixture of *E*- and *Z*- isomers) cm^{-1} : ν 2967, 2919, 1719, 1629, 1435, 1379, 1226, 1114, 1052.

Data for **4d**: ¹H NMR (400 MHz, CDCl₃) δ 5.15-5.19 (m, 1H), 5.07-5.11 (m, 1H), 3.67 (s, 3H), 2.16 (d, *J* = 7.15 Hz, 2H), 2.03-2.08 (m, 2H), 1.96-1.99 (m, 2H), 1.68 (s, 3H), 1.62 (s, 3H), 1.60 (s, 3H); ¹³C NMR (400 MHz, CDCl₃) δ 167.1, 160.7, 136.1, 131.6, 124.7, 123.8, 51.1, 40.0, 27.1, 26.8, 26.0, 18.0, 16.3; EI-MS [M]⁺ 256 (3), 213 (5), 119 (30), 81 (24), 69 (100), 41 (34); ESI-HRMS calcd. for C₁₆H₂₀D₆O₂ [M]⁺ 256.2309, found 256.2304.

Data for **3d**: ¹H NMR (400 MHz, CDCl₃) δ (5.07-5.10, m, 2H), 3.69 (s, 3H), 2.16 (d, *J* = 6.61 Hz, 2H), 1.96-2.09 (m, 4H), 1.68 (s, 3H), 1.60 (s, 6H); ¹³C NMR (400 MHz, CDCl₃) δ 167.6, 160.3, 136.5, 131.8, 124.6, 123.2, 51.1, 40.0, 27.0, 26.2, 26.0, 18.0, 16.4; EI-MS [M]⁺ 256 (7), 213 (15), 155 (9), 119 (29), 81 (33), 69 (100), 41 (46); ESI-HRMS calcd. for C₁₆H₂₀D₆O₂ [M]⁺ 256.2309, found 256.2302.

General Procedure for the Preparation of Geraniols and Farnesols. Geraniols and farnesols were prepared according to the modified method of Arigoni et al. [14]. To a solution of methyl ester **3,4a-d** (0.87 mmol) in CH₂Cl₂ (20 mL) at -78°C under argon was added dropwise diisobutylaluminium hydride (1M in hexane, 2 eq. mol). Stirring was continued at -78°C for 5h before addition of water (0.4 mL), NaOH (1N, 0.4 mL) and water (1.2 mL). The mixture is loaded to a column filled with Na₂SO₄ and eluted with MeOH (2 volumes column). The solution is concentrated and purified by flash chromatography (1:4 (v/v) ether in petroleum ether) to give the corresponding alcohol **5,6a-d**.

(2E)-[2-²H₁]-3,7-Dimethylocta-2,6-dien-1-ol [5a]. According the general procedure, reduction of **3a** (0.172 g) gave **5a** (0.127 g, 87 %) as a colorless oil. ¹H NMR (400 MHz, CDCl₃) δ 5.08-5.13 (m, 1H), 4.16 (s, 2H), 2.02-2.13 (m, 4H), 1.69 (s br, 6H), 1.61 (s, 3H); ¹³C NMR (400 MHz, CDCl₃) δ 140.1, 132.1, 124.3, 59.7, 39.9, 26.8, 26.0, 18.1, 16.6; ESI-HRMS calcd. for C₁₀H₁₅D [M-H₂O]⁺ 137.1314, found 137.1307.

(2E)-[2,4,4,9,9,9-²H₆]-3,7-Dimethylocta-2,6-dien-1-ol [5b]. According the general procedure, reduction of **3b** (0.185 g) gave **5b** (0.141 g, 90 %) as a colorless oil. ¹H NMR (400 MHz, CDCl₃) δ 5.05-5.09, m, 1H), 4.10 (s, 2H), 2.05 (d, *J* = 6.79 Hz, 2H), 1.65 (s, 3H), 1.57 (s, 6H); ¹³C NMR (400 MHz, CDCl₃) δ 139.4, 131.9, 124.2, 59.4, 26.5, 25.9, 17.9.

(2E,6E)-[2-²H₁]-3,7,11-Trimethyldodeca-2,6,10-trien-1-ol [5c]. According to the general procedure, reduction of **3c** (0.180 g) gave **5c** (0.153 g, 96 %) as a colorless oil. ¹H NMR (400 MHz, CDCl₃) δ 5.04-5.10 (m, 2H), 4.08 (s, 2H), 1.92-2.10 (m, 8H), 1.64 (s, 3H), 1.63 (s, 3H), 1.56 (s br, 6H); ¹³C NMR (400 MHz, CDCl₃) δ 139.2, 135.4, 131.4, 124.5, 124.1, 59.2, 39.9, 39.7, 26.9, 26.5, 25.8, 17.8, 16.4, 16.

(2E,6E)-[2,4,4,13,13,13-²H₆]-3,7,11-Trimethyldodeca-2,6,10-trien-1-ol [5d]. According to the general procedure, reduction of **3d** (0.179 g) gave **5d** (0.140 g, 88 %) as a colorless oil. ¹H NMR (400 MHz, CDCl₃) δ 5.10-5.12 (m, 2H), 4.15 (s, 2H), 1.98-2.11 (m, 6H), 1.69 (s, 3H), 1.61 (s, 6H); ¹³C NMR (400 MHz, CDCl₃) δ 140.0, 135.7, 131.7, 124.7, 124.1, 59.7, 40.1, 27.1, 26.5, 26.0, 18.0, 16.4.

General Procedure for the Preparation of Trisammonium Diphosphates. Trisammonium diphosphates were prepared according to the modified method of Woodside et al. [15]. To a solution of *N*-chlorosuccinimide (11.39 mmol) in CH₂Cl₂ (45 mL) at -30°C under argon was added dropwise freshly distilled dimethyl sulfide (1.1 eq. mol). The mixture was warmed to 0°C, stirred at this temperature for 10 min and cooled to -40°C. A solution of alcohol **5,6a-d** (1 eq. mol) in CH₂Cl₂ (5 mL) was slowly added before the reaction mixture was warmed to 0°C. Stirring was continued for 2 h at 0°C and 15 min at rt. The clear solution was then washed with cold saturated NaCl (25 mL). The aqueous phase was extracted with pentane (2 × 20 mL). The combined organic layers were washed with cold saturated NaCl (20 mL), dried (MgSO₄), concentrated under reduced pressure (no water bath) and completely removed under high vacuum for 2 h. Corresponding alkyl chlorides were used without further purification. Freshly prepared tris(tetrabutylammonium) hydrogen pyrophosphate (according to the method of Woodside et al. [16]) (1.2 eq. mol) was dissolved in ACN (5 mL) at rt under argon before dropwise addition of alkyl chloride in ACN (2 mL). Stirring was continued at rt overnight. The mixture was concentrated under reduced pressure. The residue was dissolved in (NH₄)₂CO₃ (3 mL) (0.25 mM, 2 % isopropyl alcohol), loaded onto a 2 × 30 cm column of Dowex 50WX8-200 (NH₄⁺ form) before elution of two volumes column of (NH₄)₂CO₃ (0.25 mM, 2 % isopropyl alcohol). The eluent was lyophilized and the resulting white powder was purified by chromatography on cellulose (1:9 (v/v) water in ACN). Fractions were monitored by TLC (silica gel, *iPr*-OH-water-AcOEt 6:3:1) and those containing trisammonium diphosphate were combined. Solvents were removed under reduced pressure and the resulting solution was lyophilized to afford **7,8a-d**.

Trisammonium (2E)-[2-²H₁]-3,7-Dimethylocta-2,6-dienyl Diphosphate [7a]. According to the general procedure, phosphorylation of **5a** (0.127 g) gave **7a** (0.153 g, 51 % from **5a**) as a flocculent white solid. mp: 157-160°C. ¹H NMR (400 MHz, D₂O/ND₄OD) δ 5.37-5.41 (m, 1H), 4.65 (d, *J* = 6.05 Hz, 2H), 2.25-2.37 (m, 4H), 1.90 (s, 3H), 1.87 (s, 3H), 1.81 (s, 3H); ¹³C NMR (400 MHz, D₂O/ND₄OD) δ 145.1, 136.4, 127.0, 65.2 (d, *J* = 5.13 Hz), 41.6,

28.5, 27.7, 19.8, 18.4; ^{31}P NMR (400 MHz, $\text{D}_2\text{O}/\text{ND}_4\text{OD}$) δ - 5.60 (d, J = 21.73 Hz, 1 P), - 9.64 (d, $J_{31\text{P},31\text{P}}$ = 21.73 Hz, 1 P); IR (ZnS, microscope) cm^{-1} : ν 3199, 3033-2922 (br), 2391, 1658, 1445, 1204, 1091, 923; ESI-HRMS calcd. for $\text{C}_{10}\text{H}_{18}\text{DO}_7\text{P}_2$ [M-H] $^-$ 314.0669, found 314.0667.

Trisammonium (2E)-[2,4,4,9,9,9- $^2\text{H}_6$]-3,7-Dimethylocta-2,6-dienyl Diphosphate [7b]. According the general procedure, phosphorylation of **5b** (0.141 g) gave **7b** (0.131 g, 40 % from **5b**) as a flocculent white solid. mp: 155-160°C. ^1H NMR (400 MHz, $\text{D}_2\text{O}/\text{ND}_4\text{OD}$) δ 5.36-5.39 (m, 1H), 4.63 (s br, 2H), 2.30 (d, J = 6.97 Hz, 2H), 1.86 (s, 3H), 1.70 (s, 3H); ^{13}C NMR (400 MHz, $\text{D}_2\text{O}/\text{ND}_4\text{OD}$) δ 144.9, 136.3, 127.1, 65.2 (d, J = 5.20 Hz), 28.4, 27.8, 19.9; ^{31}P NMR (400 MHz, $\text{D}_2\text{O}/\text{ND}_4\text{OD}$) δ - 5.58 (d, J = 21.70 Hz, 1 P), - 9.58 (d, $J_{31\text{P},31\text{P}}$ = 21.63 Hz, 1 P); IR (ZnS, microscope) cm^{-1} : ν 3150-2920 (br), 2320, 2197, 1649, 1447, 1207, 1092, 920; ESI-HRMS calcd. for $\text{C}_{10}\text{H}_{13}\text{D}_6\text{O}_7\text{P}_2$ [M-H] $^-$ 319.0983, found 319.1002.

Trisammonium (2E,6E)-[2- $^2\text{H}_1$]-3,7,11-Trimethyldodeca-2,6,10-trienyl Diphosphate [7c]. According the general procedure, phosphorylation of **5c** (0.153 g) gave **7c** (0.134 g, 45 % from **5c**) as a flocculent white solid. mp: 185-188°C. ^1H NMR (400 MHz, $\text{D}_2\text{O}/\text{ND}_4\text{OD}$) δ 5.41-5.47 (m, 2H), 4.72 (d, J = 6.05 Hz, 2H), 1.98-2.42 (m, 8H), 1.94 (s, 3H), 1.88 (s, 3H), 1.87 (s, 6H); ^{13}C NMR (400 MHz, $\text{D}_2\text{O}/\text{ND}_4\text{OD}$) δ 145.1, 139.3, 136.1, 127.3, 127.1, 65.1 (d, J = 4.59 Hz), 41.71, 41.69, 28.7, 28.6, 27.8, 19.8, 18.5, 18.1; ^{31}P NMR (400 MHz, $\text{D}_2\text{O}/\text{ND}_4\text{OD}$) δ -5.60 (d, J = 15.93 Hz, 1 P), -9.72 (d, $J_{31\text{P},31\text{P}}$ = 23.7 Hz, 1 P); IR (ZnS, microscope) cm^{-1} : ν 3165-2860 (br), 2357, 1659, 1445, 1207, 1093, 920; ESI-HRMS calcd. for $\text{C}_{15}\text{H}_{26}\text{DO}_7\text{P}_2$ [M-H] $^-$ 382.1295, found 382.1270.

Trisammonium (2E,6E)-[2,4,4,13,13,13- $^2\text{H}_6$]-3,7,11-Trimethyldodeca-2,6,10-trienyl Diphosphate [7d]. According the general procedure, phosphorylation of **5d** (0.140 g) gave **7d** (0.178 g, 66 % from **5d**) as a flocculent white solid. mp: 188-190°C. ^1H NMR (400 MHz, $\text{D}_2\text{O}/\text{ND}_4\text{OD}$) δ 5.36-5.39 (m, 2H), 4.66 (d, J = 5.75 Hz, 2H), 2.28-2.35 (m, 4H), 2.20-2.24 (m, 2H), 1.88 (s, 3H), 1.82 (s, 6H); ^{13}C NMR (400 MHz, $\text{D}_2\text{O}/\text{ND}_4\text{OD}$) δ 145.1, 139.4, 136.2, 127.3, 127.1, 65.1 (d, J = 5.35 Hz), 41.7, 28.7, 28.4, 27.7, 19.8, 18.1; ^{31}P NMR (400 MHz, $\text{D}_2\text{O}/\text{ND}_4\text{OD}$) δ - 5.63 (d, J = 15.81 Hz, 1 P), -9.65 (d, $J_{31\text{P},31\text{P}}$ = 17.78 Hz, 1 P); IR (ZnS, microscope) cm^{-1} : ν 3152-2859 (br), 2354, 2198, 1650, 1445, 1207, 1092, 921; ESI-HRMS calcd. for $\text{C}_{15}\text{H}_{21}\text{D}_6\text{O}_7\text{P}_2$ [M-H] $^-$ 387.1609, found 387.1597.

Trisammonium (E)-Geranyl and (2E,6E)-Farnesyl Diphosphates. Unlabeled GDP and FDP were synthesized from commercial geranyl and farnesyl chloride (Aldrich) respectively, according the phosphorylation procedure described above.

11.2 Manuscript II

(**Note:** ^1H , ^{13}C and ^{31}P NMR and IR spectra of the synthetic compounds are attached in CD at the end this thesis)

Supporting Information

Substrate geometry controls the cyclization cascade in Multiproduct terpene synthases from *Zea Mays*

Abith Vattekkatte,^a Nathalie Gatto,^a Tobias Köllner,^b Jörg Degenhardt,^c Jonathan Gershenzon,^b and Wilhelm Boland^{a}*

^aDepartment of Bioorganic Chemistry, Max Planck Institute for Chemical Ecology, Beutenberg Campus, Hans-Knöll-Strasse 8, D-07745 Jena, Germany

^bDepartment of Biochemistry, Max Planck Institute for Chemical Ecology, Beutenberg Campus, Hans-Knöll-Strasse 8, D-07745 Jena, Germany

^cInstitute for Pharmacy, University of Halle, Hoher Weg 8, D-06120 Halle, Germany

boland@ice.mpg.de

*To whom correspondence should be addressed. Fax: +49(0) 3641 571 202

Table of contents

Product distribution of main monoterpenes from incubations of deuterated GDP with TPS4-B73 and TPS5-*Delprim* from maize (*Zea mays*)

S5

Product distribution of main sesquiterpenes from incubations of deuterated FDP with TPS4-B73 from maize (*Zea mays*) S6

Product distribution of main sesquiterpenes from incubations of deuterated FDP with TPS5-*Delprim* from maize (*Zea mays*) S7

Oxygenated cyclic volatiles approximation S8

Complete synthetic scheme S10

Synthetic Procedure

[2,2-²H₂]-Trimethylsilylacetic acid (**2**) S11

[1,1,1,3,3-²H₅]-6-Methyl-hept-5-en-2-one (**1b**) S12

[1,1,1,3,3-²H₅]-6,10-Dimethyl-undeca-5,9-dien-2-one (**1d**) S12

Methyl (2*E*)-[2-²H]-3,7-Dimethylocta-2,6-dienoate (**3a**) S13

Methyl (2*Z*)-[2-²H]-3,7-Dimethylocta-2,6-dienoate (**4a**) S13

Methyl (2*E*)-[2,4,4,9,9,9-²H₆]-3,7-Dimethylocta-2,6-dienoate (**3b**) S14

Methyl (2*Z*)-[2,4,4,9,9,9-²H₆]-3,7-Dimethylocta-2,6-dienoate (**4b**) S14

Methyl (2*E*,6*E*)-[2-²H]-3,7,11-Trimethyldodeca-2,6,10-trienoate (**3c**) S15

Methyl (2*Z*,6*E*)-[2-²H]-3,7,11-Trimethyldodeca-2,6,10-trienoate (**4c**) S15

Methyl (2*E*,6*E*)-[2,4,4,13,13,13-²H₆]-3,7,11-Trimethyldodeca-2,6,10-trienoate (**3d**) S16

Methyl (2*Z*,6*E*)-[2,4,4,13,13,13-²H₆]-3,7,11-Trimethyldodeca-2,6,10-trienoate (**4d**) S16

(2*Z*)-[2-²H]-3,7-Dimethylocta-2,6-dien-1-ol (**6a**) S16

(2*Z*)-[2,4,4,9,9,9-²H₆]-3,7-Dimethylocta-2,6-dien-1-ol (**6b**) S17

(2Z,6E)-[2- ² H]-3,7,11-Trimethyldodeca-2,6,10-trien-1-ol (6c)	S17
(2Z,6E)-[2,4,4,13,13,13- ² H ₆]-3,7,11-Trimethyldodeca-2,6,10-trien-1-ol (6d)	S17
Trisammonium (2Z)-[2- ² H]-3,7-Dimethylocta-2,6-dienyl Diphosphate (8a)	S18
Trisammonium (2Z)-[2,4,4,9,9,9- ² H ₆]-3,7-Dimethylocta-2,6-dienyl Diphosphate (8b)	S18
Trisammonium (2Z,6E)-[2- ² H]-3,7,11-Trimethyldodeca-2,6,10-trienyl Diphosphate (8c)	S19
Trisammonium (2Z,6E)-[2,4,4,13,13,13- ² H ₆]-3,7,11-Trimethyldodeca-2,6,10-trienyl Diphosphate (8d)	

(In the attached CD)

¹H, ¹³C spectra of the synthetic compounds

[2,2- ² H ₂]-Trimethylsilylacetic acid (2)	
[1,1,1,3,3- ² H ₅]-6-Methyl-hept-5-en-2-one (1b)	
[1,1,1,3,3- ² H ₅]-6,10-Dimethyl-undeca-5,9-dien-2-one (1d)	
Methyl (2Z)-[2- ² H]-3,7-Dimethylocta-2,6-dienoate (4a)	
Methyl (2Z)-[2,4,4,9,9,9- ² H ₆]-3,7-Dimethylocta-2,6-dienoate (4b)	
Methyl (2Z,6E)-[2- ² H]-3,7,11-Trimethyldodeca-2,6,10-trienoate (4c)	
Methyl (2Z,6E)-[2,4,4,13,13,13- ² H ₆]-3,7,11-Trimethyldodeca-2,6,10-trienoate (4d)	
(2Z)-[2- ² H]-3,7-Dimethylocta-2,6-dien-1-ol (6a)	
(2Z)-[2,4,4,9,9,9- ² H ₆]-3,7-Dimethylocta-2,6-dien-1-ol (6b)	
(2Z,6E)-[2- ² H]-3,7,11-Trimethyldodeca-2,6,10-trien-1-ol (6c)	
(2Z,6E)-[2,4,4,13,13,13- ² H ₆]-3,7,11-Trimethyldodeca-2,6,10-trien-1-ol (6d)	
Trisammonium (2Z)-[2- ² H]-3,7-Dimethylocta-2,6-dienyl Diphosphate (8a)	
Trisammonium (2Z)-[2,4,4,9,9,9- ² H ₆]-3,7-Dimethylocta-2,6-dienyl Diphosphate (8b)	
Trisammonium (2Z,6E)-[2- ² H]-3,7,11-Trimethyldodeca-2,6,10-trienyl Diphosphate (8c)	

Trisammonium (2*Z*,6*E*)-[2,4,4,13,13,13-²H₆]-3,7,11-Trimethyldodeca-2,6,10-trienyl
Diphosphate (**8d**)

³¹P NMR spectra of the synthetic compounds

Trisammonium (2*Z*)-[2-²H]-3,7-Dimethylocta-2,6-dienyl Diphosphate (**8a**)

Trisammonium (2*Z*)-[2,4,4,9,9,9-²H₆]-3,7-Dimethylocta-2,6-dienyl Diphosphate (**8b**)

Trisammonium (2*Z*,6*E*)-[2-²H]-3,7,11-Trimethyldodeca-2,6,10-trienyl Diphosphate (**8c**)

Trisammonium (2*Z*,6*E*)-[2,4,4,13,13,13-²H₆]-3,7,11-Trimethyldodeca-2,6,10-trienyl
Diphosphate (**8d**)

IR spectra of the synthetic compounds

[2,2-²H₂]-Trimethylsilylacetic acid (**2**)

[1,1,1,3,3-²H₅]-6-Methyl-hept-5-en-2-one (**1b**)

[1,1,1,3,3-²H₅]-6,10-Dimethyl-undeca-5,9-dien-2-one (**1d**)

Methyl (2*Z*,6*E*)-[2-²H]-3,7,11-Trimethyldodeca-2,6,10-trienoate (**4c**)

Trisammonium (2*Z*)-[2-²H]-3,7-Dimethylocta-2,6-dienyl Diphosphate (**8a**)

Trisammonium (2*Z*)-[2,4,4,9,9,9-²H₆]-3,7-Dimethylocta-2,6-dienyl Diphosphate (**8b**)

Trisammonium (2*Z*,6*E*)-[2-²H]-3,7,11-Trimethyldodeca-2,6,10-trienyl Diphosphate (**8c**)

Trisammonium (2*Z*,6*E*)-[2,4,4,13,13,13-²H₆]-3,7,11-Trimethyldodeca-2,6,10-trienyl
Diphosphate (**8d**)

Product distribution of main monoterpenes from incubations of deuterated GDP with TPS4-B73 and TPS5-Delprim from maize (*Zea mays*)

enzyme	product distribution ^{a, b} ng/h (% composition)	substrate				
		<i>E</i> -GDP ^c	<i>E</i> -(1D)-GDP 7a	<i>Z</i> -(1D)-GDP 8a	<i>E</i> -(6D)-GDP 7b	<i>Z</i> -(6D)-GDP 8b
TPS4	α -Thujene (M ₁)*	15.4 ± 0.5 (3.3)	15.6 ± 0.2 (3.1)	20.8 ± 0.8 (3.3)	5.0 ± 0.0 (1.2)	5.7 ± 0.1 (1.0)
	Sabinene (M ₂)*	39.7 ± 1.2 (8.4)	41.8 ± 0.3 (8.4)	63.1 ± 0.6 (9.9)	18.0 ± 0.9 (4.2)	31.4 ± 0.8 (5.3)
	β -Myrcene (M ₃)	42.6 ± 2.0 (9.1)	42.9 ± 0.5 (8.6)	-	26.9 ± 0.6 (6.4)	-
	(S)-(-)-Limonene (M ₄)	101.1 ± 3.5 (21.5)	100.9 ± 1.6 (20.3)	245.9 ± 3.4 (38.6)	95.2 ± 2.1 (22.5)	236.3 ± 4.3 (39.6)
	Sabinene hydrate (M ₅)**	26.7 ± 1.2 (5.7)	31.2 ± 1.0 (6.3)	38.8 ± 1.3 (6.1)	39.6 ± 0.7 (9.3)	62.6 ± 1.2 (10.5)
	α -Terpinolene (M ₆)	21.4 ± 0.4 (4.5)	22.4 ± 0.2 (4.5)	91.9 ± 1.4 (14.4)	21.7 ± 0.5 (5.1)	89.9 ± 2.3 (15.1)
	Linalool (M ₇)*	112.1 ± 4.2 (23.9)	128.5 ± 3.6 (25.9)	17.8 ± 1.0 (2.8)	115.8 ± 2.1 (27.3)	27.9 ± 0.6 (4.7)
	α -Terpineol (M ₈)*	30.6 ± 1.7 (6.5)	34.9 ± 0.8 (7.0)	78.6 ± 3.8 (12.3)	29.7 ± 0.3 (7.0)	76.2 ± 1.2 (12.8)
	Geraniol (M ₉)	79.7 ± 3.3 (17.0)	78.7 ± 2.7 (15.8)	80.7 ± 3.0 (12.6)	71.3 ± 1.8 (16.8)	66.0 ± 0.9 (11.1)

^a Product distribution was determined by GC-FID analysis. ^b Average of three independent replicates. ^c GDP denotes the geranyl diphosphate. * Stereoisomeric pairs chromatographically not resolved. ** Compound identified by mass spectra alone.

Enzyme	product distribution ^{a, b} ng/h (% composition)	substrate				
		<i>E</i> -GDP ^c	<i>E</i> -(1D)-GDP 7a	<i>Z</i> -(1D)-GDP 8a	<i>E</i> -(6D)-GDP 7b	<i>Z</i> -(6D)-GDP 8b
TPS5	α -Thujene (M ₁)*	67.0 ± 4.5 (2.5)	66.3 ± 2.4 (2.4)	166.9 ± 3.1 (5.0)	18.4 ± 1.1 (0.8)	46.4 ± 1.1 (1.5)
	Sabinene (M ₂)*	303.9 ± 4.4 (11.2)	294.8 ± 3.5 (10.7)	644.1 ± 8.3 (19.2)	127.9 ± 1.5 (5.4)	316.7 ± 12.4 (10.2)
	β -Myrcene (M ₃)	534.1 ± 14.6 (19.6)	498.0 ± 11.1 (18.0)	11.9 ± 1.6 (0.3)	348.1 ± 2.6 (14.8)	10.2 ± 2.9 (0.3)
	(S)-(-)-Limonene (M ₄)	570.0 ± 10.2 (20.9)	546.5 ± 6.3 (19.8)	1404.0 ± 12.1 (42.0)	500.4 ± 9.9 (21.3)	1383.4 ± 33.2 (44.6)
	Sabinene hydrate (M ₅)**	198.3 ± 13.2 (7.3)	212.6 ± 2.3 (7.7)	452.0 ± 4.7 (13.5)	304.0 ± 10.2 (12.9)	648.9 ± 48.0 (20.9)
	α -Terpinolene (M ₆)	92.6 ± 2.8 (3.4)	89.0 ± 0.2 (3.2)	194.0 ± 4.7 (5.8)	86.7 ± 2.0 (3.7)	208.8 ± 8.0 (6.7)
	Linalool (M ₇)*	317.0 ± 23.2 (11.6)	339.4 ± 4.7 (12.3)	137.6 ± 18.5 (4.1)	332.2 ± 17.3 (14.1)	189.9 ± 15.4 (6.1)
	α -Terpineol (M ₈)*	140.8 ± 11.5 (5.2)	157.9 ± 4.6 (5.7)	322.1 ± 34.73 (9.6)	135.3 ± 7.0 (5.8)	286.1 ± 20.2 (9.2)
	Geraniol (M ₉)	500.0 ± 47.3 (18.4)	559.2 ± 3.5 (20.2)	12.9 ± 4.1 (0.4)	495.8 ± 34.8 (21.1)	11.2 ± 0.4 (0.3)

^a Product distribution was determined by GC-FID analysis. ^b Average of three independent replicates. ^c GDP denotes the geranyl diphosphate. * Stereoisomeric pairs chromatographically not resolved. ** Compound identified by mass spectra alone.

Product distribution of main sesquiterpenes from incubations of deuterated FDP with TPS4-B73 from maize (*Zea mays*)

enzyme	product distribution ^{a, b} ng/h (% composition)	substrate				
		<i>E</i> -FDP ^c	<i>E,E</i> -(1D)- FDP 7c	<i>Z,E</i> -(1D)-FDP 8c	<i>E,E</i> -(6D)- FDP 7d	<i>Z,E</i> -(6D)-FDP 8d
TPS4	<i>7-epi</i> -Sesquithujene (S ₁)	568.8 ± 25.4 (18.5)	713.2 ± 75.9 (20.0)	2395.1 ± 55.3 (29.3)	349.4 ± 19.4 (12.1)	1552.2 ± 30.6 (16.8)
	Sesquithujene (S ₂)	133.3 ± 6.0 (4.3)	165.4 ± 17.3 (4.6)	635.7 ± 14.5 (7.8)	55.9 ± 3.0 (1.9)	278.4 ± 5.0 (3.0)
	(<i>Z</i>)- α -Bergamotene (S ₃)	30.5 ± 1.5 (1.0)	40.2 ± 4.0 (1.1)	66.3 ± 1.4 (0.8)	21.3 ± 1.1 (0.7)	42.2 ± 0.7 (0.4)
	(<i>E</i>)- α -Bergamotene (S ₄)	47.8 ± 2.0 (1.5)	65.4 ± 7.1 (1.8)	203.8 ± 4.7 (2.5)	16.7 ± 0.8 (0.6)	80.8 ± 1.6 (0.9)
	Sesquisabinene A (S ₅)	72.9 ± 2.9 (2.4)	91.0 ± 8.0 (2.5)	328.3 ± 6.9 (4.0)	57.5 ± 3.0 (2.0)	246.7 ± 4.0 (2.7)
	Sesquisabinene B (S ₆)	29.9 ± 1.2 (1.0)	36.5 ± 2.9 (1.0)	175.7 ± 3.7 (2.1)	26.3 ± 1.3 (0.9)	144.2 ± 2.3 (1.6)
	(<i>E</i>)- β -Farnesene (S ₇)	88.2 ± 3.4 (2.9)	112.5 ± 11.2 (3.1)	-	82.8 ± 4.2 (2.9)	-
	γ -Curcumene (S ₈)*	9.4 ± 0.3 (0.3)	11.0 ± 1.0 (0.3)	68.3 ± 3.4 (0.8)	25.2 ± 1.5 (0.9)	134.6 ± 2.0 (1.4)
	Zingiberene (S ₉)*	27.6 ± 2.0 (0.9)	34.3 ± 4.5 (1.0)	122.6 ± 2.7 (1.5)	25.4 ± 1.3 (0.9)	105.3 ± 2.3 (1.1)
	(<i>S</i>)- β -Bisabolene (S ₁₀)	584.4 ± 23.0 (19.1)	737.3 ± 74.2 (20.7)	1983.6 ± 42.8 (24.3)	573.1 ± 31.2 (19.9)	2053.2 ± 41.1 (22.2)
	β -Curcumene (S ₁₁)*	19.7 ± 0.6 (0.6)	23.0 ± 1.9 (0.6)	98.5 ± 5.0 (1.2)	68.5 ± 3.6 (2.4)	299.9 ± 4.9 (3.2)
	(<i>E</i>)- γ -Bisabolene (S ₁₂)	45.0 ± 1.6 (1.5)	56.1 ± 5.5 (1.6)	152.1 ± 3.3 (1.9)	44.2 ± 2.4 (1.5)	159.9 ± 3.1 (1.7)
	<i>7-epi</i> -Sesquithujene hydrate (S ₁₃)**	174.0 ± 4.8 (5.7)	182.3 ± 0.9 (5.1)	809.6 ± 28.3 (9.9)	363.5 ± 20.9 (12.6)	1873.0 ± 22.9 (20.3)
	Sesquithujene hydrate (S ₁₄)**	116.7 ± 3.6 (3.8)	116.1 ± 0.7 (3.2)	505.9 ± 19.1 (6.2)	200.8 ± 11.8 (7.0)	1093.8 ± 25.3 (11.8)
	(3 <i>R</i>)-(<i>E</i>)-Nerolidol (S ₁₅)	458.3 ± 13.8 (14.9)	481.4 ± 10.6 (13.5)	-	344.1 ± 21.1 (11.9)	-
	Unknown (A)***	525.6 ± 14.7 (17.1)	550.2 ± 2.8 (15.4)	7.1 ± 1.4 (0.1)	411.3 ± 23.6 (14.3)	8.12 ± 0.7 (0.1)
	Unknown (B)***	29.8 ± 0.9 (1.0)	30.9 ± 0.1 (0.9)	148.9 ± 6.7 (1.8)	69.8 ± 4.1 (2.4)	393.3 ± 6.9 (4.2)
	Unknown (C)***	51.7 ± 2.4 (1.7)	51.6 ± 0.7 (1.4)	229.2 ± 10.2 (2.8)	80.8 ± 4.7 (2.0)	487.4 ± 8.5 (5.3)

^a Product distribution was determined by GC-FID analysis. ^b Average of three independent replicates. ^c GDP denotes the geranyl diphosphate. * Absolute configuration of the stereoisomeric pairs uncertain. ** Hypothetic structure. Compounds identified by mass spectra alone. *** Unknown oxygenated cyclic sesquiterpenes.

**Product distribution of main sesquiterpenes from incubations of deuterated FDP with
TPS5-Delprim from maize (*Zea mays*)**

enzyme	product distribution ^{a, b} ng/h (% composition)	substrate				
		<i>E</i> -FDP ^c	<i>E,E</i> -(1D)- FDP 7c	<i>Z,E</i> -(1D)-FDP 8c	<i>E,E</i> -(6D)- FDP 7d	<i>Z,E</i> -(6D)-FDP 8d
TPS5	7- <i>epi</i> -Sesquithujene (S ₁)	196.6 ± 2.0 (2.0)	200.4 ± 2.1 (2.0)	1035.7 ± 14.6 (3.9)	132.0 ± 5.1 (1.2)	633.0 ± 13.7 (2.4)
	Sesquithujene (S ₂)	2854.3 ± 28.8 (29.3)	2967.0 ± 35.2 (29.2)	8442 ± 129.9 (32.3)	1265.8 ± 32.8 (11.6)	3497.7 ± 95.7 (13.2)
	(<i>Z</i>)- α -Bergamotene (S ₃)	245.4 ± 2.4 (2.5)	268.4 ± 2.7 (2.6)	484.0 ± 7.1 (1.8)	134.8 ± 2.8 (1.2)	209.8 ± 5.2 (0.8)
	(<i>E</i>)- α -Bergamotene (S ₄)	33.5 ± 0.4 (0.3)	36.1 ± 0.5 (0.3)	360.7 ± 5.9 (1.4)	23.6 ± 2.0 (0.2)	274.4 ± 9.0 (1.0)
	Sesquisabinene A (S ₅)	31.8 ± 0.4 (0.3)	30.5 ± 0.4 (0.3)	187.1 ± 2.8 (0.7)	28.1 ± 1.5 (0.2)	141.8 ± 5.4 (0.5)
	Sesquisabinene B (S ₆)	526.9 ± 5.1 (5.4)	557.5 ± 7.0 (5.5)	1545.5 ± 27.0 (5.9)	438.0 ± 8.1 (4.0)	1096.1 ± 46.9 (4.1)
	(<i>E</i>)- β -Farnesene (S ₇)	299.7 ± 22.1 (3.1)	330.5 ± 3.2 (3.2)	18.4 ± 1.8 (0.1)	321.1 ± 5.3 (2.9)	-
	γ -Curcumene (S ₈)*	60.3 ± 1.0 (0.6)	63.44 ± 1.5 (0.6)	184.2 ± 2.7 (0.7)	139.0 ± 0.2 (1.3)	367.6 ± 16.5 (1.4)
	Zingiberene (S ₉)*	60.5 ± 0.7 (0.6)	60.4 ± 0.6 (0.6)	219.5 ± 4.1 (0.8)	66.3 ± 1.7 (0.6)	219.9 ± 10.8 (0.8)
	(<i>S</i>)- β -Bisabolene (S ₁₀)	2223.7 ± 19.8 (22.8)	2363.6 ± 25.8 (23.3)	8746.3 ± 165 (33.4)	2352.5 ± 91.4 (21.6)	8172.4 ± 463 (30.9)
	β -Curcumene (S ₁₁)*	82.6 ± 1.5 (0.8)	90.0 ± 2.0 (0.9)	224.9 ± 2.8 (0.8)	201.9 ± 0.6 (1.8)	510.1 ± 25.2 (1.9)
	(<i>E</i>)- γ -Bisabolene (S ₁₂)	87.4 ± 0.9 (0.9)	91.8 ± 0.9 (0.9)	314.8 ± 6.1 (1.2)	98.4 ± 3.3 (0.9)	312.5 ± 18.9 (1.2)
	7- <i>epi</i> -Sesquithujene hydrate (S ₁₃)**	58.8 ± 0.8 (0.6)	60.4 ± 1.4 (0.6)	276.3 ± 5.1 (1.0)	138.1 ± 2.6 (1.3)	575.3 ± 32.8 (2.2)
	Sesquithujene hydrate (S ₁₄)**	1185.0 ± 13.0 (12.2)	1218.1 ± 15.9 (12.0)	2104.2 ± 304 (8.0)	2578.4 ± 45.3 (23.6)	5394.2 ± 299 (20.4)
	(3 <i>R</i>)-(<i>E</i>)-Nerolidol (S ₁₅)	596.8 ± 3.9 (6.1)	592.0 ± 5.1 (5.8)	-	566.5 ± 22.1 (5.2)	-
	Unknown (A)***	230.9 ± 2.4 (2.4)	221.0 ± 2.6 (2.2)	-	206.1 ± 6.0 (0.2)	3.0 ± 3.0 (0)
	Unknown (B)***	12.5 ± 0.2 (0.1)	10.8 ± 0.9 (0.1)	69.3 ± 1.0 (0.3)	26.4 ± 0.7 (0.2)	154.0 ± 7.9 (0.6)
	Unknown (C)***	896.8 ± 9.2 (9.2)	918.6 ± 9.4 (9.0)	1792.2 ± 31.1 (6.8)	2104.1 ± 41.2 (19.3)	4449.7 ± 225 (16.8)

^a Product distribution was determined by GC-FID analysis. ^b Average of three independent replicates. ^c GDP denotes the geranyl diphosphate. * Absolute configuration of the stereoisomeric pairs uncertain. ** Hypothetic structure. Compounds identified by mass spectra alone. *** Unknown oxygenated cyclic sesquiterpenes.

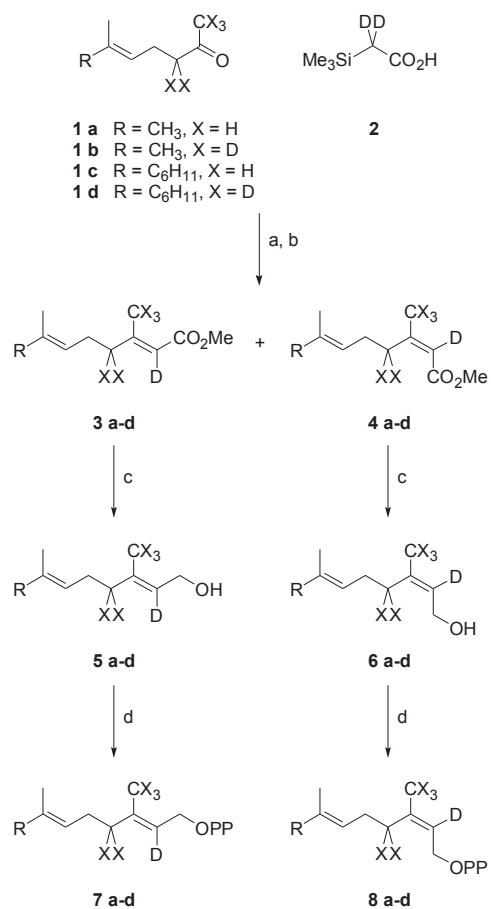
Oxygenated cyclic volatiles approximation

To estimate the weight of this approximation, quantitative kinetic measurements were carried out. Since TPS4-B73 and TPS5-*Delprim* exhibit similar basic features, only deuterium isotope effects on the catalytic activity of TPS4 were evaluated using the noncompetitive method. Both unlabeled (2*E*,6*E*)-FDP and (2*E*,6*E*)-[²H₆]-FDP **7d** substrates were used in two independent enzyme assays. Standard enzyme assays were performed in triplicate with aliquots of the same enzyme extracts under saturated substrate conditions. A decrease of 13 % (relative to the reference substrate) of the maximal rate for sesquiterpene formation was observed when (2*E*,6*E*)-[²H₆]-FDP **7d** was incubated with TPS4, while similar K_m were obtained for both substrates. Since the kinetic experiments were performed using the same enzyme extract, the total enzyme concentration $[E_T]$ was identical for both assays. Therefore, the turnover number (k_{cat}) of the enzyme, usually defined as the ratio of $V_{max}/[E_T]$, can be approximated to V_{max} . The apparent total rate isotope effect k_H/k_D , determined from the maximal rates, equals 1.15. As discussed before, similar results were obtained when the oxygenated cyclic volatiles were not considered (19 % decrease in the volatile production corresponding to a $k_H/k_D = 1.23$) and justify the approximation made above.

Experimental Section

General Methods. Reactions were performed under Ar. Solvents were dried according to standard procedures. ^1H , ^{13}C and ^{31}P NMR: Bruker AV 400 spectrometer (Bruker, D-76287 Rheinstetten/Karlsruhe, Germany). Chemical shifts of ^1H , ^{13}C and ^{31}P NMR are given in ppm (δ) based on solvent picks. CDCl_3 : 7.27 (1H NMR) and 77.4 ppm (^{13}C NMR). $\text{D}_2\text{O}/\text{ND}_4\text{OD}$: 4.79 (^1H NMR); ^{13}C NMR and ^{31}P NMR were referenced to external standard 3-(trimethylsilyl)-propionic acid- d_4 sodium salt (TSP; 3 % in D_2O) and phosphoric acid (H_3PO_4 , 10 % in D_2O), respectively. IR: Bruker Equinox 55 FTIR spectrophotometer. GC-MS: Trace MS, 2000 Series (Thermoquest, D-63329 Egelsbach, Germany) equipped with an Alltech DB5 (15 m \times 0.25 mm, 0.25 μm); helium served as carrier gas. Molecular composition of prepared compounds were determined by ESI-MS using a Micromass Quattro II (Waters, Micromass, Manchester, UK) tandem quadrupole mass spectrometer (geometry quadrupole-hexapole-quadrupole) equipped with an electrospray (ESI) source. High resolution ESI-MS (HR-EI-MS) were recorded at resolution ca 2500. High-resolution MS (EI) data were obtained using a MasSpec 2 instrument (Micromass, UK) in positive ion mode using 70 eV ionization energy. GC-HR-MS: Analyses were performed with a Hewlett Packard HP6890 gas chromatograph interfaced to a MasSpec 2. Separation was achieved on a J & W Scientific DB-5 capillary column, 30 m \times 0.25 mm, 0.25 μm film thickness using helium (30 mL s^{-1}) as carrier gas. Melting point: Büchi B-540 (Büchi Labortechnik AG, CH-9230 Flawil, Switzerland). Chromatography: Silica gel Si 60 (0.200-0.063 mm, E. Merck, Darmstadt, Germany); cellulose microcrystalline Avicel (E. Merck, Darmstadt, Germany).

Complete Synthetic Scheme



Reagents and conditions: (a) 2 eq. mol LDA, THF, -78°C to reflux; (b) Me₂SO₄, DIEA; (c) DIBAL-H, CH₂Cl₂; (d) i) NBS, Me₂S, CH₂Cl₂; ii) (Bu₄N)₃P₂O₇H, ACN; iii) ion exchange; iv) cellulose, ACN/NH₄HCO₃

Synthetic Procedure:**(2E) deuterated substrates**

We had recently reported the synthesis and characterization of (2E) deuterated substrates **3a-d**, **5a-d** and **7a-d**. We followed the same protocol for synthesis in these experiments.¹

[2,2-²H]-Trimethylsilylacetic acid [2]. A mixture of sodium acetate-*d*₃ (1.76 g, 20.7 mmol, Aldrich), 18-crown-6 ether (2g, 7.6 mmol) in dry ether (100 mL) was refluxed 2h under argon. Trimethylsilyl chloride (2.61 mL, 20.7 mmol) was added dropwise and the mixture was refluxed for 24h under argon. After cooling, the mixture was filtrated under argon. The resulting clear solution was added dropwise to a solution of lithium diisopropylamine at -78°C [prepared by reaction of *n*-butyl lithium 1.6 M in hexane (12.94 mL, 20.7 mmol) and diisopropylamine (2.90 mL, 20.7 mmol) in ether (40 mL)]. The mixture was stirred for 30 min at -78°C, warmed to rt and stirring was continued for additional 30 min. The yellow solution was then refluxed for 2h. The reaction was quenched by addition of saturated NH₄Cl at 0°C. The aqueous phase was acidified to pH = 3 with HCl (0.5 M) and the solution was extracted with ether (3 × 50 mL). The combined organic layers were dried (MgSO₄) and concentrated. Purification by flash chromatography (1:4 (v/v) ether in petroleum ether) gave **2** (1.16 g, 42 %) as a colorless oil which solidifies at low temperature. ¹H NMR (400 MHz, CDCl₃) δ 0.17 (s, 9H); ¹³C NMR (400 MHz, CDCl₃) δ (CO₂H not observed), -1.13; IR (neat) cm⁻¹: ν 2925, 2855, 1733, 1461, 1261, 799; ESI-HRMS calcd. for C₄H₇D₂O₂Si [M-CH₃]⁺ 119.0497, found 119.0501.

General Procedure for the Preparation of Pentadeuterated Ketones. A mixture of **1a,c** (39.6 mmol) and K₂CO₃ (0.25 g, previously dried at 80°C for 24h) in D₂O (8 mL) was vigorously stirred overnight at 70°C under argon. After cooling to rt, the mixture was extracted with dry CH₂Cl₂ (3 × 10 mL). The combined organic layers were dried (MgSO₄)

and concentrated. The procedure was repeated 3-5 times with fresh D₂O and K₂CO₃. The degree of labeling was monitored by GC-MS (>96 atom % ²H). The pentadeuterated ketone was purified by flash chromatography (1:9 (v/v) ether in petroleum ether).

[1,1,1,3,3-²H₅]-6-Methyl-hept-5-en-2-one [1b]. According the general procedure, deuteration of 6-methyl-hept-5-en-2-one **1a** (5g) gave **1b** (4.21 g, 81 %) as a yellow pale oil. ¹H NMR (400 MHz, CDCl₃) δ 5.0-5.04 (m, 1H), 2.20 (d, *J* = 7.09 Hz, 2H), 1.63 (s, 3H), 1.57 (s, 3H); ¹³C NMR (400 MHz, CDCl₃) δ 209.4, 133.0, 122.9, 25.9, 22.7, 17.9; IR (neat) cm⁻¹: ν 2977, 2937, 2554, 1711, 1449, 1380, 1252, 1171, 1042; EI-MS [*M*⁺] 131 (4), 113 (85), 95 (65), 69 (60), 46 (100); ESI-HRMS calcd. for C₈H₉D₅O [*M*⁺] 131.1358 found 131.1360 [21].

(5*E*)-[1,1,1,3,3-²H₅]-6,10-Dimethyl-undeca-5,9-dien-2-one [1d]. According the general procedure, deuteration of (5*E*)-6,10-dimethylundeca-5,9-dien-2-one **1c** (5g) gave **1d** (4.41 g, 86 %) as a yellow pale oil. ¹H NMR (400 MHz, CDCl₃) δ 5.07 (t, *J* = 7.8 Hz, 2H), 2.25 (d, *J* = 6.8 Hz, 2H), 1.95-2.08 (m, 4H), 1.68 (s, 3H), 1.61 (s, 3H), 1.60 (s, 3H); IR (neat) cm⁻¹: ν 2969, 2920, 2857, 1712, 1449, 1378, 1252, 1175, 1061; EI-MS [*M*⁺] 199 (3), 181 (4), 156 (28), 136 (39), 121 (15), 93 (21), 82 (9), 69 (78), 53 (17), 46 (100); ESI-HRMS calcd. for C₈H₉D₅O [*M*⁺] 199.1984, found 199.1985 [22].

General Procedure for the Preparation of Methyl Esters. Methyl esters were prepared according to the modified method of Arigoni et al. [14]. To a solution of lithium diisopropylamine (2.2 eq. mol) in THF (15 mL) at -78°C was added dropwise a solution of **2** (1.16 g, 8.64 mmol) in THF (15 mL). The mixture was stirred for 30 min at -78°C, 30 min at 0°C and then cooled to -78°C before dropwise addition of the corresponding ketones **1a-d** (1.1 eq. mol) in THF (15 mL). The reaction mixture was then stirred 1h at -78°C, 1h at -10°C and 1h at rt. The reaction mixture was quenched by dropwise addition of HCl (0.1 N) at 0°C. THF was removed under reduced pressure and the residue was dissolved in hexane (30 mL). The solution was poured into 100 mL of an hexane:HCl (0.5 N) (3:1) mixture and the

aqueous phase was extracted with hexane (3×40 mL). The combined organic layers were washed with brine, dried (MgSO_4) and concentrated. Purification by flash chromatography (1:4 (v/v) ether in petroleum ether) gave an isomeric mixture of corresponding carboxylic acids. The mixture of *E/Z* carboxylic acids was dissolved in ACN (20 mL) at 0°C and freshly distilled diisopropylamine (1.1 eq. mol) was added dropwise. The mixture was stirred 10 at 0°C , 20 min at rt and then cooled to 0°C before dropwise addition of freshly distilled dimethyl sulfate (2 eq. mol). The reaction mixture was stirred for 3h at rt. The mixture was quenched by dropwise addition of NH_4OH (0.1N) and the solvent was removed under reduced pressure. The residue was taken up in Et_2O (10 mL), poured into an ether:water (3:1) mixture (80 mL) and the aqueous phase was extracted with ether (3×30 mL). The combined organic layers were washed with brine, dried (MgSO_4) and concentrated. Silica gel column chromatography (1:9 (v/v) ether in petroleum ether) gave isomerically pure methyl esters.

Methyl (2*E*)-[2- $^2\text{H}_1$]-3,7-Dimethylocta-2,6-dienoate [3a] and Methyl (2*Z*)-[2- $^2\text{H}_1$]-3,7-Dimethylocta-2,6-dienoate [4a]. According the general procedure, condensation of **1a** (1.14 g) and **2** (1.10 g), esterification of the mixture of *E/Z* carboxylic acids and subsequent purification by flash chromatography gave **4a** (0.20 g) as a colorless oil followed by **3a** (0.31 g) as a colorless oil (total yield 35 % from **2**, *Z/E* 4:6). IR (neat, mixture of *E*- and *Z*- isomers) cm^{-1} : ν 2962, 1261, 1094, 1021, 866, 800.

Data for **4a**: ^1H NMR (400 MHz, CDCl_3) δ 5.14-5.18 (m, 1H), 3.68 (s, 3H), 2.64 (t, $J = 8.25$ Hz, 2H), 1.69 (q, $J = 7.52$ Hz, 2H), 1.90 (s, 3H); 1.69 (s br, 3H), 1.63 (s br, 3H); ^{13}C NMR (400 MHz, CDCl_3) δ 167.1, 160.8, 132.6, 124.5, 51.1, 33.8, 27.2, 26.0, 25.6, 18.0; EI-MS $[\text{M}]^+$ 183 (6), 152 (16), 124 (35), 115 (55), 84 (36), 69 (100), 41 (37); ESI-HRMS calcd. for $\text{C}_{11}\text{H}_{17}\text{DO}_2$ $[\text{M}]^+$ 183.1369, found 183.1360.

Data for **3a**: ^1H NMR (400 MHz, CDCl_3) δ 5.07-5.10 (m, 1H), 3.69 (s, 3H), 2.17 (s, 7H), 1.69 (s, 3H), 1.61 (s, 3H); ^{13}C NMR (400 MHz, CDCl_3) δ 167.6, 160.4, 132.9, 123.4, 51.1, 41.2,

26.4, 26.0, 19.2, 18.1; EI-MS $[M]^+$ 183 (15), 152 (19), 124 (47), 115 (87), 84 (59), 69 (100), 41 (57); ESI-HRMS calcd. for $C_{11}H_{17}DO_2$ $[M]^+$ 183.1369, found 183.1362.

Methyl (2E)-[2,4,4,9,9,9- 2H_6]-3,7-Dimethylocta-2,6-dienoate [3b] and Methyl (2Z)-[2,4,4,9,9,9- 2H_6]-3,7-Dimethylocta-2,6-dienoate [4b]. According the general procedure, condensation of **1b** (1.25 g) and **2** (1.16 g), esterification of the mixture of *E/Z* carboxylic acids and subsequent purification by flash chromatography gave **4b** (0.24 g) as a colorless oil followed by **3b** (0.37 g) as a colorless oil (total yield 38 % from **2**, *Z/E* 4:6). IR (neat, mixture of *E*- and *Z*- isomers) cm^{-1} : ν 2964, 2918, 1719, 1629, 1435, 1230, 1102, 1041, 792.

Data for **4b**: 1H NMR (400 MHz, $CDCl_3$) δ 5.14-5.18 (m, 1H), 3.68 (s, 3H), 2.15 (d, $J = 7.30$ Hz, 2H), 1.69 (s, 3H), 1.63 (s, 3H); ^{13}C NMR (400 MHz, $CDCl_3$) δ 167.1, 160.5, 132.5, 124.1, 51.1, 27.0, 26.0, 18.0; EI-MS $[M]^+$ 188 (10), 156 (16), 128 (38), 119 (41), 88 (36), 69 (100), 41 (47); ESI-HRMS calcd. for $C_{11}H_{12}D_6O_2$ $[M]^+$ 188.1683, found 188.1691.

Data for **3b**: 1H NMR (400 MHz, $CDCl_3$) δ 5.07-5.10 (m, 1H), 3.69 (s, 3H), 2.15 (d, $J = 6.83$ Hz, 2H), 1.69 (s, 3H), 1.61 (s, 3H); ^{13}C NMR (400 MHz, $CDCl_3$) δ 167.6, 160.2, 132.9, 123.4, 51.1, 26.3, 26.0, 18.0; EI-MS $[M]^+$ 188 (7), 156 (13), 128 (27), 119 (50), 88 (26), 69 (100), 41 (38); ESI-HRMS calcd. for $C_{11}H_{12}D_6O_2$ $[M]^+$ 183.1683, found 188.1692.

Methyl (2E,6E)-[2- 2H_1]-3,7,11-Trimethyldodeca-2,6,10-trienoate [3c] and Methyl (2Z,6E)-[2- 2H_1]-3,7,11-Trimethyldodeca-2,6,10-trienoate [4c]. According the general procedure, condensation of **1c** (1.62 g) and **2** (1.02 g), esterification of the mixture of *E/Z* carboxylic acids and subsequent purification by flash chromatography gave **4c** (0.25 g) as a colorless oil followed by **3c** (0.41 g) as a colorless oil (total yield 35 % from **2**, *Z/E* 4:6). IR (neat, mixture of *E*- and *Z*- isomers) cm^{-1} : ν 2968, 2917, 1719, 1638, 1438, 1378, 1241, 1148, 1069, 928, 792.

Data for **4c**: 1H NMR (400 MHz, $CDCl_3$) δ 5.14-5.18 (m, 1H), 5.06-5.10 (m, 1H), 3.66 (s, 3H), 2.65 (t, $J = 7.79$ Hz, 2H), 2.17 (q, $J = 7.64$ Hz, 2H), 2.03-2.08 (m, 2H), 1.95-1.99 (m,

2H), 1.88 (s, 3H), 1.67 (s, 3H), 1.61 (s, 3H), 1.59 (s, 3H); ^{13}C NMR (400 MHz, CDCl_3) δ 167.0, 160.6, 136.1, 131.5, 124.7, 123.9, 50.9, 40.0, 33.7, 27.1, 27.0, 26.0, 25.5, 17.9, 16.2; EI-MS $[\text{M}]^+$ 251 (8), 208 (21), 136 (32), 115 (55), 81 (51), 69 (100), 41 (52); ESI-HRMS calcd. for $\text{C}_{16}\text{H}_{25}\text{DO}_2$ $[\text{M}]^+$ 251.1995, found 251.1999.

Data for **3c**: ^1H NMR (400 MHz, CDCl_3) δ 5.07-5.10 (m, 2H), 3.69 (s, 3H), 2.17 (s br, 7H), 1.97-2.10 (m, 4H), 1.69 (s, 3H), 1.61 (s br, 6H); ^{13}C NMR (400 MHz, CDCl_3) δ 167.6, 160.3, 136.6, 131.7, 124.6, 123.3, 51.0, 41.3, 40.0, 27.1, 26.4, 26.0, 19.2, 18.0, 16.3; EI-MS $[\text{M}]^+$ 251 (25), 208 (56), 150 (57), 115 (60), 81 (57), 69 (100), 41 (67); ESI-HRMS calcd. for $\text{C}_{16}\text{H}_{25}\text{DO}_2$ $[\text{M}]^+$ 251.1995, found 251.2000.

Methyl (2E,6E)-[2,4,4,13,13,13- $^2\text{H}_6$]-3,7,11-Trimethyldodeca-2,6,10-trienoate [3d] and Methyl (2Z,6E)-[2,4,4,13,13,13- $^2\text{H}_6$]-3,7,11-Trimethyldodeca-2,6,10-trienoate [4d].

According to the general procedure, condensation of **1d** (1.78 g) and **2** (1.09 g), esterification of the mixture of *E/Z* carboxylic acids and subsequent purification by flash chromatography gave **4d** (0.24 g) as a colorless oil followed by **3d** (0.41 g) as a colorless oil (total yield 31 % from **2**, *Z/E* 4:6). IR (neat, mixture of *E*- and *Z*- isomers) cm^{-1} : ν 2967, 2919, 1719, 1629, 1435, 1379, 1226, 1114, 1052.

Data for **4d**: ^1H NMR (400 MHz, CDCl_3) δ 5.15-5.19 (m, 1H), 5.07-5.11 (m, 1H), 3.67 (s, 3H), 2.16 (d, $J = 7.15$ Hz, 2H), 2.03-2.08 (m, 2H), 1.96-1.99 (m, 2H), 1.68 (s, 3H), 1.62 (s, 3H), 1.60 (s, 3H); ^{13}C NMR (400 MHz, CDCl_3) δ 167.1, 160.7, 136.1, 131.6, 124.7, 123.8, 51.1, 40.0, 27.1, 26.8, 26.0, 18.0, 16.3; EI-MS $[\text{M}]^+$ 256 (3), 213 (5), 119 (30), 81 (24), 69 (100), 41 (34); ESI-HRMS calcd. for $\text{C}_{16}\text{H}_{20}\text{D}_6\text{O}_2$ $[\text{M}]^+$ 256.2309, found 256.2304.

Data for **3d**: ^1H NMR (400 MHz, CDCl_3) δ (5.07-5.10, m, 2H), 3.69 (s, 3H), 2.16 (d, $J = 6.61$ Hz, 2H), 1.96-2.09 (m, 4H), 1.68 (s, 3H), 1.60 (s, 6H); ^{13}C NMR (400 MHz, CDCl_3) δ 167.6, 160.3, 136.5, 131.8, 124.6, 123.2, 51.1, 40.0, 27.0, 26.2, 26.0, 18.0, 16.4; EI-MS $[\text{M}]^+$ 256

(7), 213 (15), 155 (9), 119 (29), 81 (33), 69 (100), 41 (46); ESI-HRMS calcd. for $C_{16}H_{20}D_6O_2$ $[M]^+$ 256.2309, found 256.2302.

General Procedure for the Preparation of Geraniols and Farnesols. Geraniols and farnesols were prepared according to the modified method of Arigoni et al. [14]. To a solution of methyl ester **4a-d** (0.87 mmol) in CH_2Cl_2 (20 mL) at $-78^\circ C$ under argon was added dropwise diisobutylaluminium hydride (1M in hexane, 2 eq. mol). Stirring was continued at $-78^\circ C$ for 5h before addition of water (0.4 mL), NaOH (1N, 0.4 mL) and water (1.2 mL). The mixture is loaded to a column filled with Na_2SO_4 and eluted with MeOH (2 volumes column). The solution is concentrated and purified by flash chromatography (1:4 (v/v) ether in petroleum ether) to give the corresponding alcohol **6a-d**.

(2Z)-[2- 2H_1]-3,7-Dimethylocta-2,6-dien-1-ol [6a]. According the general procedure, reduction of **4a** (0.164 g) gave **6a** (0.126 g, 91 %) as a colorless oil. 1H NMR (400 MHz, $CDCl_3$) δ 5.10-5.14 (m, 1H), 4.10 (s, 2H), 2.10-2.12 (m, 4H), 1.76 (s, 3H), 1.70 (s, 3H), 1.62 (s, 3H); ^{13}C NMR (400 MHz, $CDCl_3$) δ 140.3, 132.8, 124.2, 59.4, 32.4, 27.0, 26.0, 23.7, 18.0; ESI-HRMS calcd. for $C_{10}H_{15}D$ $[M-H_2O]^+$ 137.1314, found 137.1306.

(2Z)-[2,4,4,9,9,9- 2H_6]-3,7-Dimethylocta-2,6-dien-1-ol [6b]. According the general procedure, reduction of **4b** (0.166 g) gave **6b** (0.121 g, 86 %) as a colorless oil. 1H NMR (400 MHz, $CDCl_3$) δ 5.11-5.12 (m, 1H), 4.10 (s, 2H), 2.07 (d, $J = 7.07$ Hz, 2H), 1.70 (s, 3H), 1.62 (s, 3H); ^{13}C NMR (400 MHz, $CDCl_3$) δ 140.1, 132.7, 124.2, 59.3, 26.8, 26.0, 18.0.

(2Z,6E)-[2- 2H_1]-3,7,11-Trimethyldodeca-2,6,10-trien-1-ol [6c]. According the general procedure, reduction of **4c** (0.192 g) gave **6c** (0.160 g, 94 %) as a colorless oil. 1H NMR (400 MHz, $CDCl_3$) δ 5.08-5.12 (m, 2H), 4.09 (s, 2H), 1.95-2.10 (m, 8H), 1.74 (s, 3H), 1.67 (s, 3H), 1.59 (s br, 6H); ^{13}C NMR (400 MHz, $CDCl_3$) δ 140.0, 136.2, 131.7, 124.5, 123.9, 59.2, 40.0, 32.2, 27.0, 26.8, 26.0, 23.7, 18.0, 16.3.

(2Z,6E)-[2,4,4,13,13,13-²H₆]-3,7,11-Trimethyldodeca-2,6,10-trien-1-ol [6d]. According to the general procedure, reduction of **4d** (0.155 g) gave **6d** (0.125 g, 91 %) as a colorless oil. ¹H NMR (400 MHz, CDCl₃) δ 5.07-5.13 (m, 2H), 4.10 (s, 2H), 1.96-2.09 (m, 6H), 1.68 (s, 3H), 1.60 (s, 6H); ¹³C NMR (400 MHz, CDCl₃) δ 140.1, 136.3, 131.8, 124.6, 123.9, 59.3, 40.0, 27.0, 26.7, 26.0, 18.0, 16.3.

General Procedure for the Preparation of Trisammonium Diphosphates. Trisammonium diphosphates were prepared according to the modified method of Woodside et al. [15]. To a solution of *N*-chlorosuccinimide (11.39 mmol) in CH₂Cl₂ (45 mL) at -30°C under argon was added dropwise freshly distilled dimethyl sulfide (1.1 eq. mol). The mixture was warmed to 0°C, stirred at this temperature for 10 min and cooled to -40°C. A solution of alcohol **6a-d** (1 eq. mol) in CH₂Cl₂ (5 mL) was slowly added before the reaction mixture was warmed to 0°C. Stirring was continued for 2h at 0°C and 15 min at rt. The clear solution was then washed with cold saturated NaCl (25 mL). The aqueous phase was extracted with pentane (2 × 20 mL). The combined organic layers were washed with cold saturated NaCl (20 mL), dried (MgSO₄), concentrated under reduced pressure (no water bath) and completely removed under high vacuum for 2h. Corresponding alkyl chlorides were used without further purification. Freshly prepared tris(tetrabutylammonium) hydrogen pyrophosphate (according to the method of Woodside et al. [16]) (1.2 eq. mol) was dissolved in ACN (5 mL) at rt under argon before dropwise addition of alkyl chloride in ACN (2 mL). Stirring was continued at rt overnight. The mixture was concentrated under reduced pressure. The residue was dissolved in (NH₄)₂CO₃ (3 mL) (0.25 mM, 2 % isopropyl alcohol), loaded onto a 2 × 30 cm column of Dowex 50WX8-200 (NH₄⁺ form) before elution of two volumes column of (NH₄)₂CO₃ (0.25 mM, 2 % isopropyl alcohol). The eluent was lyophilized and the resulting white powder was purified by chromatography on cellulose (1:9 (v/v) water in ACN). Fractions were monitored by TLC (silica gel, *iPr*-OH-water-AcOEt 6:3:1) and those containing trisammonium

diphosphate were combined. Solvents were removed under reduced pressure and the resulting solution was lyophilized to afford **8a-d**.

Trisammonium (2Z)-[2-²H₁]-3,7-Dimethylocta-2,6-dienyl Diphosphate [8a]. According to the general procedure, phosphorylation of **6a** (0.126 g) gave **8a** (0.187 g, 63 % from **6a**) as a flocculent white solid. mp: 158-159°C. ¹H NMR (400 MHz, D₂O/ND₄OD) δ 5.36-5.38 (m, 1H), 4.63 (d, *J* = 6.24 Hz, 2H), 2.30-2.37 (m, 4H), 1.94 (s, 3H), 1.87 (s, 3H), 1.81 (s, 3H); ¹³C NMR (400 MHz, D₂O/ND₄OD) δ 145.1, 136.6, 126.8, 64.9 (d, *J* = 5.14 Hz), 34.1, 28.9, 27.7, 25.4, 19.8; ³¹P NMR (400 MHz, D₂O/ND₄OD) δ - 5.60 (d, *J* = 21.73 Hz, 1 P), - 9.61 (d, *J*_{31P,31P} = 23.71 Hz, 1 P); IR (ZnS, microscope) cm⁻¹: ν 3172-2860 (br), 2350, 1860, 1687, 1441, 1203, 1080, 911; ESI-HRMS calcd. for C₁₀H₁₈DO₇P₂ [M-H]⁻ 314.0669, found 314.0689.

Trisammonium (2Z)-[2,4,4,9,9,9-²H₆]-3,7-Dimethylocta-2,6-dienyl Diphosphate [8b]. According to the general procedure, phosphorylation of **6b** (0.121 g) gave **8b** (0.196 g, 70 % from **6b**) as a flocculent white solid. mp: 157-161°C. ¹H NMR (400 MHz, D₂O/ND₄OD) δ 5.36-5.39 (m, 1H), 4.60 (under D₂O pick, s br, 2H), 2.29 (d, *J* = 6.97 Hz, 2H), 1.87 (s, 3H), 1.80 (s, 3H); ¹³C NMR (400 MHz, D₂O/ND₄OD) δ 143.8.1, 136.5, 127.1, 65.0 (d, *J* = 5.14 Hz), 29.0, 28.0, 20.1; ³¹P NMR (400 MHz, D₂O/ND₄OD) δ - 5.63 (d, *J* = 53.64 Hz, 1 P), - 9.61 (d, *J*_{31P,31P} = 53.64 Hz, 1 P); IR (ZnS, microscope) cm⁻¹: ν 3185-2854 (br), 2196, 1892, 1649, 1445, 1204, 1087, 916; ESI-HRMS calcd. for C₁₀H₁₃D₆O₇P₂ [M-H]⁻ 319.0983, found 319.0979.

Trisammonium (2Z,6E)-[2-²H₁]-3,7,11-Trimethyldodeca-2,6,10-trienyl Diphosphate [8c]. According to the general procedure, phosphorylation of **6c** (0.160 g) gave **8c** (0.255 g, 82 % from **6c**) as a flocculent white solid. mp: 184-186°C. ¹H NMR (400 MHz, D₂O/ND₄OD) δ 5.45-5.51 (m, 2H), 4.74 (d, *J* = 6.24 Hz, 2H), 2.37-2.46 (m, 6H), 2.29-2.33 (m, 2H), 2.06 (s, 3H), 1.97 (s, 3H), 1.91 (s, 6H); ¹³C NMR (400 MHz, D₂O/ND₄OD) δ 145.2, 139.5, 136.1,

127.3, 127.0, 64.9 (d, $J = 5.14$ Hz), 41.7, 34.1, 29.0, 28.7, 27.7, 25.5, 19.8, 18.1; ^{31}P NMR (400 MHz, $\text{D}_2\text{O}/\text{ND}_4\text{OD}$) δ -5.62 (d, $J = 15.8$ Hz, 1 P), -9.61 (d, $J_{31\text{P},31\text{P}} = 17.76$ Hz, 1 P); IR (ZnS, microscope) cm^{-1} : ν 3199-2826 (br), 2330, 1914, 1658, 1448, 1205, 1088, 1021, 921; ESI-HRMS calcd. for $\text{C}_{15}\text{H}_{26}\text{DO}_7\text{P}_2$ $[\text{M}-\text{H}]^-$ 382.1295, found 382.1252.

Trisammonium(2Z,6E)-[2,4,4,13,13,13- $^2\text{H}_6$]-3,7,11-Trimethyldodeca-2,6,10-trienyl

Diphosphate [8d]. According the general procedure, phosphorylation of **6d** (0.125 g) gave **8d** (0.135 g, 56 % from **6d**) as a flocculent white solid. mp: 186-188°C. ^1H NMR (400 MHz, $\text{D}_2\text{O}/\text{ND}_4\text{OD}$) δ 5.32-5.38 (m, 2H), 4.61 (d, $J = 5.97$ Hz, 2H), 2.26-2.28 (m, 4H), 2.18-2.20 (m, 2H), 1.84 (s, 3H), 1.78 (s, 6H); ^{13}C NMR (400 MHz, $\text{D}_2\text{O}/\text{ND}_4\text{OD}$) δ 145.2, 139.7, 136.3, 127.4, 127.1, 65.0 (d, $J = 4.59$ Hz), 41.9, 27.0, 28.8, 27.9, 20.0, 18.3; ^{31}P NMR (400 MHz, $\text{D}_2\text{O}/\text{ND}_4\text{OD}$) δ -6.71 (d, $J = 15.80$ Hz, 1 P), -9.78 (d, $J_{31\text{P},31\text{P}} = 11.85$ Hz, 1 P); IR (ZnS, microscope) cm^{-1} : ν 3192-2861 (br), 2332, 2200, 1651, 1446, 1206, 1092, 917; ESI-HRMS calcd. for $\text{C}_{15}\text{H}_{21}\text{D}_6\text{O}_7\text{P}_2$ $[\text{M}-\text{H}]^-$ 387.1609, found 387.1656.

Heterologous expression of terpene synthases. The open reading frames of *tps4-B73* and *tps5-Dell* were cloned as *EcoRI-NotI* fragments and inserted into the bacterial expression vector pHis8-3 which provided the expressed proteins with a His-tag at the *N*-terminal [23]. The constructs were transformed into the *Escherichia coli* strain BL21 (DE3) and fully sequenced to avoid errors introduced by DNA amplification. The recombinant proteins TPS4 and TPS5 were purified from *E. coli* as previously described [9].

Assay for terpene synthase activity. Each 200 μL assay contained 50 μL of the bacterial extract in assay buffer (10 mM 3-(*N*)-2-hydroxypropane sulfonic acid (Mopso), pH 7.0, 1 mM DTT, and 10 % (v/v) glycerol) with 350 μM substrate, 7.5 mM MgCl_2 , 1.5 mM NaWO_4 , and 0.75 mM NaF in a 2 ml screw-capped glass vial. The assay was overlaid with 100 μL pentane containing 2.5 μM (*E*)- β -caryophyllene (Aldrich, 98 % pure) as an internal standard and incubated for 20 min at 30°C. The reaction was stopped by mixing for 1 min, and an

aliquot of the pentane layer was analyzed by GC-FID. Assay results are reported as the mean of three to six independent replicate assays. Product identification was performed by GC-MS as previously described.²

Gas chromatography for terpene synthase activity. A Hewlett-Packard model 6890 gas chromatograph was employed with the carrier gas He at 1 ml min⁻¹, splitless injection (injector temperature: 220°C, injection volume: 2 µL), a DB-WAX column (polyethylene glycol, 30 m × 0.25 mm ID × 0.25 µm film thickness, J&W Scientific, Folsom, CA, USA) for sesquiterpenes and a DB5-MS column (30 m × 0.25 mm ID × 0.25 µm film thickness, J & W Scientific) for monoterpenes, respectively. Temperature was programmed from 50°C (3 min hold) at 7°C min⁻¹ to 240°C (2 min hold). Quantification was performed with the trace of a flame ionization detector (FID) operated at 250°C. Peaks were compared with that of the internal standard assuming equal response factors.

11.3 Manuscript III

Supporting Information

Inhibition of a Multiproduct Terpene Synthase from *Medicago truncatula* by 3-Bromoprenyl diphosphates

Abith Vattekkatte^a, Nathalie Gatto^a, Eva Schulze^b, Wolfgang Brandt^b and Wilhelm Boland^{a*}

^aDepartment of Bioorganic Chemistry, Max Planck Institute for Chemical Ecology,

Hans-Knöll-Strasse 8, 07745 Jena, Germany

^b Department of Bioorganic Chemistry, Leibniz Institute of Plant Biochemistry,

Weinberg 3, 06120 Halle (Saale), Germany.

boland@ice.mpg.de

Table of contents*¹H, ¹³C spectra of the synthetic compounds*

2-((7-methyloct-6-en-2-yn-1-yl)oxy)tetrahydro-2H-pyran (**2a**)

7-methyloct-6-en-2-yn-1-ol (**3a**)

(2*E*)-3-bromo-7-methylocta-2,6-dien-1-ol (**4a**)

Trisammonium (2*E*)-1-(3-bromo-7-methylocta-2,6-dienyl)diphosphate(**5a**)

³¹P NMR spectra of the synthetic compounds

Trisammonium (2*E*)-1-(3-bromo-7-methylocta-2,6-dienyl)diphosphate(**5a**)

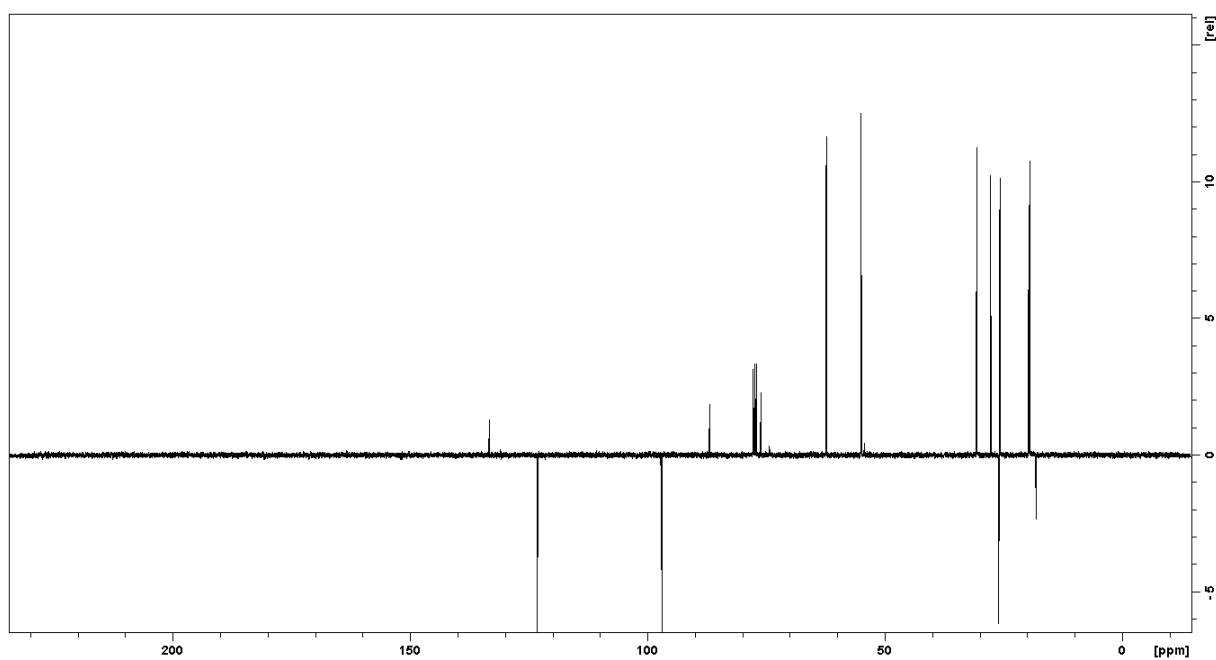
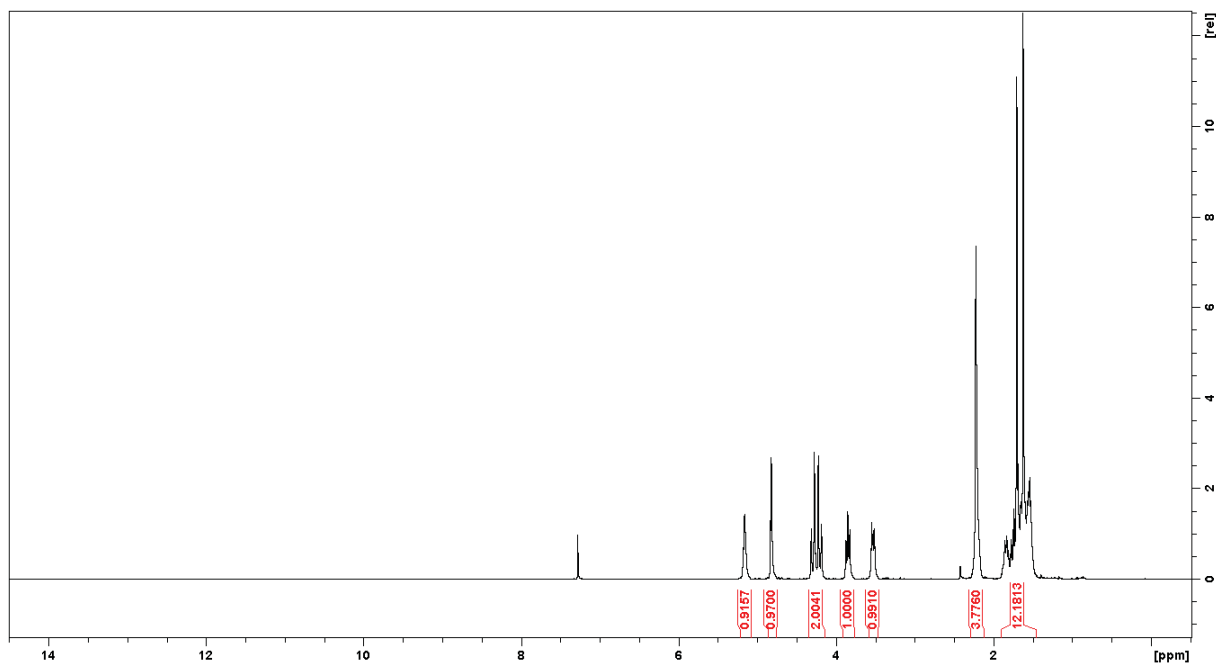
Trisammonium ((2*E*,6*E*)-3-bromo-7,11-dimethyldodeca-2,6,10-trienyl)diphosphate (**5b**)

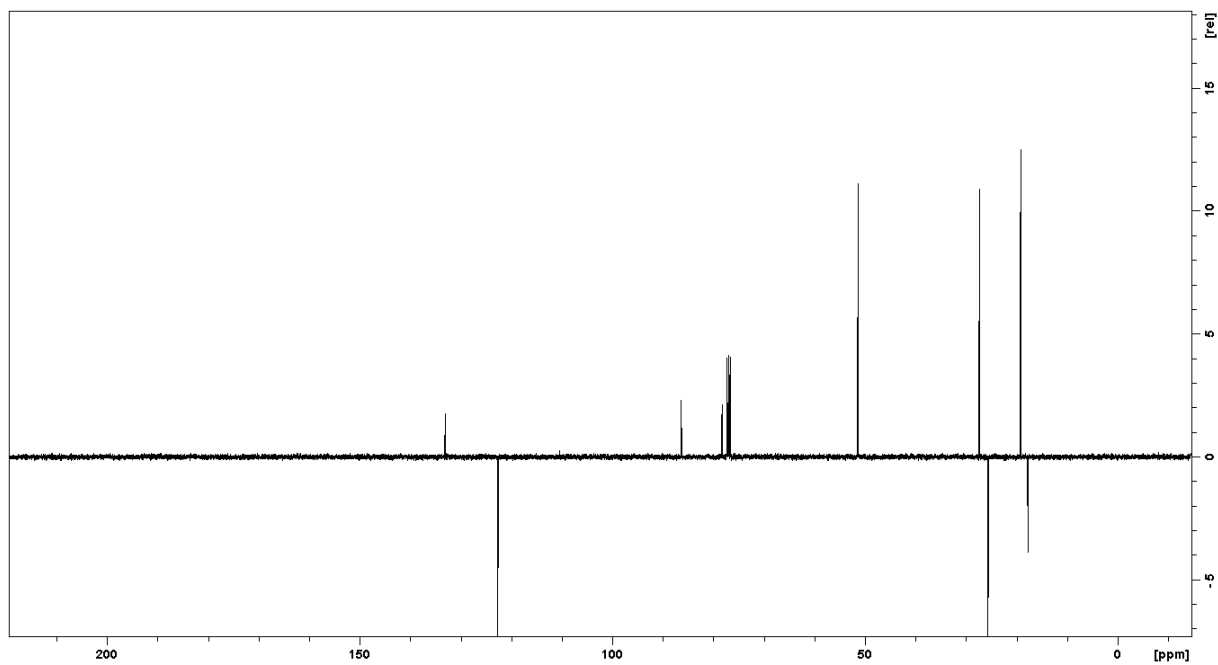
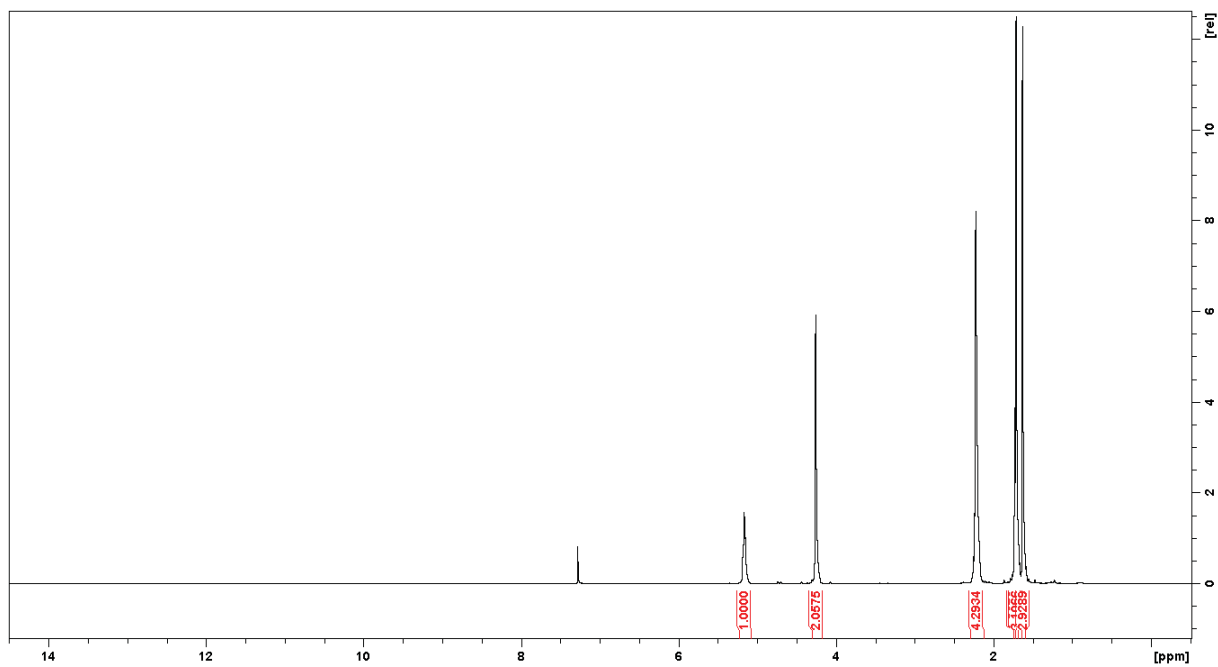
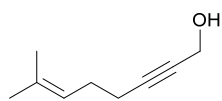
IR spectra of the synthetic compounds

Trisammonium (2*E*)-1-(3-bromo-7-methylocta-2,6-dienyl)diphosphate(**5a**)

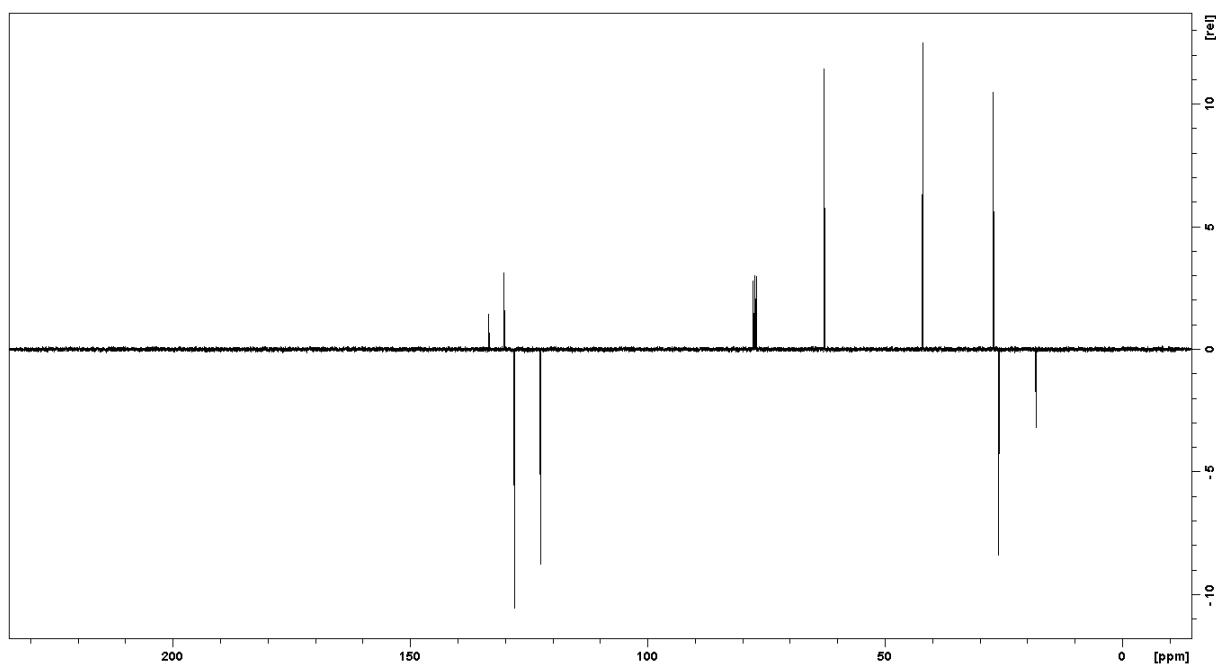
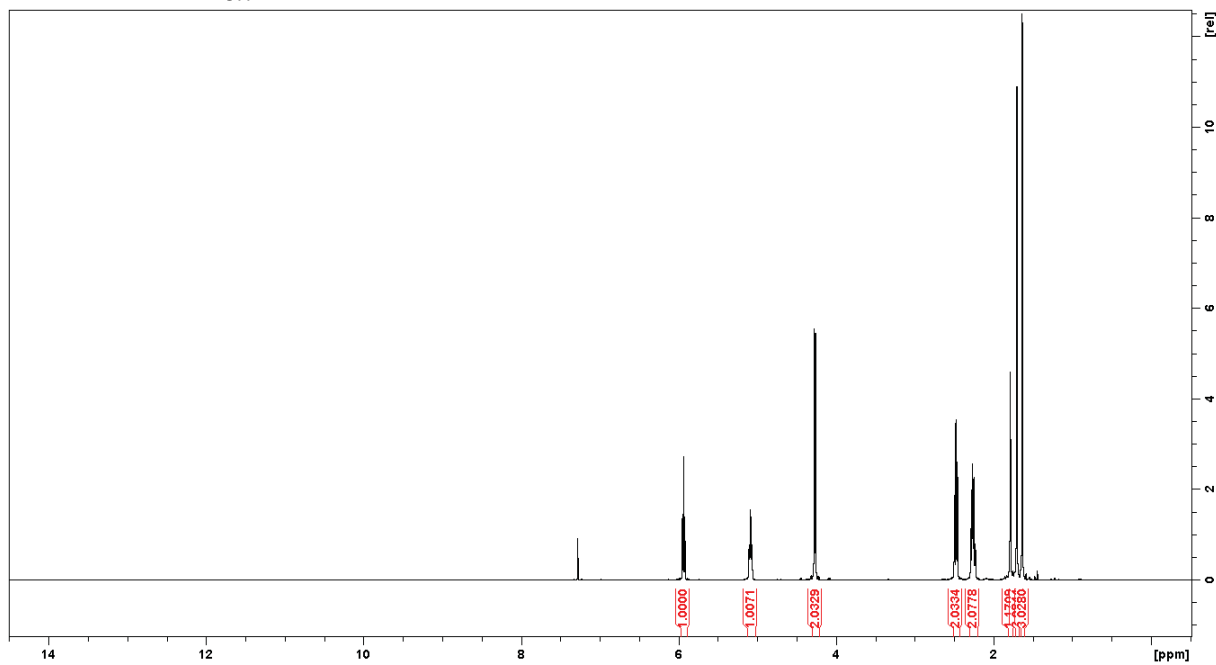
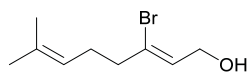
Trisammonium ((2*E*,6*E*)-3-bromo-7,11-dimethyldodeca-2,6,10-trienyl)diphosphate (**5b**)

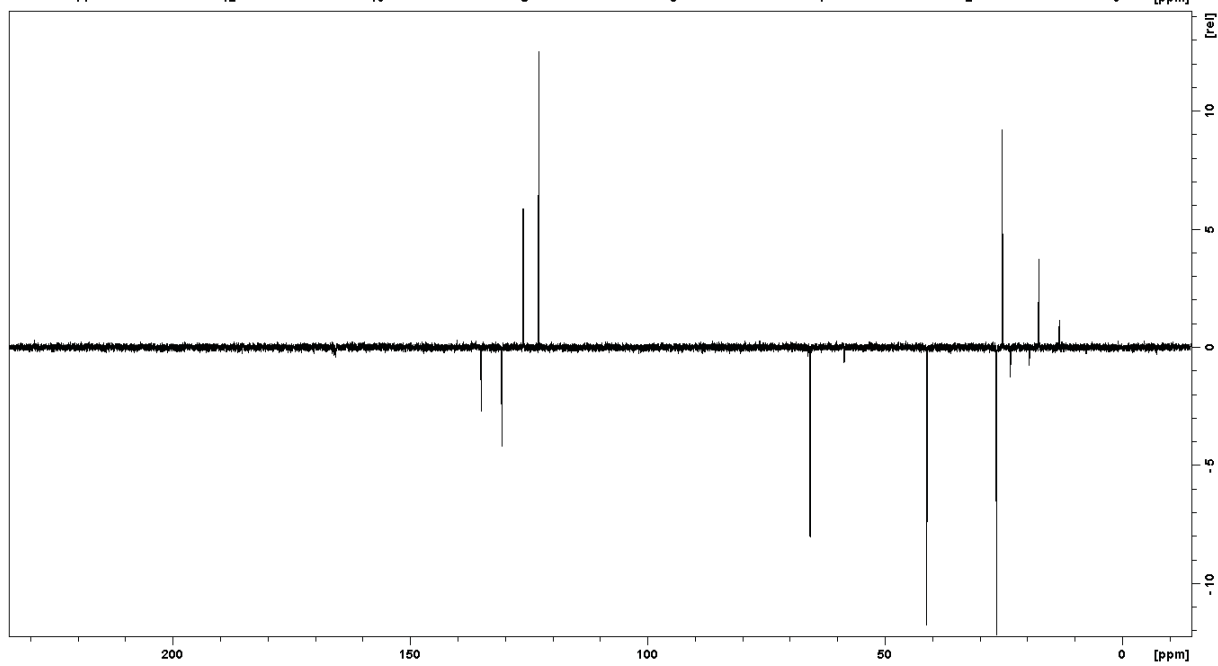
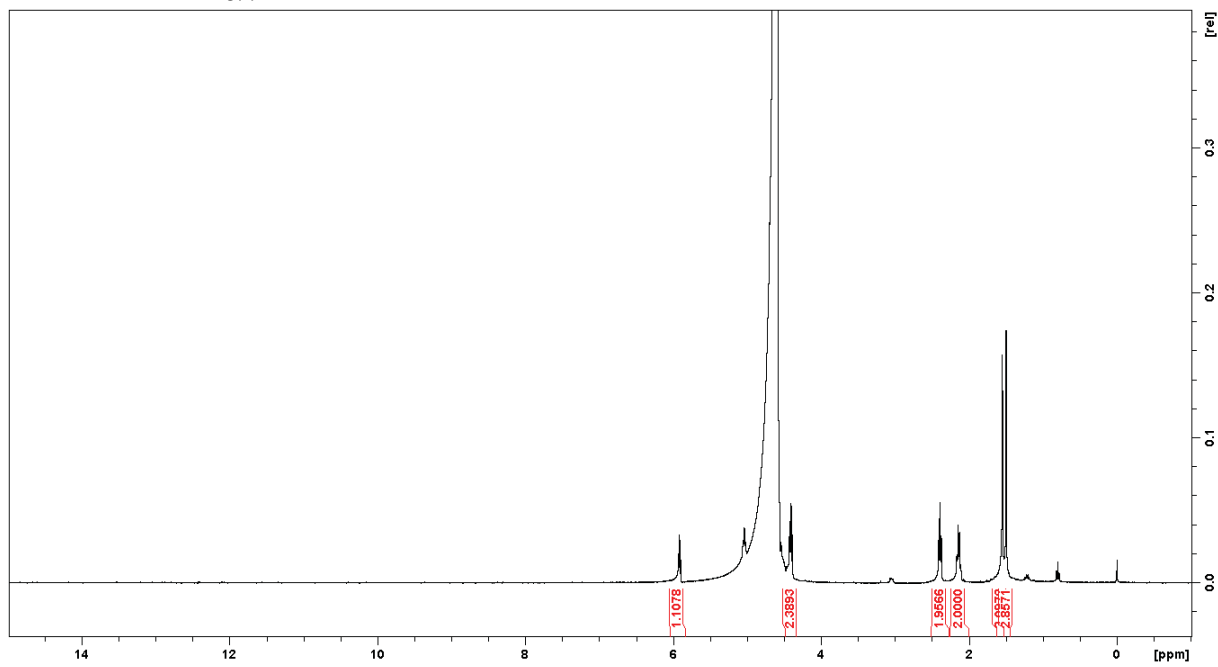
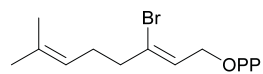
^1H , ^{13}C spectra of the synthetic compounds



7-methyloct-6-en-2-yn-1-ol (**3a**)

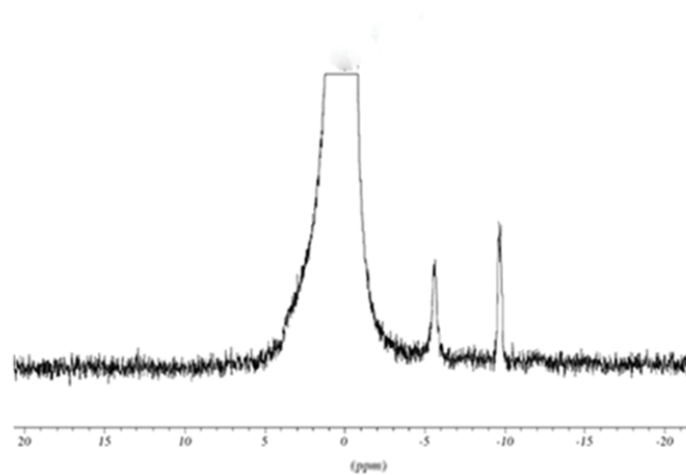
(2E)-3-bromo-7-methylocta-2,6-dien-1-ol (**4a**)



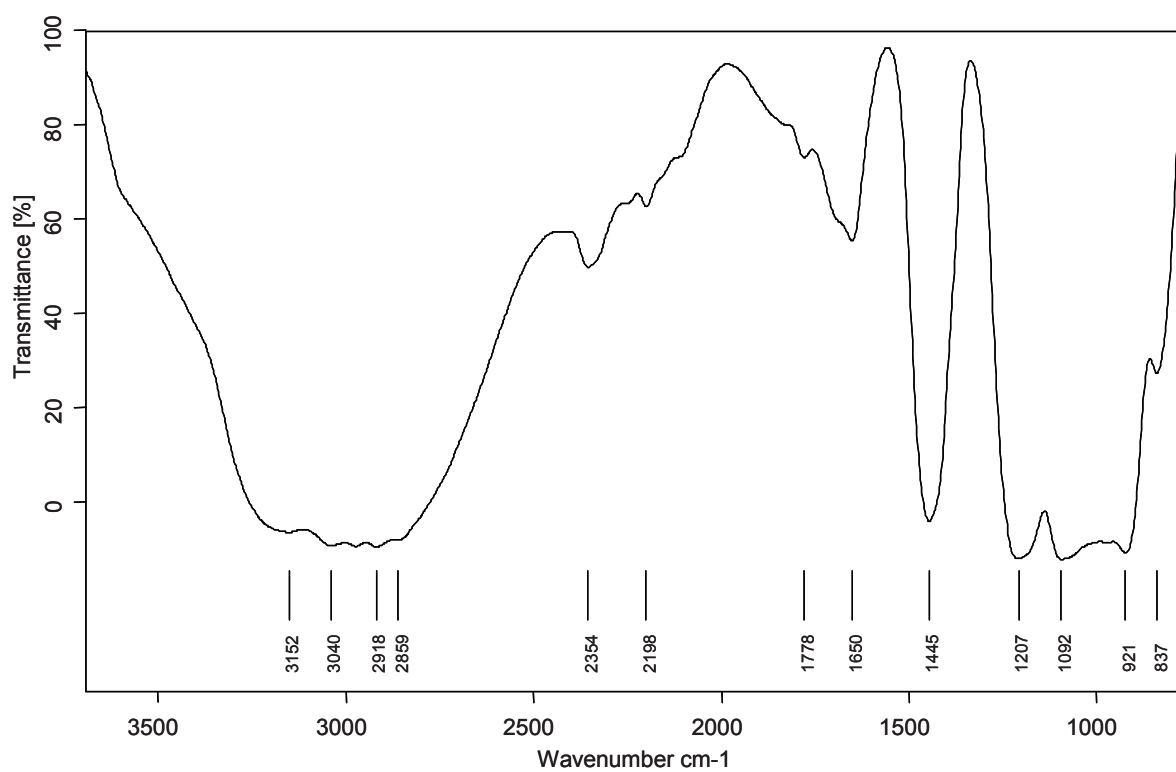
Trisammonium (2*E*)-1-(3-bromo-7-methylocta-2,6-dienyl)diphosphate(**5a**)

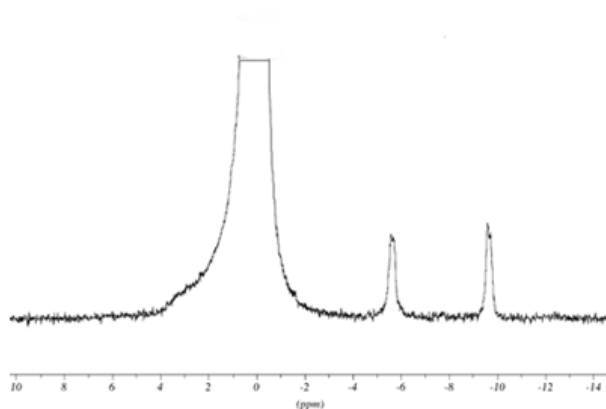
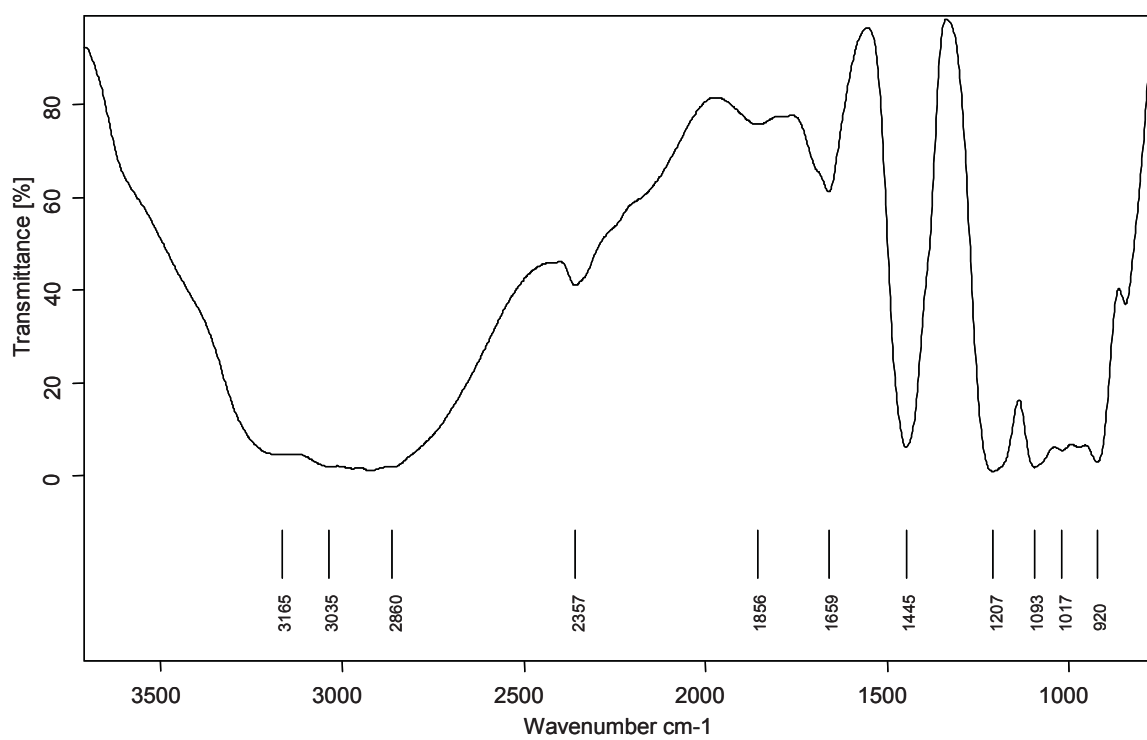
^{31}P NMR and IR spectra spectra of the synthetic compounds

Trisammonium (2*E*)-1-(3-bromo-7-methylocta-2,6-dienyl)diphosphate(**5a**)



Trisammonium (2*E*)-1-(3-bromo-7-methylocta-2,6-dienyl)diphosphate(**5a**)



Trisammonium ((2*E*,6*E*)-3-bromo-7,11-dimethyldodeca-2,6,10-trienyl)diphosphate (**5b**)Trisammonium ((2*E*,6*E*)-3-bromo-7,11-dimethyldodeca-2,6,10-trienyl)diphosphate (**5b**)

11.4 Manuscript IV

Supporting Information

Novel biosynthetic products from multiproduct
terpene synthase from *Medicago truncatula* using non-
natural isomers of prenyl diphosphates

Abith Vattekkatte,¹ Dr. Stefan Garms² and Prof. Dr. Wilhelm Boland³

^aDepartment of Bioorganic Chemistry, Max Planck Institute for Chemical Ecology,
Beutenberg Campus, Hans-Knöll-Strasse 8, D-07745 Jena, Germany

boland@ice.mpg.de

*To whom correspondence should be addressed. Fax: +49(0) 3641 571 202

Table of Contents

General Methods.....	3
Heterologous Expression of Terpene synthases.....	4
Identification of Enzyme Products.....	4
Quantification of Products.....	5
Determination of the Stereochemistry of the Enzyme Products	5
Enzyme Assays for Product Analysis.....	6
Preparative Assays.....	7
MtTPS5 Product Identification	8
Retention Indices	8
Stereochemical Analysis	9
Absolute Configuration.....	10
Mass spectra	12
Substrates.....	16
Synthesis of (2Z,6E)-Farnesyldiphosphate.....	16
Mass spectra	16
(2Z,6E)-Farnesol.....	16
NMR Spectra	17
(2Z,6E)-Farnesol.....	17
(2Z,6E)-Farnesyldiphosphate	18

Experimental Section

General Methods. Reactions were performed under Ar. Solvents were dried according to standard procedures. ^1H , ^{13}C and ^{31}P NMR: Bruker AV 400 spectrometer (Bruker, D-76287 Rheinstetten/Karlsruhe, Germany). Chemical shifts of ^1H , ^{13}C and ^{31}P NMR are given in ppm (δ) based on solvent peaks. CDCl_3 : 7.27 (1H NMR) and 77.4 ppm (^{13}C NMR). $\text{D}_2\text{O}/\text{ND}_4\text{OD}$: 4.79 (^1H NMR); ^{13}C NMR and ^{31}P NMR were referenced to external standard 3-(trimethylsilyl)-propionic acid- d_4 sodium salt (TSP; 3 % in D_2O) and phosphoric acid (H_3PO_4 , 10 % in D_2O), respectively. IR: Bruker Equinox 55 FTIR spectrophotometer. GC-MS: Trace MS, 2000 Series (Thermoquest, D-63329 Egelsbach, Germany) equipped with an Alltech DB5 (15 m \times 0.25 mm, 0.25 μm); helium served as carrier gas. Molecular composition of prepared compounds were determined by ESI-MS using a Micromass Quattro II (Waters, Micromass, Manchester, UK) tandem quadrupole mass spectrometer (geometry quadrupole-hexapole-quadrupole) equipped with an electrospray (ESI) source. High resolution ESI-MS (HR-EI-MS) were recorded at resolution ca 2500. High-resolution MS (EI) data were obtained using a MasSpec 2 instrument (Micromass, UK) in positive ion mode using 70 eV ionization energy. GC-HR-MS: Analyses were performed with a Hewlett Packard HP6890 gas chromatograph interfaced to a MasSpec 2. Separation was achieved on a J & W Scientific DB-5 capillary column, 30 m \times 0.25 mm, 0.25 μm film thickness using helium (30 mL s^{-1}) as carrier gas. Melting point: Büchi B-540 (Büchi Labortechnik AG, CH-9230 Flawil, Switzerland). Chromatography: Silica gel Si 60 (0.200-0.063 mm, E. Merck, Darmstadt, Germany); cellulose microcrystalline Avicel (E. Merck, Darmstadt, Germany).

Heterologous expression of terpene synthases.

Strains of *E. coli* (BL21-CodonPlus(DE3)) harboring the recombinant vectors of MtTPS5¹ carrying an N-terminal His₈-tag were grown to $A_{600} = 0.5$ at 37 °C in LB-medium with kanamycin at 50 $\mu\text{g mL}^{-1}$. After induction with isopropyl β -D-1-thiogalactopyranoside (IPTG, final concentration 1 mM), cultures were shaken overnight at 16 °C and 200 rpm. Cells were harvested by centrifugation for 20 min at 4000 rpm, and the pellet was resuspended in lysis buffer (50 mM NaH₂PO₄, 300 mM NaCl, 10 mM imidazole, pH 8.0) and incubated with lysozyme (1 mg mL⁻¹) for 1 h at 4 °C. Disruption of the cells was achieved by sonication for 2 \times 2 min. The cell debris was removed by centrifugation at 10000g for 30 min. The supernatant was passed over a column of Ni²⁺-NTA-Agarose (QIAGEN, Hilden, Germany), equilibrated with eight bed volumes of lysis buffer. After being washed twice with four bed volumes of washing buffer (50 mM NaH₂PO₄, 300 mM NaCl, 20 mM imidazole, pH 8.0), the protein was eluted with elution buffer (50 mM NaH₂PO₄, 300 mM NaCl, 250 mM imidazole, pH 8.0). The purified protein was desalted into a TRIS-buffer (50 mM TRIS, pH 7.5, 10 mM NaCl, 10% glycerol) by passing through a NAP 25 column (Amersham Biosciences, Uppsala, Sweden), diluted to reach a concentration of 1 mg mL⁻¹ and stored at -20 °C. Protein quantification was performed by using a method of Bradford et al.²

Identification of Enzyme Products

GC-MS analysis was performed on an instrument equipped with a ZB-5 capillary column (0.25 mm i.d. \times 15 m with 0.25 μm film). One microliter of the sample was injected in splitless mode at an injection port temperature of 220 °C. The oven temperature was kept at 50 °C for 2 min followed by a ramp of 10 °C min⁻¹ to 240 °C followed by an additional ramp of 30 °C min⁻¹ to 280 °C and finally kept for 2 min. Helium at a flow rate of 1.5 mL min⁻¹ served as carrier gas. Ionization potential was set to 70 eV, and scanning was performed from 40 to 250 amu. Compounds were identified by comparing their mass spectra

and Kováts indices (retention indices) with those of published reference spectra in MassFinders' (software version 3.5) and Adams' terpene library and in the NIST database. In addition, retention indices (RI) of sesquiterpene peaks derived by calibrating GC runs with a C8–C20 alkane standard were compared with RI values of authentic reference compounds. Essential oils with known composition containing relevant sesquiterpenoids were purchased from a commercial supplier or were generously provided by Stefan von Reuss.

Quantification of products

For quantification of enzyme products, the compounds were first separated by gas chromatography (H_2 carrier gas 1.5 mL min^{-1} , injection volume $2 \mu\text{L}$) under the conditions described above and subsequently analyzed on a flame ionization detector (FID) (250°C). Correction of the different response factors of sesquiterpene hydrocarbons and alcohols was achieved using calibration curves obtained from samples with different concentrations of (*E*)- β -caryophyllene and torreyol. The average and standard deviations of relative ratios were determined by at least four independent samples setting the sum of identified compounds to 100%.

Determination of the Stereochemistry of the Enzyme Products

The enantiomers of the enzymatic products were separated and identified by GC–MS using a heptakis(2,3-di-*O*-methyl-*O*-*tert*-butyldimethylsilyl)- β -cyclodextrin column (50% in OV1701, w/w) (FS-Hydrodex β -6TBDM) ($0.25 \text{ mm i.d.} \times 25 \text{ m} \times 0.25 \mu\text{m film}$) operated with helium at 1 mL min^{-1} as carrier gas, a splitless injection of $1 \mu\text{L}$ sample at 220°C and a temperature program starting from 60°C kept for 5 min, followed by a ramp of 2°C min^{-1} (for α -copaene (**8**) 1°C min^{-1}) to 160°C followed by an additional ramp of $30^\circ\text{C min}^{-1}$ to 220°C with 2 min hold. The separation of torreyol enantiomers was achieved by using a heptakis(2,3,6-tri-*O*-methyl)- β -cyclodextrin column (50% in OV1701, w/w) (FS-

Hydrodex β -PM) (0.25 mm i.d. \times 25 m \times 0.25 μ m film). Helium was used as carrier gas at a constant flow rate of 1 mL min⁻¹, and samples (1 μ L) were injected at 220 °C. The GC was programmed with an initial oven temperature of 110 °C (15-min hold), which was then increased 2 °C min⁻¹ up to 160 °C followed by a 30 °C min⁻¹ ramp until 220 °C (2-min hold).

Enzyme Assays for Product Analysis

Standard assays contained 600 nM purified protein in assay buffer (25 mM HEPES, pH 7.5, 10% glycerol, 10 mM MgCl₂, 1 mM DTT) with 50 μ M substrate (FDP, (1*S*)-[1-²H]-FDP, (1*R*)-[1-²H]-FDP, or [1,1-²H₂]-FDP) in a final volume of 1 mL. Deuterated FDPs were synthesized as previously described.³ The reaction mixture was covered with 100 μ L of pentane containing 1 ng μ L⁻¹ of dodecane as an internal standard to trap the reaction products. After being incubated for 90 min at 30 °C, the reaction was stopped by vortexing for 20 s. The whole mixture was frozen in liquid nitrogen, and the pentane layer was removed after thawing and analyzed by GC–MS as described above.

To analyze the protonation reaction, 50 μ L of the purified enzyme (1 mg mL⁻¹) was lyophilized and redissolved in 50 μ L of D₂O and incubated for 30 min on ice to ensure proper H–D exchange of the enzyme. An aliquot of 20 μ L of the protein sample was analyzed in assay buffer prepared with D₂O (>99% d₁) containing 50 μ M FDP. The assays were incubated for 1 h at 30 °C. The reaction products were collected by a solid-phase microextraction fiber (SPME) consisting of 100 μ m polydimethylsiloxane and analyzed by GC–MS. The labeling degree of each product was calculated from the intensities of the respective [M]⁺, [M + 1]⁺ for hydrocarbons and [M – H₂O]⁺, [M – H₂O + 1]⁺ for alcohols after correcting for the abundance of their ¹³C satellite peaks.

Preparative Assays

For identifying and determining the stereochemistry of copan-3-ol (**25**) and cubebol (**21**), two 10-mL assays containing 600 nM purified enzyme in assay buffer with 50 μ M FDP were covered with 10 mL of pentane. After being incubated overnight at 30 °C, the mixture was extracted three times with 5 mL of pentane. The combined organic phases were passed through a Pasteur pipet containing Na_2SO_4 , and the volume was reduced to \sim 100 μ L. Alcohols were separated on silica (1 g, Pasteur pipet) using pentane/ether (6:1, v/v) for elution. Two fractions highly enriched in the desired compounds were obtained, besides fractions containing both compounds.

MtTPS5 Product Identification

Retention indices

Tabelle A-1. Retention indices of enzyme products, which were formed in the presence of various substrates of MtTPS5 compared with authentic references. The origin of the reference substances is also indicated.

Enzyme product	Retentionsindex		
	WT	Reference	Source of Reference
(2Z,6E)-Produkte			
α -Ylangen (15)	1371	1370	Givaudan
α -Himachalene (16)	1447	1448	SU
Isobicyclgermacrene (17)	1476	---	n. r.
α -Amorphene (18)	1479	1480	SU
γ -Humulen (19)	1486	1485	Fluka
γ -Himachalen (20)	1487	1487	Givaudan
β -Himachalen (21)	1500	1500	SU
δ -Amorphen (23)	1507	1507	(b) ⁴
C ₁₅ H ₂₆ O - II (22)	1515	---	n. r.
C ₁₅ H ₂₆ O - III (24)	1571	---	n. r.
Humulan-6,9-dien-3-ol (25)	1576	---	n. r.
C ₁₅ H ₂₆ O - IV (26)	1632	---	n. r.
2-Himachalen-7-ol (27)	1648	1646	Givaudan

SU: *Scapania undulata*⁵ (Stefan von Reuß, Universität Hamburg); **(a):** Stefan von Reuß (Universität Hamburg); **(b):** acid-catalyzed rearrangement of Germacren D (**34**); **n. r.:** no reference available

Stereochemical Analysis

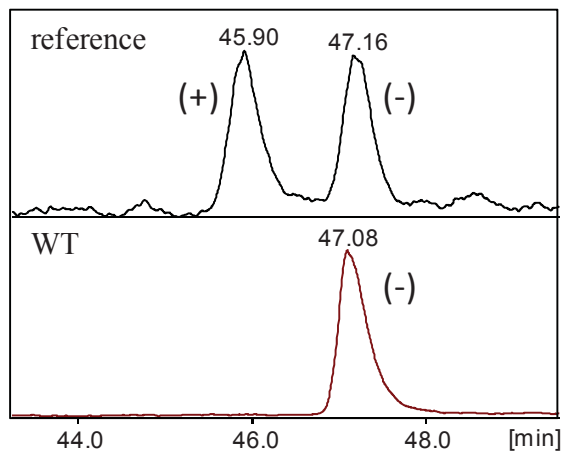
Tabelle A-2. Gas chromatographic separation factors (α -values) and resolution (R-values), origin of the references, and the elution and the separation conditions of the determination of the absolute configuration of MtTPS1- and MtTPS5 products.

Enzyme product	α -value	R-value	Origin of Reference	Elution, separation conditions
(2Z,6E)-Produkte				
(+)- α -Ylangen (15)	1,0103	2,058	EZ + (-)- 15 ^a	⁶ , (e)
(-)- α -Himachalen (16)	1,0266	5,939	SU + (-)- 16 ^b	(d), (e)
(-)- α -Amorphen (18)	1,0365	9,996	EZ + (-)- 18 ^b	⁶ , (e)
(-)- γ -Himachalen (20)	1,0169	3,998	SU + (-)- 20 ^b	(d), (e)
(+)- δ -Amorphen (23)	1,0205	5,509	(\pm)- 34 rearrangement ⁴	⁶ , (e)

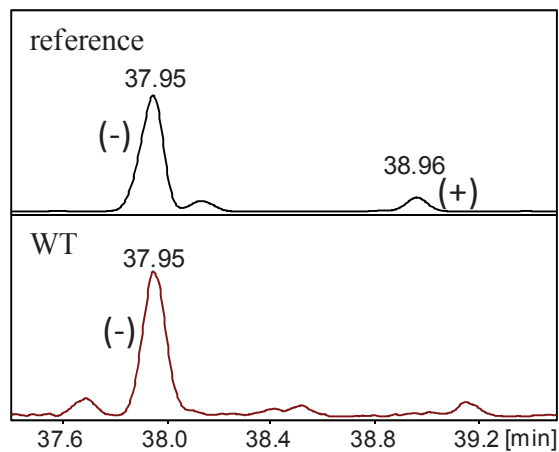
PQ: *Preissia quadrata* Pentane extract; **MA:** *Meum athamanticum*; **SU:** *Scarpania undulata*⁵; **EE:** MtTPS5 incubated with (2E,6E)-FDP (Pentane extract); **EZ:** MtTPS5 incubated with (2Z,6E)-FDP (Pentaneextrakt); **(a):** Stefan von Reuß (Universität Hamburg); **(b):** *Preissia quadrata* contains (+)-Isomer; **(c):** *Cortinarius odorifer* Britz contains (+)-**73**; **(d)** *Scapania undulata* contains (+)-Enantiomer;⁷ **(e):** Method I; **(f):** Method II; **(g):** Methode III (Methods: see experimental section). ^aStefan von Reuß (Universität Hamburg), ^bGivaudan SA, Schweiz

Illustration A-1. Identification of the absolute configuration of the products of with MtTPS5 with (2Z,6E)-FDP were obtained. Reference: Reference includes both enantiomers.

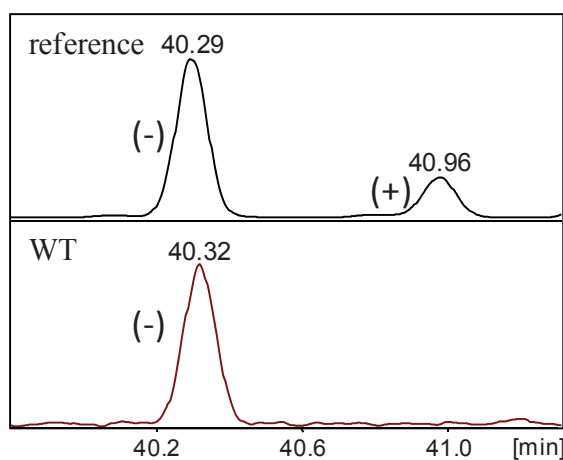
α -Ylangen (**15**)



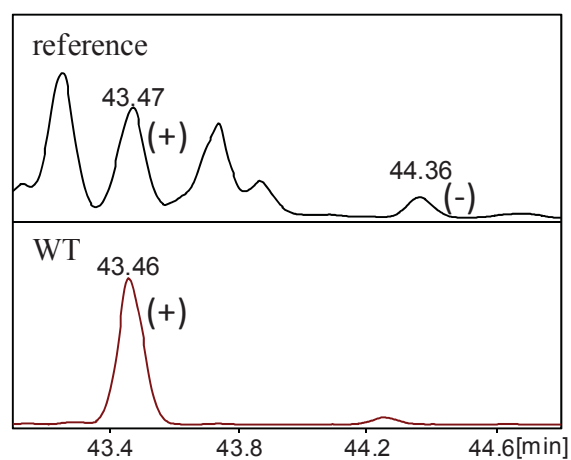
α -Himachalen (**16**)

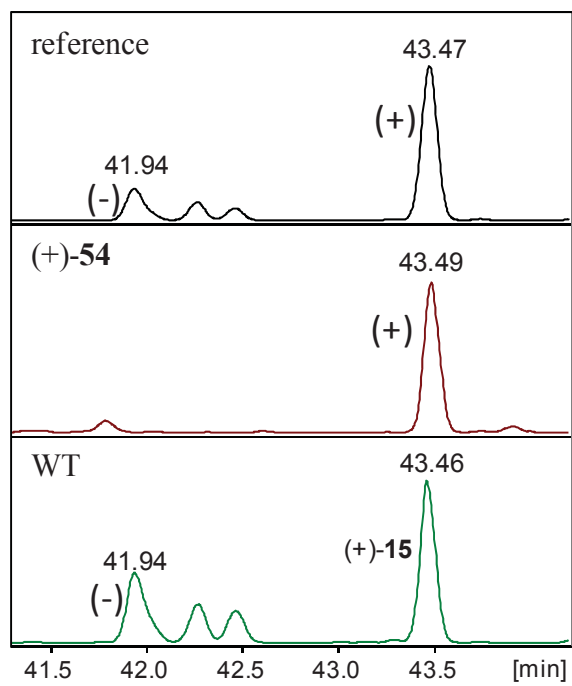


γ -Himachalen (**20**)



α -Amorphen (**18**)

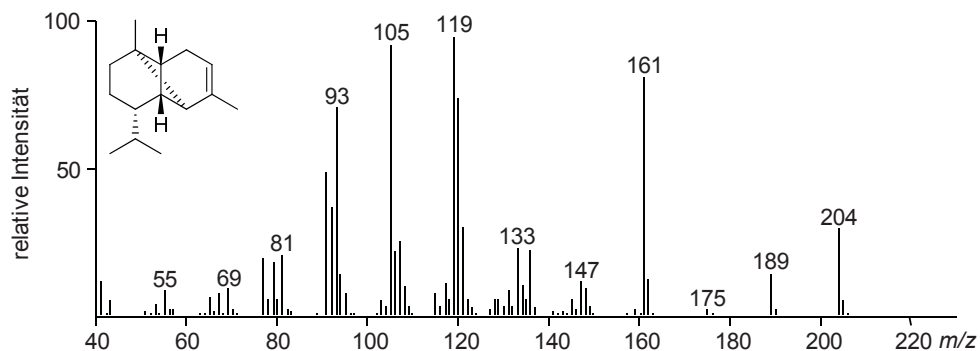


δ -Amorphen (23)

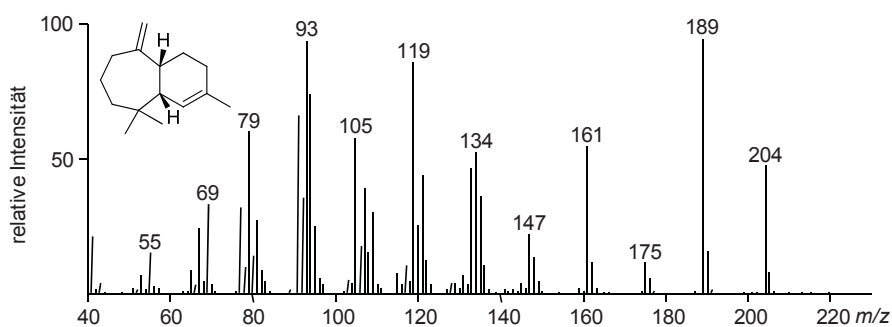
Mass spectra

Illustration A-2. The mass spectra of the products of enzyme MtTPS5 after incubation with various FDP and NDP substrates. The compounds are ordered by increasing retention index.

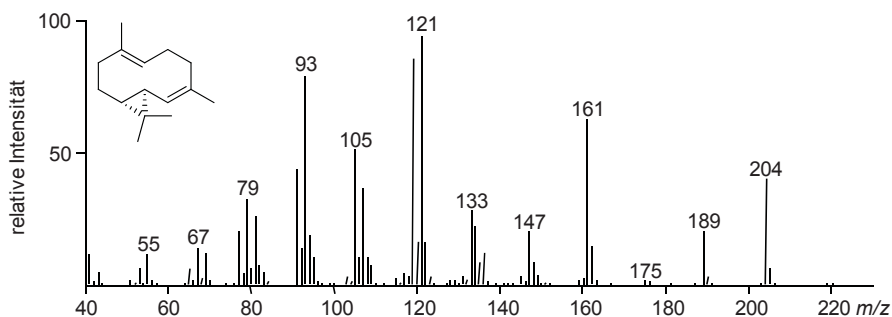
α -Ylangen (**15**) (RI = 1371)



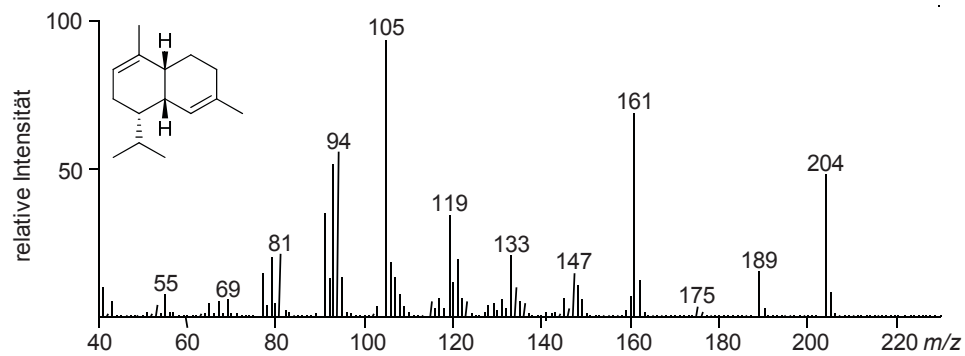
α -Himachalen (**16**) (RI = 1447)



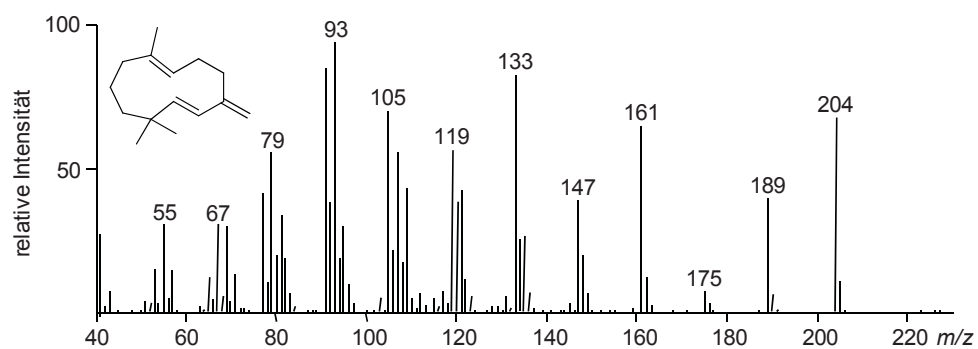
Isobicyclogermacren (**17**) (RI = 1476)



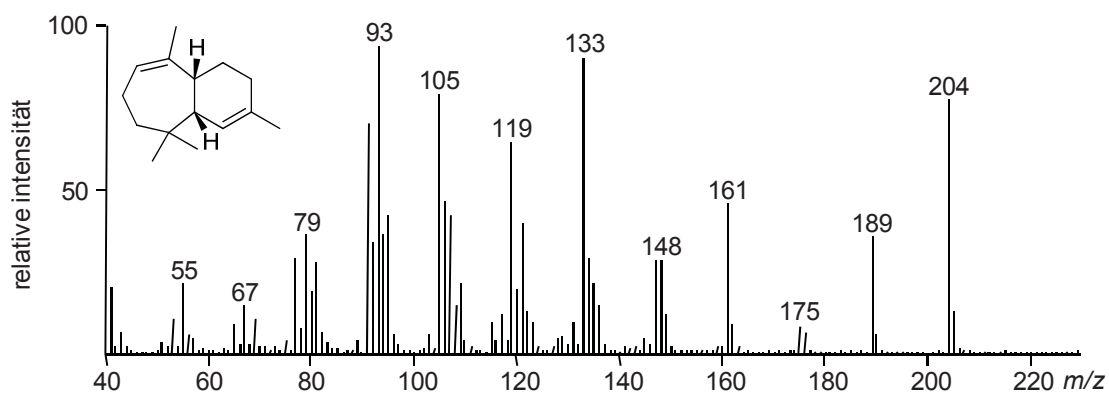
α -Amorphen (**18**) (RI = 1479)

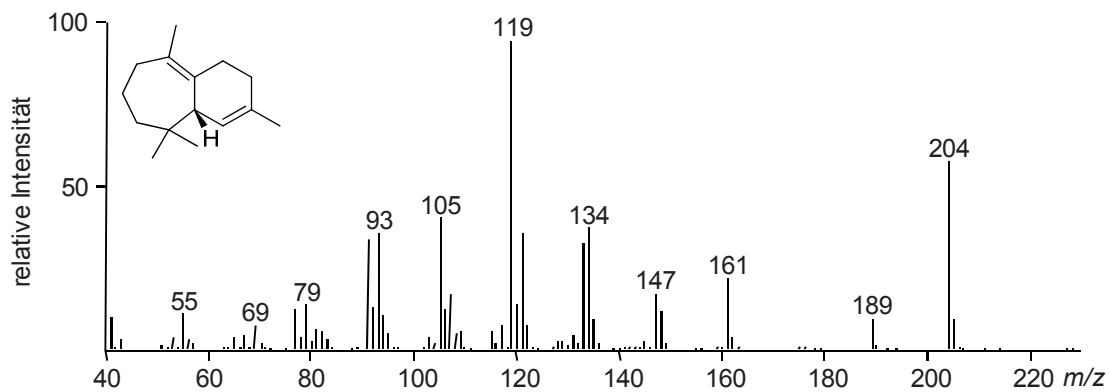
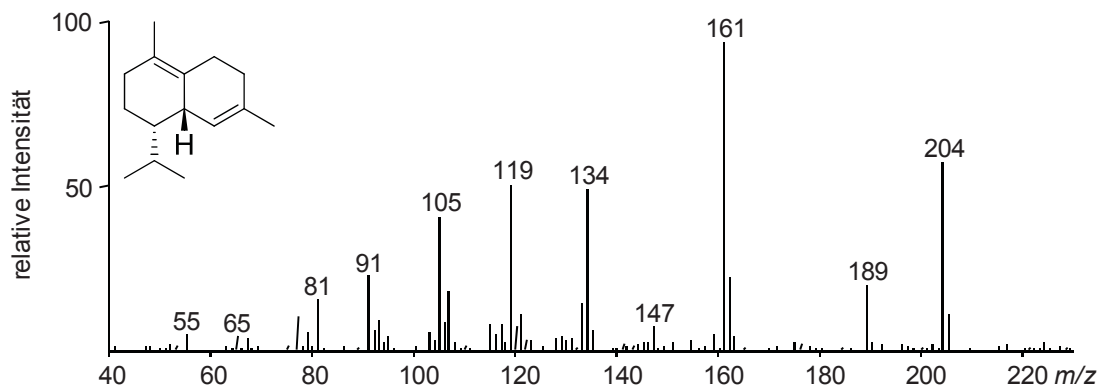
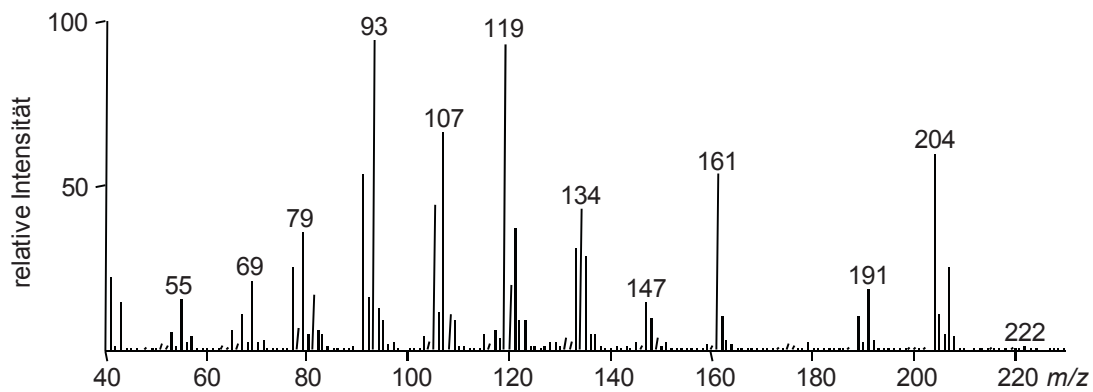


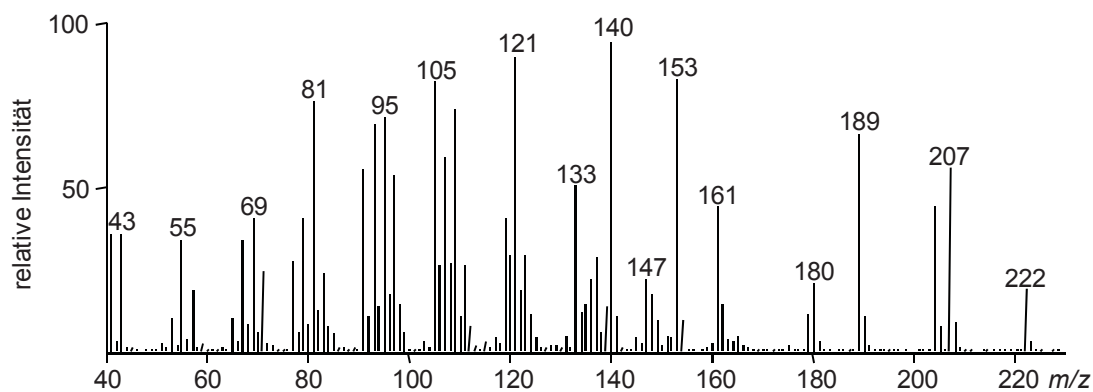
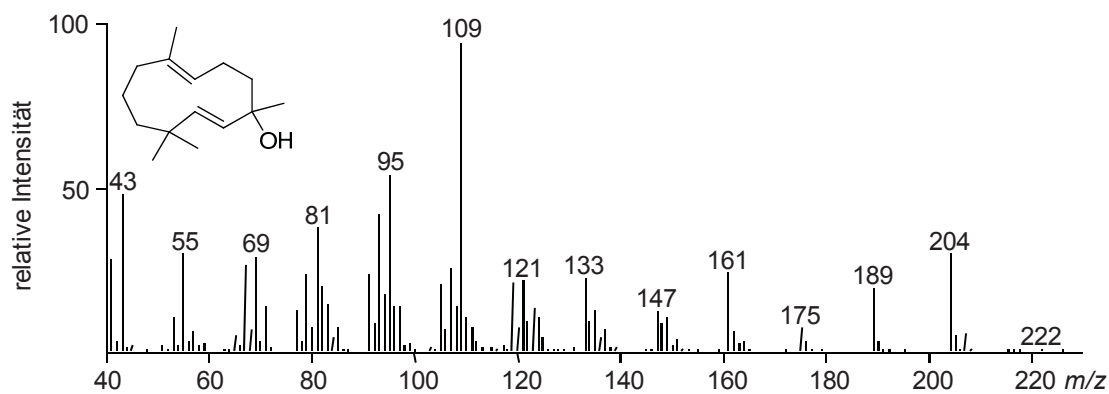
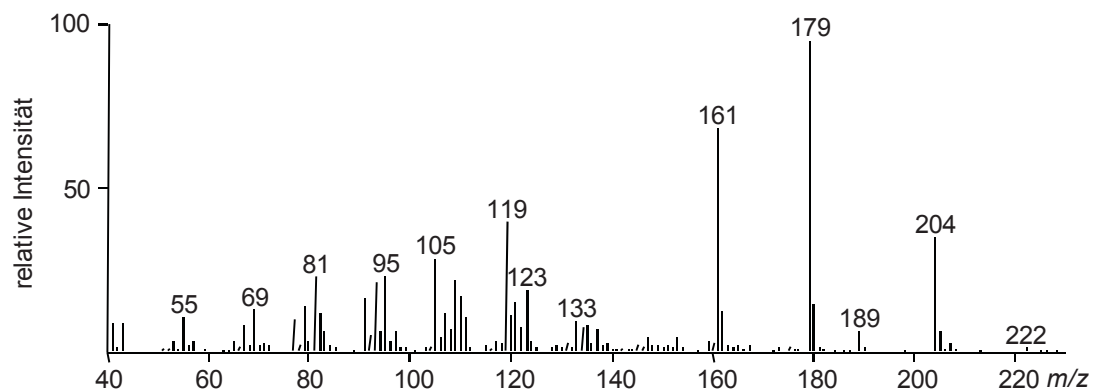
γ -Humulen (**19**) (RI = 1486)



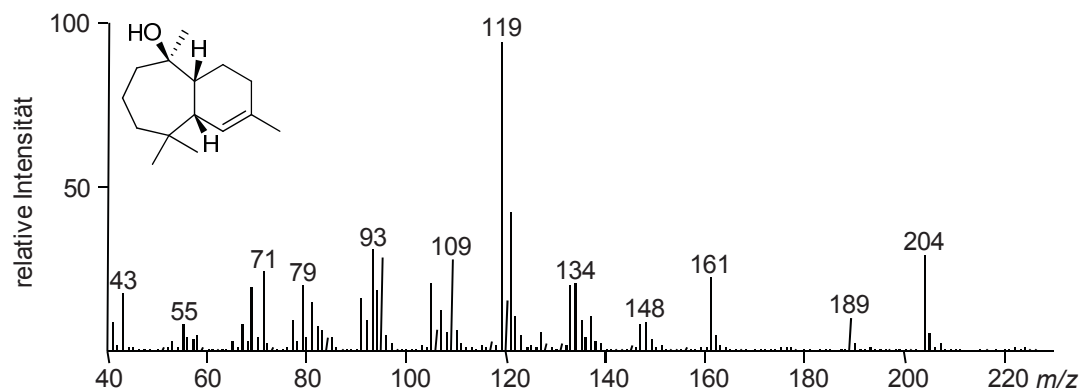
γ -Himachalen (**20**) (RI = 1486)



β -Himachalen (**21**) (RI = 1500) δ -Amorphen (**23**) (RI = 1507) $C_{15}H_{26}O$ - II (**22**) (RI = 1515)

$C_{15}H_{26}O$ - III (**24**) (RI = 1571)Humulan-6,9-dien-3-ol (**25**) (RI = 1576) $C_{15}H_{26}O$ - IV (**26**) (RI = 1632)

2-Himachalen-7-ol (**27**) (RI = 1648)



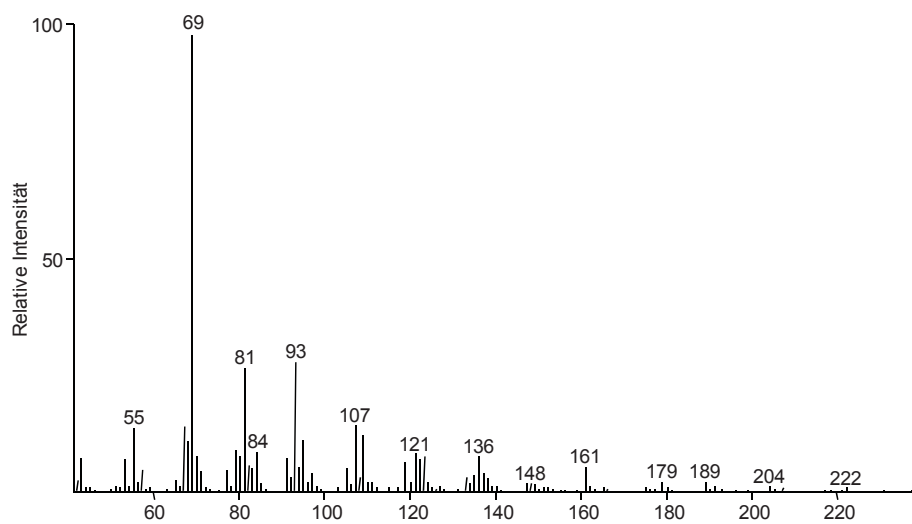
Substrates

Synthesis of (2Z,6E)-Farnesyl diphosphate

(2Z,6E)-FPP was synthesized from (2E,6E)-farnesol as described by Shao et al.⁸

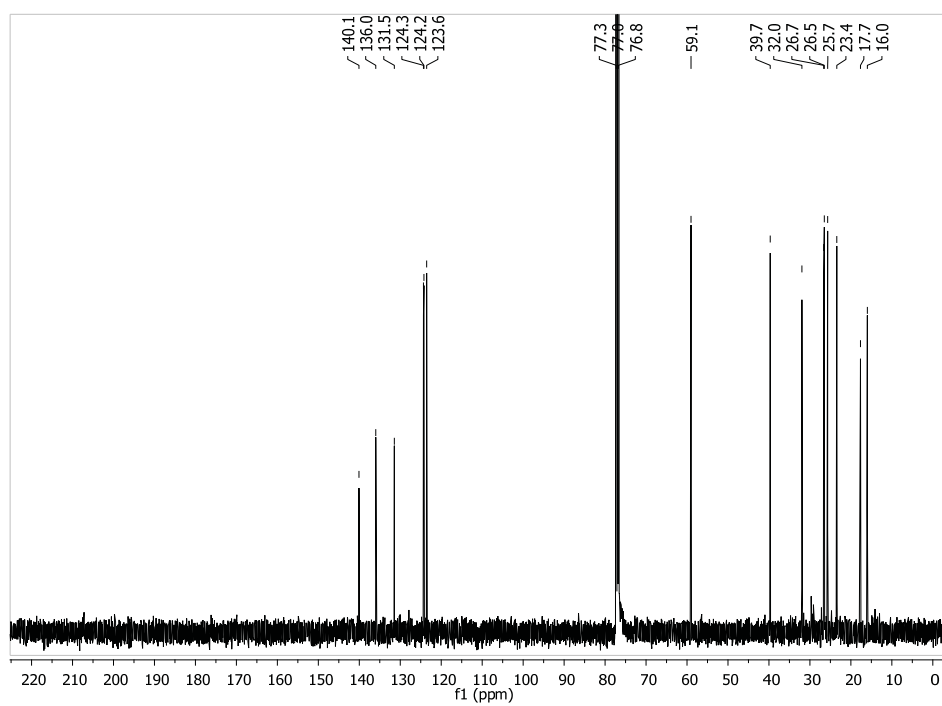
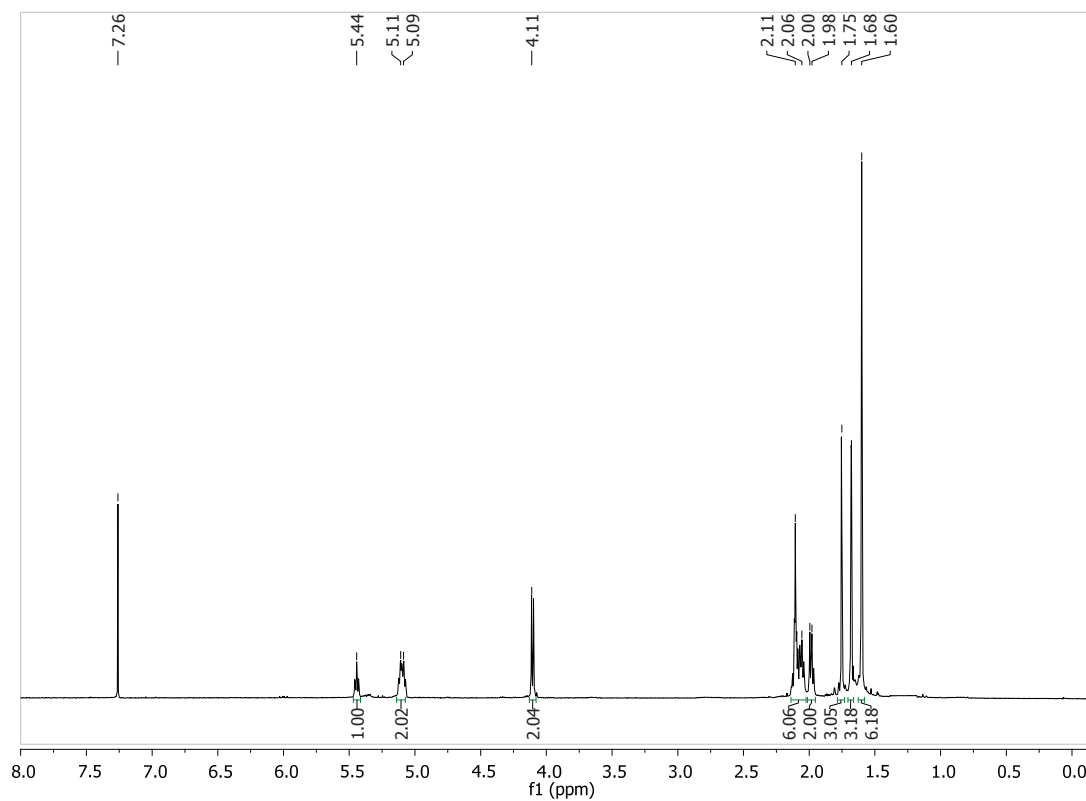
Mass spectra

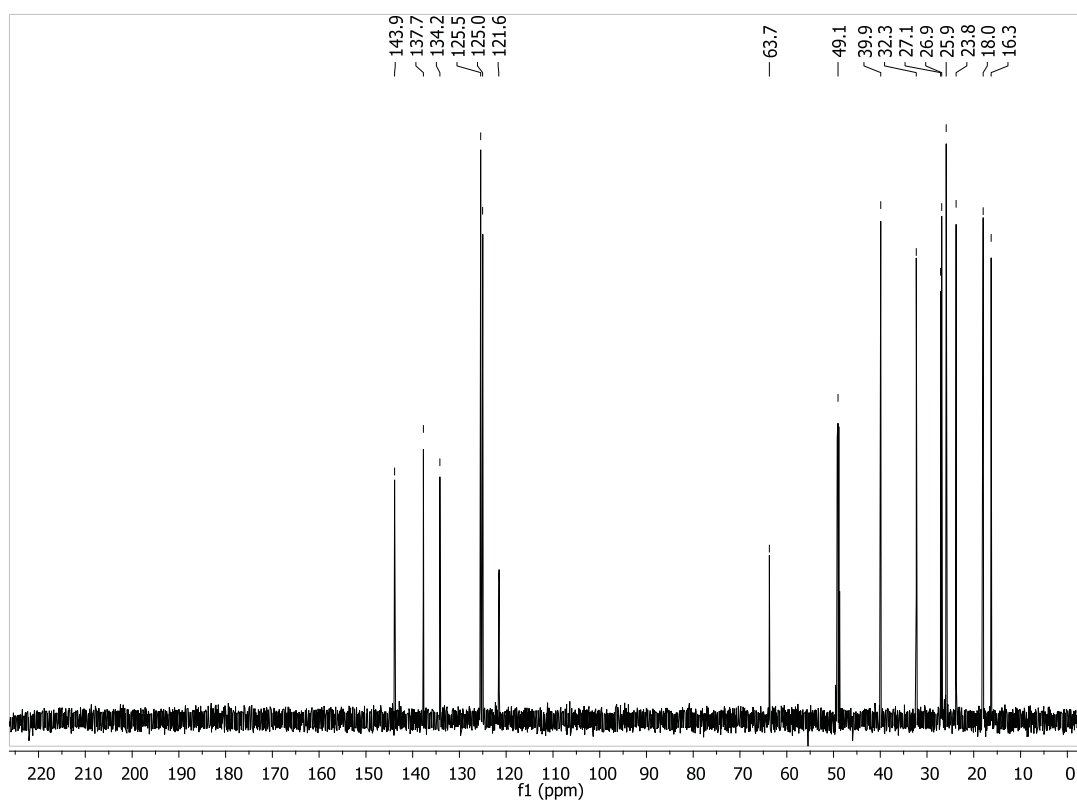
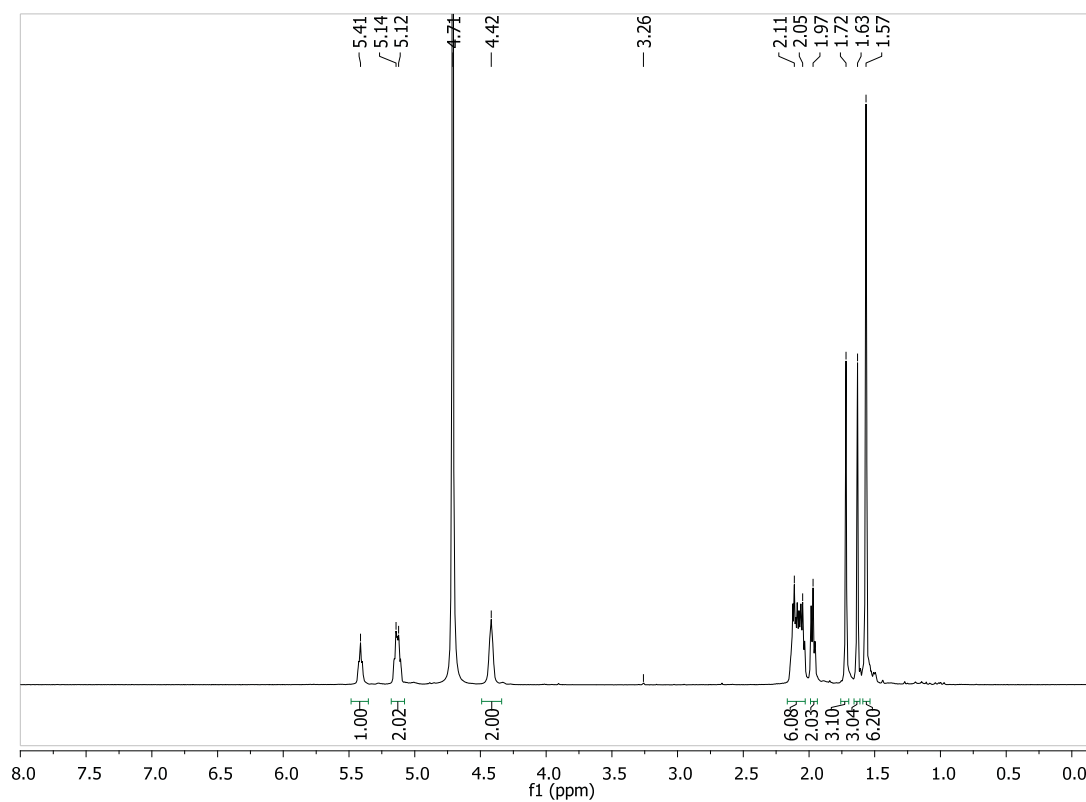
(2Z,6E)-Farnesol



NMR Spectra

(2Z,6E)-Farnesol



(2Z,6E)-Farnesylidiphosphate

- 1 G. I. Arimura, S. Garms, M. Maffei, S. Bossi, B. Schulze, M. Leitner, A. Mithöfer and W. Boland, *Planta*, 2008, **227**, 453.
- 2 M. M. Bradford, *Anal. Biochem.*, 1976, **72**, 248.
- 3(a) N. Gatto, A. Vattekkatte, T. Kollner, J. Degenhardt, J. Gershenzon and W. Boland, *Chem Commun (Camb)*, 2015, **51**, 3797; (b) A. Vattekkatte, N. Gatto, T. G. Kollner, J. Degenhardt, J. Gershenzon and W. Boland, *Organic & Biomolecular Chemistry*, 2015.
- 4 N. Bülow and W. A. König, *Phytochemistry*, 2000, **55**, 141.
- 5 A. M. Adio, C. Paul, P. Kloth and W. A. König, *Phytochemistry*, 2004, **65**, 199.
- 6 W. A. König, N. Bülow and Y. Saritas, *Flavour and Fragrance Journal*, 1999, **14**, 367.
- 7 N. H. Andersen, P. Bissonette, C. B. Liu, B. Shunk, Y. Ohta, C.-L. W. Tseng, A. Moore and S. Huneck, *Phytochemistry*, 1977, **16**, 1731.
- 8 Y. Shao, J. T. Eummer and R. A. Gibbs, *Organic Letters*, 1999, **1**, 627.

12 Citations

- 1 Connolly, J. D. & Hill, R. A. *Dictionary of Terpenoids* (Chapman & Hall, New York, 1992).
- 2 Sacchettini, J. C. & Poulter, C. D. Creating isoprenoid diversity. *Science*, 277, 1788-1789, (1997).
- 3 Yamada, Y., Kuzuyama, T., Komatsu, M., Shin-Ya, K., Omura, S., Cane, D. E. & Ikeda, H. Terpene synthases are widely distributed in bacteria. *Proceedings of the National Academy of Sciences of the United States of America*, 112, 857-862, (2015).
- 4 Christianson, D. W. Roots of biosynthetic diversity. *Science*, 316, 60-61, (2007).
- 5 Thulasiram, H. V., Erickson, H. K. & Poulter, C. D. Chimeras of two isoprenoid synthases catalyze all four coupling reactions in isoprenoid biosynthesis. *Science*, 316, 73-76, (2007).
- 6 Gershenzon, J. & Dudareva, N. The function of terpene natural products in the natural world. *Nature Chemical Biology*, 3, 408-414, (2007).
- 7 Roberts, S. C. Production and engineering of terpenoids in plant cell culture. *Nature Chemical Biology*, 3, 387-395, (2007).
- 8 Fraga, B. M. Natural sesquiterpenoids. *Natural Product Reports*, 28, 1580-1610, (2011).
- 9 Fraga, B. M. Natural sesquiterpenoids. *Natural Product Reports*, 26, 1125-1155, (2009).
- 10 Fraga, B. M. Natural sesquiterpenoids. *Natural Product Reports*, 17, 483-504, (2000).
- 11 Sato, T., Yamaga, H., Kashima, S., Murata, Y., Shinada, T., Nakano, C. & Hoshino, T. Identification of novel sesterterpene/triterpene synthase from *Bacillus clausii*. *ChemBioChem*, 14, 822-825, (2013).
- 12 Langenheim, J. H. Higher plant terpenoids: A phyto-centric overview of their ecological roles. *Journal of Chemical Ecology*, 20, 1223-1280, (1994).
- 13 Nambara, E. & Marion-Poll, A. Abscisic acid biosynthesis and catabolism. *Annual Review of Plant Biology*, 56, 165-185, (2005).
- 14 Pichersky, E. & Gershenzon, J. The formation and function of plant volatiles: Perfumes for pollinator attraction and defense. *Current Opinion in Plant Biology*, 5, 237-243, (2002).
- 15 Hilker, M., Kobs, C., Varama, M. & Schrank, K. Insect egg deposition induces *Pinus sylvestris* to attract egg parasitoids. *Journal of Experimental Biology*, 205, 455-461, (2002).
- 16 Zwenger, S. & Basu, C. Plant terpenoids: Applications and future potentials. *Biotechnology and Molecular Biology Reviews*, 3, 1-7, (2008).
- 17 Pichersky, E., Noel, J. P. & Dudareva, N. Biosynthesis of plant volatiles: Nature's diversity and ingenuity. *Science*, 311, 808-811, (2006).
- 18 Stipanovic, R., Bell, A. & Benedict, C. in *Biologically active natural products: Agrochemicals* (eds Horace G. Cutler & Stephen J. Cutler) 211-220 (CRC Press, 1999).
- 19 Unsicker, S. B., Kunert, G. & Gershenzon, J. Protective perfumes: The role of vegetative volatiles in plant defense against herbivores. *Current Opinion in Plant Biology*, 12, 479-485, (2009).
- 20 Schnee, C., Köllner, T. G., Held, M., Turlings, T. C. J., Gershenzon, J. & Degenhardt, J. The products of a single maize sesquiterpene synthase form a volatile defense signal that attracts natural enemies of maize herbivores. *Proceedings of the National Academy of Sciences of the United States of America*, 103, 1129-1134, (2006).
- 21 Dudareva, N., Negre, F., Nagegowda, D. A. & Orlova, I. Plant volatiles: Recent advances and future perspectives. *Critical Reviews in Plant Sciences*, 25, 417-440, (2006).
- 22 Wu, S. Q. Metabolic engineering of natural products in plants; tools of the trade and challenges for the future. *Current Opinion in Biotechnology*, 19, 145-152, (2008).
- 23 Gerber, N. N. & Lechevalier, H. A. Geosmin, an earthy-smelling substance isolated from actinomycetes. *Applied Microbiology*, 13, 935-938, (1965).
- 24 Ruzicka, L. The isoprene rule and the biogenesis of terpenic compounds. *Experientia*, 9, 357-367, (1953).
- 25 Lynen, F., Eggerer, H., Henning, U. & Kessel, I. Farnesyl-pyrophosphat und 3-methyl- δ^3 -butenyl-1-pyrophosphat, die biologischen vorstufen des squalens. Zur biosynthese der terpene, iii. *Angewandte Chemie*, 70, 738-742, (1958).
- 26 Chaykin, S., Law, J., Phillips, A. H., Tchen, T. T. & Bloch, K. Phosphorylated intermediates in the synthesis of squalene. *Proceedings of the National Academy of Sciences of the United States of America*, 44, 998-1004, (1958).
- 27 Tavormina, P. A. & Gibbs, M. H. The metabolism of β,γ -dihydroxy- β -methylvaleric acid by liver homogenates. *Journal of the American Chemical Society*, 78, 6210-6210, (1956).
- 28 Rohmer, M., Seemann, M., Horbach, S., Bringermeier, S. & Sahn, H. Glyceraldehyde 3-phosphate and pyruvate as precursors of isoprenic units in an alternative non-mevalonate pathway for terpenoid biosynthesis. *Journal of the American Chemical Society*, 118, 2564-2566, (1996).
- 29 Arigoni, D., Sagner, S., Latzel, C., Eisenreich, W., Bacher, A. & Zenk, M. H. Terpenoid biosynthesis from 1-deoxy-d-xylulose in higher plants by intramolecular skeletal rearrangement. *Proceedings of the National Academy of Sciences of the United States of America*, 94, 10600-10605, (1997).

- 30 Dudareva, N., Klempien, A., Muhlemann, J. K. & Kaplan, I. Biosynthesis, function and metabolic engineering of plant volatile organic compounds. *New Phytologist*, 198, 16-32, (2013).
- 31 Aharoni, A., Jongsma, M. A. & Bouwmeester, H. J. Volatile science? Metabolic engineering of terpenoids in plants. *Trends in Plant Science*, 10, 594-602, (2005).
- 32 Breitmaier, E. *Terpenes: Flavors, fragrances, pharmaca, pheromones*. 1st edn, (Wiley-VCH, 2006).
- 33 Ajikumar, P. K. Terpenoids: Opportunities for biosynthesis of natural product drugs using engineered microorganisms. *Molecular Pharmaceutics*, 5, 167-190, (2008).
- 34 Shahidi, N. T. A review of the chemistry, biological action, and clinical applications of anabolic-androgenic steroids. *Clinical Therapeutics*, 23, 1355-1390, (2001).
- 35 Bansal, R. & Acharya, P. C. Man-made cytotoxic steroids: Exemplary agents for cancer therapy. *Chemical Reviews*, 114, 6986-7005, (2014).
- 36 De Las Heras, B., Rodriguez, B., Bosca, L. & Villar, A. M. Terpenoids: Sources, structure elucidation and therapeutic potential in inflammation. *Current Topics in Medicinal Chemistry*, 3, 171-185, (2003).
- 37 Cragg, G. M. & Newman, D. J. Plants as a source of anti-cancer agents. *Journal of Ethnopharmacology*, 100, 72-79, (2005).
- 38 Newman, D. J., Cragg, G. M. & Snader, K. M. Natural products as sources of new drugs over the period 1981–2002. *Journal of Natural Products*, 66, 1022-1037, (2003).
- 39 Cragg, G. M. & Newman, D. J. Plants as a source of anti-cancer and anti-HIV agents. *Annals of Applied Biology*, 143, 127-133, (2003).
- 40 Srivastava, V., Negi, A. S., Kumar, J. K., Gupta, M. M. & Khanuja, S. P. S. Plant-based anticancer molecules: A chemical and biological profile of some important leads. *Bioorganic & Medicinal Chemistry*, 13, 5892-5908, (2005).
- 41 Charles, P. C., Narsimha, R., David, N. L. & Wyllie, S. G. Origin of (+)- δ -cadinene and the cubenols in the essential oils of the Myrtaceae. *Flavour and Fragrance Journal*, 15, 352-361, (2000).
- 42 Martin, V. J. J., Pitera, D. J., Withers, S. T., Newman, J. D. & Keasling, J. D. Engineering a mevalonate pathway in *Escherichia coli* for production of terpenoids. *Nature Biotechnology*, 21, 796-802, (2003).
- 43 Gang, D. R. Evolution of flavors and scents. *Annual Review of Plant Biology*, 56, 301-325, (2005).
- 44 Oldfield, E. & Lin, F. Y. Terpene biosynthesis: Modularity rules. *Angewandte Chemie International Edition*, 51, 1124-1137, (2012).
- 45 Weng, J.-K., Philippe, R. N. & Noel, J. P. The rise of chemodiversity in plants. *Science*, 336, 1667-1670, (2012).
- 46 Cheng, A.-X., Lou, Y.-G., Mao, Y.-B., Lu, S., Wang, L.-J. & Chen, X.-Y. Plant terpenoids: Biosynthesis and ecological functions. *Journal of Integrative Plant Biology*, 49, 179-186, (2007).
- 47 Nagegowda, D. A. Plant volatile terpenoid metabolism: Biosynthetic genes, transcriptional regulation and subcellular compartmentation. *FEBS Letters*, 584, 2965-2973, (2010).
- 48 Feeny, P. in *Herbivores: Their interactions with secondary plant metabolites (second edition)*, (ed Gerald A. Rosenthalmay R. Berenbaum) 1-44 (Academic Press, 1992).
- 49 Pimentel, D. & Bellotti, A. C. Parasite-host population systems and genetic stability. *The American Naturalist*, 110, 877-888, (1976).
- 50 Iriti, M. & Faoro, F. Chemical diversity and defence metabolism: How plants cope with pathogens and ozone pollution. *International Journal of Molecular Sciences*, 10, 3371-3399, (2009).
- 51 Berenbaum, M. & Neal, J. Synergism between myristicin and xanthotoxin, a naturally cooccurring plant toxicant. *Journal of Chemical Ecology*, 11, 1349-1358, (1985).
- 52 Akhtar, Y. & Isman, M. Binary mixtures of feeding deterrents mitigate the decrease in feeding deterrent response to antifeedants following prolonged exposure in the cabbage looper, *Trichoplusia ni* (Lepidoptera: Noctuidae). *Chemoecology*, 13, 177-182, (2003).
- 53 Phillips, M. A. & Croteau, R. B. Resin-based defenses in conifers. *Trends in Plant Science*, 4, 184-190, (1999).
- 54 Himejima, M., Hobson, K., Otsuka, T., Wood, D. & Kubo, I. Antimicrobial terpenes from oleoresin of ponderosa pine tree *Pinus ponderosa*: A defense mechanism against microbial invasion. *Journal of Chemical Ecology*, 18, 1809-1818, (1992).
- 55 Staerk, D., Skole, B., Jorgensen, F. S., Budnik, B. A., Ekpe, P. & Jaroszewski, J. W. Isolation of a library of aromadendranes from *Landolphia dulcis* and its characterization using the volsurf approach. *Journal of Natural Products*, 67, 799-805, (2004).
- 56 Dicke, M., Van Loon, J. J. A. & Soler, R. Chemical complexity of volatiles from plants induced by multiple attack. *Nature Chemical Biology*, 5, 317-324, (2009).
- 57 Dicke, M., Van Beek, T. A., Posthumus, M. A., Ben Dom, N., Van Bokhoven, H. & De Groot, A. Isolation and identification of volatile kairomone that affects acarine predator-prey interactions involvement of host plant in its production. *Journal of Chemical Ecology*, 16, 381-396, (1990).
- 58 Turlings, T. C. J., Tumlinson, J. H. & Lewis, W. J. Exploitation of herbivore-induced plant odors by host-seeking parasitic wasps. *Science*, 250, 1251-1253, (1990).

- 59 Mumm, R. & Hilker, M. The significance of background odour for an egg parasitoid to detect plants with host eggs. *Chem Senses*, 30, 337-343, (2005).
- 60 Mumm, R., Schrank, K., Wegener, R., Schulz, S. & Hilker, M. Chemical analysis of volatiles emitted by *Pinus sylvestris* after induction by insect oviposition. *Journal of Chemical Ecology*, 29, 1235-1252, (2003).
- 61 Runyon, J. B., Mescher, M. C. & De Moraes, C. M. Volatile chemical cues guide host location and host selection by parasitic plants. *Science*, 313, 1964-1967, (2006).
- 62 Bouwmeester, H. J., Matusova, R., Zhongkui, S. & Beale, M. H. Secondary metabolite signalling in host-parasitic plant interactions. *Current Opinion in Plant Biology*, 6, 358-364, (2003).
- 63 Heil, M. & Silva Bueno, J. C. Within-plant signaling by volatiles leads to induction and priming of an indirect plant defense in nature. *Proceedings of the National Academy of Sciences of the United States of America*, 104, 5467-5472, (2007).
- 64 Baldwin, I. T., Halitschke, R., Paschold, A., Von Dahl, C. C. & Preston, C. A. Volatile signaling in plant-plant interactions: "Talking trees" in the genomics era. *Science*, 311, 812-815, (2006).
- 65 Ton, J., D'alessandro, M., Jourdie, V., Jakab, G., Karlen, D., Held, M., Mauch-Mani, B. & Turlings, T. C. Priming by airborne signals boosts direct and indirect resistance in maize. *The Plant Journal*, 49, 16-26, (2007).
- 66 Dicke, M. & Bruin, J. Chemical information transfer between plants: Back to the future. *Biochemical Systematics and Ecology*, 29, 981-994, (2001).
- 67 Flesch, G. & Rohmer, M. Prokaryotic hopanoids - the biosynthesis of the bacteriohopane skeleton - formation of isoprenic units from 2 distinct acetate pools and a novel type of carbon carbon linkage between a triterpene and D-ribose. *European Journal of Biochemistry*, 175, 405-411, (1988).
- 68 Rohmer, M., Knani, M., Simonin, P., Sutter, B. & Sahn, H. Isoprenoid biosynthesis in bacteria - a novel pathway for the early steps leading to isopentenyl diphosphate. *Biochemical Journal*, 295, 517-524, (1993).
- 69 Seemann, M., Zhai, G. Z., Umezawa, K. & Cane, D. Pentalenene synthase. Histidine-309 is not required for catalytic activity. *Journal of the American Chemical Society*, 121, 591-592, (1999).
- 70 Lichtenthaler, H. K., Schwender, J., Disch, A. & Rohmer, M. Biosynthesis of isoprenoids in higher plant chloroplasts proceeds via a mevalonate-independent pathway. *FEBS Letters*, 400, 271, (1997).
- 71 Goldstein, J. L. & Brown, M. S. Regulation of the mevalonate pathway. *Nature*, 343, 425-430, (1990).
- 72 Lichtenthaler, H. K., Rohmer, M. & Schwender, J. Two independent biochemical pathways for isopentenyl diphosphate and isoprenoid biosynthesis in higher plants. *Physiologia Plantarum*, 101, 643-652, (1997).
- 73 Disch, A. & Rohmer, M. On the absence of the glyceraldehyde 3-phosphate/pyruvate pathway for isoprenoid biosynthesis in fungi and yeasts. *FEMS Microbiology Letters*, 168, 201-208, (1998).
- 74 Gershenzon, J. & Croteau, R. B. Terpenoid biosynthesis: The basic pathway and formation of monoterpenes, sesquiterpenes, and diterpenes. *Lipid metabolism in plants*, 339-388, (1993).
- 75 Mcgarvey, D. J. & Croteau, R. Terpenoid metabolism. *Plant Cell*, 7, 1015, (1995).
- 76 Brandt, W., Bräuer, L., Günnewich, N., Kufka, J., Rausch, F., Schulze, D., Schulze, E., Weber, R., Zakharaova, S. & Wessjohann, L. Molecular and structural basis of metabolic diversity mediated by prenyldiphosphate converting enzymes. *Phytochemistry*, 70, 1758-1775, (2009).
- 77 Eisenreich, W., Bacher, A., Arigoni, D. & Rohdich, F. Biosynthesis of isoprenoids via the non-mevalonate pathway. *Cellular and Molecular Life Sciences*, 61, 1401-1426, (2004).
- 78 Rodriguez-Concepcion, M. & Boronat, A. Elucidation of the methylerythritol phosphate pathway for isoprenoid biosynthesis in bacteria and plastids. A metabolic milestone achieved through genomics. *Plant Physiology*, 130, 1079-1089, (2002).
- 79 Bick, J. A. & Lange, B. M. Metabolic cross talk between cytosolic and plastidial pathways of isoprenoid biosynthesis: Unidirectional transport of intermediates across the chloroplast envelope membrane. *Archives of Biochemistry and Biophysics*, 415, 146-154, (2003).
- 80 Dudareva, N., Andersson, S., Orlova, I., Gatto, N., Reichelt, M., Rhodes, D., Boland, W. & Gershenzon, J. The nonmevalonate pathway supports both monoterpene and sesquiterpene formation in snapdragon flowers. *Proceedings of the National Academy of Sciences of the United States of America*, 102, 933-938, (2005).
- 81 Hemmerlin, A., Hoeffler, J.-F., Meyer, O., Tritsch, D., Kagan, I. A., Grosdemange-Billiard, C., Rohmer, M. & Bach, T. J. Cross-talk between the cytosolic mevalonate and the plastidial methylerythritol phosphate pathways in tobacco bright yellow-2 cells. *Journal of Biological Chemistry*, 278, 26666-26676, (2003).
- 82 Laule, O., Fürholz, A., Chang, H.-S., Zhu, T., Wang, X., Heifetz, P. B., Grisse, W. & Lange, M. Crosstalk between cytosolic and plastidial pathways of isoprenoid biosynthesis in *Arabidopsis thaliana*. *Proceedings of the National Academy of Sciences of the United States of America*, 100, 6866-6871, (2003).

- 83 Jux, A., Gleixner, G. & Boland, W. Classification of terpenoids according to the methylerythritolphosphate or the mevalonate pathway with natural $^{12}\text{C}/^{13}\text{C}$ isotope ratios: Dynamic allocation of resources in induced plants. *Angewandte Chemie International Edition*, 40, 2091-2093, (2001).
- 84 Aharoni, A., Giri, A. P., Verstappen, F. W. A., Berteau, C. M., Sevenier, R., Sun, Z. K., Jongsma, M. A., Schwab, W. & Bouwmeester, H. J. Gain and loss of fruit flavor compounds produced by wild and cultivated strawberry species. *Plant Cell*, 16, 3110-3131, (2004).
- 85 Aharoni, A., Giri, A. P., Deuerlein, S., Griepink, F., De Kogel, W. J., Verstappen, F. W. A., Verhoeven, H. A., Jongsma, M. A., Schwab, W. & Bouwmeester, H. J. Terpene metabolism in wild-type and transgenic Arabidopsis plants. *Plant Cell*, 15, 2866-2884, (2003).
- 86 Ralston, L., Kwon, S. T., Schoenbeck, M., Ralston, J., Schenk, D. J., Coates, R. M. & Chappell, J. Cloning, heterologous expression, and functional characterization of 5-*epi*-aristolochene-1,3-dihydroxylase from tobacco (*Nicotiana tabacum*). *Archives of Biochemistry and Biophysics*, 393, 222-235, (2001).
- 87 Yin, S., Mei, L., Newman, J., Back, K. & Chappell, J. Regulation of sesquiterpene cyclase gene expression. Characterization of an elicitor- and pathogen-inducible promoter. *Plant Physiology*, 115, 437-451, (1997).
- 88 Vögeli, U. & Chappell, J. Regulation of a sesquiterpene cyclase in cellulase-treated tobacco cell suspension cultures. *Plant Physiology*, 94, 1860-1866, (1990).
- 89 Devarenne, T. P., Ghosh, A. & Chappell, J. Regulation of squalene synthase, a key enzyme of sterol biosynthesis, in tobacco. *Plant Physiology*, 129, 1095-1106, (2002).
- 90 Zook, M. N., Chappell, J. & Kúć, J. A. Characterization of elicitor-induction of sesquiterpene cyclase activity in potato tuber tissue. *Phytochemistry*, 31, 3441-3445, (1992).
- 91 Zook, M. N. & Kúć, J. A. Induction of sesquiterpene cyclase and suppression of squalene synthetase activity in elicitor-treated or fungal-infected potato tuber tissue. *Physiological and Molecular Plant Pathology*, 39, 377-390, (1991).
- 92 Chappell, J., Nable, R., Fleming, P., Andersen, R. A. & Burton, H. R. Accumulation of capsidiol in tobacco cell cultures treated with fungal elicitor. *Phytochemistry*, 26, 2259-2260, (1987).
- 93 Altman, D. W., Stipanovic, R. D. & Bell, A. A. Terpenoids in foliar pigment glands of A, D, and AD genome cottons: Introgression potential for pest resistance. *Journal of Heredity*, 81, 447-454, (1990).
- 94 Steele, C. L., Katoh, S., Bohlmann, J. & Croteau, R. A. Regulation of oleoresinosis in Grand Fir (*Abies grandis*) - differential transcriptional control of monoterpene, sesquiterpene, and diterpene synthase genes in response to wounding. *Plant Physiology*, 116, 1497-1504, (1998).
- 95 Funk, C., Lewinsohn, E., Vogel, B. S., Steele, C. L. & Croteau, R. Regulation of oleoresinosis in Grand Fir (*Abies grandis*) (coordinate induction of monoterpene and diterpene cyclases and two cytochrome p450-dependent diterpenoid hydroxylases by stem wounding). *Plant Physiology*, 106, 999-1005, (1994).
- 96 Turner, G. W., Gershenson, J. & Croteau, R. B. Development of peltate glandular trichomes of peppermint. *Plant Physiology*, 124, 665-680, (2000).
- 97 Guo, Z. & Wagner, G. Biosynthesis of labdenediol and sclareol in cell-free extracts from trichomes of *Nicotiana glutinosa*. *Planta*, 197, 627-632, (1995).
- 98 Wagner, M. R., Benjamin, D. M., Clancy, K. M. & Schuh, B. A. Influence of diterpene resin acids on feeding and growth of larch sawfly, *Pristiphora erichsonii* (Hartig). *Journal of Chemical Ecology*, 9, 119-127, (1983).
- 99 Tissier, A. Glandular trichomes: What comes after expressed sequence tags? *The Plant Journal*, 70, 51-68, (2012).
- 100 Wendt, K. U., Schulz, G. E., Corey, E. J. & Liu, D. R. Enzyme mechanisms for polycyclic triterpene formation. *Angewandte Chemie International Edition*, 39, 2812-2833, (2000).
- 101 Cane, D. E. Enzymatic formation of sesquiterpenes. *Chemical Reviews*, 90, 1089-1103, (1990).
- 102 Greenhagen, B. & Chappell, J. Molecular scaffolds for chemical wizardry: Learning nature's rules for terpene cyclases. *Proceedings of the National Academy of Sciences of the United States of America*, 98, 13479-13481, (2001).
- 103 Croteau, R. Biosynthesis and catabolism of monoterpenoids. *Chemical Reviews*, 87, 929-954, (1987).
- 104 Cane, D. E., Oliver, J. S., Harrison, P. H. M., Abell, C., Hubbard, B. R., Kane, C. T. & Lattman, R. Biosynthesis of pentalenene and pentalenolactone. *Journal of the American Chemical Society*, 112, 4513-4524, (1990).
- 105 Davis, E. M. & Croteau, R. in *Biosynthesis: Aromatic polyketides, isoprenoids, alkaloids*, Vol. 209 *Topics in current chemistry* 53-95 (Springer-Verlag, 2000).
- 106 Degenhardt, J., Köllner, T. G. & Gershenson, J. Monoterpene and sesquiterpene synthases and the origin of terpene skeletal diversity in plants. *Phytochemistry*, 70, 1621-1637, (2009).
- 107 Schenk, D. J., Starks, C. M., Manna, K. R., Chappell, J., Noel, J. P. & Coates, R. M. Stereochemistry and deuterium isotope effects associated with the cyclization-rearrangements catalyzed by tobacco *epi*-

- aristolochene and hyoscyamus premnaspirodiene synthases, and the chimeric CH₄ hybrid cyclase. *Archives of Biochemistry and Biophysics*, 448, 31-44, (2006).
- 108 Bohlmann, J., Meyer-Gauen, G. & Croteau, R. Plant terpenoid synthases: Molecular biology and phylogenetic analysis. *Proceedings of the National Academy of Sciences of the United States of America*, 95, 4126-4133, (1998).
- 109 Mercke, P., Bengtsson, M., Bouwmeester, H. J., Posthumus, M. A. & Brodelius, P. E. Molecular cloning, expression, and characterization of amorpho-4,11-diene synthase, a key enzyme of artemisinin biosynthesis in *Artemisia annua* l. *Archives of Biochemistry and Biophysics*, 381, 173-180, (2000).
- 110 Corey, E. J., Matsuda, S. P. & Bartel, B. Isolation of an *Arabidopsis thaliana* gene encoding cycloartenol synthase by functional expression in a yeast mutant lacking lanosterol synthase by the use of a chromatographic screen. *Proceedings of the National Academy of Sciences of the United States of America*, 90, 11628-11632, (1993).
- 111 Lesburg, C. A., Zhai, G. Z., Cane, D. E. & Christianson, D. W. Crystal structure of pentalenene synthase: Mechanistic insights on terpenoid cyclization reactions in biology. *Science*, 277, 1820, (1997).
- 112 Starks, C. M., Back, K. W., Chappell, J. & Noel, J. P. Structural basis for cyclic terpene biosynthesis by tobacco 5-epi-aristolochene synthase. *Science*, 277, 1815, (1997).
- 113 Tarshis, L. C., Yan, M., Poulter, C. D. & Sacchettini, J. C. Crystal structure of recombinant farnesyl diphosphate synthase at 2.6-Å resolution. *Biochemistry*, 33, 10871-10877, (1994).
- 114 Wendt, K. U., Poralla, K. & Schulz, G. E. Structure and function of a squalene cyclase. *Science*, 277, 1811-1815, (1997).
- 115 Wendt, K. U., Lenhart, A. & Schulz, G. E. The structure of the membrane protein squalene-hopene cyclase at 2.0 Å resolution. *Journal of Molecular Biology*, 286, 175-187, (1999).
- 116 Caruthers, J. M., Kang, I., Rynkiewicz, M. J., Cane, D. E. & Christianson, D. W. Crystal structure determination of aristolochene synthase from the blue cheese mold, *Penicillium roqueforti*. *Journal of Biological Chemistry*, 275, 25533-25539, (2000).
- 117 Rynkiewicz, M. J., Cane, D. E. & Christianson, D. W. Structure of trichodiene synthase from *Fusarium sporotrichioides* provides mechanistic inferences on the terpene cyclization cascade. *Proceedings of the National Academy of Sciences of the United States of America*, 98, 13543, (2001).
- 118 Rynkiewicz, M. J., Cane, D. E. & Christianson, D. W. X-ray crystal structures of D100e trichodiene synthase and its pyrophosphate complex reveal the basis for terpene product diversity. *Biochemistry*, 41, 1732, (2002).
- 119 Whittington, D. A., Wise, M. L., Urbansky, M., Coates, R. M., Croteau, R. B. & Christianson, D. W. Bornyl diphosphate synthase: Structure and strategy for carbocation manipulation by a terpenoid cyclase. *Proceedings of the National Academy of Sciences of the United States of America*, 99, 15375-15380, (2002).
- 120 Pandit, J., Danley, D. E., Schulte, G. K., Mazzalupo, S., Pauly, T. A., Hayward, C. M., Hamanaka, E. S., Thompson, J. F. & Harwood, H. J., Jr. Crystal structure of human squalene synthase. A key enzyme in cholesterol biosynthesis. *Journal of Biological Chemistry*, 275, 30610-30617, (2000).
- 121 Cane, D. E. Isoprenoid biosynthesis: Overview. *Comprehensive Natural Products Chemistry*, 2, 1-13, (1999).
- 122 Bohlmann, J., Steele, C. L. & Croteau, R. Monoterpene synthases from Grand Fir (*Abies grandis*). *Journal of Biological Chemistry*, 272, 21784-21792, (1997).
- 123 Steele, C. L., Crock, J., Bohlmann, J. & Croteau, R. Sesquiterpene synthases from Grand Fir (*Abies grandis*) - comparison of constitutive and wound-induced activities, and cDNA isolation, characterization and bacterial expression of delta-selinene synthase and gamma-humulene synthase. *Journal of Biological Chemistry*, 273, 2078, (1998).
- 124 Chen, X. Y., Chen, Y., Heinsteins, P. & Davison, V. J. Cloning, expression, and characterization of (+)-delta-cadinene synthase: A catalyst for cotton phytoalexin biosynthesis. *Archives of Biochemistry and Biophysics*, 324, 255-266, (1995).
- 125 Felicetti, B. & Cane, D. E. Aristolochene synthase: Mechanistic analysis of active site residues by site-directed mutagenesis. *Journal of the American Chemical Society*, 126, 7212-7221, (2004).
- 126 Gambliel, H. & Croteau, R. Pinene cyclases i and ii. Two enzymes from sage (*Salvia officinalis*) which catalyze stereospecific cyclizations of geranyl pyrophosphate to monoterpene olefins of opposite configuration. *Journal of Biological Chemistry*, 259, 740-748, (1984).
- 127 Cane, D. E. Sesquiterpene biosynthesis: Cyclization mechanisms. *Comprehensive Natural Products Chemistry*, 2, 155-200, (1999).
- 128 Dickschat, J. S. Isoprenoids in three-dimensional space: The stereochemistry of terpene biosynthesis. *Natural Product Reports*, 28, 1917-1936, (2011).
- 129 Lin, X., Hopson, R. & Cane, D. E. Genome mining in streptomyces coelicolor: Molecular cloning and characterization of a new sesquiterpene synthase. *Journal of the American Chemical Society*, 128, 6022-6023, (2006).

- 130 Aaron, J. A., Lin, X., Cane, D. E. & Christianson, D. W. Structure of *epi*-isozizaene synthase from *Streptomyces coelicolor* a3(2), a platform for new terpenoid cyclization templates. *Biochemistry*, 49, 1787-1797, (2010).
- 131 Lin, X. & Cane, D. E. Biosynthesis of the sesquiterpene antibiotic albaflavenone in *Streptomyces coelicolor*. Mechanism and stereochemistry of the enzymatic formation of *epi*-isozizaene. *Journal of the American Chemical Society*, 131, 6332-6333, (2009).
- 132 Hohn, T. M. & Plattner, R. D. Purification and characterization of the sesquiterpene cyclase aristolochene synthase from *Penicillium roqueforti*. *Archives of Biochemistry and Biophysics*, 272, 137-143, (1989).
- 133 Dehal, S. S. & Croteau, R. Partial-purification and characterization of 2 sesquiterpene cyclases from sage (*Salvia officinalis*) which catalyze the respective conversion of farnesyl pyrophosphate to humulene and caryophyllene. *Archives of Biochemistry and Biophysics*, 261, 346-356, (1988).
- 134 Cane, D. E., Ha, H. J., Pargellis, C., Waldmeier, F., Swanson, S. & Murthy, P. P. N. Trichodiene biosynthesis and the stereochemistry of the enzymatic cyclization of farnesyl pyrophosphate. *Bioorganic Chemistry*, 13, 246-265, (1985).
- 135 Hohn, T. M. & Vanmiddlesworth, F. Purification and characterization of the sesquiterpene cyclase trichodiene synthetase from *Fusarium sporotrichioides*. *Archives of Biochemistry and Biophysics*, 251, 756-761, (1986).
- 136 King, H. L. & Rilling, H. C. Avian liver prenyltransferase. The role of metal in substrate binding and the orientation of substrates during catalysis. *Biochemistry*, 16, 3815-3819, (1977).
- 137 Poulter, C. D., Argyle, J. C. & Mash, E. A. Prenyltransferase. New evidence for an ionization-condensation-elimination mechanism with 2-fluorogeranyl pyrophosphate. *Journal of the American Chemical Society*, 99, 957-959, (1977).
- 138 Poulter, C. D., Wiggins, P. L. & Le, A. T. Farnesylpyrophosphate synthetase. A stepwise mechanism for the 1'-4 condensation reaction. *Journal of the American Chemical Society*, 103, 3926-3927, (1981).
- 139 Poulter, C. D., Satterwhite, D. M. & Rilling, H. C. Prenyltransferase. The mechanism of the reaction. *Journal of the American Chemical Society*, 98, 3376-3377, (1976).
- 140 Brems, D. N. & Rilling, H. C. On the mechanism of the prenyltransferase reaction. Metal ion dependent solvolysis of an allylic pyrophosphate. *Journal of the American Chemical Society*, 99, 8351-8352, (1977).
- 141 Rittersdorf, W. & Cramer, F. Cyclization of nerol and linalool on solvolysis of their phosphate esters. *Tetrahedron*, 24, 43-52, (1968).
- 142 Allinger, N. L. & Siefert, J. H. Organic quantum chemistry. Xxxiii. Electronic spectra and rotational barriers of vinylborane, allyl cation, and related compounds. *Journal of the American Chemical Society*, 97, 752-760, (1975).
- 143 Satterwhite, D. M., Wheeler, C. J. & Croteau, R. Biosynthesis of monoterpenes - enantioselectivity in the enzymatic cyclization of linalyl pyrophosphate to (-)-endo-fenchol. *Journal of Biological Chemistry*, 260, 3901-3908, (1985).
- 144 Cane, D. E., Prabhakaran, P. C., Oliver, J. S. & Mcilwaine, D. B. Aristolochene biosynthesis - stereochemistry of the deprotonation steps in the enzymatic cyclization of farnesyl pyrophosphate. *Journal of the American Chemical Society*, 112, 3209, (1990).
- 145 Köllner, T. G., Schnee, C., Gershenson, J. & Degenhardt, J. The variability of sesquiterpenes emitted from two *Zea mays* cultivars is controlled by allelic variation of two terpene synthase genes encoding stereoselective multiple product enzymes. *Plant Cell*, 16, 1115-1131, (2004).
- 146 Köllner, T. G., Gershenson, J. & Degenhardt, J. Molecular and biochemical evolution of maize terpene synthase 10, an enzyme of indirect defense. *Phytochemistry*, 70, 1139-1145, (2009).
- 147 Arimura, G., Garms, S., Maffei, M., Bossi, S., Schulze, B., Leitner, M., Mithofer, A. & Boland, W. Herbivore-induced terpenoid emission in *Medicago truncatula*: Concerted action of jasmonate, ethylene and calcium signaling. *Planta*, 227, 453-464, (2008).
- 148 Garms, S., Boland, W. & Arimura, G.-I. Early herbivore-elicited events in terpenoid biosynthesis. *Plant Signaling & Behaviour*, 3, 418-419, (2008).
- 149 Garms, S., Köllner, T. G. & Boland, W. A multiproduct terpene synthase from *Medicago truncatula* generates cadalane sesquiterpenes via two different mechanisms. *Journal of Organic Chemistry*, 75, 5590-5600, (2010).
- 150 Mathis, J. R., Back, K., Starks, C., Noel, J., Poulter, C. D. & Chappell, J. Pre-steady-state study of recombinant sesquiterpene cyclases. *Biochemistry*, 36, 8340-8348, (1997).
- 151 Cane, D. E., Chiu, H. T., Liang, P. H. & Anderson, K. S. Pre-steady-state kinetic analysis of the trichodiene synthase reaction pathway. *Biochemistry*, 36, 8332-8339, (1997).
- 152 Nobeli, I., Favia, A. D. & Thornton, J. M. Protein promiscuity and its implications for biotechnology. *Nature Biotechnology*, 27, 157-167, (2009).
- 153 Tokuriki, N. & Tawfik, D. S. Protein dynamism and evolvability. *Science*, 324, 203-207, (2009).

- 154 Yoshikuni, Y., Ferrin, T. E. & Keasling, J. D. Designed divergent evolution of enzyme function. *Nature*, 440, 1078-1082, (2006).
- 155 Dougherty, D. A. The cation- π interaction. *Accounts of Chemical Research*, 46, 885-893, (2013).
- 156 Mahadevi, A. S. & Sastry, G. N. Cation- π interaction: Its role and relevance in chemistry, biology, and material science. *Chemical Reviews*, 113, 2100-2138, (2013).
- 157 Rising, K. A., Starks, C. M., Noel, J. P. & Chappell, J. Demonstration of germacrene a as an intermediate in 5-*epi*-aristolochene synthase catalysis. *Journal of the American Chemical Society*, 122, 1861-1866, (2000).
- 158 Bohlmann, J. & Gershenzon, J. Old substrates for new enzymes of terpenoid biosynthesis. *Proceedings of the National Academy of Sciences of the United States of America*, 106, 10402-10403, (2009).
- 159 Schillmiller, A. L., Schauvinhold, I., Larson, M., Xu, R., Charbonneau, A. L., Schmidt, A., Wilkerson, C., Last, R. L. & Pichersky, E. Monoterpenes in the glandular trichomes of tomato are synthesized from a neryl diphosphate precursor rather than geranyl diphosphate. *Proceedings of the National Academy of Sciences of the United States of America*, -, (2009).
- 160 Wheeler, C. J. & Croteau, R. Monoterpene cyclases - stereoelectronic requirements for substrate binding and ionization. *Journal of Biological Chemistry*, 262, 8213-8219, (1987).
- 161 Wise, M. L., Savage, T. J., Katahira, E. & Croteau, R. Monoterpene synthases from common sage (*Salvia officinalis*) - cDNA isolation, characterization, and functional expression of (+)-sabinene synthase, 1,8-cineole synthase, and (+)-bornyl diphosphate synthase. *Journal of Biological Chemistry*, 273, 14891-14899, (1998).
- 162 Wise, M. L. & Croteau, R. in *Comprehensive natural products chemistry*, (ed Sir Derek Bartonkoji Nakanishiotto Meth-Cohn) 97-153 (Pergamon, 1999).
- 163 Lopez-Gallego, F., Agger, S. A., Abate-Pella, D., Distefano, M. D. & Schmidt-Dannert, C. Sesquiterpene synthases Cop4 and Cop6 from *Coprinus cinereus*: Catalytic promiscuity and cyclization of farnesyl pyrophosphate geometric isomers. *ChemBioChem*, 11, 1093-1106, (2010).
- 164 Schalk, M. & Croteau, R. A single amino acid substitution (F363I) converts the regiochemistry of the spearmint (-)-limonene hydroxylase from a c6- to a c3-hydroxylase. *Proceedings of the National Academy of Sciences of the United States of America*, 97, 11948-11953, (2000).
- 165 Wüst, M., Little, D. B., Schalk, M. & Croteau, R. Hydroxylation of limonene enantiomers and analogs by recombinant (-)-limonene 3- and 6-hydroxylases from mint (*Mentha*) species: Evidence for catalysis within sterically constrained active sites. *Archives of Biochemistry and Biophysics*, 387, 125-136, (2001).
- 166 Arigoni, D. Stereochemical aspects of sesquiterpene biosynthesis. *Pure and Applied Chemistry*, 41, 219-245, (1975).
- 167 Chen, M., Al-Lami, N., Janvier, M., D'antonio, E. L., Faraldos, J. A., Cane, D. E., Allemann, R. K. & Christianson, D. W. Mechanistic insights from the binding of substrate and carbocation intermediate analogues to aristolochene synthase. *Biochemistry*, 52, 5441-5453, (2013).
- 168 Little, D. B. & Croteau, R. B. Alteration of product formation by directed mutagenesis and truncation of the multiple-product sesquiterpene synthases δ -selinene synthase and γ -humulene synthase. *Archives of Biochemistry and Biophysics*, 402, 120-135, (2002).
- 169 Crock, J., Wildung, M. & Croteau, R. Isolation and bacterial expression of a sesquiterpene synthase cDNA clone from peppermint (*Mentha x piperita*, L.) that produces the aphid alarm pheromone (*E*)-beta-farnesene. *Proceedings of the National Academy of Sciences of the United States of America*, 94, 12833-12838, (1997).
- 170 Cai, Y., Jia, J. W., Crock, J., Lin, Z. X., Chen, X. Y. & Croteau, R. A cDNA clone for beta-caryophyllene synthase from *Artemisia annua*. *Phytochemistry*, 61, 523-529, (2002).
- 171 Chang, Y. J., Song, S. H., Park, S. H. & Kim, S. U. Amorpha-4,11-diene synthase of *Artemisia annua*: cDNA isolation and bacterial expression of a terpene synthase involved in artemisinin biosynthesis. *Archives of Biochemistry and Biophysics*, 383, 178-184, (2000).
- 172 Warke, A. & Momany, C. Addressing the protein crystallization bottleneck by cocrystallization. *Crystal Growth & Design*, 7, 2219-2225, (2007).
- 173 Tholl, D. Terpene synthases and the regulation, diversity and biological roles of terpene metabolism. *Current Opinion in Plant Biology*, 9, 297-304, (2006).
- 174 Vedula, L. S., Jiang, J., Zakharian, T., Cane, D. E. & Christianson, D. W. Structural and mechanistic analysis of trichodiene synthase using site-directed mutagenesis: Probing the catalytic function of tyrosine-295 and the asparagine-225/serine-229/glutamate-233- motif. *Archives of Biochemistry and Biophysics*, 469, 184-194, (2008).
- 175 Vedula, L. S., Rynkiewicz, M. J., Pyun, H.-J., Coates, R. M., Cane, D. E. & Christianson, D. W. Molecular recognition of the substrate diphosphate group governs product diversity in trichodiene synthase mutants. *Biochemistry*, 44, 6153-6163, (2005).
- 176 Vedula, L. S., Cane, D. E. & Christianson, D. W. Role of arginine-304 in the diphosphate-triggered active site closure mechanism of trichodiene synthase. *Biochemistry*, 44, 12719-12727, (2005).

- 177 Christianson, D. W. Unearthing the roots of the terpenome. *Current Opinion in Chemical Biology*, 12, 141-150, (2008).
- 178 Christianson, D. W. Structural biology and chemistry of the terpenoid cyclases. *Chemical Reviews*, 106, 3412-3442, (2006).
- 179 Sallaud, C., Rontein, D., Onillon, S., Jabes, F., Duffe, P., Giacalone, C., Thoraval, S., Escoffier, C., Herbertte, G., Leonhardt, N., Causse, M. & Tissier, A. A novel pathway for sesquiterpene biosynthesis from z,z-farnesyl pyrophosphate in the wild tomato *Solanum habrochaites*. *Plant Cell*, 21, 301-317, (2009).
- 180 Gatto, N., Vattekkatte, A., Kollner, T., Degenhardt, J., Gershenzon, J. & Boland, W. Isotope sensitive branching and kinetic isotope effects to analyse multiproduct terpenoid syntheses from *Zea mays*. *Chemical Communications*, 51, 3797-3800, (2015).
- 181 Vattekkatte, A., Gatto, N., Kollner, T. G., Degenhardt, J., Gershenzon, J. & Boland, W. Substrate geometry controls the cyclization cascade in multiproduct terpene syntheses from *Zea mays*. *Organic & Biomolecular Chemistry*, 13, 6021-6030, (2015).
- 182 Vattekkatte, A., Gatto, N., Schulze, E., Brandt, W. & Boland, W. Inhibition of a multiproduct terpene synthase from *Medicago truncatula* by 3-bromoprenyl diphosphates. *Organic & Biomolecular Chemistry*, 13, 4776-4784, (2015).
- 183 Arimura, G. I., Garms, S., Maffei, M., Bossi, S., Schulze, B., Leitner, M., Mithöfer, A. & Boland, W. Herbivore-induced terpenoid emission in *Medicago truncatula*: Concerted action of jasmonate, ethylene and calcium signaling. *Planta*, 227, 453-464, (2008).
- 184 Boland, W. & Garms, S. Induced volatiles of *Medicago truncatula*: Molecular diversity and mechanistic aspects of a multiproduct sesquiterpene synthase from *m. Truncatula*. *Flavour and Fragrance Journal*, 25, 114-116, (2010).
- 185 Schmelz, E. A., Alborn, H. T. & Tumlinson, J. H. Synergistic interactions between volicitin, jasmonic acid and ethylene mediate insect-induced volatile emission in *Zea mays*. *Physiologia Plantarum*, 117, 403-412, (2003).
- 186 Schmelz, E. A., Alborn, H. T., Banchio, E. & Tumlinson, J. H. Quantitative relationships between induced jasmonic acid levels and volatile emission in *Zea mays* during *Spodoptera exigua* herbivory. *Planta*, 216, 665-673, (2003).
- 187 Köllner, T. G., Schnee, C., Gershenzon, J. & Degenhardt, J. The sesquiterpene hydrocarbons of maize (*Zea mays*) form five groups with distinct developmental and organ-specific distribution. *Phytochemistry*, 65, 1895-1902, (2004).
- 188 Köllner, T. G., O'maille, P. E., Gatto, N., Boland, W., Gershenzon, J. & Degenhardt, J. Two pockets in the active site of maize sesquiterpene synthase TPS4 carry out sequential parts of the reaction scheme resulting in multiple products. *Archives of Biochemistry and Biophysics*, 448, 83-92, (2006).
- 189 Arimura, G.-I., Kopke, S., Kunert, M., Volpe, V., David, A., Brand, P., Dabrowska, P., Maffei, M. E. & Boland, W. Effects of feeding *Spodoptera littoralis* on lima bean leaves: Iv. Diurnal and nocturnal damage differentially initiate plant volatile emission. *Plant Physiology*, 146, 965-973, (2008).
- 190 Boland, W. & Garms, S. Induced volatiles of *Medicago truncatula*: Molecular diversity and mechanistic aspects of a multiproduct sesquiterpene synthase from *m. Truncatula*. *Flavour and Fragrance Journal*, 25, 114-116, (2010).
- 191 Matsuo, A., Nozaki, H., Kubota, N., Uto, S. & Nakayama, M. Structures and conformations of (-)-isobicyclogermacrene and (-)-lepidozene - 2 key sesquiterpenoids of the cis-10,3-bicyclic and trans-10,3-bicyclic ring-systems, from the liverwort *Lepidozia-vitrea* - X-ray crystal-structure analysis of the hydroxy derivative of (-)-isobicyclogermacrene. *Journal of the Chemical Society-Perkin Transactions 1*, 203-214, (1984).
- 192 Cane, D. E. & Tandon, M. Epicubenol synthase and the stereochemistry of the enzymatic cyclization of farnesyl and nerolidyl diphosphate. *Journal of the American Chemical Society*, 117, 5602-5603, (1995).
- 193 Benedict, C. R., Lu, J.-L., Pettigrew, D. W., Liu, J., Stipanovic, R. D. & Williams, H. J. The cyclization of farnesyl diphosphate and nerolidyl diphosphate by a purified recombinant δ -cadinene synthase. *Plant Physiology*, 125, 1754-1765, (2001).
- 194 Alchanati, I., Patel, J. a. A., Liu, J., Benedict, C. R., Stipanovic, R. D., Bell, A. A., Cui, Y. & Magill, C. W. The enzymatic cyclization of nerolidyl diphosphate by [δ]-cadinene synthase from cotton stele tissue infected with *Verticillium dahliae*. *Phytochemistry*, 47, 961-967, (1998).
- 195 Northrop, D. B. Steady-state analysis of kinetic isotope-effects in enzymic reactions. *Biochemistry*, 14, 2644, (1975).
- 196 Miwa, G. T., Harada, N. & Lu, A. Y. H. Kinetic isotope effects on cytochrome P-450-catalyzed oxidation reactions: Full expression of the intrinsic isotope effect during the o-deethylation of 7-ethoxycoumarin by liver microsomes from 3-methylcholanthrene-induced hamsters. *Archives of Biochemistry and Biophysics*, 239, 155-162, (1985).

- 197 Miwa, G. T., Walsh, J. S., Kedderis, G. L. & Hollenberg, P. F. The use of intramolecular isotope effects to distinguish between deprotonation and hydrogen atom abstraction mechanisms in cytochrome P-450- and peroxidase-catalyzed n-demethylation reactions. *Journal of Biological Chemistry*, 258, 14445-14449, (1983).
- 198 Hjelmeland, L. M., Aronow, L. & Trudell, J. R. Intramolecular determination of substituent effects in hydroxylations catalyzed by cytochrome P-450. *Molecular Pharmacology*, 13, 634-639, (1977).
- 199 Hjelmeland, L. M., Aronow, L. & Trudell, J. R. Intramolecular determination of primary kinetic isotope effects in hydroxylations catalyzed by cytochrome P-450. *Biochemical and Biophysical Research Communications*, 76, 541-549, (1976).
- 200 Jones, J. P., Korzekwa, K. R., Rettie, A. E. & Trager, W. F. Isotopically sensitive branching and its effect on the observed intramolecular isotope effects in cytochrome-P-450 catalyzed-reactions -a new method for the estimation of intrinsic isotope effects. *Journal of the American Chemical Society*, 108, 7074, (1986).
- 201 Harada, N., Miwa, G. T., Walsh, J. S. & Lu, A. Y. Kinetic isotope effects on cytochrome P-450-catalyzed oxidation reactions. Evidence for the irreversible formation of an activated oxygen intermediate of cytochrome P-448. *Journal of Biological Chemistry*, 259, 3005-3010, (1984).
- 202 Samuelson, A. G. & Carpenter, B. K. The induced kinetic isotope effect as a tool for mechanistic discrimination. *Journal of the Chemical Society-Chemical Communications*, 354-356, (1981).
- 203 Lesburg, C. A., Caruthers, J. M., Paschall, C. M. & Christianson, D. W. Managing and manipulating carbocations in biology: Terpenoid cyclase structure and mechanism. *Current Opinion in Structural Biology*, 8, 695-703, (1998).
- 204 Wagschal, K. C., Pyun, H. J., Coates, R. M. & Croteau, R. Monoterpene biosynthesis - isotope effects associated with bicyclic olefin formation catalyzed by pinene synthases from sage (*Salvia officinalis*). *Archives of Biochemistry and Biophysics*, 308, 477, (1994).
- 205 Wagschal, K., Savage, T. J. & Croteau, R. Isotopically sensitive branching as a tool for evaluating multiple product formation by monoterpene cyclases. *Tetrahedron*, 47, 5933-5944, (1991).
- 206 Pyun, H. J., Coates, R. M., Wagschal, K. C., Mcgeady, P. & Croteau, R. B. Regiospecificity and isotope effects associated with the methyl methylene eliminations in the enzyme-catalyzed biosynthesis of (*R*)-limonene and (*S*)-limonene. *Journal of Organic Chemistry*, 58, 3998-4009, (1993).
- 207 Pyun, H. J., Wagschal, K. C., Jung, D. I., Coates, R. M. & Croteau, R. Stereochemistry of the proton elimination in the formation of (+)-alpha-pinene and (-)-alpha-pinene by monoterpene cyclases from sage (*Salvia officinalis*). *Archives of Biochemistry and Biophysics*, 308, 488-496, (1994).
- 208 Zu, L., Xu, M., Lodewyk, M. W., Cane, D. E., Peters, R. J. & Tantillo, D. J. Effect of isotopically sensitive branching on product distribution for pentalenene synthase: Support for a mechanism predicted by quantum chemistry. *Journal of the American Chemical Society*, 134, 11369-11371, (2012).
- 209 Tantillo, D. J. Biosynthesis via carbocations: Theoretical studies on terpene formation. *Natural Product Reports*, 28, 1035-1053, (2011).
- 210 Miller, D. J. & Allemann, R. K. Sesquiterpene synthases: Passive catalysts or active players? *Natural Product Reports*, 29, 60-71, (2012).
- 211 Kim, S.-H., Heo, K., Chang, Y.-J., Park, S.-H., Rhee, S.-K. & Kim, S.-U. Cyclization mechanism of amorpho-4,11-diene synthase, a key enzyme in artemisinin biosynthesis. *Journal of Natural Products*, 69, 758-762, (2006).
- 212 Picaud, S., Mercke, P., He, X. F., Sterner, O., Brodelius, M., Cane, D. E. & Brodelius, P. E. Amorpho-4,11-diene synthase: Mechanism and stereochemistry of the enzymatic cyclization of farnesyl diphosphate. *Archives of Biochemistry and Biophysics*, 448, 150-155, (2006).
- 213 Cane, D. E., Shim, J. H., Xue, Q., Fitzsimons, B. C. & Hohn, T. M. Trichodiene synthase - identification of active-site residues by site-directed mutagenesis. *Biochemistry*, 34, 2480-2488, (1995).
- 214 Arigoni, D., Cane, D. E., Shim, J. H., Croteau, R. & Wagschal, K. A. Monoterpene cyclization mechanisms and the use of natural-abundance deuterium nmr-short-cut or primrose path. *Phytochemistry*, 32, 623-631, (1993).
- 215 Köllner, T. G., Schnee, C., Li, S., Svatoš, A., Schneider, B., Gershenzon, J. & Degenhardt, J. Protonation of a neutral (*S*)-β-bisabolene intermediate is involved in (*S*)-β-macrocarpene formation by the maize sesquiterpene synthases TPS6 and TPS11. *Journal of Biological Chemistry*, 283, 20779-20788, (2008).
- 216 Cane, D. E., Sohng, J. K., Lamberson, C. R., Rudnicki, S. M., Wu, Z., Lloyd, M. D., Oliver, J. S. & Hubbard, B. R. Pentalenene synthase - purification, molecular-cloning, sequencing, and high-level expression in *Escherichia-coli* of a terpenoid cyclase from *Streptomyces uc5319*. *Biochemistry*, 33, 5846-5857, (1994).

- 217 Back, K. & Chappell, J. Cloning and bacterial expression of a sesquiterpene cyclase from
Hyoscyamus-muticus and its molecular comparison to related terpene cyclases. *Journal of Biological*
Chemistry, 270, 7375-7381, (1995).
- 218 Shishova, E. Y., Yu, F., Miller, D. J., Faraldos, J. A., Zhao, Y., Coates, R. M., Allemann, R. K., Cane,
D. E. & Christianson, D. W. X-ray crystallographic studies of substrate binding to aristolochene
synthase suggest a metal ion binding sequence for catalysis. *Journal of Biological Chemistry*, 283,
15431-15439, (2008).
- 219 Shishova, E. Y., Di Costanzo, L., Cane, D. E. & Christianson, D. W. X-ray crystal structure of
aristolochene synthase from *Aspergillus terreus* and evolution of templates for the cyclization of
farnesyl diphosphate. *Biochemistry*, 46, 1941-1951, (2007).
- 220 Cane, D. E., Pawlak, J. L., Horak, R. M. & Hohn, T. M. Studies of the cryptic allylic pyrophosphate
isomerase activity of trichodiene synthase using the anomalous substrate 6,7-dihydrofarnesyl
pyrophosphate. *Biochemistry*, 29, 5476-5490, (1990).
- 221 Hohn, T. M. & Beremand, P. D. Isolation and nucleotide sequence of a sesquiterpene cyclase gene
from the trichothecene-producing fungus *Fusarium sporotrichioides*. *Gene*, 79, 131-138, (1989).
- 222 Gennadios, H. A., Gonzalez, V., Di Costanzo, L., Li, A., Yu, F., Miller, D. J., Allemann, R. K. &
Christianson, D. W. Crystal structure of (+)- δ -cadinene synthase from *Gossypium arboreum* and
evolutionary divergence of metal binding motifs for catalysis. *Biochemistry*, 48, 6175-6183, (2009).
- 223 Lin, F.-Y., Liu, C.-I., Liu, Y.-L., Zhang, Y., Wang, K., Jeng, W.-Y., Ko, T.-P., Cao, R., Wang, A. H.-J.
& Oldfield, E. Mechanism of action and inhibition of dehydrosqualene synthase. *Proceedings of the*
National Academy of Sciences of the United States of America, 107, 21337-21342, (2010).
- 224 Faraldos, J. A. & Allemann, R. K. Inhibition of (+)-aristolochene synthase with iminium salts
resembling eudesmane cation. *Organic Letters*, 13, 1202-1205, (2011).
- 225 Miller, D. J., Yu, F., Knight, D. W. & Allemann, R. K. 6- and 14-fluoro farnesyl diphosphate:
Mechanistic probes for the reaction catalysed by aristolochene synthase. *Organic & Biomolecular*
Chemistry, 7, 962-975, (2009).
- 226 Noel, J. P., Dellas, N., Faraldos, J. A., Zhao, M., Hess, B. A., Smentek, L., Coates, R. M. & O'maille,
P. E. Structural elucidation of cisoid and transoid cyclization pathways of a sesquiterpene synthase
using 2-fluorofarnesyl diphosphates. *ACS Chemical Biology*, 5, 377-392, (2010).
- 227 Bondi, A. Van der waals volumes and radii. *Journal of Physical Chemistry*, 68, 441-451, (1964).
- 228 Frick, S., Nagel, R., Schmidt, A., Bodemann, R. R., Rahfeld, P., Pauls, G., Brandt, W., Gershenzon, J.,
Boland, W. & Burse, A. Metal ions control product specificity of isoprenyl diphosphate synthases in
the insect terpenoid pathway. *Proceedings of the National Academy of Sciences of the United States of*
America, 110, 4194-4199, (2013).
- 229 Dauter, Z., Dauter, M. & Rajashankar, K. R. Novel approach to phasing proteins: Derivatization by
short cryo-soaking with halides. *Acta Crystallographica Section D*, 56, 232-237, (2000).
- 230 Bijvoet, J. M., Peerdeman, A. F. & Van Bommel, A. J. Determination of the absolute configuration of
optically active compounds by means of x-rays. *Nature*, 168, 271-272, (1951).
- 231 Song, M. C., Kim, E. J., Kim, E., Rathwell, K., Nam, S.-J. & Yoon, Y. J. Microbial biosynthesis of
medicinally important plant secondary metabolites. *Natural Product Reports*, 31, 1497-1509, (2014).
- 232 Lauchli, R., Pitzer, J., Kitto, R. Z., Kalbarczyk, K. Z. & Rabe, K. S. Improved selectivity of an
engineered multi-product terpene synthase. *Organic & Biomolecular Chemistry*, 12, 4013-4020,
(2014).
- 233 Lauchli, R., Rabe, K. S., Kalbarczyk, K. Z., Tata, A., Heel, T., Kitto, R. Z. & Arnold, F. H. High-
throughput screening for terpene-synthase-cyclization activity and directed evolution of a terpene
synthase. *Angewandte Chemie International Edition*, 52, 5571-5574, (2013).
- 234 Cleland, W. W. The use of isotope effects to determine enzyme mechanisms. *Archives of Biochemistry*
and Biophysics, 433, 2-12, (2005).

13 Curriculum Vitae

Personal Data

Name: Abith Ramadevan Vattekkatte

Date of Birth: 12 July 1982

Permanent Address: Krishna Kripa, 11A Cross Road, Udaya Nagar,
Ayyanthole, Thrissur, Kerala, India. 680003

Email Address: abith.ramadevan@gmail.com

Education

Max Planck Institute for Chemical Ecology

Hans Knöll Straße 8, Jena, Thuringia, Germany, 07745

February 2011- Present

Doctoral Candidate in Chemistry

Advisor: Prof. Dr. Wilhelm Boland

Thesis: Mechanisms of Terpene Biosynthesis in Plants

University at Albany, State University of New York

1400 Washington Ave, Albany, New York, United States of America, 12222

December 2010

Master of Science in Organic Chemistry

Advisor: Prof. Eric Block, Carla Rizzo Delray Distinguished Professor

Thesis: Synthesis and Characterization of Organoselenium & Organosulfur
Compounds

University of Mumbai

M.G.Road, Fort, Mumbai, Maharashtra, India, 400032

May 2004

Master of Science in Organic Chemistry

May 2002

Bachelor of Science in Chemistry

Awards and Fellowships

- Gesellschaft Deutscher Chemiker (GDCh) travel award for Gordon Conference on Bioorganic Chemistry (2015)
- Travel award by Gordon Conference on Natural Products (2014)
- Selected for 128th BASF International Summer Course, Germany (2014)
- Doctoral Fellowship from Max Planck Society (2011- present)
- Best Speaker Award, Life Science Research Symposium, SUNY Albany (2010)
- State University of New York at Albany Teaching Fellowship (2006- 2010)
- Research Foundation of SUNY Albany Summer Fellowship (2006- 2010)
- Advanced Training in Water and Effluent Analysis at Advanced Training Institute, Govt. of India, Mumbai, India (2004)

Teaching Experience

University at Albany, State University of New York

August 2009-December 2010

Instructor, Organic Chemistry

January 2007 - May 2009

Teaching Assistant, Organic Chemistry I & II

January 2006 - December 2006

Teaching Assistant, General Chemistry I & II

International Max Planck Research School

Courses:

- Collection of Volatiles, speaker: Dr. Meredith Schuman
- Introduction to Molecular Biology, speaker: Dr. M. Schuman & others
- Introduction into the statistical program R, speaker: Dr. G. Kunert
- MS-based Proteomics, speaker: Dr. A. Svatos & others
- Analysis of Small Molecules, speaker: Dr. M. Schöttner & others
- Advanced Training in Mass Spectrometry, speaker: Dr. A. Attygalle, Stevens Institute, USA
- Structure elucidation of natural products using NMR, speaker: Dr. Markus Nett

14 List of Publications

- **Abith Vattekkatte**, Nathalie Gatto, Eva Schulze, Wolfgang Brandt and Wilhelm Boland, “Inhibition of a Multiproduct Terpene Synthase from *Medicago truncatula* by 3-Bromoprenyl diphosphates” *Org. Biomol. Chem.*, 2015, 13, 4776-4784
- **Abith Vattekkatte**, Nathalie Gatto, Tobias Köllner and Wilhelm Boland, “Substrate geometry controls the cyclization cascade in Multiproduct terpene synthases from *Zea mays*” *Org. Biomol. Chem.*, 2015, 13, 6021-6030
- Nathalie Gatto, **Abith Vattekkatte**, Tobias Köllner, Jörg Degenhardt, Jonathan Gershenzon, and Wilhelm Boland, “Isotope sensitive branching and kinetic isotope effects to analyze multiproduct terpenoid synthases from *Zea mays*”, *Chem. Commun.*, 2015, 51, 3797-3800
- Roman Kubec, Robert B. Cody, A. John Dane, Rabi A. Musah, Jan Schraml, **Abith Vattekkatte** and Eric Block, Applications of Direct Analysis in Real Time–Mass Spectrometry (DART-MS) in Allium Chemistry. (*Z*)-Butanethial S-Oxide and 1-Butenyl Thiosulfinates and Their *S*-(*E*)-1-Butenylcysteine S-Oxide Precursor from *Allium siculum*, *J. Agric. Food Chem.*, 2010, 58 (2) 1121–1128
- Eric Block, Robert B. Cody, A. John Dane, Rabi A. Musah, R. Sheridan, **Abith Vattekkatte** and Kai Wang,” Allium Chemistry: Use of New Instrumental Techniques to “See” Reactive Organosulfur Species formed upon Crushing Garlic and Onion”, *Pure Appl. Chem.*, 2010, 82 (3) 535-539
- **Abith Vattekkatte**, Stefan Garms and Wilhelm Boland, “Novel biosynthetic products from multiproduct terpene synthase from *Medicago truncatula* using non-natural isomers of prenyl diphosphates” (under preparation)

15 Conference Presentations

15.1 Oral Presentations

Vattekkatte A., Boland W. (April 2015). Mechanistic insights into multiproduct terpenoid syntheses. Talk presented at 49. Doktorandenworkshop: Naturstoffe: Chemie, Biologie, Ökologie, at Max Planck Institute for Chemical Ecology, Abteilung Bioorganische Chemie, Jena, DE.

Vattekkatte A., Boland W. (April 2015). Mechanistic insights into multiproduct terpenoid syntheses from *Zea mays* using isotope sensitive branching. Talk presented at Joint Symposium of Rothamsted Research, the Institute of Organic Chemistry and Biochemistry (IOCB) Prague and the MPI-CE, at Max Planck Institute for Chemical Ecology, Jena, DE.

Vattekkatte A., Boland W. (August 2014). Chemical wizardry with substrates: multiproduct sesquiterpene synthase from *Medicago truncatula*. Talk presented at 128th BASF International Summer Course, at BASF, Ludwigshafen, DE.

Vattekkatte A., Boland W. (July 2014). Single template, multiple currencies: multiproduct sesquiterpene synthase from *Medicago truncatula*. Talk presented at 30th ISCE Meeting, International Society of Chemical Ecology, at University of Illinois, Urbana-Champaign, IL, USA.

Vattekkatte A., Boland W. (February 2014). Substrates for chemical wizardry: multiproduct sesquiterpene synthase from *Medicago truncatula*. Talk presented at 13th IMPRS Symposium, at MPI for Chemical Ecology, Dornburg, DE.

Vattekkatte A., Block E. (September 2010). (S)-Trifluoroselenomethionine, a novel unnatural amino acid and expression in protein. Life Science Research Symposium, Talk presented at SUNY Albany, Albany, NY, USA (Best Speaker Award).

Vattekkatte A., Bhawe V.G. (January 2003). Inductively Coupled Plasma Spectroscopy; DR. R.A. Kulkarni R&D Foundation & Ramanarain Ruia College, at University of Mumbai, India.

15.2 Poster Presentations

Vattekkatte A., Boland W. (July 2015) Isotope sensitive branching and kinetic isotope effects to analyse multiproduct terpenoid synthases. Poster presented at Gordon Conference Series on Bioorganic Chemistry, Proctor Academy, Andover, NH, USA.

Vattekkatte A., Gatto N., Köllner T., Boland W. (June 2015). Isotope sensitive branching and kinetic isotope effects to analyse multiproduct terpenoid synthases. Poster presented at TERPNET 2015 - 12th International Meeting on Biosynthesis, Functions, and Synthetic Biology of Isoprenoids, Vancouver, BC, CA.

Vattekkatte A., Boland W. (July 2014). Substrates for chemical wizardry: Multiproduct Sesquiterpene Synthase from *Medicago truncatula*. Poster presented at Gordon Conference Series on Natural Products, Proctor Academy, Andover, NH, USA.

Vattekkatte A., Boland W. (June 2014). Substrates for chemical wizardry: Multiproduct Sesquiterpene Synthase from *Medicago truncatula*. Poster presented at Embo Conference Series on Enzyme Mechanisms By Biological Systems, Manchester, GB.

Vattekkatte A., Boland W. (February 2013). Multiproduct sesquiterpene synthase MtTPS5: structural studies and the journey so far. Poster presented at 12th IMPRS Symposium, MPI for Chemical Ecology, Jena, DE.

Vattekkatte A., Boland W. (February 2012). Multiproduct Sesquiterpene Synthase MtTPS5: Structural studies into the treasure source. Poster presented at 11th IMPRS Symposium, MPI for Chemical Ecology, Dornburg, DE.

16 Eigenständigkeitserklärung

Declaration of authorship / Selbständigkeitserklärung

Ich erkläre, dass ich die vorliegende Arbeit selbständig und unter Verwendung der angegebenen Hilfsmittel, persönlichen Mitteilungen und Quellen angefertigt habe.

I certify that the work presented here is, to the best of my knowledge and belief, original and the result of my own investigations, except as acknowledged, and has not been submitted, either in part or whole, for a degree at this or any other university.

Abith Ramadevan Vattekkatte

Jena, 10.08.2015

